



HAL
open science

Development of new methodologies in organic synthesis for the preparation of bioactive molecules

Marwa Hussein

► **To cite this version:**

Marwa Hussein. Development of new methodologies in organic synthesis for the preparation of bioactive molecules. Organic chemistry. Université de Rennes; Université Libanaise, 2017. English. NNT : 2017REN1S046 . tel-01682268

HAL Id: tel-01682268

<https://theses.hal.science/tel-01682268>

Submitted on 12 Jan 2018

HAL is a multi-disciplinary open access archive for the deposit and dissemination of scientific research documents, whether they are published or not. The documents may come from teaching and research institutions in France or abroad, or from public or private research centers.

L'archive ouverte pluridisciplinaire **HAL**, est destinée au dépôt et à la diffusion de documents scientifiques de niveau recherche, publiés ou non, émanant des établissements d'enseignement et de recherche français ou étrangers, des laboratoires publics ou privés.



THÈSE / UNIVERSITÉ DE RENNES 1
sous le sceau de l'Université Bretagne Loire

avec
Université Libanaise

pour le grade de
DOCTEUR DE L'UNIVERSITÉ DE RENNES 1
Mention : Chimie

Ecole doctorale Sciences de la Matière, Rennes

présentée par

Marwa Hussein

préparée à l'unité de recherche UMR 6226 CNRS / Institut des Sciences
Chimiques de Rennes / Equipe PNSCM
Composante universitaire : S. P. M.

**Development of new
methodologies in
organic synthesis to
prepare bioactive
compounds**

**Thèse soutenue à Beyrouth
le 20 Mars 2017**

devant le jury composé de :

Thierry DURAND

Directeur de Recherche CNRS, Université de
Montpellier / *rapporteur*

Kamal H. BOUHADIR

Professeur, Université Américaine Beyrouth /
rapporteur

Jean-Pierre BAZUREAU

Professeur, Université de Rennes1 / *examineur*

Fares FARES

Professeur, Université Libanaise Beyrouth /
examineur

Ali HACHEM

Professeur, Université Libanaise Beyrouth / *co-
directeur de thèse*

René GREE

Directeur de Recherche CNRS (Em.), Université de
Rennes 1 / *co-directeur de thèse*

Table of Schemes

Scheme I. 1: Main strategies for the synthesis of 2-Azetidinone ring	10
Scheme I. 2: The Kinugasa reaction	11
Scheme I. 3: Original β -lactam synthesis through Kinugasa reaction [31]	11
Scheme I. 4: Synthesis of β -lactam by Ding and Irwin [32].....	12
Scheme I. 5: Mechanism for the Kinugasa reaction as proposed by Ding and Irwin..	12
Scheme I. 6: Thermal non-catalyzed alkyne- nitronc cycloaddition reaction	13
Scheme I. 7: Catalytic intermolecular Kinugasa reaction developed by Miura	13
Scheme I. 8: Catalytic asymmetric synthesis of β -lactams by using chiral ligands	15
Scheme I. 9: Enantioselective Kinugasa reaction catalyzed by Cu(II)/TOX 13 chiral complex.....	15
Scheme I. 10: Highly stereoselective ynamide Kinugasa reaction	16
Scheme I. 11: Diastereoselective synthesis of Carbapenems via a Kinugasa reaction	17
Scheme I. 12: Synthesis of the cholesterol absorption inhibitor Ezetimibe 25	17
Scheme I. 13: Asymmetric Kinugasa reaction on water.....	18
Scheme I. 14: Synthesis of α -methylene β -lactams via ester enolate imine condensation reaction.....	20
Scheme I. 15: synthesis of α -ethylidene β -lactams via ester enolate imine condensation reaction.....	20
Scheme I. 16: Kinugasa reaction in the presence of L-proline	21
Scheme I. 17: The way of formation of 30 proposed by Basak.....	21
Scheme I. 18: General method for the preparation of 6-methylidene penems 40	22
Scheme I. 19: Synthesis of α -methylene β -lactams via PPh ₃ -catalyzed umpolung cyclization of propiolamides	22
Scheme I. 20: Proposed mechanism for the synthesis of α -methylene β -lactam via PPh ₃ catalyst.....	23
Scheme I. 21: Synthesis of α -alkylidene- β -lactam using Kinugasa reaction with alkynes bearing a <i>gem</i> -difluoro group at propargylic position	23
Scheme I. 22: Mechanism of the Kinugasa reaction proposed by Tang and coworkers	27
Scheme I. 23: Our working hypothesis towards a new synthesis of α -methylene- and α -alkylidene- β -lactams.....	28

Scheme I. 24: Grignard reaction for the preparation of 47a	32
Scheme I. 25: Kinugasa reaction between alkynes 47 and nitrene 2a	33
Scheme I. 26: Kinugasa reaction between nitrene 2a and alkynes 49 and 51	39
Scheme I. 27: Kinugasa reaction between nitrene 2a and alkyne 53	40
Scheme I. 28: Kinugasa reaction between alkyne 47d and nitrene 55	41
Scheme I. 29: Kinugasa reaction between alkyne 47d and nitrene 57	41
Scheme I. 30: Kinugasa reaction between alkyne 47d and nitrene 59	41
Scheme I. 31: Kinugasa reaction between alkyne 47d and cyclic nitrene 61	42
Scheme I. 32: Kinugasa reaction between nitrene 2a and alkynes 63	42
Scheme I. 33: Kinugasa reaction between simple alkyne 63d and nitrenes 57 , 59 and 61	44
Scheme I. 34: Direct synthesis of α -methylene and α -alkylidene β -lactams via Kinugasa reaction.....	48
Scheme II. 1: Brook rearrangement of acylsilanes.....	93
Scheme II. 2: Proposed mechanism by Brook for the formation of aldehydes from acylsilanes	93
Scheme II. 3: Reaction of alkoxides with acylsilane 15	94
Scheme II. 4: Reverse Brook rearrangement	94
Scheme II. 5: First acylsilane compound synthesized by Brook	95
Scheme II. 6: Different methods for the synthesis of acylsilanes.....	95
Scheme II. 7: Acylsilane 25 from α -silyl alcohols 24	96
Scheme II. 8: Acylsilanes 31 from silyl alcohols 30 using mild oxidation conditions. 96	
Scheme II. 9: Acylsilanes 34 from silyl alcohols 33 using Dess-Martin oxidant.....	97
Scheme II. 10: Acylsilanes 38 from masked aldehydes 36	97
Scheme II. 11: Acylsilanes 41 from esters 39	98
Scheme II. 12: Acylsilanes 44 from esters 43 and silyllithium derivative 42	98
Scheme II. 13: oxidation of disilyl alcohols 46' to afford acylsilanes 48	99
Scheme II. 14: Acylsilanes 50 from amides 49	99
Scheme II. 15: Synthesis of acylsilanes 50 from morpholine amides 51	100
Scheme II. 16: Rearrangement observed starting from aryl morpholine amides 53 . 100	
Scheme II. 17: Acylsilane using aromatic/heteroaromatic morpholine amide precursors	101
Scheme II. 18: Acylsilanes 62 from <i>S</i> -2-pyridyl esters 61	101
Scheme II. 19: Acylsilanes 50 and 65 from acyl chlorides 63	102

Scheme II. 20: Acylsilanes 69 from acyl chlorides 67 using palladium catalyst	102
Scheme II. 21: Nucleophilic addition on acylsilane 70 bearing achiral center on the α -carbon.....	103
Scheme II. 22: Nucleophilic addition on acylsilane 73 bearing achiral center on the β -carbon.....	104
Scheme II. 23: Grignard additions on acylsilanes 76	104
Scheme II. 24: Addition reaction of lithium enolate on acylsilane 78	105
Scheme II. 25: Diastereoselective aldolizations of acylsilane 84	105
Scheme II. 26: Radical reactions of acylsilanes 89, 91 and 93	106
Scheme II. 27: Mechanism proposed for the radical reactions of acylsilanes.	106
Scheme II. 28: Synthesis of bicyclic alcohol 97 from acylsilane 96 through a radical reaction.....	107
Scheme II. 29: Cyclization reaction of acylsilanes 98	107
Scheme II. 30: Cyclization of bis-silyl compounds 101 and 103 using <i>p</i> -TsOH as a catalyst	108
Scheme II. 31: Enantioselective reduction of 105 and 107 using a chiral borane	108
Scheme II. 32: Enantioselective reduction of α,β -unsaturated acylsilane 109 using chiral lithium amine 110	109
Scheme II. 33: Organocatalyzed Michael reactions	110
Scheme II. 34: Pd-catalyzed cross coupling reaction of arylsilane 11	111
Scheme II. 35: Intramolecular aldol reaction starting from bifunctional acylsilane-aldehyde molecules	116
Scheme II. 36: preparation of the key intermediate 128	120
Scheme II. 37: Synthesis of phosphonate amide 124	121
Scheme II. 38: Direct addition of phosphonate 124 on the starting <i>o</i> -phthalaldehyde 119	126
Scheme II. 39: Intramolecular aldolization reaction of 128 using LDA as a base	127
Scheme II. 40: Intramolecular aldolization using quinidine-derived catalyst	128
Scheme II. 41: comparison of enol contents between ketone and acylsilane	129
Scheme II. 42: Mechanism for enamine formation	130
Scheme II. 43: Preparation of acylsilane 141	132
Scheme II. 44: Two models of acylsilane intermediates	140
Scheme III. 1: Condensation of hydrazine 19 with diketone 18	203
Scheme III. 2: Protection of hydrazine	203

Scheme III. 3: Deprotection of pyrrole 20	205
Scheme III. 4: Preparation of hydrazone 23	206
Scheme III. 5: Condensation reaction of pyrrolidines 24R and 24S with aldehyde 22	207
Scheme III. 6: Palladium catalyzed arylation of 3-formylthiophene 26 with bromobenzene 27	209
Scheme III. 7: Reduction of aldehyde 29	212
Scheme III. 8: Preparation of phosphonium salt 31	213
Scheme III. 9: Wittig reaction between phosphonium 31 and aldehyde 32	215
Scheme III. 10: Protection of trihydroxybenzaldehyde 22 using MOMCl.....	215
Scheme III. 11: Deprotection of MOM groups.....	218
Scheme III. 12: Preparation of phosphonium salt 36	221
Scheme III. 13: Wittig reaction between phosphonium salt 36 and aldehyde 32	221
Scheme III. 14: Deprotection of MOM group of 37E and 37Z	222
Scheme III. 15: General sequence for the preparation of oxazoles	223
Scheme III. 16: Esterification reaction of carboxyl group.....	223
Scheme III. 17: Preparation of amide 42a	225
Scheme III. 18: Preparation of phosphonate 44a	227
Scheme III. 19: Preparation of phosphonate 48	230
Scheme III. 20: Cyclization reaction of 44a to obtain the oxazole product 53a	231

Table of Tables

Table I. 1: Alkylidene β -lactams 48 produced via scheme 25	33
Table I. 2: Results of Kinugasa reaction between nitrene 2a and simple alkyne 63 ...	43
Table I. 3: Crystal data and structure refinement for 52Z	71
Table II. 1: Infrared C=O absorption and NMR data of some acylsilanes [28, 30].....	92
Table III. 1: Results of IC ₅₀ (μ M) of the compounds on HaCaT and B16 lines.....	234

Table of Figures

Fig.I. 1: Structure of original penicillin G (Thiazolidine ring)	6
Fig.I. 2: Structure of 2-Azetidinone (β -lactam)	7
Fig.I. 3: Some major classes of β -lactams that act as antibiotics.....	7
Fig.I. 4: β -Lactam compounds exhibit interesting biological activities	8
Fig.I. 5: Bis-oxazoline type ligands used for asymmetric intermolecular Kinugasa reaction.....	14
Fig.I. 6: Structure of <i>cis</i> -carbapenem.....	16
Fig.I. 7: General structures of α -methylene and α -alkylidene β -lactams.....	19
Fig.I. 8: Representative examples of bioactive α -alkylidene β -lactams	19
Fig.I. 9: β -lactam inhibitors	20
Fig.I. 10: ^1H NMR spectrum of compound 48E	34
Fig.I. 11: ^{13}C NMR spectrum of compound 48E	34
Fig.I. 12: ^1H - ^1H NOESY spectrum of compound 48E	35
Fig.I. 13: ^1H NMR spectrum of compound 48Z	36
Fig.I. 14: ^{13}C NMR spectrum of compound 48Z	36
Fig.I. 15: ^1H - ^1H NOESY spectrum of compound 48Z	37
Fig. I. 16: Structure of 52Z by X-Ray diffraction	39
Fig.II. 1: Structure of acylsilanes.....	89
Fig.II. 2: The proposed dual activation mode of guanidine 114 catalyzed Michael reaction between an acylsilane and a nitroolefin.	108
Fig.II. 3: ^1H NMR spectrum of α,β -unsaturated amide 125	119
Fig.II. 4: ^1H NMR spectrum of saturated amide 126	120
Fig.II. 5: ^1H NMR spectrum of acylsilane 127	121
Fig.II. 6: ^1H NMR spectrum of the key intermediate 128	122
Fig.II. 7: Quinidine and proline catalysts.....	125
Fig.II. 8: ^1H NMR spectrum of the <i>cis</i> and <i>trans</i> mixture of 133 -indanole	128
Fig.II. 9: ^1H NMR spectrum of amide 136	130
Fig.II. 10: ^1H NMR spectrum of amide 137	131
Fig.II. 11: ^1H NMR spectrum of aldehyde 138	135
Fig.II. 12: ^1H NMR spectrum of acetal 139	136
Fig.III. 1: Activation of the caspase protease cascade during apoptosis.....	172
Fig.III. 2: DISC formation and caspase-8 activation in extrinsic pathway.....	174

Fig.III. 3: Apoptosis via mitochondrial membrane.....	175
Fig.III. 4: Members of BCL-2 family proteins	177
Fig.III. 5: Interaction between the three types of BCL-2 family proteins regulating MOMP and induce apoptosis.....	178
Fig.III. 6: Role of MCL-1 in survival and apoptotic conditions.....	179
Fig.III. 7: Structures of ABT-737, ABT-263, and ABT-199 BCL-2 inhibitors.	182
Fig.III. 8: Structures of Indole-2-carboxylic acid derivatives.....	184
Fig.III. 9: Structures of class I and class II compounds suggested by Fesik.	185
Fig.III. 10: Co-crystal structure of benzothiophene 3 with MCL-1.....	186
Fig.III. 11: Structure of 6/MIM1, a selective MCL-1 inhibitor.....	186
Fig.III. 12: Co-crystal structure of MIM-1 compound with MCL-1	187
Fig.III. 13: MCL-1 inhibitors developed by Walensky.	188
Fig.III. 14: Co-crystal structure of compound 8 with MCL-1	188
Fig.III. 15: Developed MCL-1 inhibitors.	189
Fig.III. 16: Co-crystal structure of compound 8 with MCL-1	189
Fig.III. 17: AbbVie's aryl sulfonamide-based MCL-1 inhibitors	190
Fig.III. 18: Co-crystal structure of compound 14 with MCL-1	187
Fig.III. 19: Deconstruction of dual MCL-1/BCL-2 inhibitor 15 and rebuilding of MCL-1 selective inhibitor.....	192
Fig.III. 20: Co-crystal structure of compound 17 with MCL-1	192
Fig.III. 21: Molecular modeling of MIM-1 in MCL-1 pocket.....	196
Fig.III. 22: First model prepared in our group.....	197
Fig.III. 23: Second model of synthesis	197
Fig.III. 24: Thiophene docked in MCL-1 protein	204
Fig.III. 25: Oxazole docked in MCL-1 protein	205
Fig.III. 26: ¹ H NMR spectrum of 20	204
Fig.III. 27: ¹³ C NMR spectrum of 20	205
Fig.III. 28: ¹ H NMR spectrum of 23	200
Fig.III. 29: ¹³ C NMR spectrum of 23	201
Fig.III. 30: ¹ H NMR spectrum of 25R	202
Fig.III. 31: ¹³ C NMR spectrum of 25R	209
Fig.III. 32: ¹ H NMR spectrum of 29	204
Fig.III. 33: ¹³ C NMR spectrum of 29	205
Fig.III. 34: ¹ H- ¹ H NOESY spectrum of 29	205

Fig.III. 35: ^1H NMR spectrum of 30	206
Fig.III. 36: ^{13}C NMR spectrum of 30	207
Fig.III. 37: ^1H NMR spectrum of 31	208
Fig.III. 38: ^{13}C NMR spectrum of 31	208
Fig.III. 39: ^1H NMR spectrum of 33E	210
Fig.III. 40: ^{13}C NMR spectrum of 33E	210
Fig.III. 41: ^1H NMR spectrum of 33Z	211
Fig.III. 42: ^{13}C NMR spectrum of 33Z	211
Fig.III. 43: ^1H NMR spectrum of 34E	213
Fig.III. 44: ^{13}C NMR spectrum of 34E	213
Fig.III. 45: ^1H NMR spectrum of 34Z	214
Fig.III. 46: ^{13}C NMR spectrum of 34Z	214
Fig.III. 47: ^1H NMR spectrum of 40	218
Fig.III. 48: ^{13}C NMR spectrum of 40	219
Fig.III. 49: ^1H NMR spectrum of 42a	220
Fig.III. 50: ^{13}C NMR spectrum of 42a	220
Fig.III. 51: ^1H NMR spectrum of 44a	221
Fig.III. 52: ^{13}C NMR spectrum of 44a	222
Fig.III. 53: ^{31}P NMR spectrum of 44a	223
Fig.III. 54: Other analogs starting from alanine amino acid	223
Fig.III. 55: Phosphonate intermediates starting from glycine	224

Table of Contents

I.A.Introduction:.....	1
I.A.a.Antibiotics.....	5
I.A.b.Beta-lactams.....	7
I.A.c.Kinugasa reaction... ..	11
I.A.d. α -Methylene- and α -Alkylidene β -lactams... ..	19
I.B.Objective and Strategy.....	27
I.C.Results and discussion.....	32
I.D.Conclusion.. ..	48
I.E.Experimental Part.....	52
I.F.References.....	82
II.A.Introduction	91
II.A.a.General Introduction.....	91
II.A.b.Physical properties of acylsilanes	92
II.A.c.Brook and reverse Brook rearrangements.....	93
II.A.d.Synthesis of acylsilanes	95
II.A.d.1.Acylsilanes from α -silyl alcohol.....	96
II.A.d.2.Acylsilanes from masked aldehydes.....	97
II.A.d.3.Acylsilanes from esters.....	98
II.A.d.4.Acylsilanes from amides.....	99
II.A.d.5.Acylsilanes from S-2-pyridyl ester... ..	101
II.A.d.6.Acylsilanes from acyl chloride... ..	101
II.A.e.Reactions and uses of acylsilanes in organic synthesis	102
II.A.e.1.Stereocontrolled nucleophilic additions on acylsilanes.....	103
II.A.e.2.Stereocontrolled aldol reactions of acylsilanes.. ..	105
II.A.e.3.Acylsilanes in radical reactions.....	106

II.A.e.4.Cyclization reactions of acylsilanes.....	107
II.A.e.5.Enantioselective reduction of acylsilanes.....	108
II.A.e.6.Organocatalytic asymmetric Michael reactions with acylsilane donors.....	109
II.A.e.7.Palladium catalyzed cross coupling reaction of acylsilanes.....	111
II.B.Objective and strategy.....	116
II.C.Results and discussion.....	120
II.D.Conclusion.....	140
II.E.Experimental Part.....	145
II.F.References.....	161
III.A.Introduction.....	171
III.A.a.Apoptosis.....	171
III.A.a.1.The extrinsic pathway.....	173
III.A.a.2.The intrinsic pathway... ..	174
III.A.b.BCL-2 Family Proteins.....	176
III.A.b.1.Mcl-1 protein.....	178
III.A.c.BCL-2 Inhibitors.....	180
III.A.c.1.MCL-1 inhibitor... ..	183
III.B.Objective and Strategy.....	196
III.C.Results and discussion.....	203
III.C.a.Hydrazone type analogs.....	203
III.C.b.Alkene type analogs.....	209
III.C.c.Biological tests.....	231
III.D.Conclusion.....	240
III.E.Experimental Part.....	244
III.F.References.....	295

Acknowledgments

This thesis was done at the "Institute for Chemical Sciences of the University of Rennes 1", in the laboratory of "Natural Products, Synthesis and Medicinal Chemistry" (PNSCM) of the UMR CNRS 6226, in the group of Prof. René GRÉE, as well as at the "Laboratory of Medicinal Chemistry and Natural Product" (LCMPN) at the Lebanese University, under the direction of Pr. Ali HACHEM.

This thesis would not have been possible without the encouragement of my academic advisors, Professors René GRÉE and Ali HACHEM who have been greatly generous in their invaluable councils and relevant remarks as well as their confidence in me and for welcoming me to their research team. Without their guidance, support and good nature, I would have never been able to pursue my goal.

Also, I would like to thank Dr. Paul MOSSET, for his support and for his valuable advices he gave me during my thesis work.

I would also like to thank Mr. Olivier TASSEAU, for all the information he provided to me, and helped me to learn many important and needed techniques.

I would like to express my profound thanks to Doctor Thierry Durand from the University of Montpellier and Kamal BouHadir from the American University of Beirut, reporters who gave valuable time to the study of this manuscript.

I cannot but express my gratitude to Professor Bazureau from the University of Rennes 1, for agreeing to be a member of the jury of this thesis.

Many thanks from the deep of my heart for each member of the laboratory (LCMPN): Dr. Fares Fares (Co-director), Dr. Hassan ABDALLAH, Dr. Nada JABER, and Dr. Ali KHALAF, for their advice.

Thanks for the Doctoral Schools at the Lebanese University (EDST) and the University of Rennes 1 (SDLM), which gave me the opportunity to do my PhD.

I would like to thank the CRMPO at the University of Rennes 1 for the mass spectroscopic analysis and the NMR experiments as well as CDIFX for the X-Ray.

Thanks to all people from both laboratories for their kindness and support: Assaad, Hiba, Layal, Rima, Rim, Ranin, and Johal.

I dedicate this thesis manuscript very sincerely to my parents, my brothers and to the SOUL of my sister who have always supported throughout my studies and always encouraged me to go further.

Most sincerely, I am utterly thankful to the person who always been an inspiration and has motivated me to aspire for a demanding and meaningful Education, I am deeply thankful to my Love of my life, who always encourages me and being beside me at every hard moment, and giving me a lot of moral supports!

Standard Equipments and Techniques

Nuclear Magnetic Resonance (NMR)

The NMR spectra were obtained using the spectrometer BRUCKER AVANCE 300 and 400 with sample changer and BBO ATMA multinuclear sensor automatically tunable (300 or 400 MHz for the proton, 75 or 100 MHz for the carbon 13 and 121 MHz for the phosphorus 31).

The chemical shifts δ are expressed in parts per million (ppm) with respect to the signal of the solvent ($\delta = 7.26$ for CDCl_3) used as a reference for the proton and carbon NMR. The coupling constants are expressed in Hertz (Hz), to describe the multiplicity of signals. The following abbreviations have been used: s: singlet, d: doublet, t: triplet, q: quadriplet, dd: doublet of doublet, dt: doublet of triplet, etc. The ^{13}C spectra were determined from fully decoupled proton spectra.

The assignment of signals for complex structures was confirmed using 2D experiment(NOESY).

Mass Spectrometry(HRMS)

High-resolution mass spectra were performed by CRMPO on a VARIAN MAT double-focusing spectrometer (mode electronic impact) or high resolution micromass MS / MS Mass Spectrometer ZABSpecOF (electrospray mode)

Melting Point

The melting points were determined with an error of ± 2 ° C. using a KOFLER BENCH.

Chromatography

The thin-film analytical chromatographies are carried out using aluminum sheets Merck silica gel 60F254. After elution, the plates are revealed in 254 nm UV light then by a solution of para-anisaldehyde (375 mL of 95% EtOH, 18.5 mL of *p*-anisaldehyde, 25 mL of concentrated H₂SO₄, and 7.5 mL glacial acetic acid) and / or potassium permanganate (1.5 g of KMnO₄, 10 g of K₂CO₃, 1.25 mL of 10% NaOH and 200 mL water). Purifications by column chromatography were carried out with Acros Organics 60A silica gel (0.040-0.063 mm).

Glassware

The reactions requiring anhydrous conditions were all carried out under an inert atmosphere (Nitrogen) using glassware previously dried and Cooled under argon or nitrogen.

Solvents and reagents

Diethyl ether and THF are distilled over sodium/benzophenone. Dichloromethane and Toluene are distilled over calcium hydride.

Nomenclature

The names of the molecules were assigned using the Chemdraw 8.0 software according to the nomenclature IUPAC

Abbreviations

Apaf-1: Apoptotic protease activating factor

Bax: Bcl-2-associated x protein

BCl-2: B-cell lymphoma 2

BCl-xL: B-cell lymphoma-extra large

BH: Bcl-2 Homology

CDCl₃: Chloroform

CDI: Carbonyldiimidazole

CuI: Copper iodide

DAST: Diethylaminosulfurtrifluoride

DBU: 1,8-diazabicyclo[5.4.0]undec-7-ene

DCC: N,N'-Dicyclohexylcarbodiimide

DCM: Dichloromethane

DMAP: 4-Dimethylamino pyridine

DMF: Dimethylformamide

DMSO: Dimethylsulfoxide

DNA: Deoxyribonucleic acid

dppb: 1,4-Bis(diphenylphosphino)butane

equiv: Equivalent

Et₃N: Triethylamine

EtAc: Ethylacetate

EtOH: Ethanol

h: hour

HCl: Hydrochloric acid

HIV: Human Immunodeficiency virus

HRMS: High resolution mass spectrometry

Hz: Hertz

IBX: 2-Iodoxybenzoic acid

IC₅₀: Average concentration inhibitor

IR: Infra-red

K₂CO₃: Potassium carbonate

LDA: Lithium diisopropyl amide

LiAlH₄: Lithium aluminium hydride

LiCl: Lithium chloride
MCl-1: Myeloid Cell Leukemia 1
MeCN: Acetonitrile
MeOH: Methanol
MgSO₄: Magnesium sulfate
MIM-1: Mcl-1 inhibitor molecule 1
min: Minute
mol: Mole
MOM: Methoxymethyl
MOMP: Mitochondrial outer membrane permeabilization
mp: Melting point
Na₂CO₃: Sodium carbonate
NaBH₄: Sodium borohydride
NaCl: Sodium chloride
NaH: Sodium hydride
NaHCO₃: Sodium bicarbonate
NaOH: Sodium hydroxide
n-BuLi: n-butyllithium
NH₄Cl: ammonium chloride
NMR: Nuclear magnetic resonance
NOESY: Nuclear Overhauser Effect Spectroscopy
Ph: Phenyl
pH: potential hydrogen
pka: Acid dissociation constant
ppm: parts per million
PPTs: Pyridinium *para*-toluene sulfonate
***p*-TSA:** *Para*-toluene sulfonic acid
R_f: Retention factor
Rt: Room temperature
SOCl₂: Thionyl chloride
***t*-BuO⁻:** tert-Butyl alcohol
THF: Tetrahydrofuran
TLC: Thin layer chromatography
UV: Ultraviolet

I. FIRST CHAPTER

**A new direct synthesis of α -methylene and
alkylidene β -lactames**

I.A. INTRODUCTION

Introduction:

Antibiotics:

To begin, the definition of "antibiotic" as first proposed by *Selman Waksman* (who discovered the streptomycin): it is a natural product produced by bacteria and fungi that inhibits, or kills, microbes by specific interactions with bacterial targets, without any consideration of the source of the particular compound or class [1]. Afterward the notion of "antibiotic" has been extended to molecules obtained by hemisynthesis, or even by total synthesis, and to some substances exhibiting antifungal, antiviral or anticancer properties, provided that they are of natural origin.

Antibiotics were first discovered in September 1928 by Alexander Fleming, who accidentally observed that something unusual was occurring on the plate of one of his experiments, which was dotted with colonies, except for one area where a blob of mold was growing [2]. The zone immediately around the mold -later identified as a rare strain of *Penicillium notatum*- was clear, as if the mold had secreted something that inhibited bacterial growth. Fleming found that his "mold juice" was capable of killing a wide range of harmful bacteria, such as *Streptococcus*, *Meningococcus*, and the *Diphtheria Bacillus*. That marked the beginning of the discovery of penicillin which, together with several other different antimicrobial agents, save millions of humans and animals from infectious disease-causing organisms.

In 1939, during the World War II, Howard Florey, Ernst Chain, and their colleagues at the Sir William Dunn School of Pathology at Oxford University, turned penicillin from a laboratory curiosity into a life-saving drug. They focused their work on the purification and chemistry of penicillin G (the original form of penicillin). This molecule was used as a therapeutic agent for the first time in 1941 in Oxford on a patient suffered from septicemia (serious bloodstream infection). In 1945, a Nobel prize in Physiology or Medicine was awarded jointly to Sir Alexander Fleming, Ernst Boris Chain and Sir Howard Walter Florey "*for the discovery of penicillin and its curative effect in various infectious diseases*".

From an historical point of view, it is interesting to note that the real discoverer of penicillin was a french military physician, Ernest Duchesne. Duchesne was studying the interaction between *Escherichia coli* and *Penicillium glaucum* and he demonstrated that the mold could eliminate the bacteria in a culture. He also proved that an animal inoculated with a lethal dose of *Salmonella typhi* (typhoid agent) was still alive-if beforehand inoculated with *Penicillium glaucum*. E. Duchesne defended his thesis with general indifference...it was in 1897...thirty years before Fleming's (serendipity) observation.

An expanded role for the penicillins came from the discovery that natural penicillins (G and V) can be modified chemically and mainly enzymatically (by amidases), by removing the acyl group to leave 6-aminopenicillanic acid (6-APA) and then adding other acyl groups that confer new biological and pharmacokinetic properties (Figure I.1). These modern semi-synthetic penicillins such as oxacillin, ampicillin, amoxicillin, and carbenicillin, have various specific properties such as: resistance to stomach acids so that they can be taken orally, a degree of resistance to penicillinase (a penicillin-destroying enzyme produced by some bacteria) that extended their range of activity against some Gram-negative bacteria.

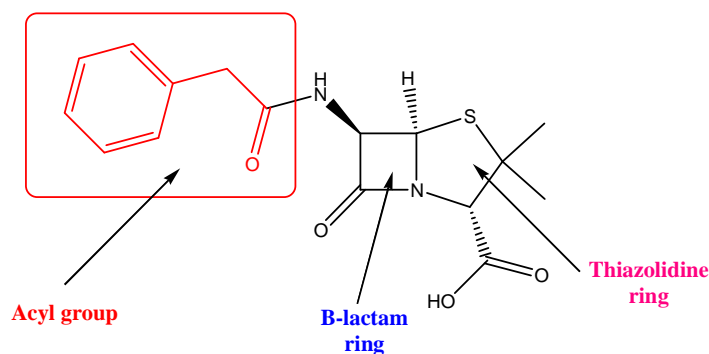


Fig. I. 1: Structure of original penicillin G (Thiazolidine ring)

Among many antibiotics used nowadays in clinical medicine we can notice *cephalosporins*, β -lactams with an identical mode of action to that of penicillins, as one of the most significant family of antibiotics [3]. Moreover, penicillins and cephalosporins follow the same biogenetic way, except for the last step.

It is necessary to note that the most important aspect for the synthesis of β -lactam derivatives has been the construction of the four-membered ring.

Beta-lactams:

2-Azetidinone (β -lactam), a four membered cyclic amide (Figure I.2), has been recognized as the fundamental pharmacophore group for a large number of bioactive compounds, especially antibiotics [4].

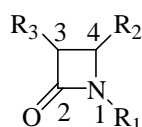
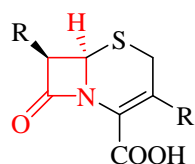
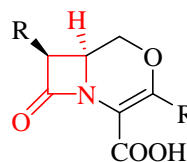


Fig. I. 2: Structure of 2-Azetidinone (β -lactam)

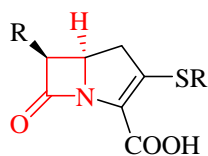
β -lactams are present in a variety of antibiotics, such as penicillins, carbapenems, cephalosporins, and monobactams (azthreonam, the only one in medicine) (Figure I.3), since they occupied a central role in the fight against pathogenic bacteria [5].



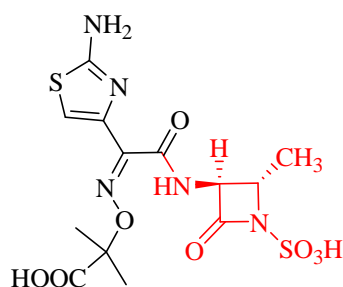
Cephalosporins



Isooxacephems



Carbapenems



Monobactam: azthreonam

Fig. I. 3: Some major classes of β -lactams that act as antibiotics

In addition to their antibiotic significance, β -lactams exhibit interesting non-antibacterial properties including cholesterol-lowering effects [6, 7, 8, 9], antifungal [10], anticancer [11, 12], analgesic [13], and antihyperglycemic activity [14] (Figure I.4).

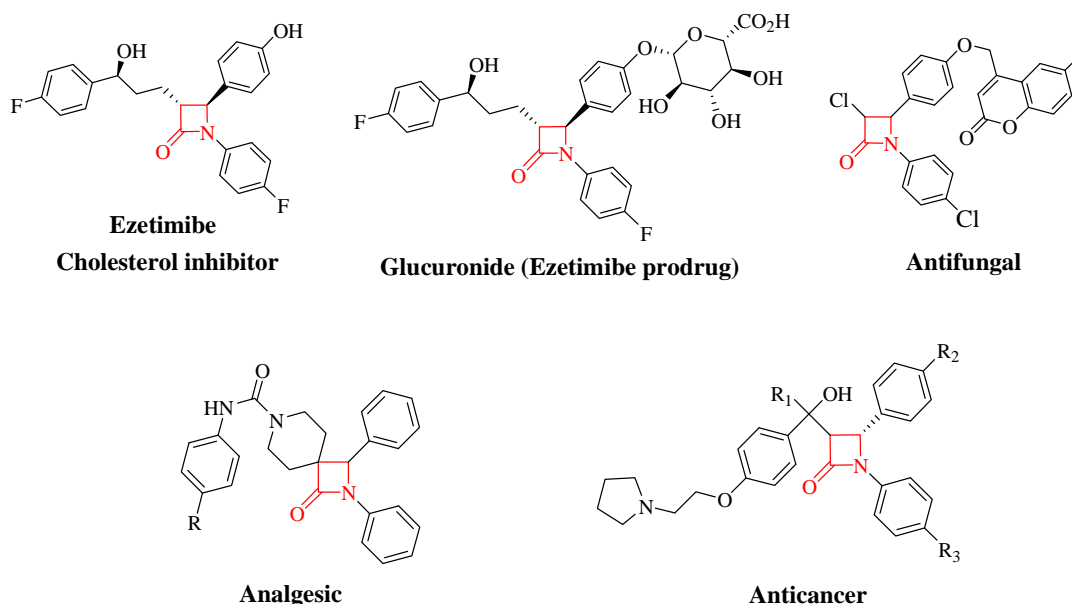


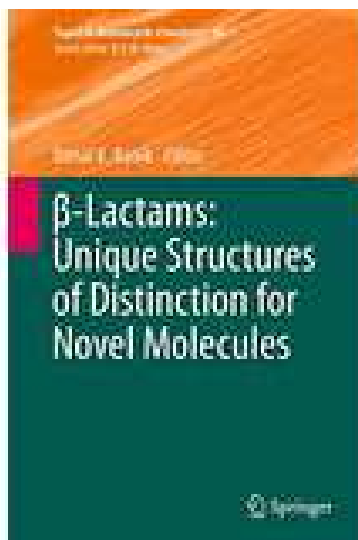
Fig. I. 4: β -Lactam compounds exhibit interesting biological activities

Furthermore, many reports on serine protease [15, 16, 17] inhibition by certain β -lactams were also published as well as discovery of 2-azetidinones' antagonism of vasopressin V1a receptor [18] and inhibition of HIV-1 protease [19] and β -lactamase [20].

The uncontrolled use of β -lactams against bacterial infection resulted in increasing the number of antibiotic-resistant bacterial strains, thus β -lactams with greater potency and broader spectrum of action become urgently required. The search for highly active β -lactam antibiotics, as well as more effective β -lactamase inhibitors, has motivated from a long time ago, academic and industrial laboratories to design new functionalized β -lactam structures.

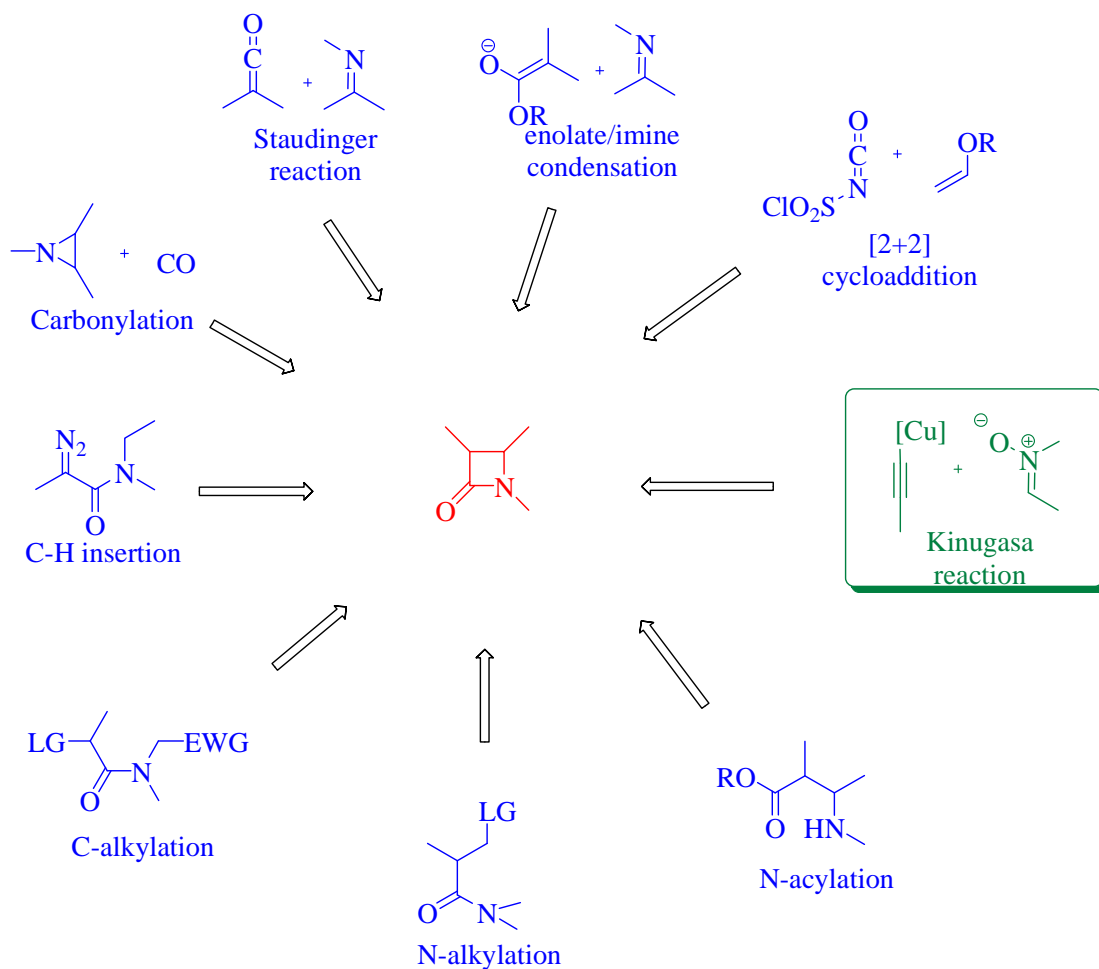
So, based on either new or already established methodologies, or on the modification of preexisting groups attached to the 2-azetidinone ring, many methodologies were

developed for the stereoselective construction of the four-membered β -lactam ring as reviewed for instance in the following book [21, 22].



β -lactams: Unique Structures of Distinction for Novel Molecules by Bimal K. Banik

The most popular classical methods for the construction of β -lactams are ketene/imine cycloadditions (also known as the Staudinger reaction) [14, 23, 24, 25], ester or amide enolate-imine condensations [14, 26], and [2+2] cycloadditions of isocyanates with vinyl ethers [27] (Scheme I.1).



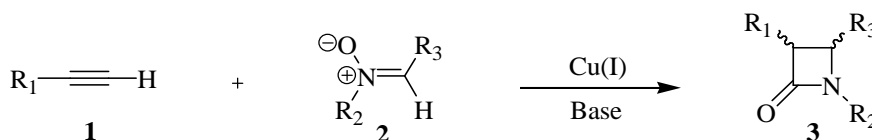
Scheme I. 1: Main strategies for the synthesis of 2-Azetidinone ring

Other important reactions for the synthesis of β -lactams involves formation of the β -lactam ring via *N*-acylation of β -amino acids and *N*-alkylation of amides after introduction of a β -leaving group [14, 28], and the formation of C3-C4 bond by direct C-alkylation, but this reaction is very rare [14, 29] (Scheme I.1). On the other hand, rhodium-catalyzed intramolecular C-H insertions of diazoamides [30] are also known.

Among the different synthetic routes for the construction of β -lactam ring is the Kinugasa reaction, which is an interesting and direct method for such a preparation. This reaction has been discovered 40 years ago by Kinugasa and Hashimoto [31] and several reviews have been already published on this topic [32, 33].

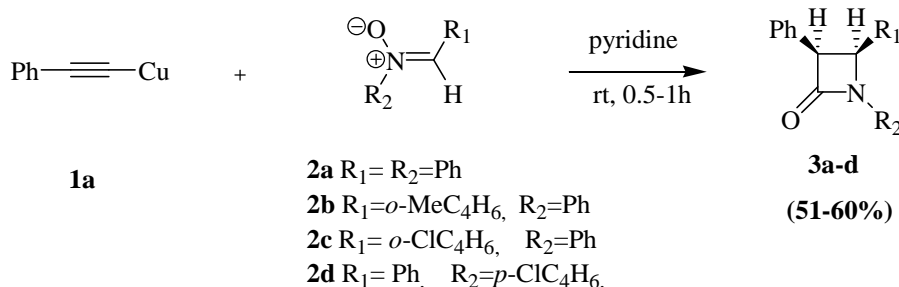
Kinugasa reaction:

The Kinugasa reaction is formally a simple [3+2] cycloaddition reaction between alkyl/arylacetylide **1** with a nitron **2** in the presence of a base and copper (I) (Scheme I.2).



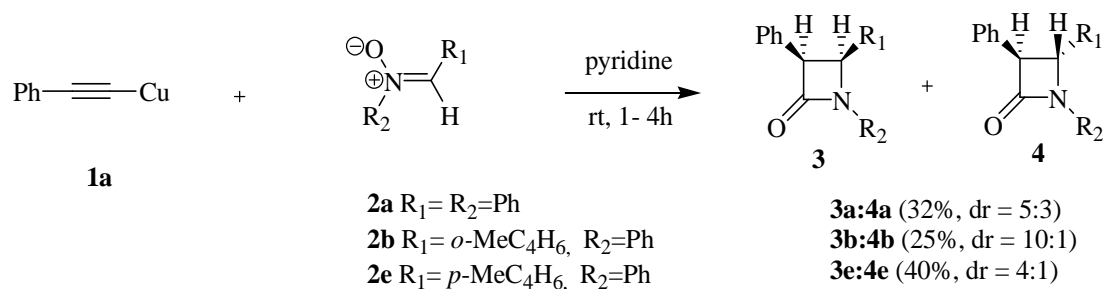
Scheme I. 2: The Kinugasa reaction

In 1972 Kinugasa and Hashimoto [31] reported the first reaction of copper(I) phenylacetylide **1a** with nitrones **2a-d**, providing a new and facile way to synthesize β -lactams (Scheme I.3). The reaction was carried out in dry pyridine for 0.5-1 h, and only the *cis* products **3a-d** were obtained by these authors, in fair yields (51-60%). This process was the first Kinugasa-type synthesis of *cis* β -lactams in a stereoselective manner.



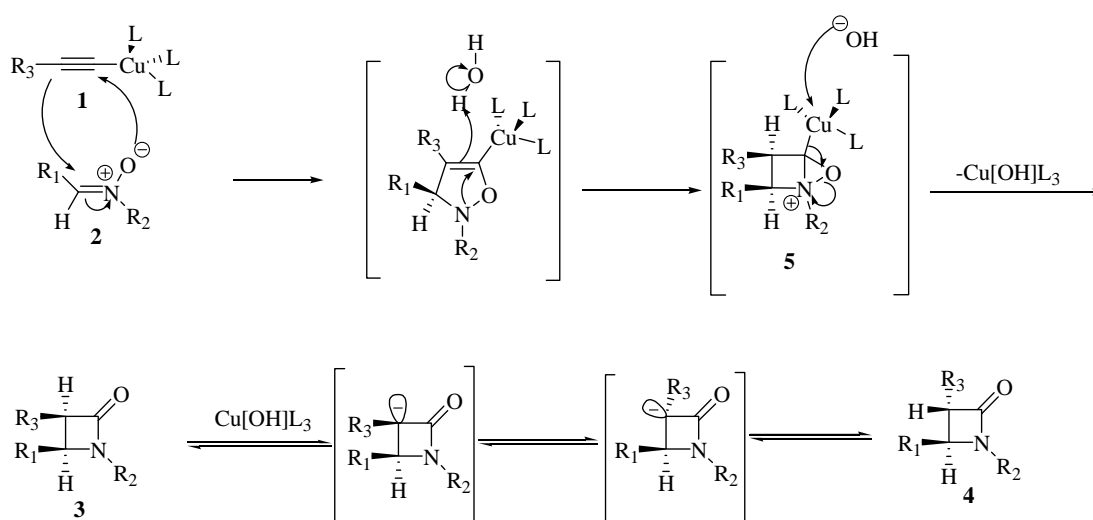
Scheme I. 3: Original β -lactam synthesis through Kinugasa reaction [31]

In 1976, Ding and Irwin [34] studied the reaction of different nitrones **2a,b,e** with copper (I) phenylacetylide **1a** and discovered that a mixture of *cis*- and *trans*- β -lactams was always obtained, in different ratios. The *cis*- β -lactam **3** was the major diastereomer in most cases and it was converted into the *trans*-isomer **4** under basic conditions through an epimerization process. This isomerisation process was also depending on the type of substituent at C3 position (Scheme I.4).



Scheme I. 4: Synthesis of β -lactam by Ding and Irwin [32]

Ding and Irwin proposed a first mechanism for the Kinugasa reaction, which is still one of the mechanisms considered today (Scheme I.5).

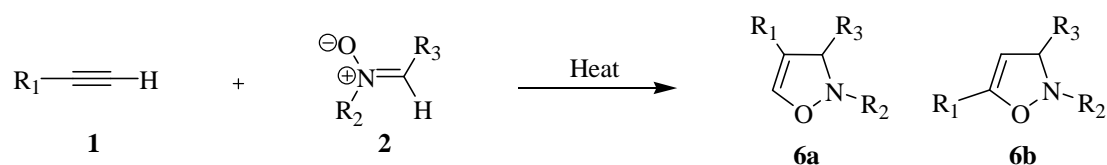


Scheme I. 5: Mechanism for the Kinugasa reaction as proposed by Ding and Irwin

As illustrated in the above scheme, the process consists of a two-step cascade reaction involving a 1,3-dipolar cycloaddition, followed by a rearrangement. It has been suggested by these authors that β -lactam formation proceeds through a highly strained bicyclic oxaziridinium intermediate **5**. *Cis*-azetidinone was formed under kinetic control, due to the protonation of isoxazoline intermediate from sterically less hindered face.

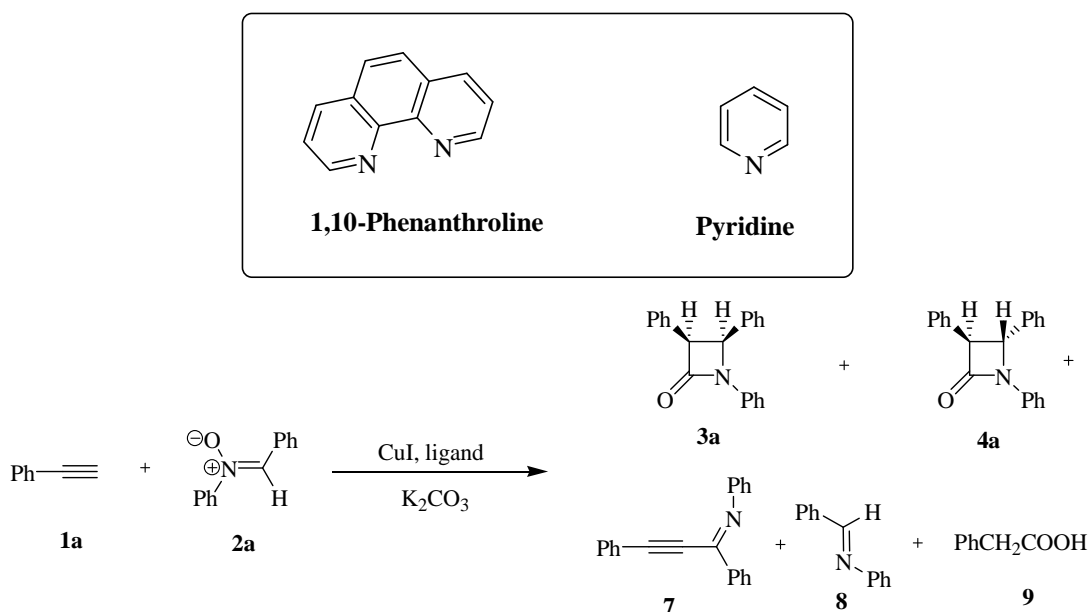
It has to be noticed that the classical, copper-free cycloaddition of nitrones to terminal alkynes proceeds under thermal conditions and leads to regioisomeric isoxazolines **6a,b** (Scheme I.6) [35]. The presence of Cu (I) changes the overall outcome of this

process and the reaction takes place at room temperature, leading to 2-azetidinone products **3** instead of isoxazolines **6**.



Scheme I. 6: Thermal non-catalyzed alkyne- nitrone cycloaddition reaction

The first catalytic version of the Kinugasa reaction was developed by Miura and coworkers [36] in 1993, where the coupling between a terminal alkyne and *C, N*-diarylnitrones was accomplished with a catalytic amount of copper iodide (CuI) and potassium carbonate (Scheme I.7). The yields of the resulting products **3a**, **4a**, **7-9** were depending on the type of phosphanes, or nitrogen-containing compounds, used as ligands. In the absence of ligands, or with ligands containing phosphanes, the *trans*- β -lactam **4a** was isolated in a very poor yield as the only product. When the reaction was performed in the presence of pyridine or 1,10-phenanthroline as ligands, the yields of the β -lactams were improved (55–71%), and mixtures of *cis***3a** and *trans***4a** isomers were obtained in a 2:1 ratio for pyridine, and in a 1:1.2 ratio for 1,10-phenanthroline respectively.



Scheme I. 7: Catalytic intermolecular Kinugasa reaction developed by Miura

In another report, two years later, Miura and coworkers [37] described the first examples of the asymmetric intermolecular Kinugasa reaction with chiral bis-oxazoline-type ligands (Figure I.5). When compound **10a** was used as ligand, the reaction of alkyne **1a** with nitron **2a** provided β -lactams **3a** and **4a** in 45% yield (dr 35:65) and $ee = 40\%$ for each isomer. The ee improved to 68% when the amount of CuI was increased to 0.1 equivalent. Furthermore, the reaction with the ligands **10b** and **11** generated similar products with ee 's of 67% and 45%, respectively, while the slow addition of phenylacetylene **1a** to a mixture of nitron **2a**, CuI (0.1 mmol), and **10a** (0.2 mmol) afforded a 57% ee . Under the same reaction conditions with ligands **10b** or **11**, copper (I) phenylacetylide precipitated preventing further reaction.

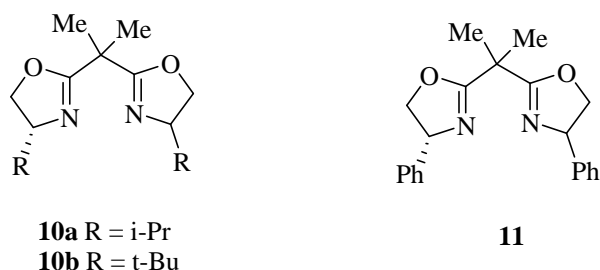
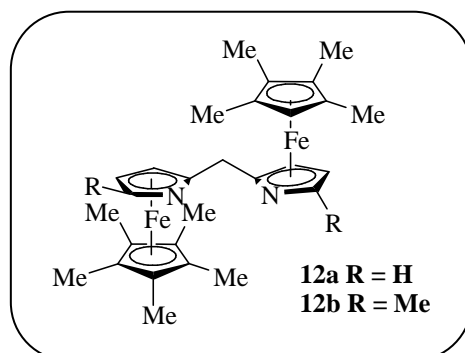
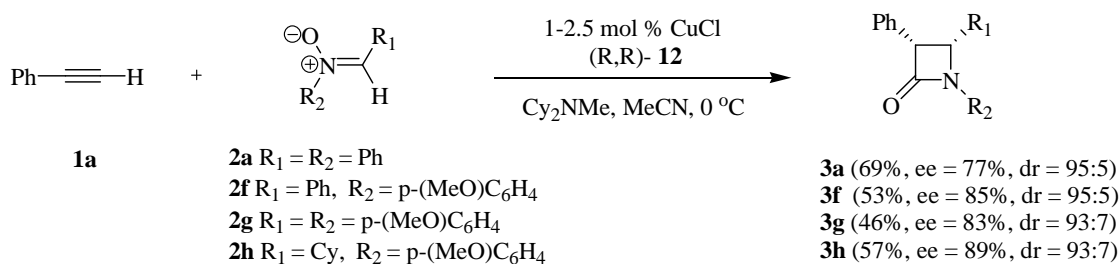


Fig. I. 5: Bis-oxazoline type ligands used for asymmetric intermolecular Kinugasa reaction

In 2002, Lo and Fu examined the Kinugasa reaction under Miura's conditions, using a new C_2 -symmetric planar-chiral bis(azaferrrocene) ligand **12** and the sterically hindered base N,N -dicyclohexylmethylamine [38] (Scheme I.8). Thus, the reaction between phenylacetylene **1a** and C, N -diphenyl substituted nitrones **2** in the presence of ligand **12a** with catalytic amounts of copper (I) chloride revealed a moderate stereoselection. On the contrary, the use of a methyl-substituted ligand **12b** afforded the β -lactams **3** with excellent cis diastereoselectivity (95:5) and good ee 's (from 77 to 89%).

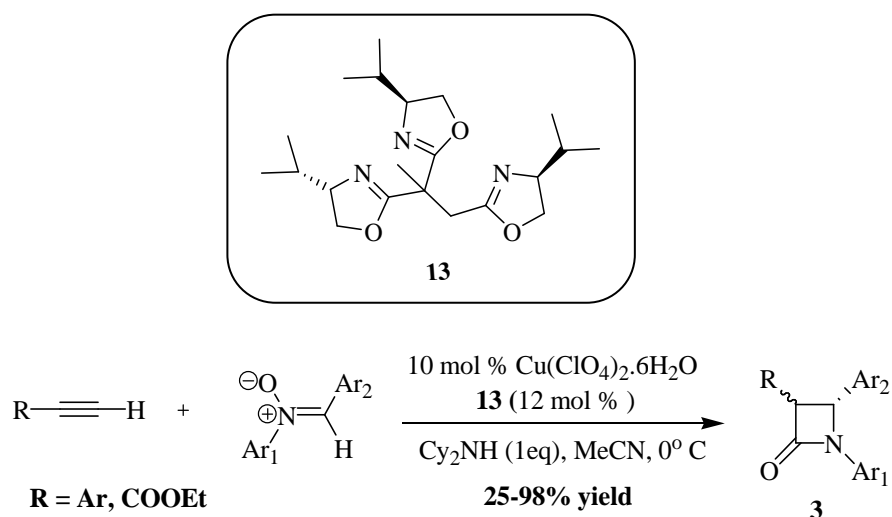




Scheme I. 8: Catalytic asymmetric synthesis of β -lactams by using chiral ligands

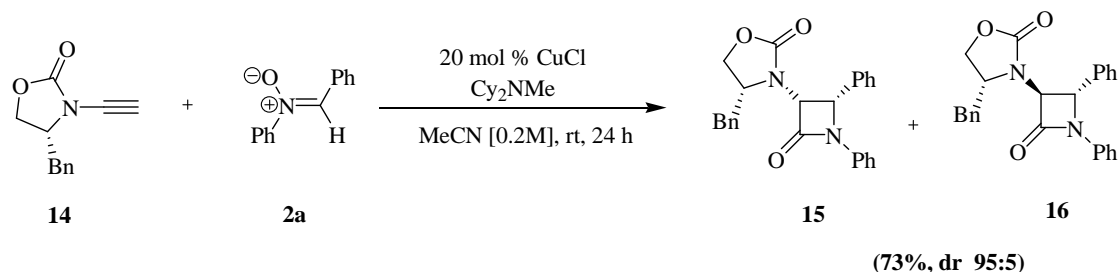
It should be noted that, until now, the Kinugasa reaction was performed strictly under nitrogen atmosphere in order to avoid the Glaser oxidative coupling reaction, which is a coupling between two terminal alkynes in the presence of a base and Cu(I), that occurs via a radical mechanism [39].

In 2003, Tang and coworkers [38] reported that the Kinugasa reaction in the presence of a catalytic amount of pseudo C_3 -symmetric trisoxazoline ligand (TOX ligand) **13**, $\text{Cu}(\text{ClO}_4)_2 \cdot 6\text{H}_2\text{O}$, and Cy_2NH , as a base, in acetonitrile at 0°C , obtained the desired the *cis*- β -lactams **3** in moderate to good yields (25-98%) and with *ee*'s up to 91:9 (Scheme I.9).



Scheme I. 9: Enantioselective Kinugasa reaction catalyzed by Cu(II)/TOX **13** chiral complex

In 2008, Hsung's [41] described a highly stereoselective synthesis of chiral α -amino- β -lactams through an ynamide-Kinugasa reaction. The reaction was carried out in the presence of CuCl in MeCN [0.2 M] at room temperature and produced *cis* β -lactam **15** as the major isomer and *trans* β -lactam **16** as minor isomer (Scheme I.10).



Scheme I. 10: Highly stereoselective ynamide Kinugasa reaction

During the same year, the research group of M. Chmielewski was working on the synthesis of a highly bioactive β -lactam family of products, the "carbapenems" that has higher resistance to β -lactamases than other β -lactams [42]. On the other hand, it has to be noticed that carbapenem is a saturated carbapenem β -lactam that exists primarily as biosynthetic intermediate on the way to the carbapenem antibiotics (Figure I.6).

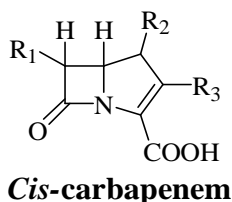
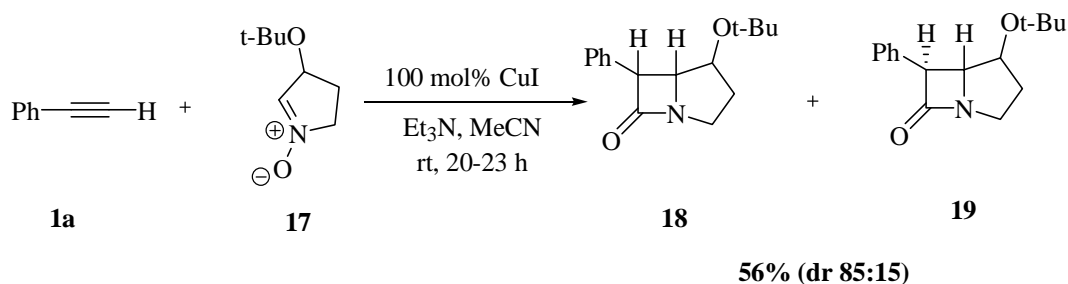


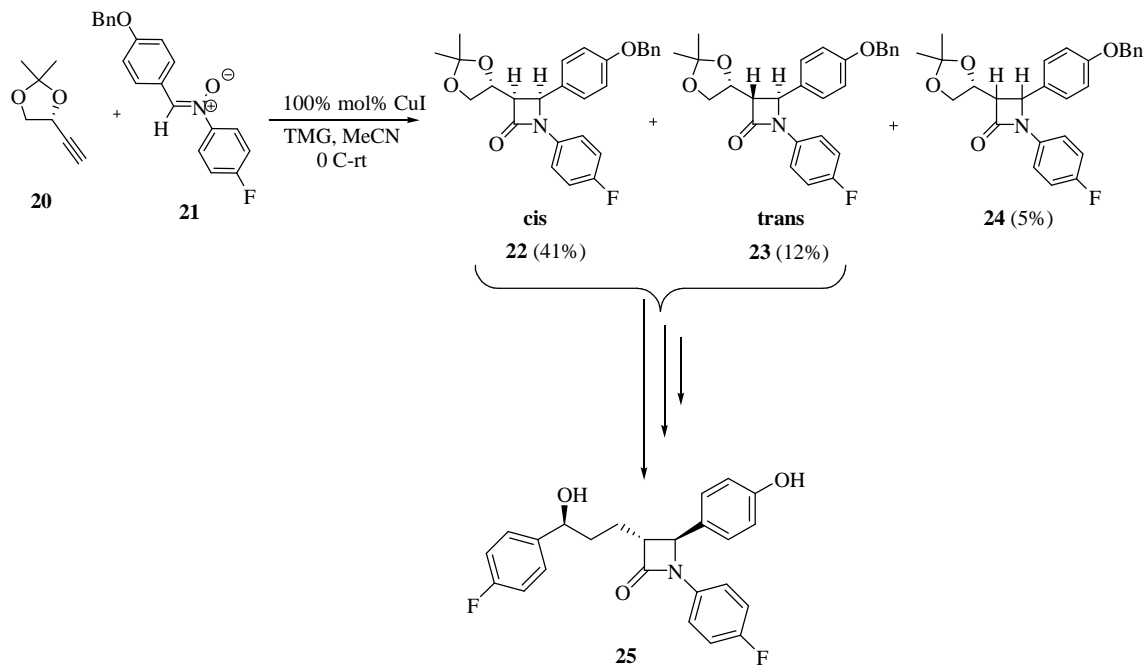
Fig. I. 6: Structure of *cis*-carbapenem

Chmielewski reported a stereoselective synthesis of carbapenems via Kinugasa reaction between a terminal alkyne and a nonracemic cyclic nitronium salt [42]. The reaction of phenylacetylene **1a** with nitronium salt **17** gave two bicyclic products **18** and **19** in a 85:15 ratio and 56% yield (Scheme II.11). The use of other acetylenes provided products with high diastereoselectivity, but a rather poor yield (32-36%).



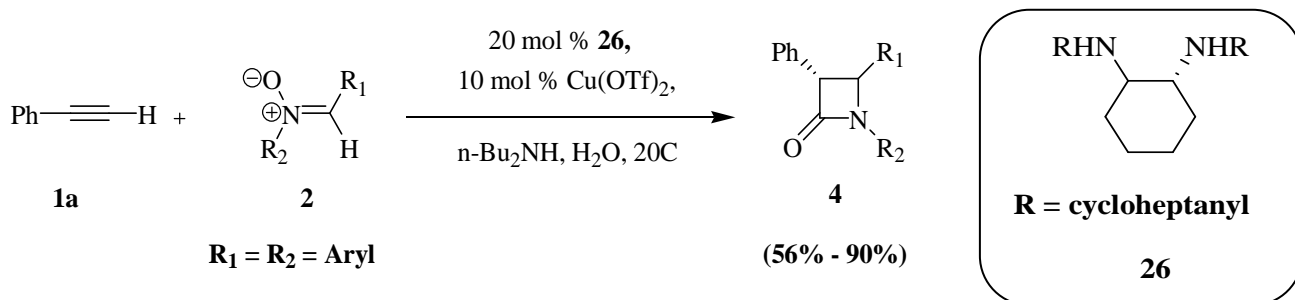
Scheme I. 11: Diastereoselective synthesis of Carbapenems via a Kinugasa reaction

In 2011, M. Chmielewski and coworkers developed also a novel approach for the synthesis of the cholesterol absorption inhibitor "Ezetimibe" **25** [41]. The key step was the Kinugasa cycloaddition/rearrangement cascade between terminal acetylene **20** and nitronium **21** with *N,N,N',N'*-tetramethylguanidine (TMG) as the base (Scheme II.12). The *cis*-azetidinone **22** (ezetimibe is *trans*-azetidinone with configuration (3*R*, 4*S*)) was obtained along with two other isomers: the *trans*-azetidinone **23** and a mixture of diastereoisomers **24**. It should be noted that the *cis*-azetidinone **22** and the *trans*-azetidinone **23** have the same configuration at the C4 carbon of the azetidin-2-one ring. Thus, **22** and **23** could be used for the next steps without separation.



Scheme I. 12: Synthesis of the cholesterol absorption inhibitor Ezetimibe **25**

Recently, Feng and coworkers [44] described a new chiral diamine–Cu(OTf)₂ complex for the catalytic asymmetric Kinugasa reaction. Furthermore, the reaction was performed in water without the need of any organic co-solvent. In contrast to most enantioselective Kinugasa reactions, this mild and operationally simple method provided a one-step route to optically active *trans*-β-lactams **4** in good yields, enantioselectivities and diastereoselectivities. The *trans* isomer **4** is the result of epimerization at the C3 position under the basic reaction conditions used (Scheme I.13).



Scheme I. 13: Asymmetric Kinugasa reaction on water

α -Methylene- and α -Alkylidene β -lactams:

The α -methylene and α -alkylidene β -lactams (Figure I.7) have not been extensively studied, even if some are known as bioactive natural products.

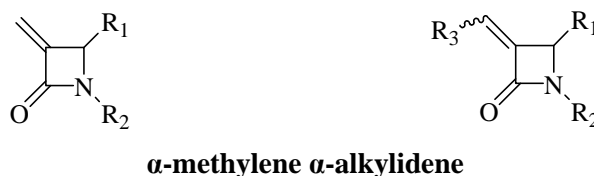


Fig. I. 7: General structures of α -methylene and α -alkylidene β -lactams

These attractive structures are important motifs that exist in biologically active β -lactam products such as the β -lactamase inhibitors Asparenomicin A [45] and 6-(acetylmethylene)-penicinallic acid (Figure I.8) [46].

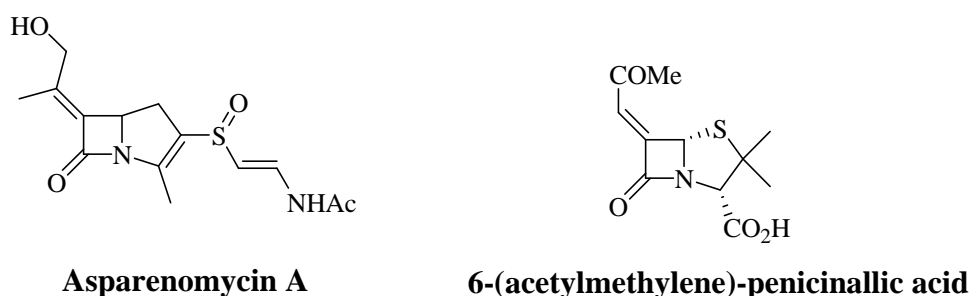


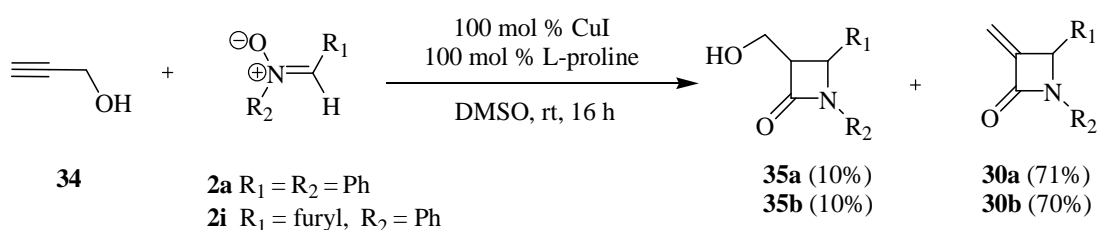
Fig. I. 8: Representative examples of bioactive α -alkylidene β -lactames

In addition to their biological activity, α -methylene and α -alkylidene β -lactams are valuable synthetic intermediates in organic chemistry that can serve for the preparation of other useful targets.

The bacterial resistance to the β -lactam antibiotics is a serious medical problem; one of the resistance mechanism is due to the production of β -lactamases enzymes that hydrolyze the azetidinone. For this reason, these antibiotics are used, in the case of resistant germs, in combination with β -lactamases inhibitors. They act as decoy molecules for the deleterious enzymes and so they protect the antibiotic from bacterial

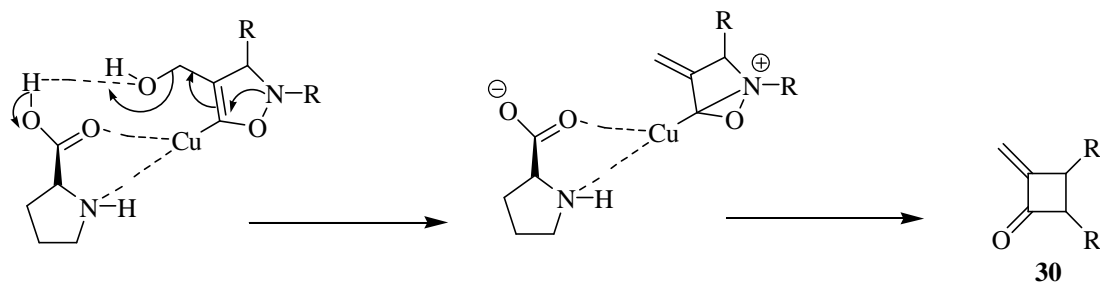
It should be noted that the lithium enolate esters were obtained by the treatment of β -amino esters with LDA under usual conditions for the generation of enolates from simple esters.

In 2004, Basak developed another route for the synthesis of α -methylene β -lactam **30** using the Kinugasa reaction. He performed the reaction between nitrones **2** and propargyl alcohol **34** in the presence of CuI and L-proline in DMF at room temperature (Scheme I.16) [49].



Scheme I. 16: Kinugasa reaction in the presence of L-proline

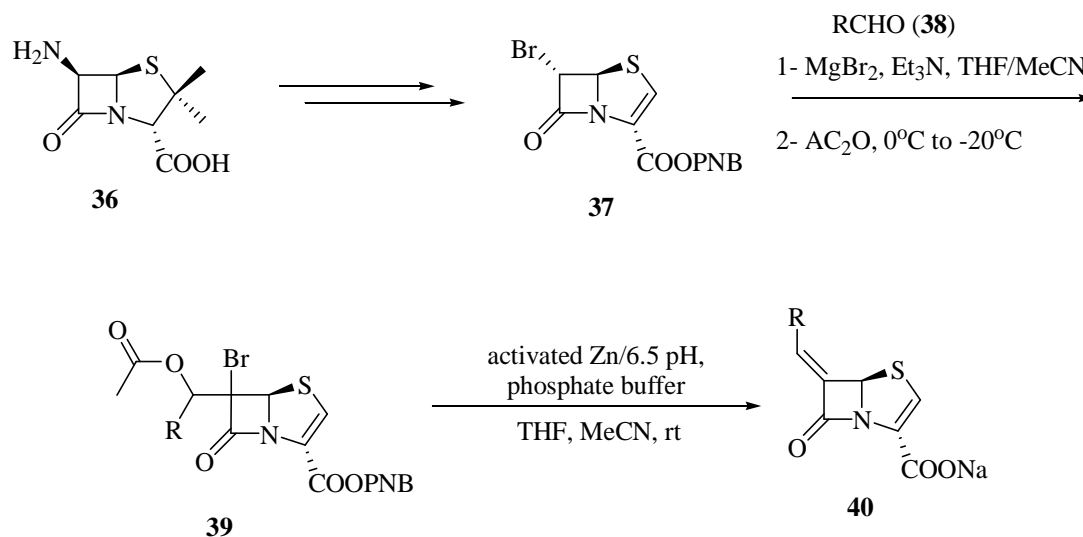
The reaction afforded two products, the *cis*- β -lactams **35** along with the 3-exomethylene β -lactams **30**. When DMSO was used as solvent, the α -methylene adduct **30** became the major product. The presence of the amphoteric L-proline molecule is important for this one-step reaction sequence. The authors suggested that the synthesis of the α -methylene product **30** proceeded via L-proline-mediated elimination of water molecule at the stage of isoxazoline, before the formation of β -lactam, rather than simple water elimination from azetidinone **35** (Scheme I.17).



Scheme I. 17: The way of formation of **30** proposed by Basak

Two years later, Venkatesan and coworkers designed a new series of 6-methylidene penems containing [6,5] fused bicycles as a novel class of β -lactamase inhibitors [50].

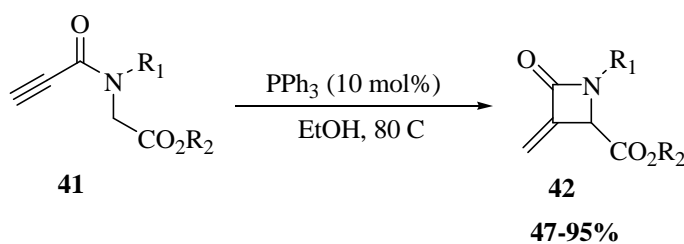
The preparation of these methyldene penicillins was achieved by a direct aldol condensation between an aldehyde **38** and 6-bromo-7-oxo-4-thia-1-azabicyclo [3,2,0] hept-2-ene-2-carboxylic acid-4-nitrobenzyl ester **37** in the presence of triethylamine and anhydrous MgBr_2 , followed by reductive elimination to introduce the double bond at the 6-position of the penem nucleus (Scheme I.18).



Scheme I. 18: General method for the preparation of 6-methyldene penems **40**

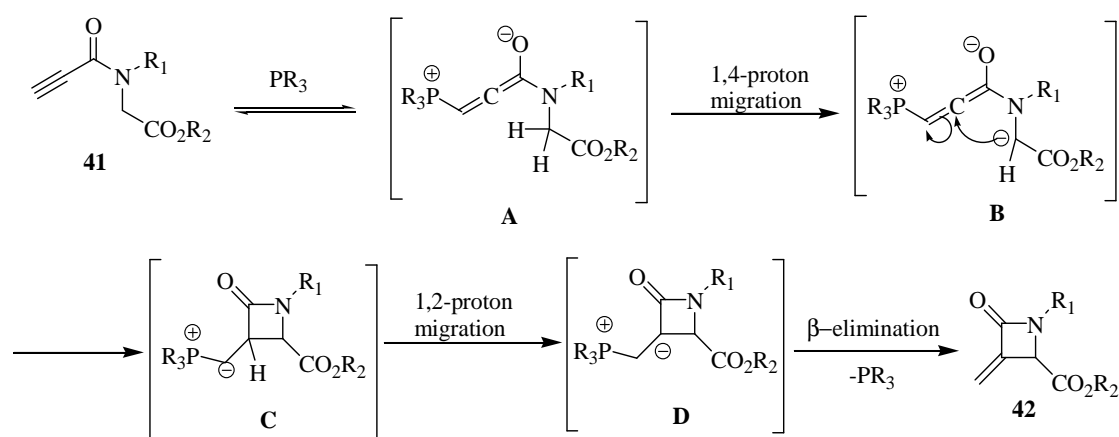
The starting material **37** was prepared from the commercially available 6-aminopenicilanic acid (6-APA) **36** by a modified multistep procedure [51, 52].

In 2014, Zhu L. and coworkers developed a new and facile synthesis of α -methylene β -lactams. Umpolung cyclization of 2-propiolamidoacetates **41** (or α -propiolamido ketones) under the catalysis of triphenylphosphine, afforded the desired 4-substituted 3-methyleneazetidion-2-ones **42** in high yields [53] (scheme I.19).



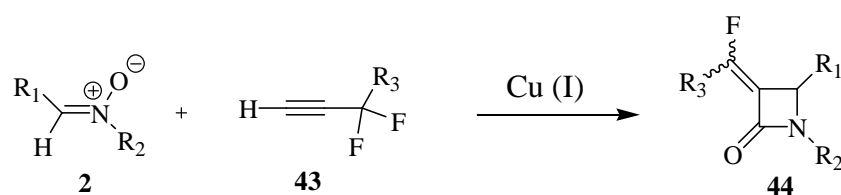
Scheme I. 19: Synthesis of α -methylene β -lactams via PPh_3 -catalyzed umpolung cyclization of propiolamides

The scheme below illustrates the mechanism for this catalyzed umpolung cyclization proposed by the authors. The conjugated addition of a tertiary phosphine to propiolamides **41** generates the zwitterionic intermediate **A** that undergo 1,4-proton migration to give α -ester anion **B**. Then **B** undergoes intramolecular conjugate addition and affords β -lactam intermediate **C**. After that, the 1,2-proton migration followed by β -elimination furnishes α -methylene β -lactam **42** as the final product and regenerates the tertiary phosphine, which enters into the next catalytic cycle.



Scheme I. 20: Proposed mechanism for the synthesis of α -methylene β -lactam via PPh_3 catalyst

The α -alkylidene β -lactams were also synthesized very recently in our group using the Kinugasa reaction. When the reaction was applied to the *gem*-difluoro propargylic systems **43**, it gave the unexpected α -alkylidene- β -lactams with a fluorine atom in vinylic position **44** [54] (Scheme I.21).



Scheme I. 21: Synthesis of α -alkylidene- β -lactam using Kinugasa reaction with alkynes bearing a *gem*-difluoro group at propargylic position

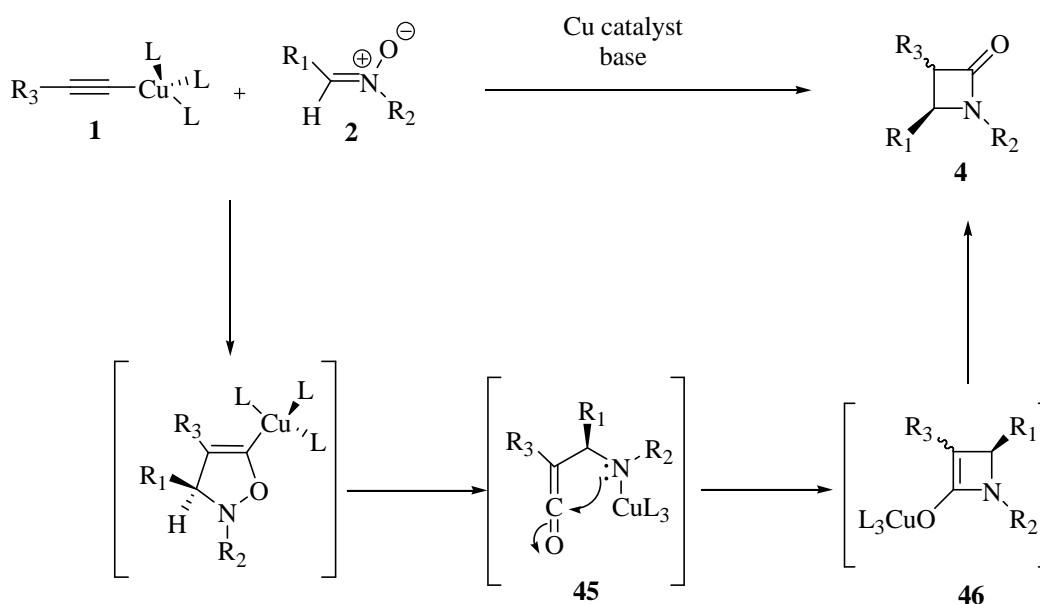
These results obtained in our group opened the gate for us towards a new and direct synthesis of α -methylene and α -alkylidene- β -lactams using the Kinugasa reaction, as indicated there after.

I.B. OBJECTIVE AND STRATEGY

Objective and Strategy:

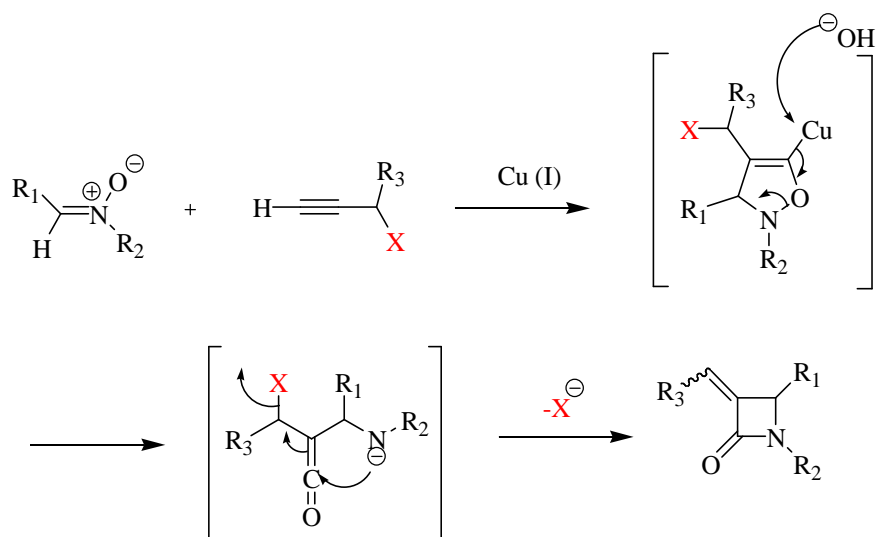
As mentioned earlier, the Kinugasa reaction has already proved to be of much use in the synthesis of β -lactams.

Two mechanisms have been proposed for the Kinugasa reaction. The first mechanism, via oxaziridinum intermediates, was previously shown in scheme I.5, while a second, via ketenes, was proposed by Tang and coworkers [55], almost 30 years later, as shown in Scheme I.22.



Scheme I. 22: Mechanism of the Kinugasa reaction proposed by Tang and coworkers

Our strategy towards the title target molecules is based on the mechanism proposed by Tang and coworkers [55], and our working hypothesis is indicated in Scheme I.23, where the Kinugasa reaction has to be performed with an alkyne bearing a nucleofuge in propargylic position. Thus, at the ketene open intermediate stage, the classical ring closure to the β -lactam could be in competition with the simultaneous loss of this X^- (atom or leaving group) to afford directly the corresponding α -methylene and α -alkylidene β -lactams.



Scheme I. 23: Our working hypothesis towards a new synthesis of α -methylene- and α -alkylidene- β -lactams

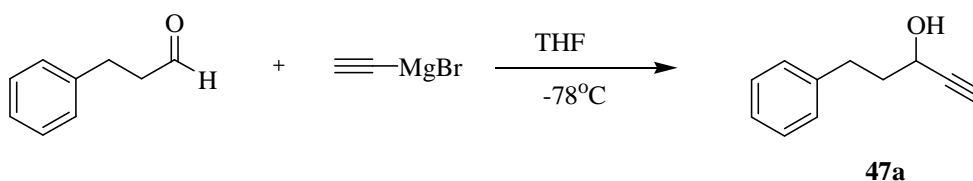
As we mentioned earlier, this working hypothesis was supported by the last results of Kinugasa reaction obtained recently in our groups [54].

I.C. RESULTS AND DISCUSSION

Results and discussion:

At the beginning, the first priority of our work was to choose the most suitable leaving group at the propargylic position in order to obtain the best yield of the desired α -alkylidene β -lactam products (Scheme I.25). Thus different classical leaving groups were chosen for this purpose, as indicated in Table 1.

Acetate, benzoate, and carbonate groups were selected to activate the alcohol at the propargylic position. First of all, the propargylic alcohols were prepared from the Grignard reaction between the corresponding aldehyde and ethynyl magnesium bromide. Alcohol **47a** (Scheme I.24), for instance, was obtained in 78% yield from the reaction between 3-phenyl propionaldehyde and ethynyl magnesium bromide.

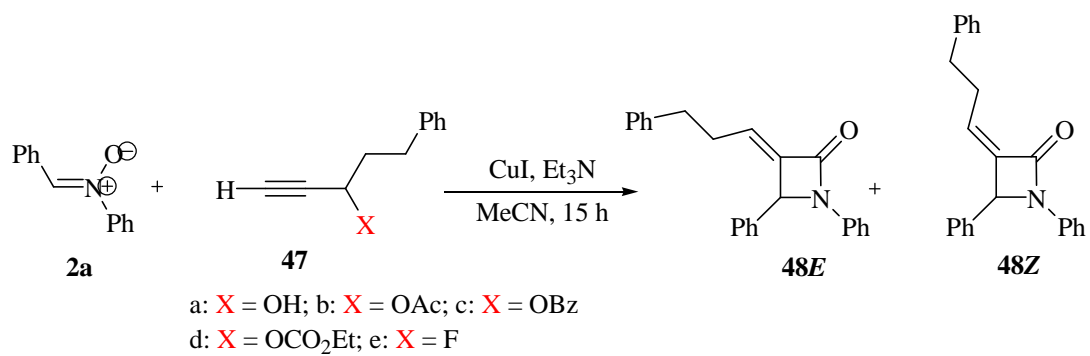


Scheme I. 24: Grignard reaction for the preparation of **47a**

In all three cases (acetate, benzoate, and carbonate), the reaction was performed in CH_2Cl_2 at room temperature, using Et_3N as a base. Acetyl chloride was used to prepare the acetate, and gave **47b** in 81% yield. The reaction with benzoyl chloride gave the desired benzoate **47c** in 83% yield, while the protection using ethyl chloroformate, gave the desired carbonate **47d** in 88% yield. These propargylic esters were used then for the Kinugasa reaction with different nitrones.

We selected the conditions that have been already optimized in our group, with reactions performed at room temperature in a 3:1 mixture of acetonitrile and water for 15h [52].

The reaction was performed first with the *C,N*-diphenyl nitron **2a** and alkyne **47**, selected as models (Scheme I.25, Table I.1). The base used was Et_3N , in the presence of copper iodide as copper (I) salt and the mixture was stirred for 15h.



Scheme I. 25: Kinugasa reaction between alkynes **47** and nitrene **2a**

Entry	X	Temperature	Yield %	Z/E
1	OH	RT	-	-
2	OH	50°C	-	-
3		RT	22	31/69
4		RT	24	29/71
5		RT	40	38/62
6		50°C	74	28/72
7		Reflux (3hr)	65	42/48
8	F	50°C	58	36/64

Table I. 1: Alkyldene β-lactams **48** produced via scheme 25

No reaction was observed with the propargylic alcohol **47a**, neither at room temperature nor at 50°C (Table I.1, entries 1 and 2), while the Kinugasa reaction with the acetate **47b** (Table I.1, entry 3) gave a 31:69 mixture of the desired α -alkylidene- β -lactams **48E** and **48Z**, but in low yield (22%). A similar result was obtained (24% yield), starting from the corresponding benzoate **47c** (Table I.1, entry 4).

A significant improvement was observed by using carbonate **47d** as starting material, in which the desired target molecules **48E** and **48Z** (71:29) were obtained in 40% overall yield (Table I.1, entry 5). Furthermore, a 74% overall yield was obtained when the reaction was performed with the same carbonate **47d**, but at 50°C with a 28:72 mixture of the **Z** and **E** isomers (Table I.1, entry 6). However, no further improvement was obtained when the reaction was done at reflux for 3h (Table I.1, entry 7).

Finally, the use of fluoride as nucleofuge proved to be also a possible good choice since the mono-fluoro propargylic derivative **47e** gave the target molecules in 58% overall yield (Table I.1, entry 8). It should be noticed that this mono-fluoro propargylic group was easily prepared by the fluorination reaction of alcohol **47a** using DAST.

It has been checked that the reaction was under kinetic control. No interconversion between **48E** and **48Z** was observed by heating each of them, alone, at 50°C. The same result was obtained by heating either **48E** or **48Z** in the presence of the other reagents (copper, base...) used under the Kinugasa reaction conditions.

After purification by chromatography on silica gel, compounds **48E** and **48Z** were isolated in pure form and their structures were clearly established from NMR data.

For compound **48E**, the ^1H NMR spectrum in Figure I.10 shows a triplet of doublet at 6.25 ppm with coupling constants $^3J = 7.8$ Hz and $^4J = 1.6$ Hz, which can be assigned to the vinylic proton **H_b**. Then a small doublet at 5.14 ppm with coupling constant $^4J = 1.6$ Hz corresponds to the β -lactam proton **H_c**.

The ^{13}C NMR spectrum, shown in Figure I.11, is also in full agreement with the structure.

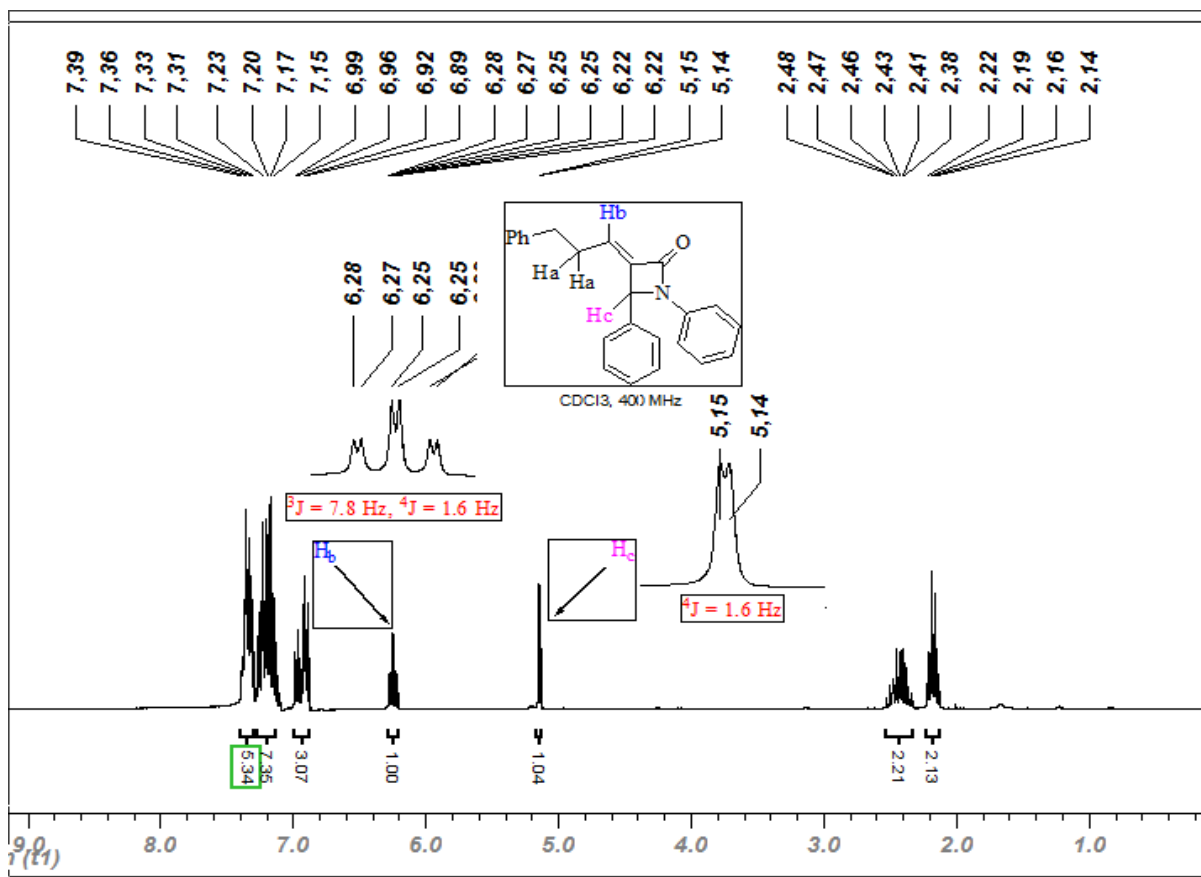


Fig. I. 10: ^1H NMR spectrum of compound **48E**

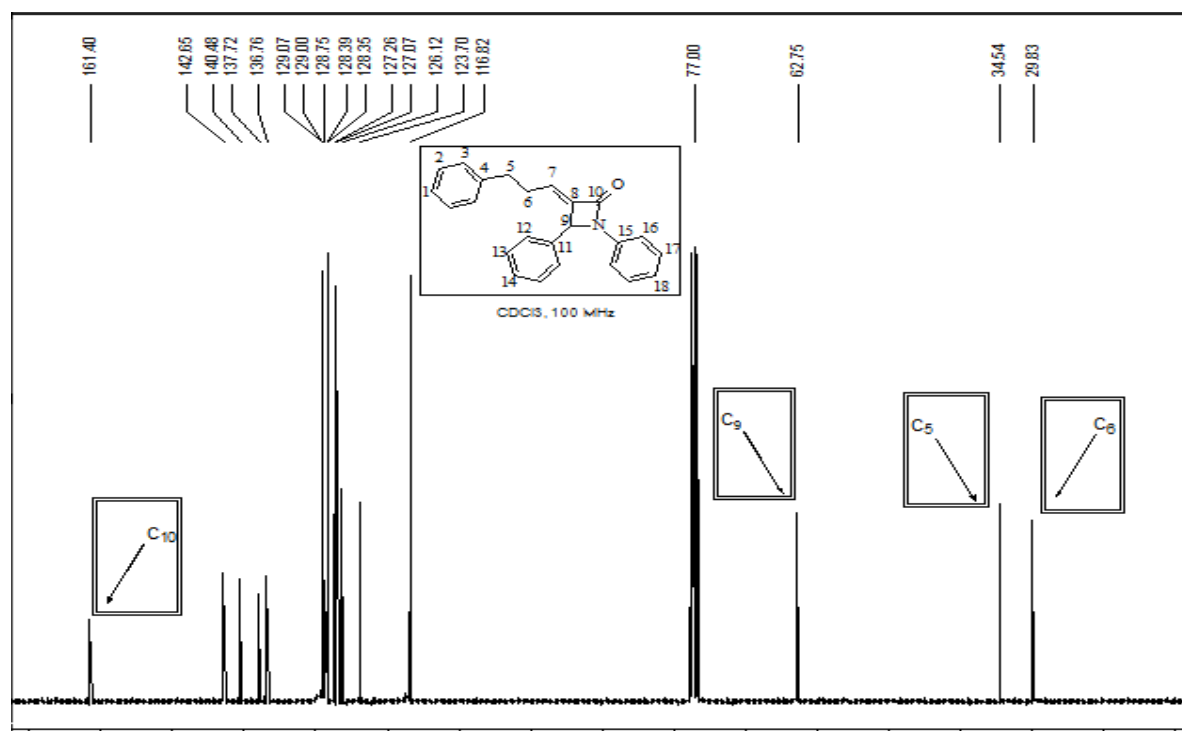


Fig. I. 11: ^{13}C NMR spectrum of compound **48E**

In addition to that, ^1H - ^1H NOESY spectrum (Figure I.12) illustrates clearly the *trans* configuration of the *exo*-double bond.

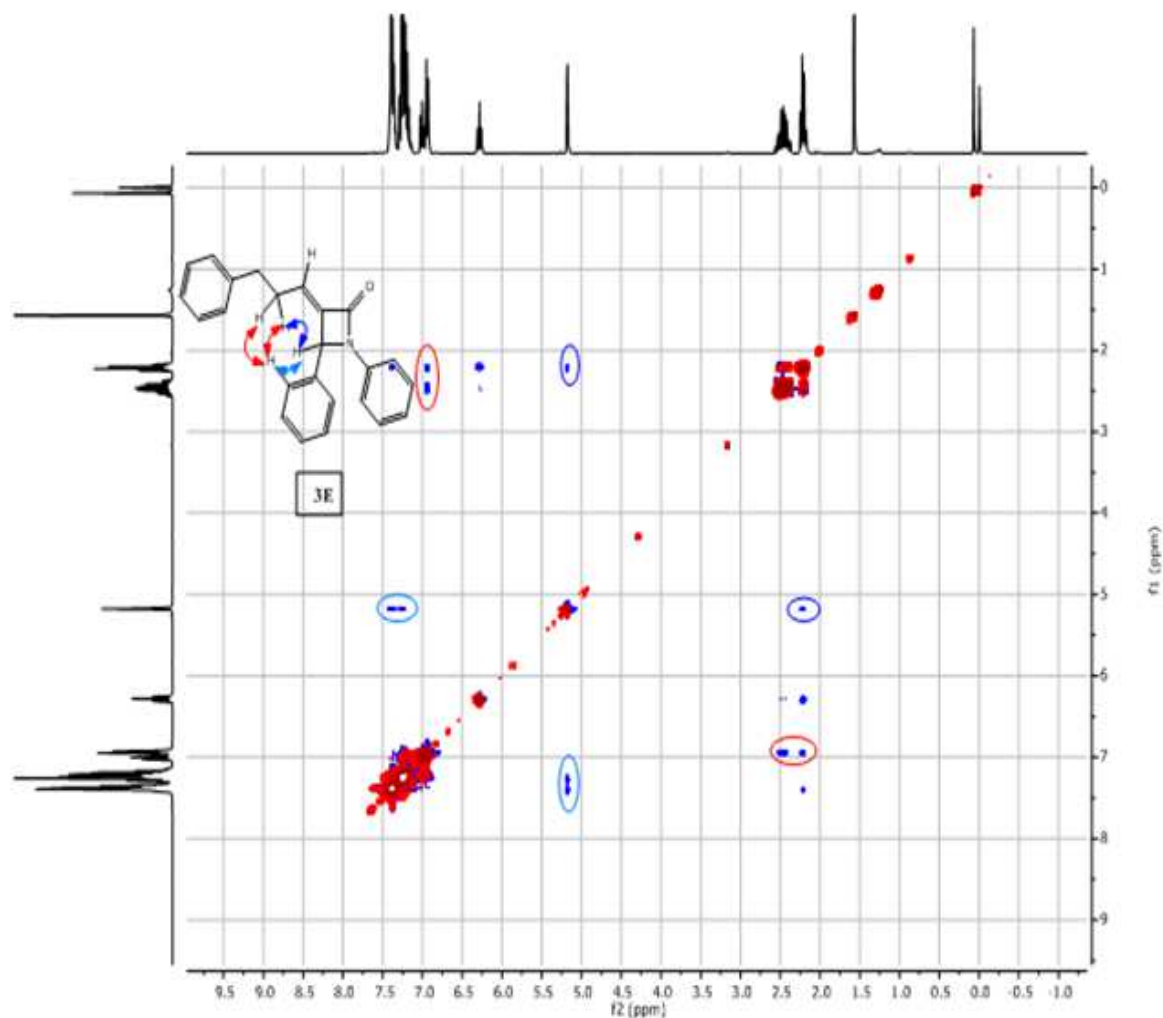


Fig. I. 12: ^1H - ^1H NOESY spectrum of compound **48E**

As shown in Figure I.12, there is a clear correlation between the allylic methylene protons **Ha** and the β -lactam proton **Hc** and also with the *ortho* aromatic proton. This indicates that the methylene protons are close to the β -lactam proton **Hc** in compound **48E**.

On the other hand, ^1H NMR spectrum of the compound **48Z**(Figure I.13) shows a small difference -in comparison with **48E** in the chemical shifts of vinylic proton, β -lactam proton **Hc**, and the methylene protons that appear as one multiplet system with their neighbour benzylic protons (2.88-2.69 ppm). ^{13}C NMR spectrum of **48Z**is also represented in Figure I.14.

proton. Furthermore, no correlation between the methylene protons with the β -lactam proton was observed. These data clearly demonstrates that the vinylic proton in compound **48Z** is close to both the β -lactam proton and the phenyl proton.

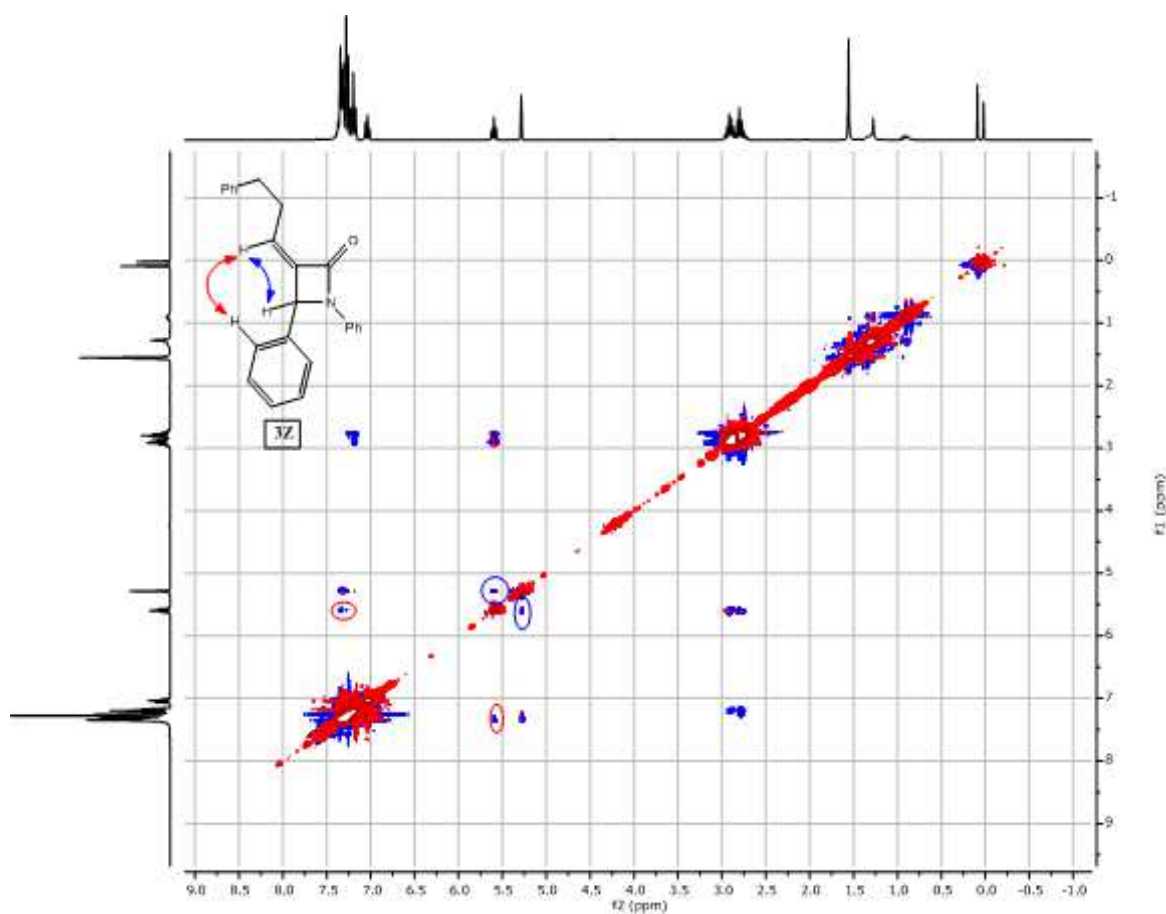
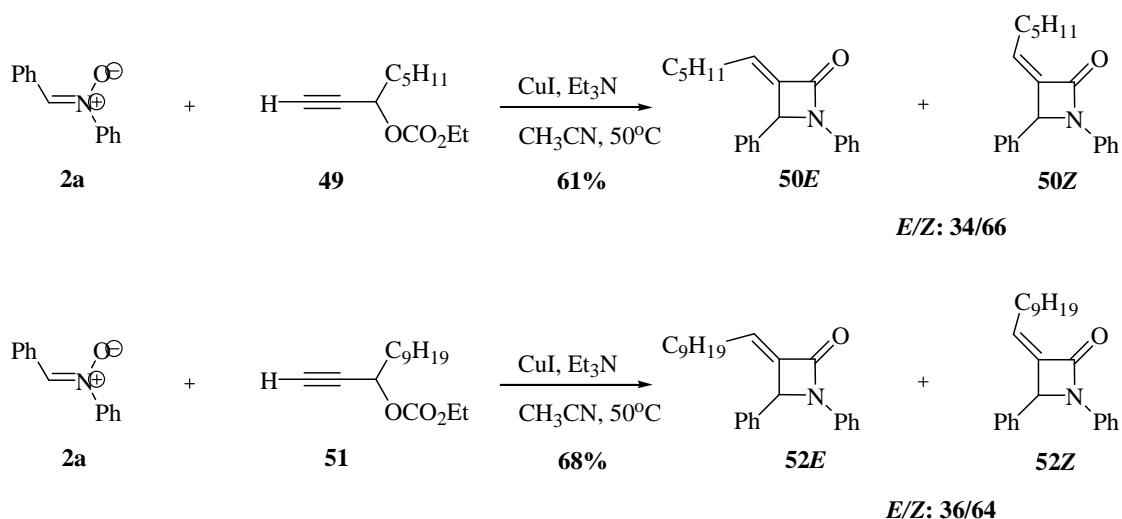


Fig. I. 15: ^1H - ^1H NOESY spectrum of compound **48Z**

Thus carbonate group showed to be the best leaving group since it gave the highest overall yield for the desired α -alkylidene- β -lactam products. Therefore this group was selected as nucleofuge for the other alkynes in our work.

Under previously optimized reaction conditions, the Kinugasa reaction was also performed between *C,N*-diphenyl nitron **2a** and other alkynes **49** and **51** bearing an linear alkyl side chain, affording the desired β -lactam products **50** and **52** in good yields and with different ratios of *E* and *Z* isomers (Scheme I.26).



Scheme I. 26: Kinugasa reaction between nitron **2a** and alkynes **49** and **51**

The α -alkylidene- β -lactam products **50** and **52**, obtained in 61% and 68% overall yields respectively, were isolated by chromatography and their structures were established as previously by ^1H and ^{13}C NMR. Furthermore, ^1H - ^1H NOESY experiments performed on each isomer shows a clear correlation between the methylene protons with the β -lactam proton for the *E* isomers, and a clear correlation between the vinylic proton with both the β -lactam proton and the *ortho* aromatic proton for the *Z* isomers.

In addition to that, the structure of **52Z** was also confirmed by X-Ray crystallography analysis (Figure I.16).

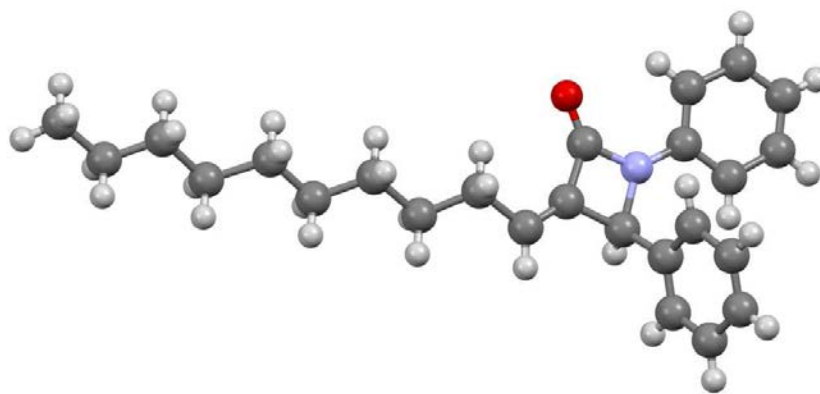
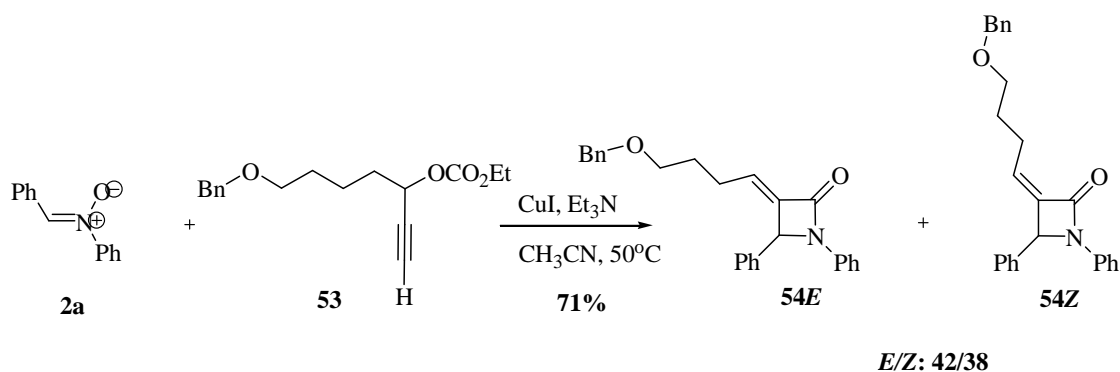


Fig. I. 16: Structure of **52Z** by X-Ray diffraction

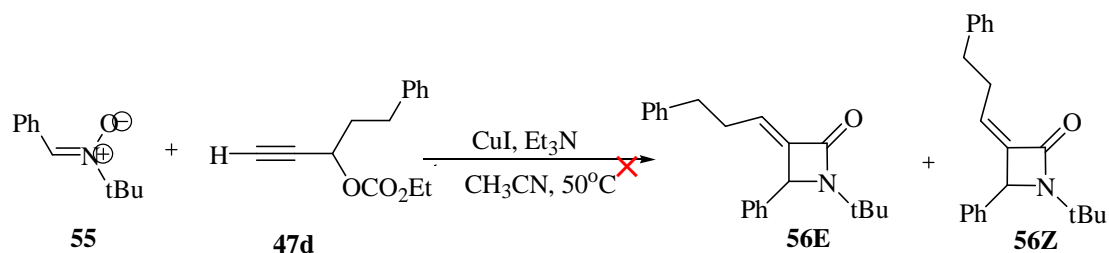
Furthermore, *C,N*-diphenyl nitron **2a** reacted also smoothly with the alkyne **53** that bears a remote protected alcohol function, to afford in 71% overall yield a 42:58 mixture of **54E** and **54Z** (Scheme I.27).



Scheme I. 27: Kinugasa reaction between nitron **2a** and alkyne **53**

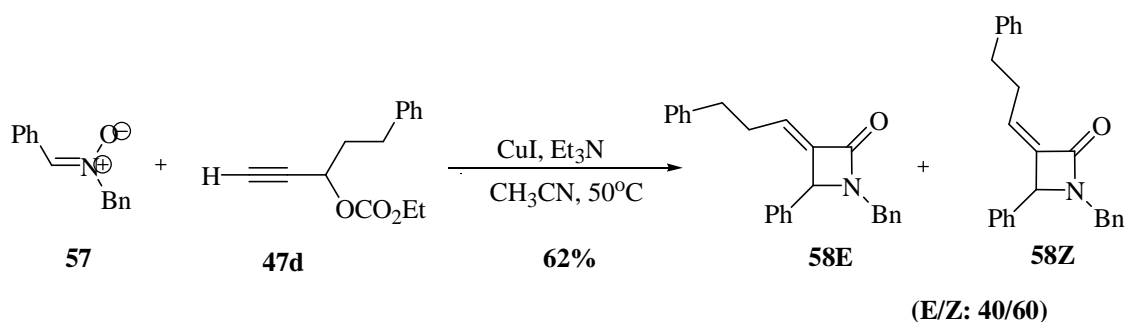
Similarly, the structures of **54E** and **54Z** were established by NMR data (^1H , ^{13}C , and ^1H - ^1H NOESY), as for **48E** and **48Z**.

Other nitrones were also used in this reaction, for example *C*-phenyl-*N*-*t*Bu nitron **55** which reacted very slowly with alkyne **47d** affording at best very little of, non-purified, alkylidene- β -lactam products **56** and mostly decomposition products (Scheme I.28).



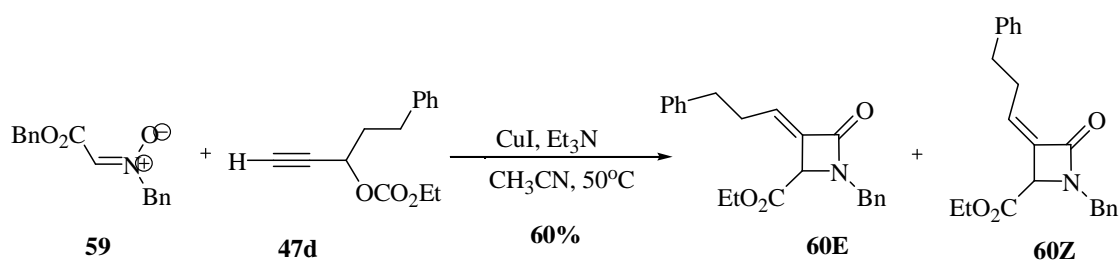
Scheme I. 28: Kinugasa reaction between alkyne **47d** and nitron **55**

On the contrary, the *C*-Phenyl-*N*-Benzyl nitron **57** reacted with **47d** together to give the target molecules **58** in 62% overall yield and as a 40:60 mixture of *E* and *Z* isomers (Scheme I.29).



Scheme I. 29: Kinugasa reaction between alkyne **47d** and nitron **57**

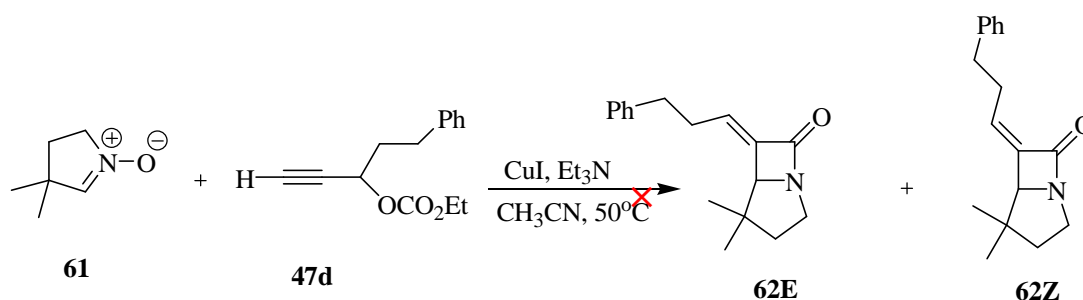
The functionalized nitron **59** reacted smoothly with alkyne **47d** to give the target derivatives **60** in 60% yield, as a 47:53 mixture of *E* and *Z* isomers (Scheme I.30).



Scheme I. 30: Kinugasa reaction between alkyne **47d** and nitron **59**

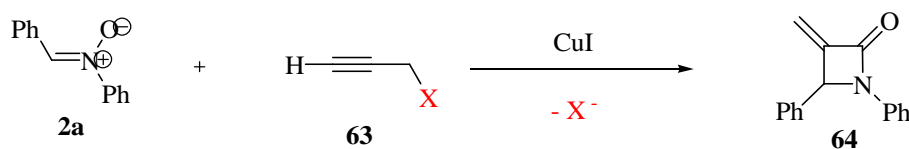
Again, the structures of **58** and **60** were established by NMR data and their stereochemistry demonstrated by 2D experiments (^1H - ^1H NOESY), as for **48E** and **48Z**.

Finally nitron **61**, selected as a model of cyclic nitron, was treated with alkyne **47d**, but unfortunately the reaction didn't work in this case, and the desired **62E** and **62Z** products were not obtained (Scheme I.31).



Scheme I. 31: Kinugasa reaction between alkyne **47d** and cyclic nitron **61**

In addition to that, the Kinugasa reaction was extended to simple model alkynes **63** (Scheme I.32), by using the same reaction conditions.



a: X = OH, **b:** X = OAc, **c:** X = OBz, **d:** X = OCO₂Et
e: X = OTs, **f:** X = Br, **g:** X = Cl

Scheme I. 32: Kinugasa reaction between nitron **2a** and alkynes **63**

Different leaving groups were also chosen for this simple propargylic system and protection of this simple propargylic alcohol was performed using the same reaction conditions as mentioned earlier for the first alkyne model **47**. On the other hand, the propargylic tosylate **63e**, the propargylic bromide **63f**, and the propargylic chloride **63g** are commercially available.

The results obtained in these Kinugasa reactions are shown in Table I. 2.

Entry	X	Yield
a	OH	37%
b	$\begin{array}{c} \text{O} \\ \parallel \\ -\text{O}-\text{C}-\text{CH}_3 \end{array}$	38%
c	$\begin{array}{c} \text{O} \\ \parallel \\ -\text{O}-\text{C}-\text{Ph} \end{array}$	47%
d	$\begin{array}{c} \text{O} \\ \parallel \\ -\text{O}-\text{C}-\text{OEt} \end{array}$	52%
e	-OTs	40%
f	Br	22%
g	Cl	24%

Table I. 2: Results of Kinugasa reaction between nitron **2a** and simple alkyne **63**

The reaction was working already with the propargylic alcohol **63a**, affording the known α -methylene- β -lactam **64** in 37% yield. A similar result was obtained with acetate **63b** (38% yield), while some improvement was observed with benzoate **63c** (47% yield). Here again the carbonate **63d** was found to give the best result with a 52% yield. The corresponding tosylate **63e** gave a 40% yield while the bromo- and chloro- derivatives **63f** and **63g** gave lower yields, respectively 22% and 24%.

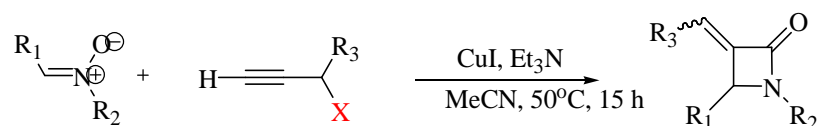
The structure of **64** was established by comparison of its spectral data with literature [47].

The reaction of the simple alkyne **63d** was also studied with three more nitrones **57**, **59** and **61**, and the results are shown in Scheme I.33.

I.D. CONCLUSION

Conclusion:

To conclude, application of the Kinugasa reaction to alkynes bearing a nucleofuge in propargylic position gives a very direct entry (1 step) to new α -methylene and α -alkylidene β -lactams (Scheme I.34).



Scheme I. 34: Direct synthesis of α -methylene and α -alkylidene β -lactams via Kinugasa reaction

Our working hypothesis towards the desired β -lactam products was thus validated.

The process is very simple and uses only cheap and easily available reagents. Thus it expands the scope of the use of the Kinugasa reaction to a family of derivatives which have been less studied previously but becomes now easily available for biological studies

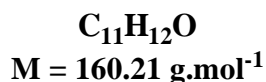
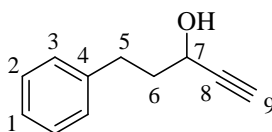
I.E. EXPERIMENTAL PART

Experimental Part:

General procedure of the Grignard reaction for the preparation of propargyl alcohol intermediates

To a solution of aldehyde (1eq) in THF, ethylene magnesium bromide (1.3eq) was added dropwise at 0°C. The reaction mixture was stirred at 0°C for 3 hrs, then the temperature left to increase to room temperature, after 30 mins at room temperature; the reaction was quenched with saturated solution of ammonium chloride, extracted with ether (3 times). The combined organic phase was then washed with water, dried over MgSO₄, and then concentrated under vacuo.

Synthesis of 5-Phenyl-pent-1-yn-3-ol(47a)



The reaction was performed between 3-phenylpropionaldehyde (1g, 1 equiv) and ethylene magnesium bromide (19.4 ml, 1.3 equiv) in THF (15 ml) according to the general procedure of Grignard reaction. After purification on column chromatography 5-phenyl-pent-1-yn-3-ol was obtained as yellow oil in 70% yield.

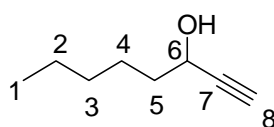
$R_f = 0.38$ (hexane/ethyl acetate 9/1).

$^1\text{H NMR}$ (CDCl₃, 300 MHz), δ ppm: 7.33-7.23 (m, 5H); 4.40 (td, 1H, H₇, $^3J = 6.7$ Hz, $^4J = 2.1$ Hz); 2.84 (t, 2H, H₅, $^3J = 7.9$ Hz); 2.51 (d, 1H, H₉, $^4J = 2.1$ Hz); 2.06 (m, 2H, H₆).

^{13}C NMR (CDCl₃, 75 MHz), δ ppm: 141.06 (1C, C₄); 128.37 (2C); 128.33 (2C); 125.89 (1C, C₁); 84.64 (1C, C₈); 73.18 (1C, C₉); 61.29 (1C, C₇); 38.90 (1C, C₅); 31.14 (1C, C₆).

HRMS (ESI) calculated for C₁₁H₁₂ONa: [M +Na]⁺ : m/z 183.0785, Found: m/z. 183.0786 (0 ppm).

Synthesis of Oct-1-yn-3-ol



C₈H₁₄O
M = 126.20 g.mol⁻¹

The reaction was performed between hexanal (1 g, 1 equiv) and ethylene magnesium bromide (20.6 ml, 1.3eq) in THF (18 ml) according to the general procedure of Grignard reaction. After purification on column chromatography using 9/1 of hexane/ethyl acetate mixture, oct-1-yn-3-ol was obtained as yellow oil in 75% yield.

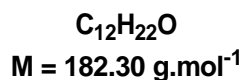
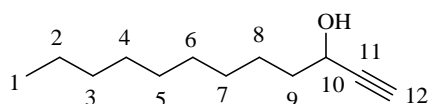
R_f = 0.31 (hexane/ethyl acetate 9/1);

^1H NMR (CDCl₃, 300 MHz), δ ppm: 4.33 (td, 1H, H₆, ³J= 6.6 Hz, ⁴J= 1.8 Hz); 2.44 (d, 1H, H₈, ⁴J= 1.8 Hz); 1.66 (m, 2H), 1.42 (m, 2H); 1.28 (m, 4H); 0.87 (m, 3H).

^{13}C NMR (CDCl₃, 75 MHz), δ ppm: 85.07 (1C, C₇); 72.66 (1C, C₈); 62.16 (1C, C₆); 37.52 (1C, C₅); 31.35 (1C); 24.65 (1C); 22.47 (1C); 13.91 (1C, C₁).

HRMS (ESI) calculated for C₈H₁₄ONa: [M +Na]⁺ : m/z 126.1045. Found: m/z. 126.1044 (0 ppm).

Synthesis of Dodec-1-yn-3-ol



The reaction was performed between decanal (1.5 g, 1 equiv) and ethylene magnesium bromide (21.42 ml, 1.3eq) in THF (16 ml) according to the general procedure of Grignard reaction. After purification on column chromatography using 9/1 of hexane/ethyl acetate mixture, dodec-1-yn-3-ol was obtained as slightly yellow oil in 81% yield.

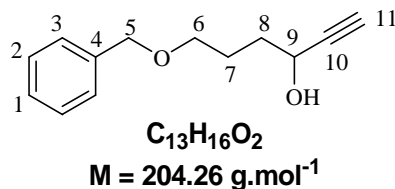
R_f = 0.36 (hexane/ethyl acetate 9/1);

¹H NMR (CDCl₃, 300 MHz), δ ppm: 3.60 (m, 1H, H₁₀); 2.32 (d, 1H, H₁₂, ⁴J= 2.5 Hz); 1.26 (m, 16H), 0.87 (t, 3H, H₁, ³J= 6.9 Hz).

¹³C NMR (CDCl₃, 75 MHz), δ ppm: 75.13 (1C, C₁₁); 73.79 (1C, C₁₂); 62.48 (1C, C₁₀); 31.87 (1C); 29.51 (1C); 29.43 (1C); 29.28 (1C); 29.26 (1C); 29.18 (1C); 22.65 (2C); 14.09 (1C).

HRMS (ESI) calculated for C₁₂H₂₂ONa: [M +Na]⁺: m/z 182.1671 Found: m/z. 182.1673 (1 ppm).

Synthesis of 6-Benzyloxy-hex-1-yn-3-ol



The reaction was performed between 5-Benzyloxy-pentan-2-one (2 g, 1 equiv) (which is already prepared from the oxidation reaction of 4-Benzyloxy-butan-1-ol) and ethylene magnesium bromide (29.17 ml, 1.3eq) in THF (25 ml) according to the general procedure of Grignard reaction. After purification on column chromatography using 9/1 of hexane/ethyl acetate mixture, 6-benzyloxy-hex-1-yn-3-ol was obtained as colorless oil in 72% yield.

R_f = 0.38 (hexane/ethyl acetate 9/1).

¹H NMR (CDCl₃, 400 MHz), δ ppm: 7.32 (m, 5H); 4.52 (s, 2H, H₅); 4.42 (m, 1H, H₉); 3.54 (t, 2H, H₆, ³J = 8.5 Hz); 2.45 (d, 1H, H₁₁, ⁴J = 2.1 Hz); 1.86 (m, 4H, H_{7,8}).

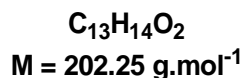
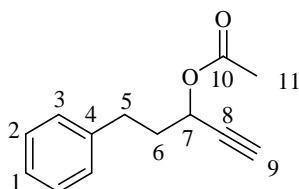
¹³C NMR (CDCl₃, 75 MHz), δ ppm: 137.97 (1C, C₄); 128.41 (2C); 127.71 (2C); 127.68 (1C, C₁); 84.85 (1C, C₁₀); 73.00 (1C, C₁₁); 72.72 (1C, C₅); 69.98 (1C, C₆); 61.90 (1C, C₉); 35.07 (1C); 25.38 (1C).

HRMS (ESI) calculated for C₁₃H₁₆O₂Na: [M +Na] +: m/z 204.1150. Found: m/z 204.1149 (0 ppm).

General reaction for the protection of propargylic alcohol

To a solution of alcohol (1 equiv) in DCM, triethylamine base (3.5 equiv) was added with 2.5 equiv of alkyl acyl chloride (protecting group) and 0.2 mol % of DMAP, the reaction mixture was stirred under nitrogen for 1 hour at room temperature, after this time the reaction was quenched with saturated solution of ammonium chloride, then extracted with ethyl acetate (3 times), the combined organic layer was then washed with water, dried over MgSO_4 and concentrated under vacuo.

Synthesis of acetic acid 1-phenethyl-prop-2-ynyl ester (47b)



The reaction was performed between 5-phenyl-pent-1-yn-3-ol (0.5 g, 1 equiv) in DCM (10 ml), with triethylamine base (1.52 ml, 3.5 equiv), acetylchloride (0.56 ml, 2.5 equiv) and DMAP (0.075g, 0.2 mol %), according to the general procedure mentioned above. After purification on column chromatography using 9/1 of hexane/ethyl acetate mixture, acetate **47b** was obtained as yellow oil in 82% yield.

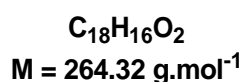
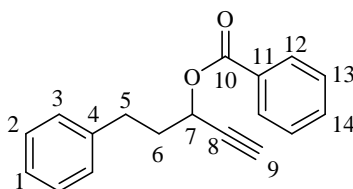
$R_f = 0.61$ (hexane/ethyl acetate 9/1);

$^1\text{H NMR}$ (CDCl_3 , 300 MHz), δ ppm: 7.35 (m, 2H); 7.28 (m, 3H); 5.42 (td, 1H, H_7 , $^3J = 6.6 \text{ Hz}$, $^4J = 2.1 \text{ Hz}$); 2.85 (t, 2H, H_5 , $^3J = 7.8 \text{ Hz}$); 2.56 (d, 1H, H_9 , $^4J = 2.1 \text{ Hz}$); 2.18 (m, 2H, H_6); 2.13 (s, 3H, H_{11}).

$^{13}\text{C NMR}$ (CDCl_3 , 75 MHz), δ ppm: 169.72 (1C, C_{10}); 140.51 (1C, C_4); 128.44 (2C); 128.30 (2C); 126.10 (1C, C_1); 80.90 (1C, C_8); 73.86 (1C, C_9); 63.19 (1C, C_7); 36.01 (1C, C_5); 31.09 (1C, C_6); 20.83 (1C, C_{11}).

HRMS (ESI) calculated for $C_{13}H_{14}O_2Na$: $[M + Na]^+$: m/z 225.0891. Found: m/z . 225.0891 (0 ppm).

Synthesis of benzoic acid 1-phenethyl-prop-2-ynyl ester (47c)



The reaction was performed between 5-phenyl-pent-1-yn-3-ol (0.5 g, 1 equiv) in DCM (10 ml), with triethylamine base (1.52 ml, 3.5 equiv), benzoylchloride (0.9 ml, 2.5 equiv) and DMAP (0.075g, 0.2 mol %), according to the general procedure. After purification on column chromatography using 9/1 of hexane/ethyl acetate mixture, benzoate **47c** was obtained as yellow oil in 85% yield.

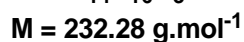
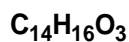
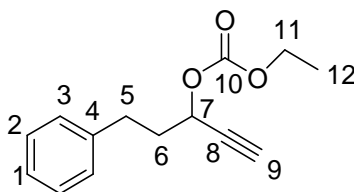
$R_f = 0.64$ (hexane/ethyl acetate 9/1).

1H NMR (CDCl₃, 300 MHz), δ ppm: 8.06 (m, 2H); 7.58 (m, 1H); 7.48 (m, 2H); 7.23 (m, 5H); 5.60 (td, 1H, H_7 , $^3J = 6.5$ Hz, $^4J = 2.1$ Hz); 2.89 (t, 2H, H_5 , $^3J = 7.8$ Hz); 2.54 (d, 1H, H_9 , $^4J = 2.1$ Hz); 2.27 (m, 2H, H_6).

^{13}C NMR (CDCl₃, 75 MHz), δ ppm: 165.40 (1C, C_{10}); 140.60 (1C); 133.23 (1C); 129.78 (2C); 129.71 (1C); 128.53 (2C); 128.41 (2C); 128.39 (2C); 128.17 (1C); 80.95 (1C, C_8); 74.11 (1C, C_9); 63.80 (1C, C_7); 38.23 (1C, C_5); 31.24 (1C, C_6).

HRMS (ESI) calculated for $C_{18}H_{16}O_2Na$: $[M + Na]^+$: m/z 287.1042. Found: m/z . 287.1042 (0ppm).

Synthesis of carbonic acid ethyl ester 1-phenethyl-pro-2-ynyl ester (**47d**)



The reaction was performed between 5-phenyl-pent-1-yn-3-ol (0.5 g, 1 equiv) in DCM (10 ml), with triethylamine base (1.52 ml, 3.5 equiv), ethyl chloroformate (0.3 ml, 2.5 equiv) and DMAP (0.075g, 0.2 mol %), according to the general procedure. After purification on column chromatography using 9/1 of hexane/ethyl acetate mixture, carbonate **47d** was obtained as yellow oil in 81% yield.

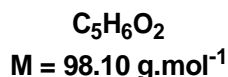
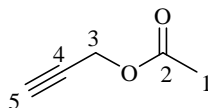
$R_f = 0.60$ (hexane/ethyl acetate 9/1).

$^1\text{H NMR}$ (CDCl_3 , 300 MHz), δ ppm: 7.28 (m, 3H); 7.19 (m, 2H); 5.19 (td, 1H, H_7 , $^3J = 6.6$ Hz, $^4J = 2.1$ Hz); 4.20 (q, 2H, H_{11} , $^3J = 7.3$ Hz); 2.80 (t, 2H, H_5 , $^3J = 7.4$ Hz); 2.56 (d, 1H, H_9 , $^4J = 2.1$ Hz); 2.14 (m, 2H, H_6); 1.31 (t, 3H, H_{12} , $^3J = 7.3$ Hz).

$^{13}\text{C NMR}$ (CDCl_3 , 75 MHz), δ ppm: 154.14 (1C, C_{10}); 140.32 (1C, C_4); 128.44 (2C); 128.30 (2C); 126.13 (1C, C_1); 80.28 (1C, C_8); 74.75 (1C, C_9); 66.82 (1C, C_{11}); 64.29 (1C, C_7); 36.08 (1C, C_5); 30.90 (1C, C_6); 14.13 (1C, C_{12}).

HRMS (ESI) calculated for $\text{C}_{14}\text{H}_{16}\text{O}_3\text{Na}$: $[\text{M} + \text{Na}]^+$: m/z 232.1099. Found: m/z . 232.1099 (0 ppm).

Synthesis of acetic acid prop-2-ynyl ester (63b)



The reaction was performed between commercially available propargyl alcohol (0.6 g, 1 equiv) in DCM (22 ml), with triethylamine base (5.2 ml, 3.5 equiv), acetyl chloride (2 ml, 2.5 equiv) and DMAP (0.26 g, 0.2 mol %), according to the general procedure. After purification on column chromatography using 9/1 of hexane/ethyl acetate mixture, acetate **63b** was obtained as yellow oil in 72% yield.

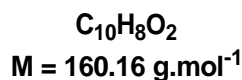
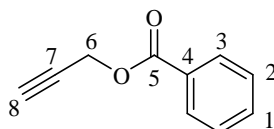
R_f = 0.65 (hexane/ethyl acetate 9/1).

¹H NMR (CDCl₃, 300 MHz), δ ppm: 4.80 (d, 2H, H₃, ⁴J = 2.4 Hz); 2.49 (t, 1H, H₅, ⁴J = 2.4 Hz); 2.39 (s, 3H, H₁).

¹³C NMR (CDCl₃, 75 MHz), δ ppm: 166.11 (1C, C₂); 77.42 (1C, C₄); 75.05 (1C, C₅); 51.81 (1C, C₃); 26.18 (1C, C₁).

HRMS (ESI) calculated for C₅H₆O₂Na: [M +Na]⁺ : m/z 183.07858. Found: m/z. 183.07857 (0 ppm).

Synthesis of benzoic acid prop-2-ynyl ester (63c)



The reaction was performed between commercially available propargyl alcohol (0.4 g, 1 equiv) in DCM (18 ml), with triethylamine base (3.46 ml, 3.5 equiv), benzoyl chloride (2.1 ml, 2.5 equiv) and DMAP (0.17 g, 0.2 mol %), according to the general

procedure. After purification on column chromatography using 9/1 of hexane/ethyl acetate mixture, benzoate **63c** was obtained as colorless oil in 75% yield.

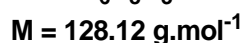
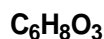
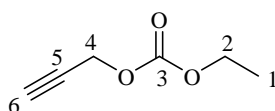
$R_f = 0.62$ (hexane/ethyl acetate 9/1).

$^1\text{H NMR}$ (CDCl_3 , 300 MHz), δ ppm: 8.05 (m, 2H); 7.56 (m, 1H); 7.43 (m, 2H); 4.92 (d, 2H, H_6 , $^4J = 2.2$ Hz); 2.53 (t, 1H, H_8 , $^4J = 2.2$ Hz).

$^{13}\text{C NMR}$ (CDCl_3 , 75 MHz), δ ppm: 165.65 (1C, C_5); 133.23 (1C, C_1); 129.69 (2C); 129.27 (1C, C_4); 128.33 (2C); 77.64 (1C, C_7); 74.97 (1C, C_8); 52.34 (1C, C_6).

HRMS (ESI) calculated for $\text{C}_{10}\text{H}_8\text{O}_2\text{Na}$: $[\text{M} + \text{Na}]^+$: m/z 183.0422. Found: m/z. 183.0422 (0 ppm).

Synthesis of carbonic acid ethyl ester prop-2-ynyl ester(**63d**)



The reaction was performed between commercially available propargyl alcohol (0.8 g, 1 equiv) in DCM (10 ml), with triethylamine base (6.94 ml, 3.5 equiv), ethyl chloroformate (3.4 ml, 2.5 equiv) and DMAP (0.35 g, 0.2 mol %), according to the general procedure. After purification on column chromatography using 9/1 of hexane/ethyl acetate mixture, carbonate **63d** was obtained as colorless oil in 70% yield.

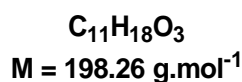
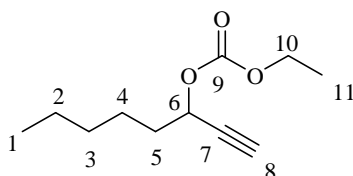
$R_f = 0.64$ (hexane/ethyl acetate 9/1).

$^1\text{H NMR}$ (CDCl_3 , 300 MHz), δ ppm: 4.72 (d, 2H, H_4 , $^4J = 2.5$ Hz); 4.22 (q, 2H, H_2 , $^3J = 7.1$ Hz); 2.52 (d, 1H, H_6 , $^4J = 2.5$ Hz); 1.31 (t, 3H, H_1 , $^3J = 7.1$ Hz).

$^{13}\text{C NMR}$ (CDCl_3 , 75 MHz), δ ppm: 154.38 (1C, C_3); 75.88 (1C, C_5); 75.42 (1C, C_6); 64.40 (1C, C_2); 54.89 (1C, C_4); 14.05 (1C, C_1).

HRMS (ESI) calculated for $C_6H_8O_3Na$: $[M + Na]^+$: m/z 151.0365. Found: m/z . 151.0367 (1 ppm).

Synthesis of carbonic acid ethyl ester -1-ethynyl hexyl ester (49)



The reaction was performed between oct-1-yn-3-ol (1 g, 1 equiv) in DCM (20 ml), with triethylamine base (3.85 ml, 3.5 equiv), ethyl chloroformate (1.88 ml, 2.5 equiv) and DMAP (0.2 g, 0.2 mol %), according to the general procedure. After purification on column chromatography using 9/1 of hexane/ethyl acetate mixture, carbonate **49** was obtained as yellow oil in 73% yield.

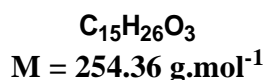
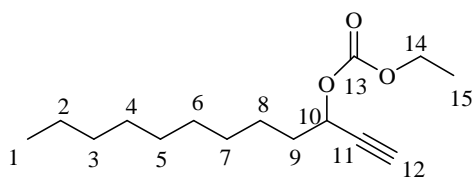
$R_f = 0.58$ (hexane/ethyl acetate 9/1).

$^1\text{H NMR}$ (CDCl_3 , 300 MHz), δ ppm: 5.17 (td, 1H, H_6 , $^3J = 6.9$ Hz, $^4J = 2.1$ Hz); 4.16 (q, 2H, H_{10} , $^3J = 7.2$ Hz); 2.48 (d, 1H, H_8 , $^4J = 2.1$ Hz); 1.77 (m, 2H), 1.25 (m, 9H); 0.85 (t, 3H, H_{11} , $^3J = 6.9$ Hz).

$^{13}\text{C NMR}$ (CDCl_3 , 75 MHz), δ ppm: 154.23 (1C, C_9); 80.57 (1C, C_7); 74.18 (1C, C_8); 67.48 (1C, C_{10}); 64.14 (1C, C_6); 34.46 (1C); 31.07 (1C); 24.34 (1C); 22.33 (1C); 14.09 (1C, C_{11}), 13.81 (1C, C_1).

HRMS (ESI) calculated for for $C_{11}H_{18}O_3$: $[M + Na]^+$: m/z 221.1154. Found: m/z . 221.1153 (0 ppm).

Synthesis of carbonic acid ethyl ester -1-ethynyl decyl ester (**51**)



The reaction was performed between dodec-1-yn-3-ol (1 g, 1 equiv) in DCM (20 ml), with triethylamine base (3.85 ml, 3.5 equiv), ethyl chloroformate (1.88 ml, 2.5 equiv) and DMAP (0.2 g, 0.2 mol %), according to the general procedure. After purification on column chromatography using 9/1 of hexane/ethyl acetate mixture, carbonate **51** was obtained as yellow oil in 80% yield.

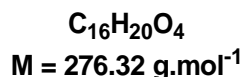
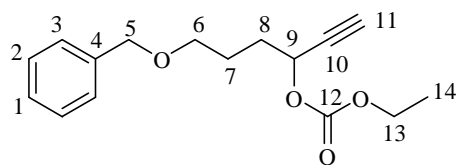
R_f = 0.64 (hexane/ethyl acetate 9/1).

¹H NMR (CDCl₃, 300 MHz), δ ppm: 5.20 (td, 1H, H₁₀, ³J= 6.6 Hz, ⁴J= 2.0 Hz); 4.20 (q, 2H, H₁₄, ³J= 7.2 Hz); 2.49 (d, 1H, H₁₂, ⁴J= 2.0 Hz); 1.80 (m, 2H), 1.29 (m, 17H); 0.87 (t, 3H, H₁₅, ³J= 7.2 Hz).

¹³C NMR (CDCl₃, 75 MHz), δ ppm: 154.33 (1C, C₁₃); 80.70 (1C, C₁₁); 74.22 (1C, C₁₂); 67.61 (1C, C₁₄); 64.26 (1C, C₁₀); 34.60 (1C); 31.84 (1C); 29.43 (1C); 29.38 (1C); 29.23 (1C); 29.03 (1C); 24.77 (1C); 22.64 (1C); 14.19 (1C), 14.06 (1C).

HRMS (ESI) calculated for C₁₅H₂₆O₃Na: [M +Na]⁺ : m/z 277.1779. Found: m/z. 277.1779 (0 ppm).

Synthesis of carbonic acid-4-benzyloxy-1-ethynyl-butyl ester ethyl ester (**53**)



The reaction was performed between 6-benzyloxy-hex-1-yn-3-ol (1.5 g, 1 equiv) in DCM (20 ml), with triethylamine base (3.60 ml, 3.5 equiv), ethyl chloroformate (1.75 ml, 2.5 equiv) and DMAP (0.18 g, 0.2 mol %), according to the general procedure. After purification on column chromatography using 9/1 of hexane/ethyl acetate mixture, carbonate **53** was obtained as yellow oil in 83% yield.

R_f = 0.69 (hexane/ethyl acetate 9/1).

¹H NMR (CDCl₃, 400 MHz), δ ppm: 7.34 (m, 5H); 5.25 (td, 1H, H₉, ³J= 6.5 Hz, ⁴J= 2.1 Hz); 4.50 (s, 2H, H₅); 4.20 (q, 2H, H₁₃, ³J= 7.2 Hz); 3.51 (t, 2H, H₆, ³J= 6.2 Hz); 2.52 (d, 1H, H₁₁, ⁴J= 2.1 Hz); 1.94 (m, 2H); 1.81 (m, 2H); 1.25 (t, 3H, ³J= 7.2 Hz).

¹³C NMR (CDCl₃, 100 MHz), δ ppm: 154.16 (1C, C₁₂); 138.12 (1C, C₄); 128.25 (2C); 127.46 (2C); 127.43 (1C, C₁); 80.37 (1C, C₁₀); 74.54 (1C, C₁₁); 72.76 (1C, C₅); 69.27 (1C, C₆); 67.23 (1C, C₁₃); 64.19 (1C, C₉); 31.46 (1C); 25.01 (1C); 14.10 (1C, C₁₄).

HRMS (ESI) calculated for C₁₆H₂₀O₄Na: [M +Na]⁺ : m/z 276.1362. Found: m/z. 276.1361 (0 ppm).

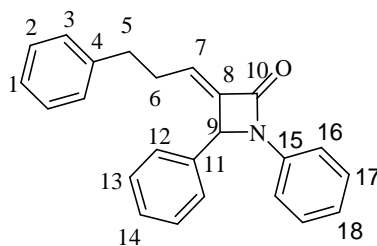
General procedure for Kinugasa reaction

H₂O (4 ml) was first degazed by bubbling nitrogen. Then CuI (1.1 equiv) was added with 6ml MeCN, and the solution was stirred under nitrogen at room temperature (Solution X). In another flask, to a solution of propargylic protected alcohol intermediate (1eq) in MeCN (6 ml) under nitrogen at 0 °C, Et₃N (1.2 equiv) was added drop wise and the mixture was stirred for 30 min (Solution Y). Solution Y was added dropwise to the solution X at room temperature. After which a 6 ml MeCN solution of the nitron (1.2 equiv) was added slowly over a period of 10 min. The reaction mixture was stirred upon heating at 50 °C for 16 hrs. After completion of the reaction, the reaction mixture was diluted with H₂O (15 ml) and filtered through celite. The celite was washed with EtAc (20 ml). The combined filtrate was extracted with EtAc (3 x 10 ml). The organic layer was washed with NH₄Cl, H₂O and brine, dried over MgSO₄ and evaporated. The residue, obtained after evaporation, upon flash chromatography using hexane / EtAc as eluent (90/10), afforded the two isomers of exoalkylidene-β-lactames (cis and trans). These were separated by chromatography over silica gel using hexane/EtAc, as eluent

The kinugasa reaction between 37d and nitron 2a

The reaction was performed between propargylic carbonate **47d** (0.25 g, 1.1mmol) and nitron **2a** (commercially available nitron) (0.255 g, 1.3mmol) according to the general mentioned above. After purification by chromatography on silica gel, using hexane/EtAc as eluent (90/10), two isomers of exoalkylidene-β-lactames **48E** and **48Z** were purely isolated; the two isomers were obtained in 50% yield of the **48E** isomer and 24.2 of the **48Z**. The combined yield of the reaction is 74 %.

(E) 1, 4-Diphenyl-3-(3-phenyl-propylidene)-azetidin-2-one (48E)



C₂₄H₂₁NO
M = 339.42 g.mol⁻¹

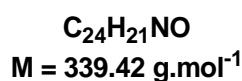
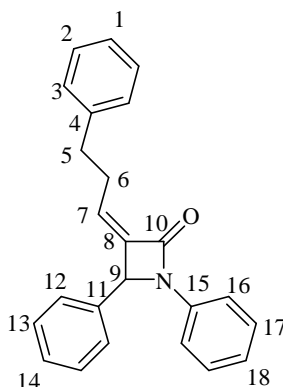
White solid, mp= 57°C, **R_f** = 0.33 (hexane/ethyl acetate 9/1).

¹H NMR (CDCl₃, 400 MHz), δ ppm: 7.36 (m, 5H); 7.15 (m, 7H); 6.92 (m, 3H); 6.25 (td, 1H, H₇, ³J= 7.8 Hz, ⁴J= 1.6 Hz); 5.14 (d, 1H, H₉, ³J= 7.8 Hz, ⁴J= 1.6 Hz); 2.42 (m, 2H, H₅, ³J= 7.8 Hz); 2.16 (m, 2H, H₆).

¹³C NMR (CDCl₃, 100 MHz), δ ppm: 161.40 (1C, C₁₀); 142.64 (1C); 140.48 (1C); 137.72 (1C); 136.76 (1C); 129.07 (2C); 129.00 (2C); 128.74 (1C), 128.39 (2C); 128.34 (2C); 127.26 (1C); 127.06 (2C); 126.12 (1C); 123.70 (1C); 116.82 (2C); 62.75 (1C, C₉); 34.54 (1C, C₅); 29.83 (1C, C₆).

HRMS (ESI) calculated for C₂₄H₂₁NONa: [M +Na]⁺ : m/z 362.1520. Found: m/z. 362.1516 (1 ppm).

(Z) 1, 4-Diphenyl-3-(3-phenyl-propylidene)-azetid-2-one (48Z)



White solid, mp= 96°C, **R_f** = 0.40 (hexane/ethyl acetate 9/1).

¹H NMR (CDCl₃, 400 MHz), δ ppm: 7.23 (m, 9H); 7.11 (m, 5H); 6.93 (m, 1H); 5.51 (td, 1H, H₇, ³J= 7.8 Hz, ⁴J= 1.5 Hz); 5.20 (s, 1H, H₉); 2.80 (m, 4H, H_{5,6}).

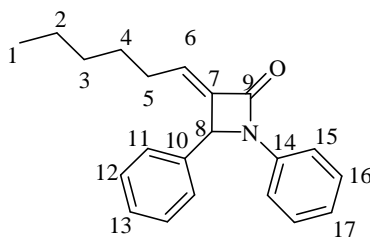
¹³C NMR (CDCl₃, 100 MHz), δ ppm: 161.55 (1C, C₁₀); 141.98 (1C); 140.63 (1C); 137.88 (1C); 137.14 (1C); 131.12 (1C); 129.03 (2C); 128.95 (2C); 128.51 (2C); 128.48 (2C); 128.36 (2C); 126.62 (1C); 126.01 (1C); 123.72 (1C); 116.83 (2C); 62.67 (1C, C₉); 35.35 (1C, C₅); 30.03 (1C, C₆).

HRMS (ESI) calculated for for C₂₄H₂₁NONa: [M +Na]⁺ : m/z 362.1520. Found: m/z. 362.1517 (1 ppm).

The Kinugasa reaction between 49 and nitrene 2a

The reaction was performed between carbonate **49** (0.2 g, 1 mmol) and nitrene **2a** (0.236 g, 1.2 mmol) according to the general procedure. After purification by chromatography on silica gel, using hexane/EtAc as eluent (90/10), two isomers of exoalkylidene-β-lactames **50E** and **50Z** were purely isolated; the two isomers were obtained in 38.38% yield of the **50E** and 22.5% of the **50Z**. The combined yield of the reaction is 61%.

(E) 3-Hexylidene-1, 4-diphenyl-azetidin-2-one (50E)



C₂₁H₂₃NO
M = 305.41 g.mol⁻¹

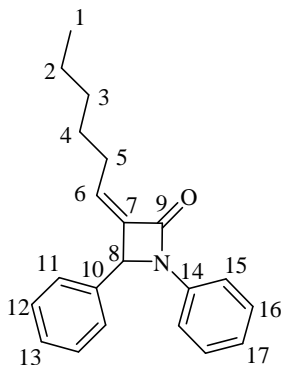
White solid, mp= 64°C, **R_f** = 0.45 (hexane/ethyl acetate 9/1).

¹H NMR (CDCl₃, 300 MHz), δ ppm: 7.38-7.12 (m, 9H); 6.92 (m, 1H); 6.19 (td, 1H, H₆, ³J= 7.1 Hz, ⁴J= 1.5 Hz); 5.34 (d, 1H, H₈, ⁴J= 1.5 Hz); 1.85 (m, 2H, H₅); 1.20-0.93 (m, 6H); 0.70 (t, 3H, H₁, ³J= 7.6 Hz).

¹³C NMR (CDCl₃, 75 MHz), δ ppm: 161.68 (1C, C₉); 141.81 (1C); 137.81 (1C); 136.89 (1C); 128.98 (2C); 128.97 (2C); 128.94 (1C); 128.64 (1C); 127.01 (2C); 123.61 (1C); 116.81 (2C); 62.87 (1C, C₈); 31.05 (1C, C₃); 27.96 (1C, C₄); 27.75 (1C, C₅); 22.19 (1C, C₂); 13.85 (1C, C₁).

HRMS (ESI) calculated for C₂₁H₂₃NONa: [M +Na]⁺ : m/z 328.1677. Found: m/z. 328.1678 (0 ppm).

(Z) 3-Hexylidene-1, 4-diphenyl-azetidin-2-one (50Z)



C₂₁H₂₃NO
M = 305.41 g.mol⁻¹

White solid, mp= 80°C, R_f = 0.60 (hexane/ethyl acetate 9/1).

$^1\text{H NMR}$ (CDCl_3 , 300 MHz), δ ppm: 7.21 (m, 9H); 6.91 (m, 1H); 5.49 (td, 1H, H_6 , $^3J = 7.6$ Hz, $^4J = 1.1$ Hz); 5.19 (s, 1H, H_8); 2.45 (m, 2H, H_5); 1.20 (m, 6H); 0.80 (m, 3H, H_1).

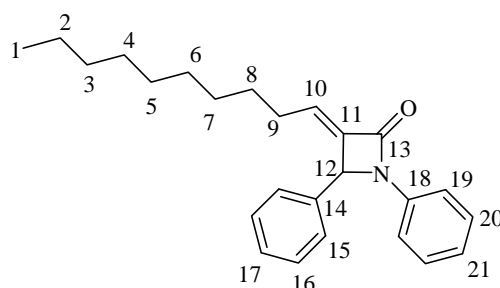
$^{13}\text{C NMR}$ (CDCl_3 , 75 MHz), δ ppm: 161.84 (1C, C_9); 141.24 (1C); 137.95 (1C); 137.35 (1C); 132.65 (1C); 129.03 (2C); 128.97 (2C); 128.48 (1C); 126.54 (2C); 123.65 (1C); 116.80 (2C); 62.66 (1C, C_8); 31.19 (1C, C_3); 28.81 (1C, C_4); 28.75 (1C, C_5); 22.37 (1C, C_2); 13.96 (1C, C_1).

HRMS (ESI) calculated for $\text{C}_{21}\text{H}_{23}\text{NONa}$: $[\text{M} + \text{Na}]^+$: m/z 328.1677. Found: m/z. 328.1684 (2 ppm).

The Kinugasa reaction between **51** and nitrone **2a**

The reaction was performed between **51** (0.3 g, 1.18 mmol) and nitrone **2a** (0.28 g, 1.42 mmol) according to the general procedure. After purification by chromatography on silica gel, using hexane/EtAc as eluent (90/10), two isomers of exoalkylidene- β -lactames **52E** and **52Z** were purely isolated, the two isomers were obtained in 43.90 % yield of the **52E** and 24.18 of the **52Z**. The combined yield of the reaction is 68 %.

(*E*) 3-Decylidene-1, 4-diphenyl-azetidin-2-one (**52E**)



$\text{C}_{25}\text{H}_{31}\text{NO}$
 $M = 361.52 \text{ g}\cdot\text{mol}^{-1}$

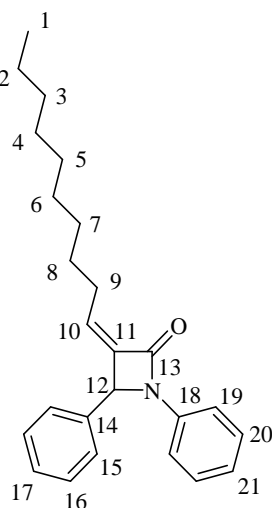
White solid, mp= 71°C, R_f = 0.42 (hexane/ethyl acetate 9/1).

¹H NMR (CDCl₃, 400 MHz), δ ppm: 7.40 (m, 7H); 7.28 (m, 2H); 7.02 (m, 1H); 6.30 (td, 1H, H₁₀, ³J= 7.1 Hz, ⁴J= 1.5 Hz); 5.44 (d, 1H, H₁₂, ⁴J= 1.5 Hz); 1.96 (m, 2H); 1.16 (m, 14H); 0.92 (t, 3H, H₁, ³J= 6.7 Hz).

¹³C NMR (CDCl₃, 100 MHz), δ ppm: 161.70 (1C, C₁₃); 141.76 (1C); 137.80 (1C); 136.88 (1C); 129.01 (4C); 128.66 (2C); 127.02 (1C); 123.63 (1C); 116.81 (2C); 62.86 (1C, C₁₂); 31.83 (1C); 29.37 (2C); 29.20 (2C); 28.88 (1C); 28.31 (1C); 27.82 (1C); 22.65 (1C); 14.11 (1C, C₁).

HRMS (ESI) calculated for C₂₅H₃₁NONa: [M +Na]⁺ : m/z 384.2297. Found: m/z. 384.2297 (0 ppm).

(Z) 3-Decylidene-1, 4-diphenyl-azetidin-2-one (52Z)



C₂₅H₃₁NO
M = 361.52 g.mol⁻¹

White solid, mp= 89°C, **R_f** = 0.62 (hexane/ethyl acetate 9/1).

¹H NMR (CDCl₃, 400 MHz), δ ppm: 7.35 (m, 7H); 7.26 (m, 2H); 7.04 (m, 1H); 5.60 (td, 1H, H₁₀, ³J= 7.9 Hz, ⁴J= 0.9 Hz); 5.31 (s, 1H, H₁₂); 2.58 (m, 2H); 1.27 (s, 14H); 0.90 (m, 3H).

¹³C NMR (CDCl₃, 100 MHz), δ ppm: 161.82 (1C, C₁₃); 141.25 (1C); 137.97 (1C); 137.37 (1C); 132.65 (1C); 129.02 (2C); 128.97 (2C); 128.48 (1C); 126.54 (2C);

123.63 (1C); 116.80 (2C); 62.65 (1C, C₁₂); 31.86 (1C); 29.49 (1C); 29.34 (1C); 29.24 (1C); 29.17 (1C); 29.04 (1C); 28.83 (1C); 22.65 (1C); 14.09 (1C).

HRMS (ESI) calculated for C₂₅H₃₁NONa: [M +Na]⁺ : m/z 384.2297. Found: m/z. 384.2300 (0 ppm).

Empirical formula	C ₂₅ H ₃₁ N O
Formula weight	361.51
Temperature	150(2) K
Wavelength	0.71073 Å
Crystal system, space group	monoclinic, <i>P</i> 2 ₁
Unit cell dimensions	a = 5.622(2) Å, α = 90 ° b = 8.232(4) Å, β = 90.683(10) ° c = 45.170(18) Å, γ = 90 °
Volume	2090.3(15) Å ³
Z, Calculated density	4, 1.149 (g.cm ⁻³)
Absorption coefficient	0.069 mm ⁻¹
<i>F</i> (000)	784
Crystal size	0.53 x 0.1 x 0.03 mm
Crystal color	Colorless
Theta range for data collection	3.06 to 27.7 °
h_min, h_max k_min, k_max l_min, l_max	-7, 7 -10, 10 -58, 55
Reflections collected / unique	14306 / 9220 [R(int) ^a = 0.0503]
Reflections [I > 2σ]	6077
Completeness to theta_max	0.982
Absorption correction type	multi-scan
Max. and min. transmission	0.998 , 0.830
Refinement method	Full-matrix least-squares on F ²
Data / restraints / parameters	9220 / 1 / 431
Flack parameter	1(9)

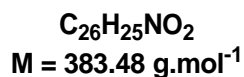
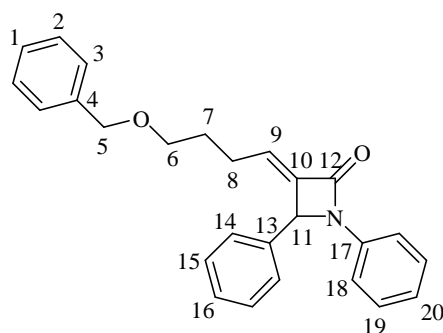
^b Goodness-of-fit	1.569
Final <i>R</i> indices [<i>I</i> >2σ]	<i>R</i> 1 ^c = 0.1489, <i>wR</i> 2 ^d = 0.4081
<i>R</i> indices (all data)	<i>R</i> 1 ^c = 0.1961, <i>wR</i> 2 ^d = 0.4514
Largest diff. peak and hole	0.628 and -0.844 e ⁻ .Å ⁻³

Table I. 3: Crystal data and structure refinement for **52Z**

The Kinugasa reaction between **53** and nitron **2a**

The reaction was performed between carbonate **53** (0.2 g, 0.72 mmol) and nitron **2a** (0.17 g, 0.86mmol) according to the general procedure. After purification by chromatography on silica gel, using hexane/EtAc as eluent (80/20), two isomers of exoalkylidene-β-lactames **54E** and **54Z** were purely isolated, the two isomers were obtained in 41% yield of the **54E** and 30% of the **54Z**. The combined yield of the reaction is 71%.

(*E*) Carbonic acid 4-benzyloxy-1-ethyl-butyl ester ethyl ester(**54E**)



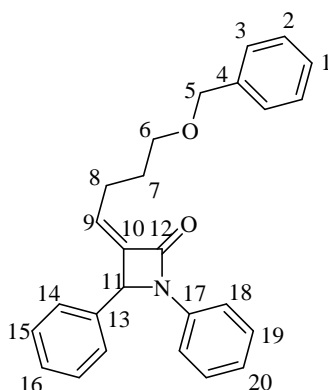
Brown solid, mp= 52°C, **R_f** = 0.37 (hexane/ethyl acetate 8/2).

¹H NMR (CDCl₃, 300 MHz), δ ppm: 7.35-7.15 (m, 14H); 6.93 (m, 1H); 6.23 (t, 1H, H₉, ³J= 6.4 Hz); 5.33 (s, 1H, H₁₁); 4.35 (s, 2H, H₅); 3.21 (m, 2H, H₆); 2.07 (m, 2H, H₈); 1.92 (m, 2H, H₇).

¹³C NMR (CDCl₃, 75 MHz), δ ppm: 161.38 (1C, C₁₂); 142.20 (1C); 138.23 (1C); 137.61 (1C); 136.65 (1C); 128.89 (2C); 128.54 (1C); 128.22 (2C); 127.87 (1C); 127.45 (4C); 126.87 (2C); 123.58 (2C); 116.73 (2C); 72.65 (1C, C₅); 68.85 (1C, C₆); 62.65 (1C, C₁₁); 28.22 (1C, C₇); 24.48 (1C, C₈).

HRMS (ESI) calculated for C₂₆H₂₅NO₂Na: [M +Na]⁺ : m/z 406.1777. Found: m/z. 406.1779 (0 ppm).

(Z) Carbonic acid 4-benzyloxy-1-ethyl-butyl ester ethyl ester (54Z)



C₂₆H₂₅NO₂
M = 383.48 g.mol⁻¹

Brown solid, mp= 74°C, **R_f** = 0.62 (hexane/ethyl acetate 8/2).

¹H NMR (CDCl₃, 300 MHz), δ ppm: 7.26-7.16 (m, 14H); 6.94 (m, 1H); 5.52 (t, 1H, H₉, ³J= 8.0 Hz); 5.18 (s, 1H, H₁₁); 4.40 (s, 2H, H₅); 3.42 (t, 2H, H₆, ³J= 8.8 Hz); 2.55 (m, 2H, H₈); 1.69 (quintet, 2H, H₇, ³J= 6.9 Hz).

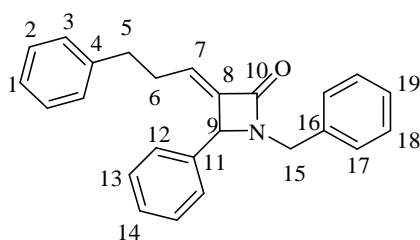
¹³C NMR (CDCl₃, 75 MHz), δ ppm: 161.59 (1C, C₁₂); 141.50 (1C); 138.37 (1C); 137.83 (1C); 137.13 (1C); 131.75 (1C); 128.99 (2C); 128.93 (2C); 128.47 (1C); 128.27 (2C); 127.61 (2C); 127.45 (1C); 126.45 (2C); 123.67 (1C); 116.78 (2C); 72.88 (1C, C₅); 69.48 (1C, C₆); 62.57 (1C, C₁₁); 29.21 (1C, C₇); 25.72 (1C, C₈).

HRMS (ESI) calculated for $C_{26}H_{25}NO_2Na$: $[M + Na]^+$: m/z 406.1777. Found: m/z . 406.1779 (0 ppm).

The Kinugasa reaction between **47d** and nitron **57**

The reaction was performed between **47d** (0.25 g, 1.08 mmol) and nitron **57** (0.27 g, 1.30 mmol) according to the general procedure. After purification by chromatography on silica gel, using hexane/EtAc as eluent (80/20), two isomers of exoalkylidene- β -lactams **58E** and **58Z** were purely isolated, the two isomers were obtained in 37.27% yield of the **58E** and 24.67% of the **58Z**. The combined yield of the reaction is 62%.

(*E*) 1-Benzyl-4-phenyl-3-(3-phenyl-propylidene)-azetidin-2-one (**58E**)



$C_{25}H_{23}NO$
 $M = 353.45 \text{ g}\cdot\text{mol}^{-1}$

Brown solid, $mp = 59^\circ\text{C}$, $R_f = 0.33$ (hexane/ethyl acetate 9/1).

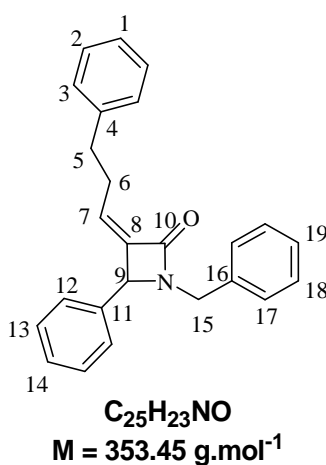
$^1\text{H NMR}$ (CDCl_3 , 400 MHz), δ ppm: 7.35-7.26 (m, 6H); 7.20-7.10 (m, 7H); 6.90 (m, 2H); 6.16 (td, 1H, H_7 , $^3J = 7.8 \text{ Hz}$, $^4J = 1.4 \text{ Hz}$); 4.84 (AB_{sys} , 1H, H_{15} , $J = 15.1 \text{ Hz}$); 4.54 (d, 1H, H_9 , $^4J = 1.4 \text{ Hz}$); 3.78 (AB_{sys} , 1H, H_{15} , $J = 15.1 \text{ Hz}$); 2.46 (m, 2H, H_5); 2.10 (m, 2H, H_6).

$^{13}\text{C NMR}$ (CDCl_3 , 100 MHz), δ ppm: 161.19 (1C, C_{10}); 143.38 (1C); 140.59 (1C); 136.38 (1C); 135.58 (1C); 128.86 (1C), 128.67 (2C); 128.64 (2C), 128.41 (2C);

128.38 (2C); 128.30 (2C); 127.59 (1C); 126.02 (1C); 125.36 (1C); 61.62 (1C, C₉); 44.00 (1C, C₁₅); 34.57 (1C, C₅); 29.96 (1C, C₆).

HRMS (ESI) calculated for C₂₅H₂₃NONa: [M +Na]⁺ : m/z 376.1672. Found: m/z. 376.1674 (1 ppm).

(Z) 1-Benzyl-4-phenyl-3-(3-phenyl-propylidene)-azetidin-2-one (58Z)



Brown solid, mp= 105°C, **R_f** = 0.40 (hexane/ethyl acetate 9/1).

¹H NMR (CDCl₃, 400 MHz), δ ppm: 7.32-7.26 (m, 7H); 7.18-7.13 (m, 8H); 5.42 (td, 1H, H₇, ³J= 7.4 Hz, ⁴J= 1.0 Hz); 4.84 (AB_{sys}, 1H, H₁₅, J= 15.1 Hz); 4.68 (s, 1H, H₉); 3.82 (AB_{sys}, 1H, H₁₅, J= 15.1 Hz); 2.80 (m, 4H, H_{5,6}).

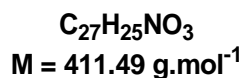
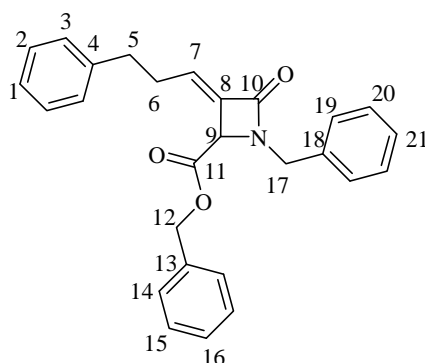
¹³C NMR (CDCl₃, 100 MHz), δ ppm: 161.41 (1C, C₁₀); 142.88 (1C); 140.78 (1C); 136.92 (1C); 135.71 (1C); 129.21 (1C), 128.73 (2C); 128.68 (2C), 128.56 (2C); 128.47 (2C); 128.44 (2C); 128.32 (1C); 127.44 (1C); 125.93 (1C); 61.71 (1C, C₉); 44.09 (1C, C₁₅); 35.36 (1C, C₅); 29.80 (1C, C₆).

HRMS (ESI) calculated for C₂₅H₂₃NONa: [M +Na]⁺ : m/z 376.1672. Found: m/z. 376.1670 (0 ppm).

The Kinugasa reaction between 47d and ester nitrone 59

The reaction was performed between carbonate **47d** (0.2 g, 0.72 mmol) and nitrone **59** (0.17 g, 0.86 mmol) according to the general procedure. After purification by chromatography on silica gel, using hexane/EtAc as eluent (80/20), two isomers of exoalkylidene- β -lactames **60E** and **60Z** were purely isolated, the two isomers were obtained in 31.64% yield of the **60E** and 28.16% of the **60Z**. The combined yield of the reaction is 60 %.

(*E*) 1-Benzyl-4-oxo-3-(3-phenyl-propylidene)-azetidine-2-carboxylic acid benzyl ester (**60E**)



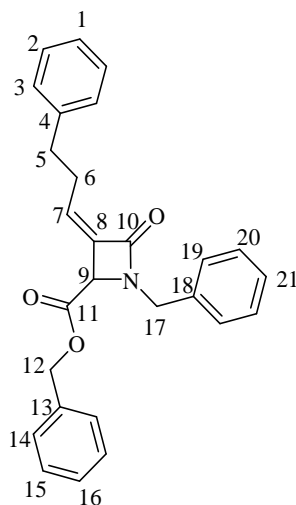
Brown oil, mp=82°C, $R_f = 0.51$ (hexane/ethyl acetate 8/2).

$^1\text{H NMR}$ (CDCl_3 , 300 MHz), δ ppm: 7.29-6.11 (m, 15H); 6.16 (td, 1H, H_7 , $^3J = 7.6$ Hz, $^4J = 1.3$ Hz); 5.10 (AB_{sys} , 2H, H_{12} , $J = 5.7$ Hz); 4.86 (AB_{sys} , 1H, H_{17} , $J = 17.3$ Hz); 4.15 (s, 1H, H_9); 4.11 (AB_{sys} , 1H, H_{17} , $J = 17.3$ Hz); 2.56 (m, 2H, H_5); 2.32 (m, 2H, H_6).

¹³C NMR (CDCl₃, 75 MHz), δ ppm: 168.80 (1C, C₁₁); 161.03 (1C, C₁₀); 140.31 (1C); 137.05 (1C); 134.80 (1C); 134.72 (1C); 128.78 (2C), 128.63 (2C); 128.46 (2C), 128.38 (2C); 128.34 (2C); 127.85 (1C); 127.67 (1C); 126.10 (1C); 67.31 (1C, C₉); 58.34 (1C, C₁₂); 45.08 (1C, C₁₇); 34.55 (1C, C₅); 29.77 (1C, C₆).

HRMS (ESI) calculated for C₂₇H₂₅NO₃Na: [M +Na]⁺: m/z 434.1726. Found: m/z. 434.1731 (1 ppm).

(Z) 1-Benzyl-4-oxo-3-(3-phenyl-propylidene)-azetidine-2-carboxylic acid benzyl ester(60Z)



C₂₇H₂₅NO₃
M = 411.49 g.mol⁻¹

Brown oil, mp=122°C, **R_f** = 0.67 (hexane/ethyl acetate 8/2).

¹H NMR (CDCl₃, 300 MHz), δ ppm: 7.32-7.15 (m, 15H); 5.66 (td, 1H, H₇, ³J= 7.9 Hz, ⁴J= 1.2 Hz); 5.14 (AB_{sys}, 2H, H₁₂, J= 17.6 Hz); 4.92 (AB_{sys}, 1H, H₁₇, J= 14.7 Hz); 4.22 (s, 1H, H₉); 4.17 (AB_{sys}, 1H, H₁₇, J= 14.7 Hz); 2.72 (m, 4H, H_{5,6}).

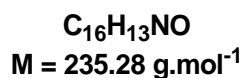
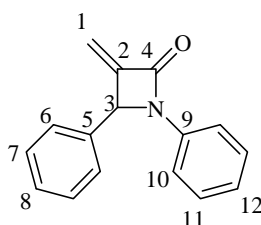
¹³C NMR (CDCl₃, 75 MHz), δ ppm: 168.98 (1C, C₁₁); 162.95 (1C, C₁₀); 140.52 (1C); 136.37 (1C); 136.05 (1C); 134.96 (1C); 130.43 (1C), 128.81 (2C); 128.66 (2C), 128.60 (2C); 128.46 (2C); 128.44 (2C); 128.36 (1C); 128.30 (1C); 127.84 (1C); 126.06 (1C); 67.15 (1C, C₉); 57.91 (1C, C₁₂); 45.09 (1C, C₁₇); 35.17 (1C, C₅); 30.05 (1C, C₆).

HRMS (ESI) calculated for C₂₇H₂₅NO₃Na: [M +Na]⁺: m/z 434.1732. Found: m/z. 434.1732 (0 ppm).

The Kinugasa reaction between **63d** and nitrene **2a**

The reaction was performed between carbonate **63d** (0.25 g, 1.9mmol) and nitrene **2a** (0.46 g, 2.34mmol) according to the general procedure. After purification by chromatography on silica gel, using hexane/EtAc as eluent (90/10), only one product of exoalkylidene- β -lactames **64** was obtained in 52 % yield.

3-Methylene-1, 4-diphenyl-azetidin-2-one (**64**)



White solid, mp=138°C, R_f = 0.34 (hexane/ethyl acetate 9/1).

¹H NMR (CDCl₃, 300 MHz), δ ppm: 7.27-7.11 (m, 9H); 6.93 (m, 1H); 5.72 (d, 1H, H_1 , 2J = 1.8 Hz); 5.28 (t, 1H, H_3 , 4J = 1.3 Hz); 5.04 (d, 1H, H_1 , 2J = 1.8 Hz).

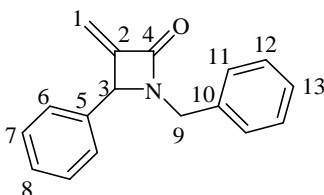
¹³C NMR (CDCl₃, 75 MHz), (ppm): 160.87 (1C, C₄); 149.79 (1C); 137.51 (1C); 136.39 (1C); 129.05 (2C); 129.02 (2C); 128.70 (2C); 126.51(2C); 124.08 (1C); 117.06 (1C); 110.77 (1C); 63.43 (1C, C₃).

HRMS (ESI) calculated for C₁₆H₁₃NONa: [M +Na]⁺ : m/z 258.0889. Found: m/z. 258.0892 (1 ppm).

The Kinugasa reaction between **53d** and nitrone **57**

The reaction was performed between carbonate **53d** (0.2 g, 1.56 mmol) and nitrone **57** (0.4 g, 1.87 mmol) according to the general procedure. After purification by chromatography on silica gel, using hexane/EtAc as eluent (80/20), only one product of exoalkylidene- β -lactam **65** was obtained in 54 % yield.

1-Benzyl-3-methylene-4-phenyl-azetid-2-one (**65**)



White solid, mp=142°C, R_f = 0.5 (hexane/ethyl acetate 8/2).

¹H NMR (CDCl₃, 300 MHz), δ ppm: 7.34-7.15 (m, 10H); 5.71 (d, 1H, H₁, ²J= 1.5 Hz); 5.00 (d, 1H, H₁, ²J= 1.5 Hz); 4.90 (AB_{sys}, 1H, H₉, J= 15.3 Hz); 4.79 (s, 1H, H₃); 3.85 (AB_{sys}, 1H, H₉, J= 15.3 Hz).

¹³C NMR (CDCl₃, 75 MHz), δ ppm: 163.78 (1C, C₄); 150.63 (1C); 136.09 (1C); 135.17 (1C); 128.82 (2C); 128.70 (2C); 128.40 (2C); 127.70 (2C); 127.32 (2C); 109.60 (1C); 62.43 (1C, C₃); 44.24 (1C, C₉).

HRMS (ESI) calculated for C₁₇H₁₅NONa: [M +Na]⁺ : m/z 272.1045. Found: m/z. 272.1045 (0 ppm).

I.F. REFERENCES

References

1. Waksman S. A., "History of the word 'antibiotic'." *J. Hist. Med. Allied Sci.*, **1973**, 284.
2. Fleming A. *British Journal of Experimental Pathology*, **1929**, 10, 226.
3. Montgomery E. H, Kroeger D. C, *Dent. Clin. North Amer.* **1984**, 28 (3), 433.
4. Alcaide B., Almendros P. *Curr. Med. Chem.*, **2004**, 11, 1921.
5. Morin R. B., Gorman M., "Chemistry and Biology of β -Lactam Antibiotics," *Academic: New York*, **1982**.
6. Bays H. E., Moore P. B., Drehobl M. A., Rosenblatt S., Toth P. D., Dujovne C. A., Knopp R. H., Lipka L. J., LeBeaut A. P., Yang B., Mellars L. E., Cuffie-Jackson C., Veltri E. P. *Clin. Ther.*, **2001**, 23, 1209.
7. Knopp R. H., Gitter H., Truitt T., Bays H., Manion C. V., Lipka L. J., LeBeaut A. P., Suresh R., Yang B., Veltri E. P., *J. Eur. Heart*, **2003**, 24, 729.
8. Clader J. W., *J. Med. Chem.* **2003**, 47, 1.
9. Ghosal A., Zbaida S., Chowdhury S. K., Iannucci R. M., Feng W., Alton K. B., Patrick J. E., Davis H. R., *Pat. Appl.*, **2002**.
10. Keri R. S., Hosamani K. M., Reddy H. S., Shingalapur R. V., *Arch. Pharmacol.*, **2010**, 343, 237.
11. Banik I., Becker F. F., Banik B. K., *J. Med. Chem.*, **2003**, 46, 12.
12. Meegan M. J., Carr M., Knox A. J. S., Zisterer D. M., Lloyd D. G., *J. Enzyme Inhib. Med. Chem.*, **2008**, 23, 668.
13. Aslanian R. G., Bennett C. E., Burnett D. A., Chan T.-Y., Kiselgof E. Y., Knutson C. E., Harris J. M., McKittrick B. A., Palani A., Smith E. M., Vaccaro H. M., Xiao D., Kim H. M. *Pat. Appl.* WO 2008/033464A2, **2008**.
14. Troisi L., Granito C., Pindinelli E., "Novel and Recent Synthesis and Applications of β -Lactams", Banik B. K., "Heterocyclic Scaffolds I," *Springer: Berlin/ Heidelberg, Germany*, **2010**; Vol. 22, 101.
15. Ogilvie W. W., Yoakim C., Do F., Haché, B., Lagacé, L., Naud, J., O'Meara, J. A., Deziel, R. *Bioorg. Med. Chem.*, **1999**, 7, 1521.
16. Wilmouth R. C., Kassamally S., Westwood N. J., Sheppard R. J., Claridge T. D. W., Aplin R. T., Wright P. A., Pritchard G. J., Schofield C., *J. Biochemistry* **1999**, 38, 7989.
17. Malachowski W. P., Tie C., Wang K., Broadrup R. L., *J. Org. Chem.*, **2002**, 67, 8962.

18. Jard S., Elands J., Schmidt A., Barberis C., "In Progress in Endocrinology," Imura H., Shizume, K., Eds.; Elsevier: Amsterdam, The Netherlands, **1998**, 1183.
19. Sperka T., Pitlik J., Bagossi P., Tözser J., *J. Bioorg. Med. Chem. Lett.*, **2005**, *15*, 3086.
20. Moellering R. C. J., *J. Antimicrob. Chemother.*, **1993**, *31*, 1.
21. France S., Weatherwax A., Taggi A. E., Lectka T., *Acc. Chem. Res.*, **2004**, *37*, 592.
22. Brandi A., Cicchi S., Cordero F., *M. Chem. Rev.*, **2008**, *108*, 3988.
23. Bose A. K., Manhas M. S., Mathur A., Wagle D. R., "In Recent Progress in the Chemical Synthesis of Antibiotics and Related Microbial Products, Lukacs G.," *Springer-Verlag: Berlin/Heidelberg, Germany*, **1993**; *2*, 551.
24. Staudinger H., Liebigs *Ann. Chem.* 1908, 356, 51.
25. Palomo C., Aizpurua J. M., Ganboa I., Oiarbide M. *Eur. J. Org. Chem.*, **1999**, 3223.
26. (a) Gilman H., Speeter M., *J. Am. Chem. Soc.*, **1943**, *65*, 2255; (b) Hart D. J., Ha D. C. *Chem. Rev.*, **1989**, *89*, 1447; (c) Benaglia M., Cinquini M., Cozzi F., *Eur. J. Org. Chem.*, **2000**, 563.
27. (a) Lysek R., Furman B., Kaluza Z., Frelek J., Suwinska K., Urbanczyk-Lipkowska Z., Chmielewski M. *Tetrahedron: Asymmetry* **2000**, *11*, 3131, (b) Furman B., Kaluza, Z., Stencel A., Grzeszczyk B., Chmielewski M. "β-Lactams from Carbohydrates In Ashry., Heterocycles from Carbohydrate Precursors," *Springer: Berlin/Heidelberg, Germany*, **2007**; *7*, pp 101.
28. (a). The Chemistry of β-Lactams; Page, M. I., Ed.; *Blackie Academic & Professional: New York, NY*, **1992**; (b) Georg G. I. "The Organic Chemistry of β-Lactams," *Wiley VCH: New York, NY*, **1993**; (c) Bruggink A., "Synthesis of β-Lactam Antibiotics," *Kluwer: Dordrecht, the Netherlands*, **2001**.
29. Ojima I., Delalogue F., *Chem. Soc. Rev.*, **1997**, *26*, 377.
30. (a) McCarthy N., McKervey M. A., Ye T., McCann M., Murphy E., Doyle M. P. *Tetrahedron Lett.* **1992**, *33*, 5983; (b) Watanabe N., Anada M., Hashimoto S., Ikegami S., *Synlett* **1994**, 1031; (c) Anada, M.; Watanabe, N. *Chem. Commun.*, **1998**, 1517.
31. Kinugasa M., Hashimoto S., *J. Chem. Soc., Chem. Commun.*, **1972**, 466.
32. Stecko S., Furman B., Chmielewski M., *Tetrahedron*, **2014**, *70*, 7817.
33. Khangarot K., Kaliappan K., *Eur. J. Org. Chem.*, **2013**.
34. Ding L. K., Irwin W. J., *J. Chem. Soc., Perkin Trans.*, **1976**, *1*, 2382.
35. (a) Feuer H. "Nitrile Oxides, Nitrones and Nitronates in Organic Synthesis: Novel Strategies in Synthesis," *Wiley: Weinheim, Germany*, **2008**, (b) Grigor'ev, I. A. "Nitrones: novel strategies in synthesis in Nitrile Oxides, Nitrones, and Nitronates in Organic Synthesis," *John Wiley and Sons: Weinheim, Germany*, **2007**, 129.

36. Okuro K., Enna M., Miura M., Nomura M., *J. Chem. Soc., Chem. Commun.*, **1993**, 1107.
37. Miura M., Enna M., Okuro K., Nomura M., *J. Org. Chem.*, **1995**, *60*, 4999.
38. Lo M.-C M., Fu G. C., *J. Am. Chem. Soc.*, **2002**, *124*, 4572.
39. Glaser C. *Ber. Dtsch. Chem. Ges.* **1869**, *2*, 422.
40. Ye M. C, Zhou J., Z.-Z., Tang Y., *Chem. Commun.*, **2003**, 2554; Zhou J., Tang Y., *Top Organomet. Chem.*, **2011**, *36*, 287.
41. Zhang X., Hsung R. P., Li H., Zhang Y., Johnson W. L., Figueroa R., *Org. Lett.*, **2008**, *10*, 3477.
42. Stecko S., Mames A., Furman B., Chmielewski M., *J. Org. Chem.*, **2008**, *73*, 7402.
43. Michalak M., Stodulski M., Stecko S., Mames A., Panfil I., Soluch M., B. Chmielewski M., *J. Org. Chem.*, **2011**, *76*, 6931.
44. Chen Z., Lin L., Wang M., Liu X. Feng X., *Chem. Eur. J.*, **2013**, *19*, 7561.
45. a) Tanaka K., Shoji J., Terui Y., Kondo E., Mayama M., Kawamura Y., Hattori T., Matsumoto K., Yoshida T. *J. Antibiot.*, **1981**, *34*, 909; b) Arisawa, M.; Then, R. L. *J. Antibiot.*, **1982**, *35*, 1578.
46. Buynak J. D., Rao M. N., Pajouhesh H., Chandrasekaran R. Y., Finn K. *J. Org. Chem.*, **1985**, *50*, 4245.
47. Livermore D. M., *J. Antimicrob Chemother* **1993**; *31*, 9.
48. Alcaide B., Esteban G., Cantalejo Y., Plumet J., Roderigues J., *J. Org. Chem.*, **1994**, *59*, 7994.
49. Basak A., Ghosh S. C., *Synlett*, **2004**, 1637.
50. Venkatesan, A. M., Agarwal A., Abe T., Ushirogochi H., Yamamura I., Ado M., Tsuyoshi T., Santos O., Gu Y., Sum F., Li Z., Francisco G., Lin Y., Peterson P., Yang Y., Kumagai T., Weiss W., Shlaes D., Knox J., Mansour T. *J. Med. Chem.*, **2006**, *49*, 4623.
51. Abe T., Matsunaga H., Mihira A., Sato C., Ushirogochi H., Takaska T., Venkatesan A. M., Mansour T., **2003**, WO-2003093277
52. Osborne N. F., Atkins R.J, Broom N.J.P., Coulton S., Harbridge J. B., Harris M. A., Francisco I. S., *J. Chem. Soc., Perkin Trans.* **1994**, *1*, 179.
53. Zhu L., Xiong Y., Li C., *J. Org. Chem.*, **2015**, *80*, 628.
54. Nasr el Dine A., Grée D., Roisnel T., Caytan E., Hachem, A., Grée R. *Eur. J. Org. Chem.*, **2016**, 556.
55. a) Ye M.-C., Zhou J., Whang Z.-Z., Tang Y. *Chem. Commun.* **2003**, 2554; b) Ye M.-C., Zhou J., Tang Y. *J. Org. Chem.* **2006**, *71*, 3576.

II. SECOND CHAPTER

Synthesis of New Acylsilanes and Preliminary Studies of their Intramolecular Aldol Reactions

II.A. INTRODUCTION

Introduction

General Introduction

Acylsilanes (RCOSiR'_3) were discovered first by Brook in 1957 [1–3]. Acylsilanes have the silicon directly attached to the carbonyl group, and this induces particular physical and chemical properties to such molecules (Figure II.1) [4–8]. From a synthetic point of view, this special functional group can be easily transformed in one pot into many different derivatives, such as acid [9–12], ketone [13–15], alcohol [16,17], aldehyde [11,18,19], nitrile [20], amide [12, 20, 21] and ester [20, 22]. In addition to these transformations, a great deal of efforts has been devoted to the development of other reactions with acylsilanes, for instance, stereocontrolled nucleophilic additions [23], stereocontrolled aldol reactions [24], cyclizations [25], coupling reactions [26], α -halogenations [3] and enantioselective reductions [27].

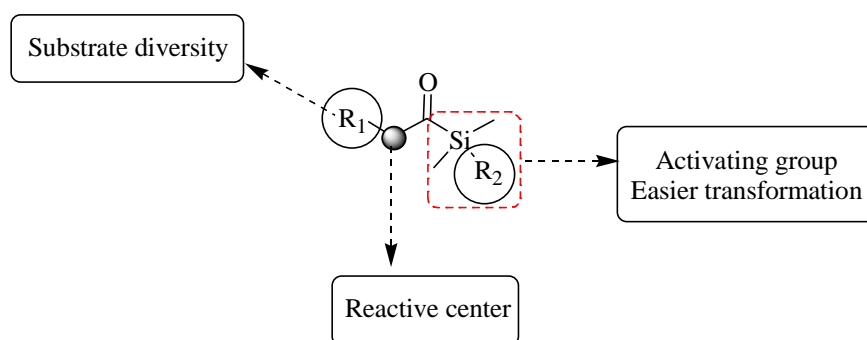


Fig. II. 1: Structure of acylsilanes.

Due to their slightly higher pK_a values (the values being approximately 16) [28], the α -alkylation of acylsilanes induced by the deprotonation of its α position by a base (achiral or chiral) is more difficult and remains a challenge.

Many important reviews on the chemistry of acylsilane were published, showing different ways for their synthesis and their important uses in organic chemistry [29].

Physical properties of acylsilanes

The spectral data of acylsilanes have been well described by Brook [30] and Page and co-workers [31]. The inductive effect of the silicon favors the polarization of the carbonyl group, which absorbs at a lower frequency than simple ketones in the infrared and ultraviolet spectra. In ^{13}C NMR spectroscopy, the signals for the carbonyl carbon are quite different from the corresponding ketones, appearing at higher chemical shift values. The anisotropy effect and electronegativity differences also lead to higher chemical shift values in the ^1H NMR spectra for the hydrogens attached to the α -carbon of acylsilanes. Table II.1 shows some examples of IR and NMR data for acylsilanes. Another important characteristic of acylsilanes is the abnormally long Si-CO bond (1.926 Å), first observed by Trotter [32] based on X-ray analysis, which can be compared to the analogous bond length in C-CO (1.51 Å) compounds [30].

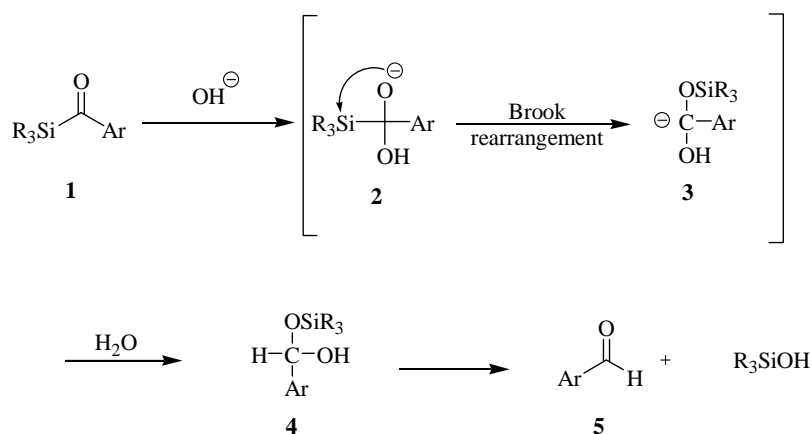
Acylsilane	IR $\nu_{\text{C=O}}(\text{cm}^{-1})$	^{13}C NMR Chemical shift C=O	^1H NMR Chemical shift CHCO
MeCOSiMe ₃	1645 (1710)	247.6 (215)	2.20 (2.08)
PhCOSiMe ₃	1618 (1675)	233.6 (207)	-
MeCOSiPh ₃	1645	240.1	2.30 (2.01)
PhCOSiPh ₃	1618 (1692)	-	-
<i>t</i> -BuCOSiMe ₃	1636	249.0 (215)	-
Me ₃ SiCOSiMe ₃	1570	318.2	-
PhCH ₂ COSiMe ₃	1635	-	3.77 (3.55)

Table II. 1: Infrared C=O absorption and NMR data of some acylsilanes [28, 30].

(Note: values in parenthesis are for analogues in which the silicon atom has been replaced by carbon).

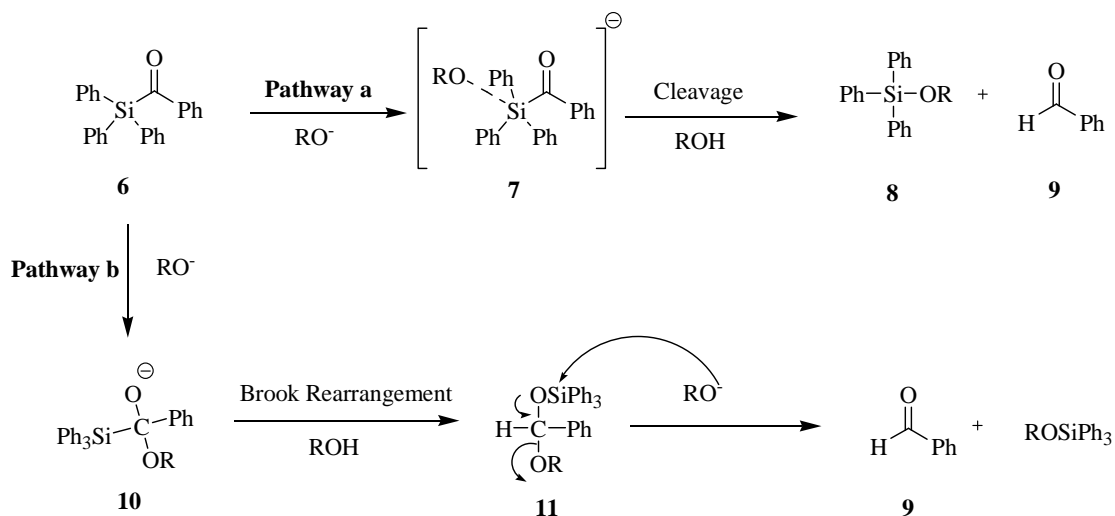
Brook and reverse Brook rearrangements

Studies have shown that acylsilanes, in general, behave as ordinary ketones. However, in some cases, these compounds have an abnormal chemical behavior, due to the intrinsic properties already mentioned. For example, in reactions of aroylsilanes with nucleophiles, the Brook rearrangement is very common [33]. Hydrolysis of aroylsilanes **1**, for instance, to the corresponding aldehydes **5**, promoted by traces of OH^- (Scheme II.1) involves Brook rearrangement (**2** to **3**). This Brook rearrangement, after carbonyl addition of a nucleophilic reagent, involves migration of the silyl group from carbon to oxygen. It is reversible and thermodynamically controlled. Thus it is commonly observed in aroylsilanes due to the relative stabilization of the carbanion intermediate **3** by the aromatic ring.



Scheme II. 1: Brook rearrangement of aroylsilanes

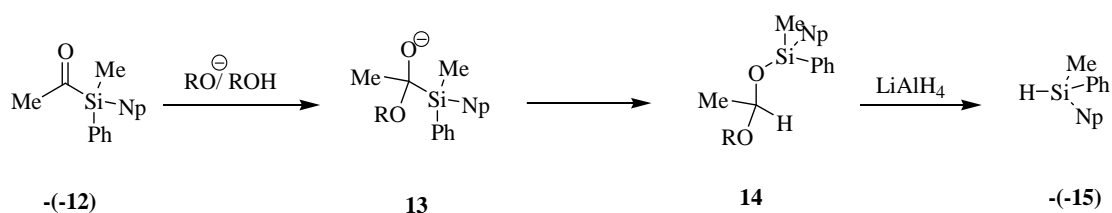
Brook studied the reaction mechanism for the nucleophilic attack of alkoxide on acylsilane group. He suggested two pathways **a** and **b** (shown in Scheme II.2).



Scheme II. 2: Proposed mechanism by Brook for the formation of aldehydes from acylsilanes

In pathway **a**, he suggested that the alkoxide ion attacks directly on the silicon atom of acylsilane **6** to afford aldehyde **9**. Another competitive pathway (pathway **b**) was proposed by Brook later, where the alkoxide ion attacks the carbonyl group of **6** to afford intermediate **10** that undergoes a rearrangement (so called now “Brook rearrangement”) and gives aldehyde **9** in the last step.

To know which pathway was more favorable, Brook used the optically active acylsilane (-)-**12** in reactions with different alkoxide ions, affording intermediates **14**. Then, reduction of **14** using LiAlH_4 gave (-)-**15** (Scheme II.3). Although the optical purities of (-)-**15** were observed to be depending on the bulk of the alkoxide ions used (EtO^- 22% vs. $t\text{-BuO}^-$ 65%), in all reactions with chiral acylsilane (-)-**12**, the enantiomer (-)-**15** was predominant, showing the retention of configuration at silicon. Therefore the bulkier alkoxides find it more difficult to attack at silicon and, consequently, the attack at the carbonyl group becomes relatively easier.

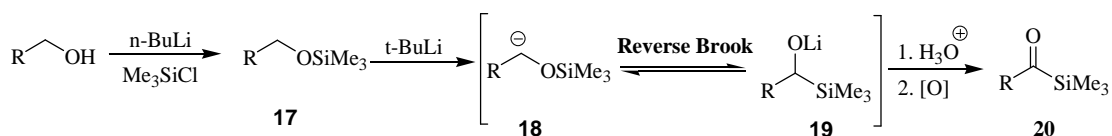


Np: Naphthyl

Scheme II. 3: Reaction of alkoxides with acylsilane **15**

In contrast, reverse Brook rearrangement (Scheme II.4) involves the transfer of silyl group from oxygen to carbon upon treating silyloxy intermediate **17** with $t\text{-BuLi}$. Then treatment of **19** with water followed by oxidation reaction ends up with the formation of acylsilane **20**.

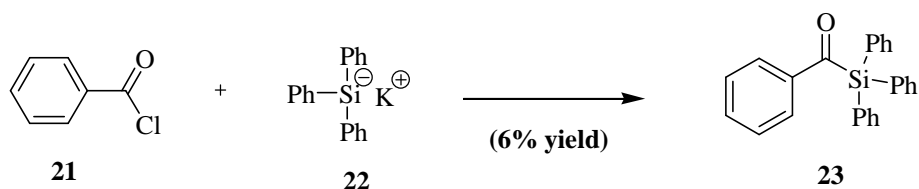
Reverse Brook rearrangement



Scheme II. 4: Reverse Brook rearrangement

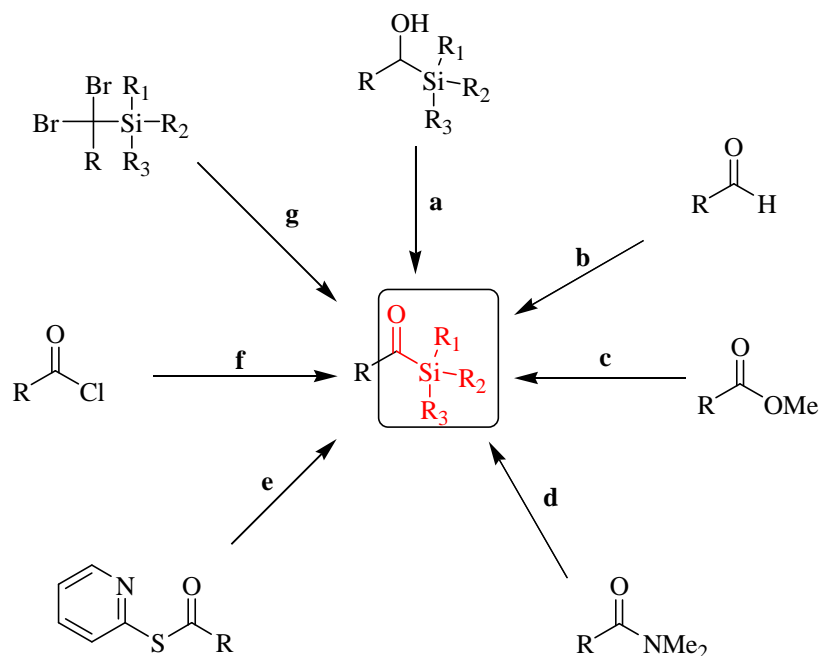
Synthesis of acylsilanes

As we mentioned at the beginning, the first acylsilane compound was reported by Brook in 1957, who prepared benzoyltriphenylsilane **23** from triphenylsilyl potassium **22** and benzoyl chloride **21** (Scheme II.5), albeit in only 6% yield.



Scheme II. 5: First acylsilane compound synthesized by Brook

The main problem in the synthesis of acylsilanes is the instability of these compounds, under many reaction conditions, which may lead to C-Si bond cleavage. Many methodologies for the synthesis of acylsilanes have been developed during the last decades [7]. Scheme 6 summarizes different methods established for the synthesis of this important and useful functional group and we will briefly comment these methods.

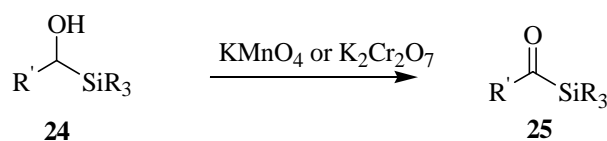


Scheme II. 6: Different methods for the synthesis of acylsilanes

Acylsilanes from α -silyl alcohols

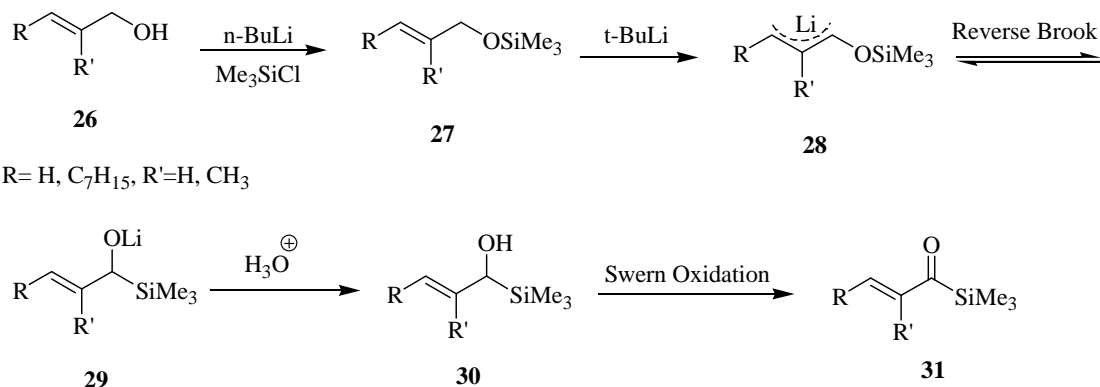
α -Silyl alcohols can be prepared by several methods, such as the condensation of trialkylsilyl anions with aldehydes [34] or the transmetalation of trialkylstannanes followed by a reverse Brook rearrangement [35].

The oxidation of α -silyl alcohol **24** with ordinary oxidizing reagents like potassium permanganate and chromic acid leads to acylsilanes **25** (Scheme II.7). However, this route has several limitations since a Si-C bond cleavage may compete [30], and the products may suffer over-oxidation to carboxylic acids.



Scheme II. 7: Acylsilane **25** from α -silylalcohols **24**

Very mild conditions, such as those present in Swern oxidation, are the most indicated options. In the example shown in Scheme II.8 [31, 36], the “reverse Brook rearrangement” (**28** to **29**), followed by a mild oxidation, is employed for the synthesis of α,β -unsaturated acylsilanes **31**.

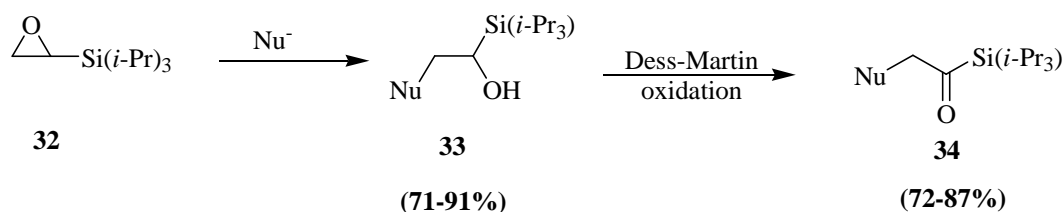


R= H, C₇H₁₅, R'=H, CH₃

(64-79% overall yield)

Scheme II. 8: Acylsilanes **31** from silylalcohols **30** using mild oxidation conditions

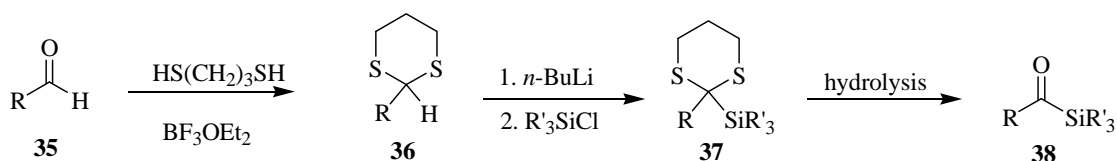
Silylalcohols **33**, prepared by nucleophilic opening of epoxides **32**, were oxidized under mild condition by the use of the Dess-Martin reagent, giving acylsilanes **34** in good to excellent overall yields (Scheme II.9) [37].



Scheme II. 9: Acylsilanes **34** from silylalcohols **33** using Dess-Martin oxidant

Acylsilanes from masked aldehydes

As we just mentioned above, the addition of silyllithium reagents to aldehydes gives α -silyl alcohols, which may be oxidized to acylsilanes. However, aldehydes **35** are more commonly converted into acylsilanes **38** by the dithiane route (the umpolung methodology, Scheme II.10).

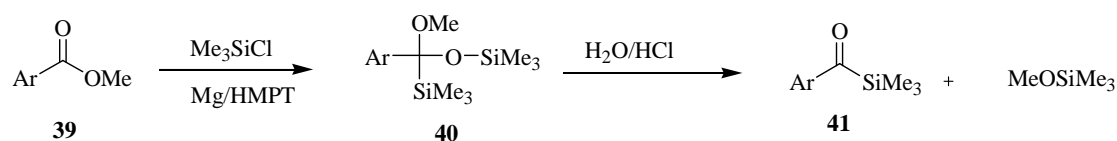


Scheme II. 10: Acylsilanes **38** from masked aldehydes **35**

The hydrolysis of 2-silyl-1,3-dithianes **37** was first investigated simultaneously by Brook [38] and Corey [39], and it is one of the most useful methodologies for the synthesis of acylsilanes. The great advantage of this method is the variety of compounds that can be prepared, including aroylsilanes, alkanoylsilanes, and functionalized acylsilanes. In general, the first and second steps (Scheme II.10) afford the products in high yields, but the hydrolysis step may be problematic. The most frequently applied method for the hydrolysis of 2-silyldithianes **37** are mercury salts (the oldest methodology) which is very slow, and thus causes degradation of the acylsilane product. For this reason, different methods have been developed, like treatment with methyl iodide [40], anodic oxidation [41], and oxidative hydrolysis mediated by *N*-bromosuccinimide [42], to regenerate the masked carbonyl group, giving acylsilanes in good yields.

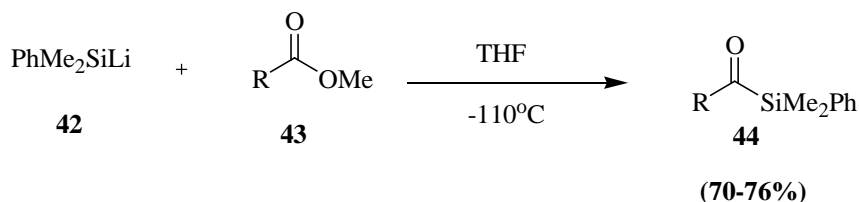
Acylsilanes from esters

Reductive silylation is also a known method for the synthesis of acylsilanes, proceeding by the reaction of esters with silyl-Grignard derivatives. This Grignard addition of a silyl nucleophile onto an ester leads to the formation of silylacetals **40** (Scheme II.11) [43], which upon hydrolysis with water in acidic medium gives the desired acylsilane **41**. However, this method generally gives poor yields and hence has been seldom employed.



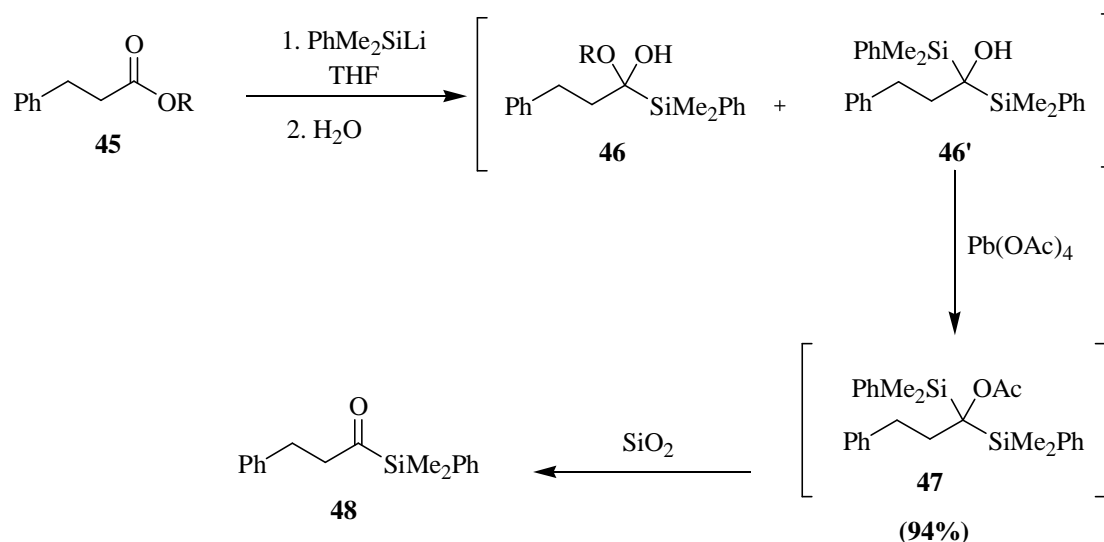
Scheme II. 11: Acylsilanes **41** from esters **39**

Compounds containing lithium attached to the silicon are extremely important reagents in organosilane chemistry. Dimethylphenylsilyllithium **42**, for example, is the most useful silyllithium derivative in these series. This is due to the aryl group that gives a good anion stability (at least one aryl group is required for this metalation procedure with Li metal) and also to the fact that this reagent can be readily prepared from the corresponding chlorodimethylphenylsilane by its reaction with lithium in THF [44]. On the other hand, trimethylsilyllithium is readily obtained by the reaction of hexamethyldisilane with methyl lithium [45]. These compounds react with esters at very low temperature only (around -110°C) to afford acylsilanes in good yields (Scheme II.12) [46].



Scheme II. 12: Acylsilanes **44** from esters **43** and silyllithium derivative **42**

Double nucleophilic attack of the silyllithium on the carbonyl group of ester yields the disilylalcohols as undesirable by-product (Scheme II.13).

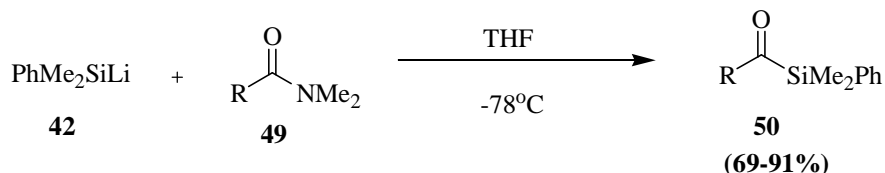


Scheme II. 13: oxidation of disilyl alcohols **46'** to afford acylsilanes **48**

These alcohols, such as **46'**, have been oxidized by PDC (pyridinium dichromate) [46], *tert*-butyl hypochlorite [47] and lead tetraacetate [48] (Scheme II.13) to the corresponding acylsilanes. This method involves a “radical Brook rearrangement”, providing acylsilanes in good yields after treatment with silica gel.

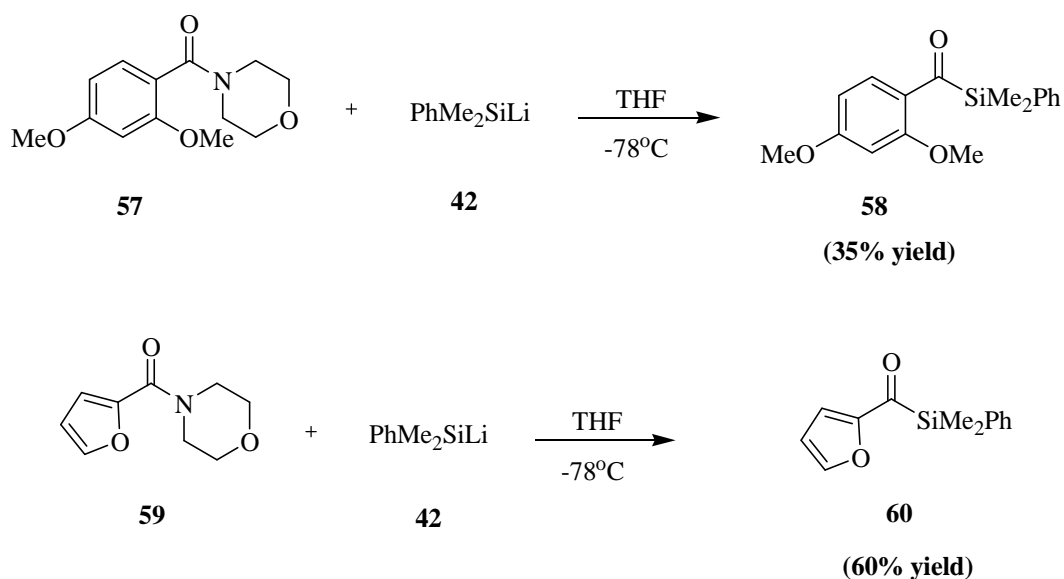
Acylsilanes from amides

Silyllithium compounds are also employed for the synthesis of acylsilanes from amides **49** (Scheme II.14) [46]. Amides appear to be more useful, since they give better yields than the traditional reaction with esters, which also requires much lower temperatures.



Scheme II. 14: Acylsilanes **50** from amides **49**

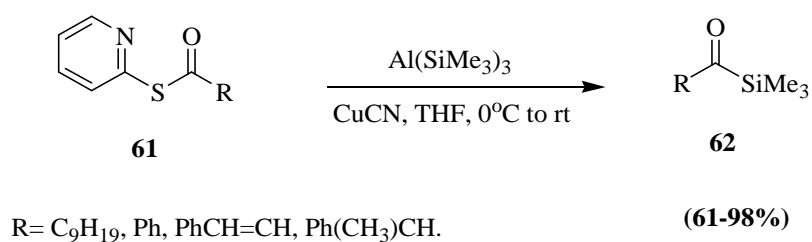
Morpholine amides, for instance, appears to be the best acylsilane precursors. Scheidt and coworkers [49] used morpholine amides **51** with silyllithium derivative **22** as the starting material for the synthesis of acylsilanes **50**. These authors suggested that this reaction occurs via a stable tetrahedral intermediate **52** (Scheme II.15). This approach



Scheme II. 17: Acylsilane using aromatic/heteroaromatic morpholine amide precursors

Acylsilanes from S-2-pyridyl esters

S-2-Pyridyl esters **61** react very smoothly with $\text{Al}(\text{SiMe}_3)_3$ in the presence of CuCN to afford acylsilanes **62** in good to excellent yields (Scheme II.18). This method is very useful and may be applied to substrates having various groups such as alkoxy, acetal, ester, or an isolated double bond [50].

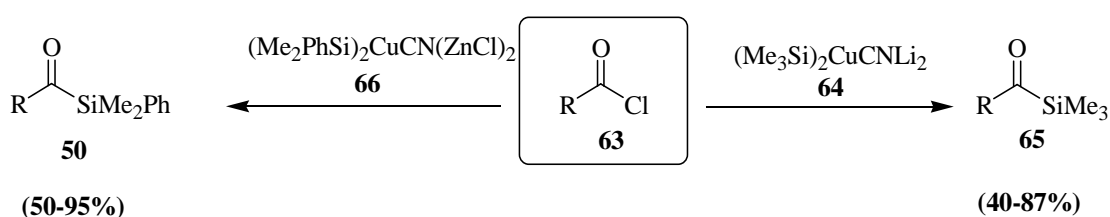


Scheme II. 18: Acylsilanes **62** from S-2-pyridyl esters **61**

Acylsilanes from acyl chlorides

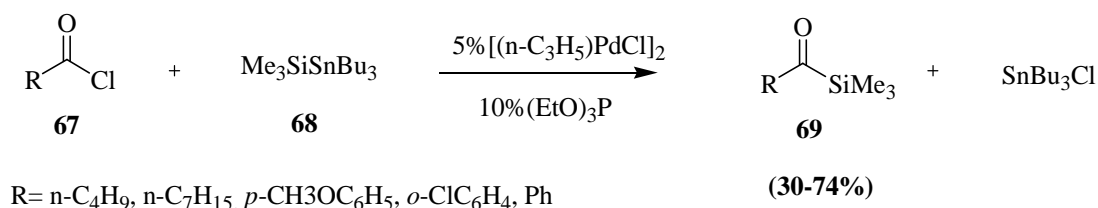
It is well known that the treatment of silyllithium derivatives with acid chloride could give acylsilanes, but this procedure is not useful due to the complex reaction mixtures that it provides. On the other hand, lithium silylcuprates like **64** (Scheme II.19) react

with a variety of acid chlorides, giving acylsilanes with good yields (40-87%), offering advantages over the silyllithium methodology since fewer by-products are formed [51]. These cuprates are traditionally obtained from the reaction of an alkylsilyllithium with CuCN or CuI [52]. But this methodology is very limited due to the use of high order cuprates which are very reactive towards a variety of functional groups. For this reason the mixed Cu-Zn complex **66** which is less reactive than ordinary cuprates could be used instead, affording the desired acylsilanes in moderate to excellent yields (50-95%). This type of method has been applied to the synthesis of acylsilanes containing cyano, halo, ester and other groups (Scheme II.19) [53, 54].



Scheme II. 19: Acylsilanes **50** and **65** from acyl chlorides **63**

Yamamoto and co-workers [55] used the reactions of disilanes (compounds with Si-Si bond) with benzoyl chloride under palladium catalysis to prepare aroylsilanes. But this method showed to be not suitable for aliphatic acylsilanes, since it gives very low yields of the desired products. Thus, an alternative methodology using polarized Si-Sn bond (weaker than the Si-Si bond in the disilanes), presented in Scheme II.20, was used, and provided both aroyl and alkanoylsilanes in good yields (up to 70%) [56].



Scheme II. 20: Acylsilanes **69** from acyl chlorides **67** using palladium catalyst

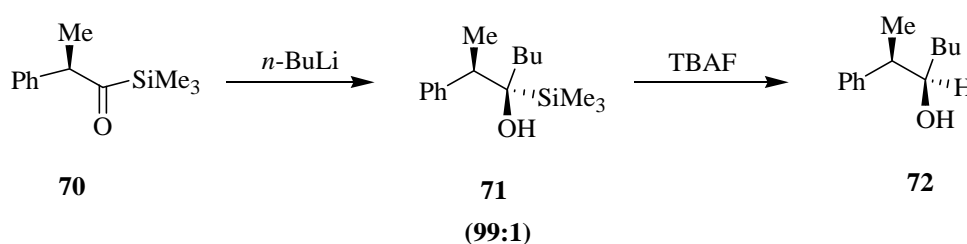
Reactions and uses of acylsilanes in organic synthesis

The use of acylsilanes in organic synthesis has increased significantly over the last two decades due to the discovery of valuable new reactions and the improvement of

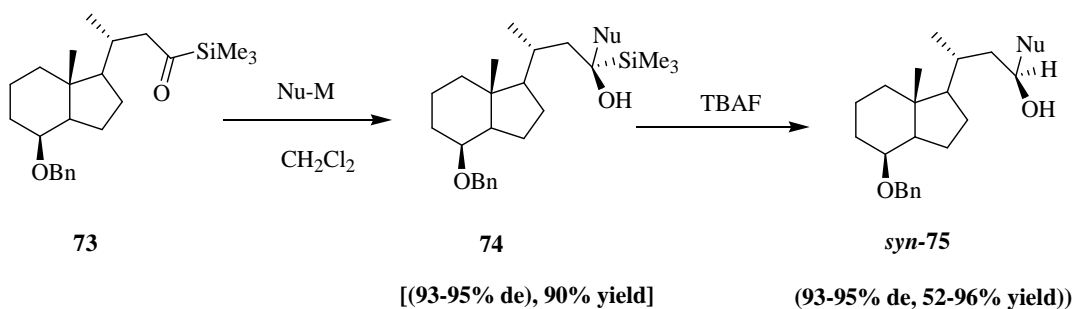
methods for acylsilane synthesis. The substantial effect of the electronic properties and the bulk of the silyl groups (possibly modulated by the nature of substituents), may be used to control the stereochemistry of reactions [57]. One of the well-established uses of acylsilanes in organic synthesis is to act as an aldehyde equivalent, in which a stereoselective nucleophilic attack on the carbonyl group, α to a chiral center, is followed by stereospecific replacement of the silyl group by hydrogen. Moreover, acylsilanes can be used as ester equivalents for chirality induction, since acylsilanes can be smoothly oxidized to esters.

Stereocontrolled nucleophilic additions on acylsilanes

The first study involving enantioselective addition to acylsilanes was reported in 1971 by Mosher [58], who used an optically active Grignard reagent to reduce benzoyltriphenylsilane and benzoyltrimethylsilane in low enantiomeric excess. Due to the relative facility for the removal of the silyl moiety and its replacement by hydrogen, acylsilanes can be considered as aldehyde equivalents in nucleophilic additions. Highly selective nucleophilic additions on acylsilanes bearing achiral center on the α -carbon as in **70** (Scheme II.21), and even on the β -carbon, as in **73** (Scheme II.22) were performed. In both cases, it was followed by a fluoride-induced desilylation process.



Scheme II. 21: Nucleophilic addition on acylsilane **70** bearing achiral center on the α -carbon

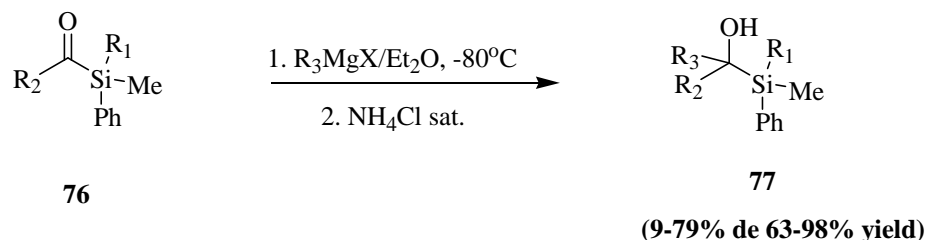


Nu-M = Allyl-SiMe₃, Methallyl-SiMe₃

Scheme II. 22: Nucleophilic addition on acylsilane **73** bearing achiral center on the β -carbon

In general, the protodesilylation (replacement of the R₃Si moiety by H) occurs with a high level of stereoselectivity, through the Brook rearrangement [59]. As shown in Scheme II.22, high stereocontrol was obtained in asymmetric induction in the synthesis of calcitriol lactone derivatives **75** [60].

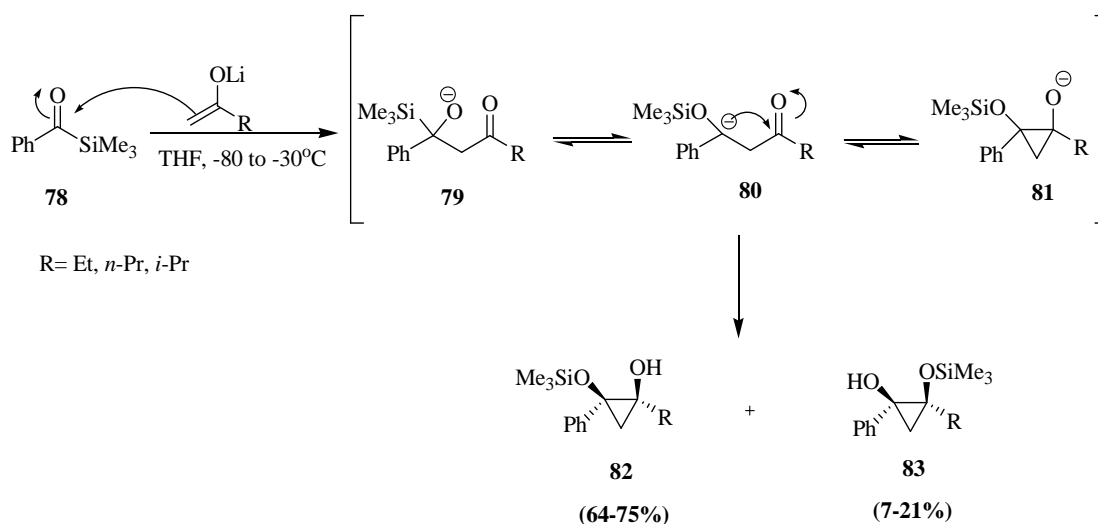
The addition of alkyl and phenyl lithium [61, 62] or Grignard reagents (Scheme II.23) [63] to acylsilanes **76** having a chiral center at silicon is also diastereoselective.



R₁= n-Bu, t-Bu, Np., R₂= Me, Ph., R₃= Me, Ph.

Scheme II. 23: Grignard additions on acylsilanes **76**

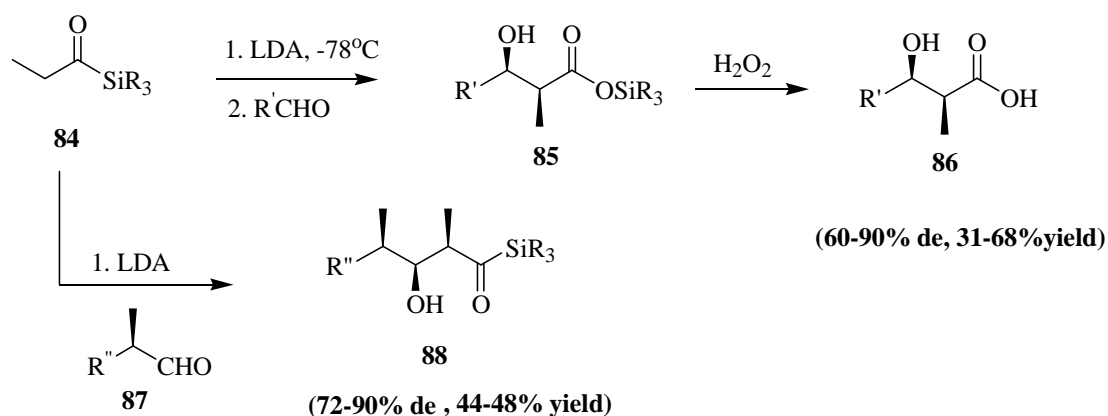
Cyclopropanediol monosilyl ethers **82** and **83** are obtained with good diastereoselectivity from the reaction of benzoylsilane **74** with lithium enolates derived from methyl ketones (Scheme II.24) [64].



Scheme II. 24: Addition reaction of lithium enolate on acylsilane **78**

Stereocontrolled aldol reactions of acylsilanes

Lithium enolates of propanoyl silanes **84** react with aryl and alkyl aldehydes to afford mainly *syn*- β -hydroxyacylsilanes **85**, which can be converted into **86** as the major products (Scheme II.25) in 31-68% overall yields [65]. While benzaldehyde gives a modest *syn/anti* ratio, isobutyraldehyde gives a good diastereoselectivity (*syn/anti* > 20). In addition, aldehydes having a chiral center on the α -carbon **87** react with **84**, giving **88** in good diastereoselectivities (72-90% de).

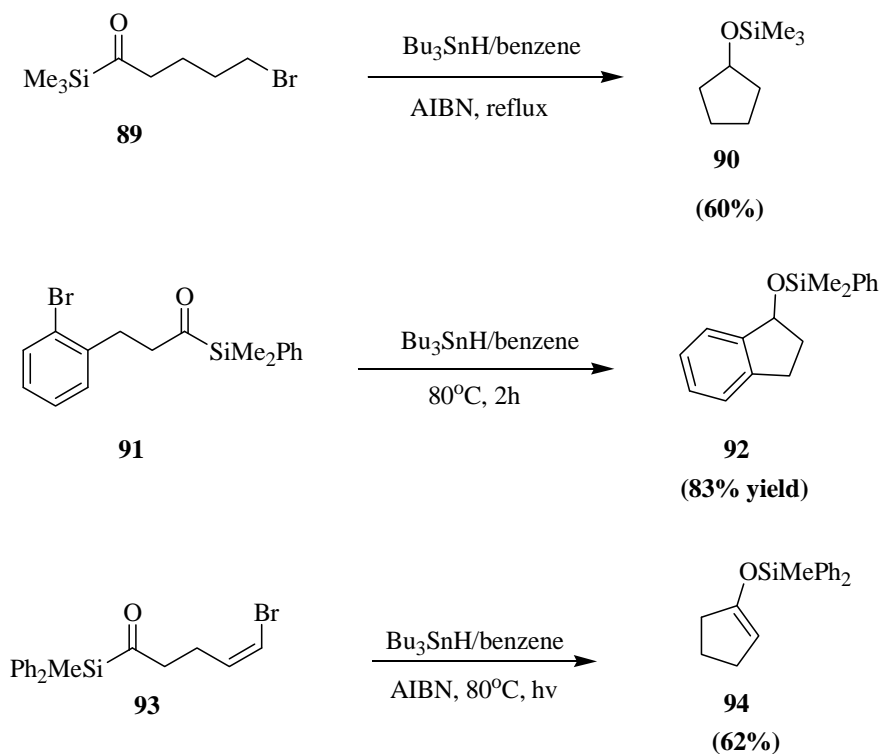


R = Et, R' = Ph, *i*-Pr, R'' = Ph, (CH₃)₂C=CH

Scheme II. 25: Diastereoselective aldolizations of acylsilane **84**

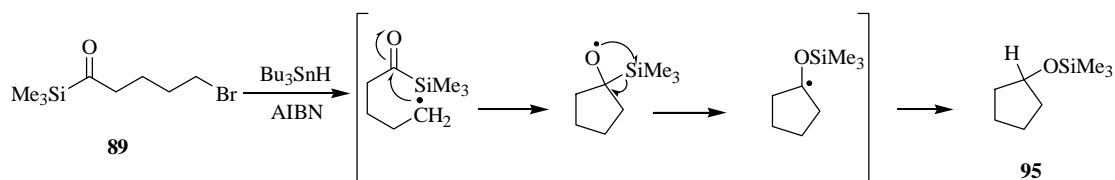
Acylsilanes in radical reactions

Radical reactions of acylsilanes have been also explored. For instance, trialkyltin radicals (Bu_3SnH) can promote intramolecular cyclization of acylsilanes **89**, **91**, and **93** which delivers alkyl, aryl and vinyl radicals, affording cyclopentyl silyl ethers **90** and **92** and enol silyl ether **94** (Scheme II.26) [66].



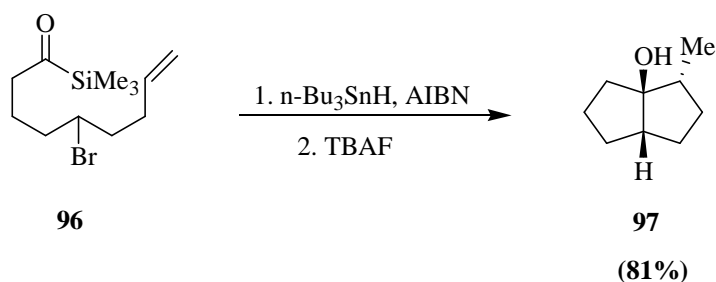
Scheme II. 26: Radical reactions of acylsilanes **89**, **91** and **93**

The mechanism of formation of **90**, **92** and **94** involves a radical Brook rearrangement, as shown in the example outlined in the Scheme II.27 [66c].



Scheme II. 27: Mechanism proposed for the radical reactions of acylsilanes.

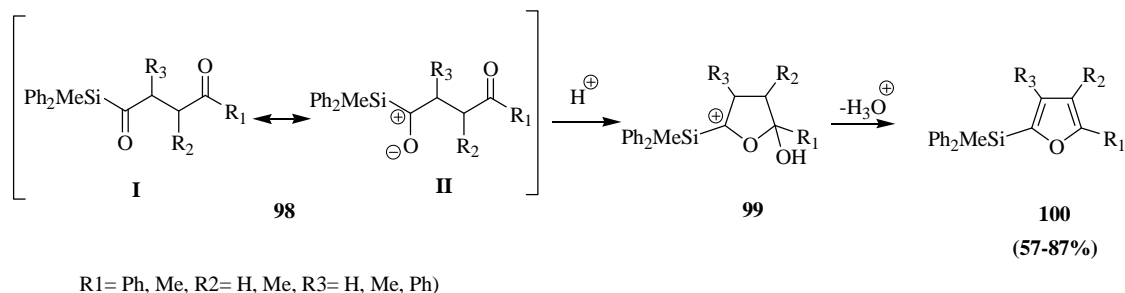
An interesting application of this method is the diastereoselective synthesis of *endo* bicyclic alcohol **97** from acylsilane **96** (Scheme II.28) [66a].



Scheme II. 28: Synthesis of bicyclic alcohol **97** from acylsilane **96** through a radical reaction

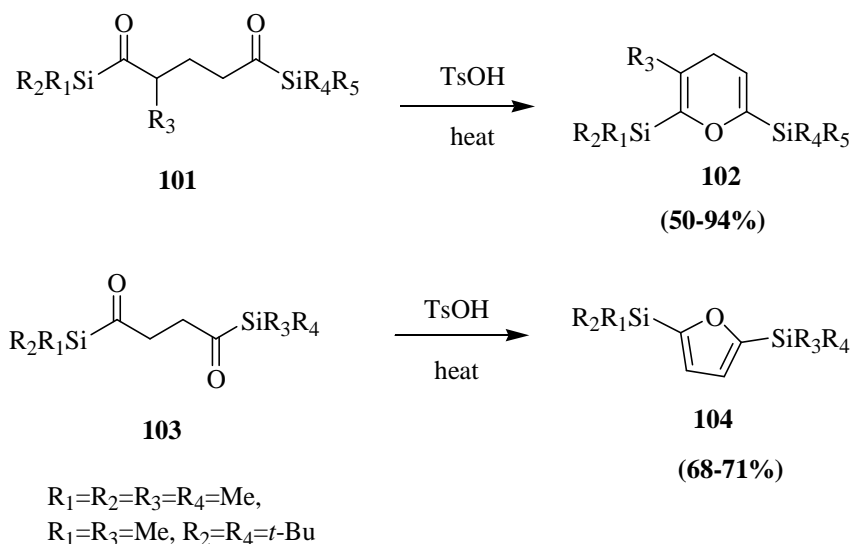
Cyclization reactions of acylsilanes

In addition to the examples mentioned before, many other cyclization reactions involving acylsilanes were developed. Acylsilanes **98** with a γ -carbonyl group provide furans **100** under milder conditions and in higher yields than the common cyclization reactions of dicarbonyl compounds. This advantage is derived from the high nucleophilicity of the oxygen atom in acylsilanes, due to the contribution of the polarized resonance form **II** (Scheme II.29) [67].



Scheme II. 29: Cyclization reaction of acylsilanes **98**

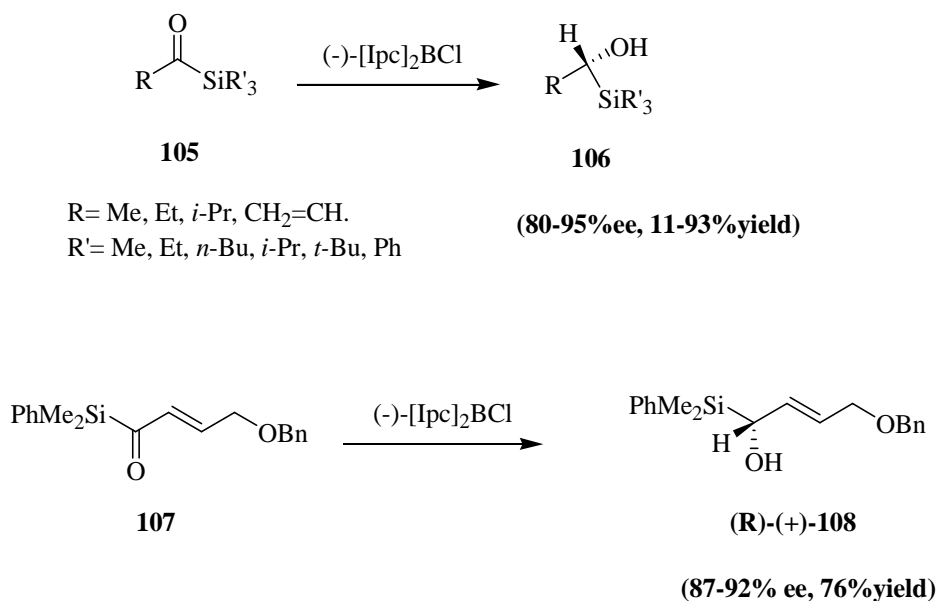
Furthermore, Scheme II.30 presents examples for the synthesis of bis-silylhydropyrans **102** and bis-silylfurans **104** through a similar cyclization of 1,5-bis-acylsilanes **101** [68] and 1,4-bis-acylsilanes **103** [69] respectively, catalyzed by *p*-toluenesulfonic acid (TsOH).



Scheme II. 30: Cyclization of bis-silyl compounds **101** and **103** using *p*-TsOH as a catalyst

Enantioselective reduction of acylsilanes

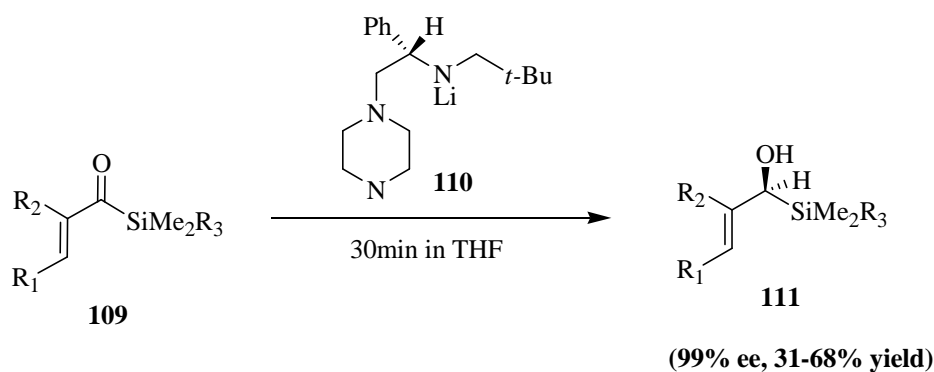
Chiral boranes have been used for the enantioselective reduction of acylsilanes affording optically active alcohols (Scheme II.31) [70, 71].



(-)-[Ipc]₂BCl: (-)-B-chlorodiisopinocampheylborane

Scheme II. 31: Enantioselective reduction of **105** and **107** using a chiral borane

In addition to that, an unusual reduction of α,β -unsaturated acylsilanes **109**, shown in Scheme II.32, was also performed. It is mediated by the chiral lithium amide **110** affording alcohols **111** in excellent enantiomeric excesses through hydride transfer from chiral lithium amide [72].



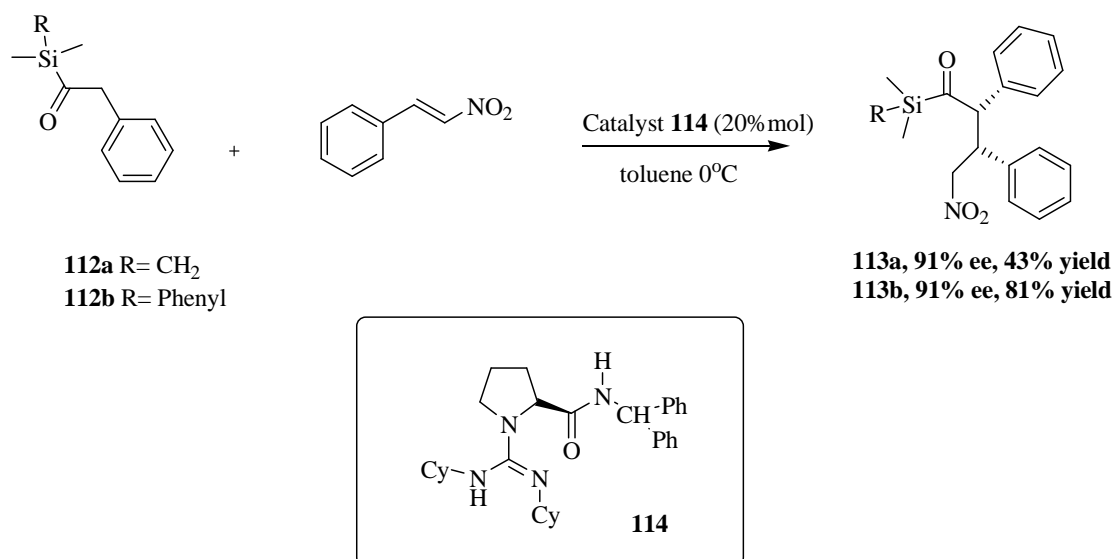
$\text{R}_1 = \text{Me}, i\text{-Pr}, -(\text{CH}_2)_3, \text{R}_2 = \text{H}, \text{R}_3 = t\text{-Bu or Ph}$

Scheme II. 32: Enantioselective reduction of α,β -unsaturated acylsilane **109** using chiral lithium amine **110**

Organocatalytic asymmetric Michael reactions with acylsilane donors

As we know, Michael reactions are among the most powerful and efficient methods for carbon-carbon bond formation. In particular, the development of organocatalytic asymmetric Michael reactions of carbonyl compounds with nitroalkenes has generated great interest in recent years [73-77]. Asymmetric Michael reactions using acylsilanes as donors showed to be very interesting, affording diverse and structurally complex α -alkyl acylsilanes with high diastereo- and enantioselectivity.

Chiral guanidines characterized by high pKa values and hydrogen-bonding activation, proved to be efficient catalysts for enantioselective reactions with acylsilanes [78-80]. Thus different substituents on guanidine catalysts were studied, but **114** (Scheme II.33) gave the best results with 99:1 dr and 91% ee.



Scheme II. 33: Organocatalyzed Michael reactions

Feng and co-workers [82] suggested that the nitroolefin and the acylsilane substrates, might be activated simultaneously by the guanidine catalyst **114** (Figure II.2), and the NH proton of the amide moiety is vital for the high activity and enantioselectivity. As illustrated in Figure II.2, the guanidine moiety of the catalyst likely functions as a base, thus enabling intracomplex deprotonation, while the N–H moiety of the amide in the catalyst might act as a Brønsted acid to activate the Michael acceptor.

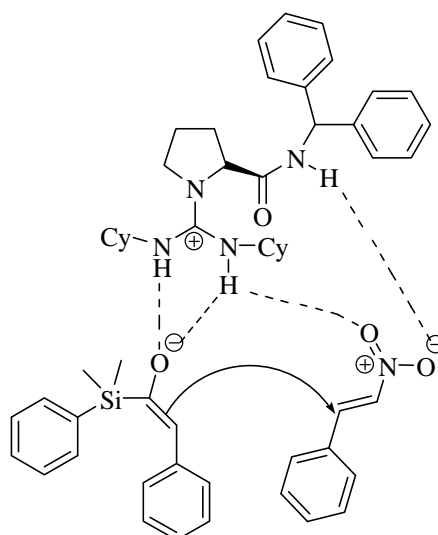
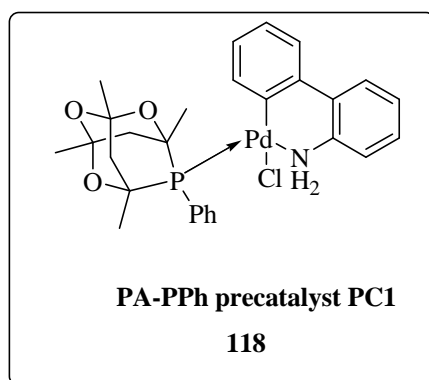
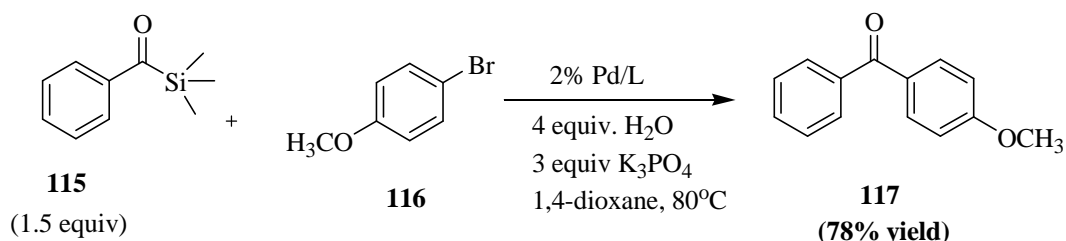


Fig. II. 2: The proposed dual activation mode of guanidine **114** catalyzed Michael reaction between an acylsilane and a nitroolefin.

Palladium catalyzed cross coupling reaction of acylsilanes

Palladium-catalyzed cross-coupling reactions are also one of the most powerful tools for carbon carbon bond formation [83]. Accordingly, Pd catalysis has been used extensively in the formation of aryl-aryl, alkyl-aryl, and alkyl-alkyl ketones. Many reports describe the formation of ketones by coupling activated carboxylic acid derivatives with various transmetalating reagents [84] or via carbonylative coupling of an aryl halide with an organometallic species [85].

Acylsilanes serve as acyl anion equivalents in a palladium-catalyzed cross-coupling reaction with aryl bromides to give unsymmetrical diaryl ketones. Water plays a unique and crucial activating role in these reactions. Thus in a successful development of Pd-catalyzed cross coupling between arylsilanes and aryl bromides, using phosphonate ligand **118**, the corresponding unsymmetrical diaryl ketone **113** was obtained in good yield (78%) (Scheme II.34) [86].

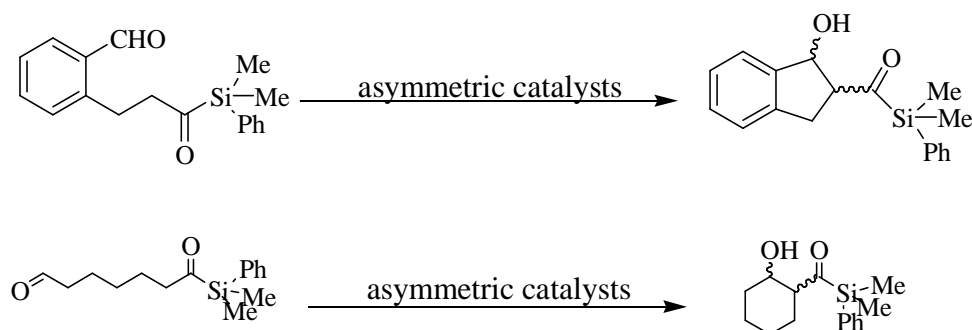


Scheme II. 34: Pd-catalyzed cross coupling reaction of arylsilane **11**

II.B. OBJECTIVE AND STRATEGY

Objective and strategy

The major goal of our research in this area was to perform **asymmetric catalytic intramolecular aldol** reactions on acylsilane derivatives bearing an aldehyde functional group in a remote position within the same molecule. Scheme II.35 shows the two different acylsilanes that we choose as model substrates to explore this type of aldol reaction.



Scheme II. 35: Intramolecular aldol reaction starting from bifunctional acylsilane-aldehyde molecules

Therefore, the first step of our research was the preparation of such key intermediates, previously unknown, bearing both the acylsilane unit and the carbonyl moiety in a remote position. For this purpose, we focused our attention on the addition reaction of dimethylphenyl silyllithium into the morpholine amide group.

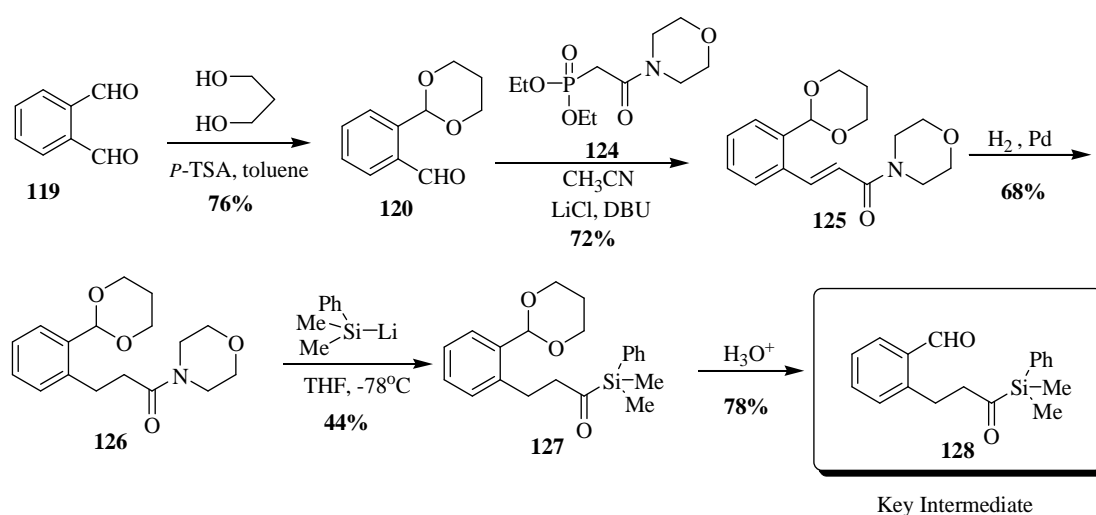
II.C. RESULTS AND DISCUSSION

Results and discussion

Our first goal was to prepare the key intermediates for the asymmetric intramolecular aldol reaction, with the acylsilane group and the remote aldehyde on the same molecule, thus two models were selected for this purpose. The first model includes the use of an aromatic linker (starting from commercially available *o*-phthalaldehyde), while the second model includes the use of an aliphatic linker (starting from commercially available 2, 3-dihydropyran).

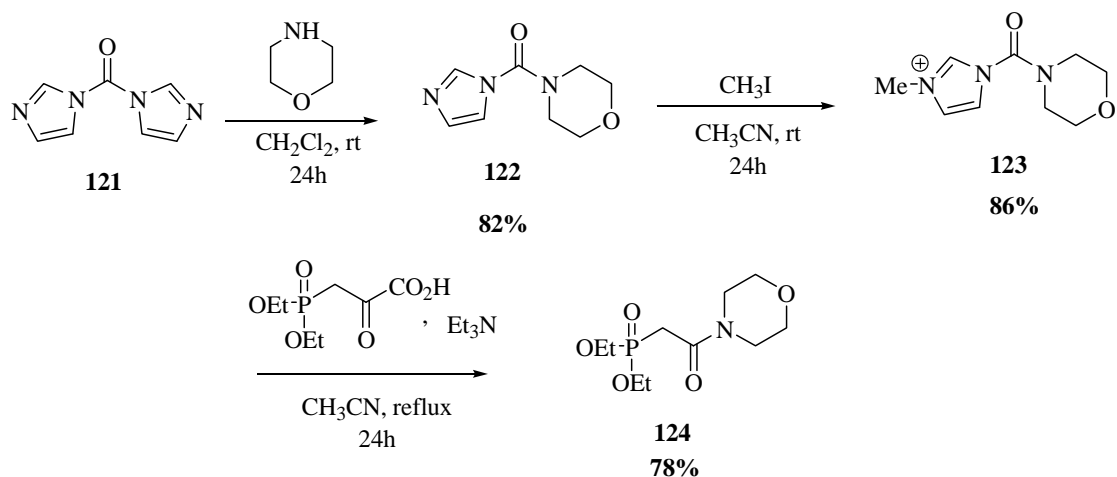
1. Synthesis of model 1 with aromatic linker

For the first model, we succeeded in obtaining the desired acylsilane intermediate **128** through five steps, according to the sequence described in Scheme II.36:



Scheme II. 36: preparation of the key intermediate **128**

Protection of *o*-phthalaldehyde **119** with propan-1, 3-diol and *p*-TSA using a Dean-Stark apparatus [87] gave two major products, the mono-protected aldehyde (lower polarity according to the TLC plate) and the di-protected one, and these two products could be easily separated by column chromatography affording 76% of the desired mono-protected aldehyde **120**.



Scheme II. 37: Synthesis of phosphonate amide **124**

As shown in scheme II.37, phosphonate amide **124** could be easily obtained in a three steps reaction sequence, following the procedures described in the literature [91], and the structures of **122**, **123**, and **124** were established by comparison of their spectral data with the literature.

Then a Horner-Wadsworth-Emmons (HWE) reaction between aldehyde **120** and phosphonate amide **124** in the presence of LiCl and DBU in CH₃CN (Scheme II.36) gave the desired α,β -unsaturated amide **125** in 72% yield [88]. ¹H NMR spectrum of the crude product shows the presence of the *trans* isomer only, which was purified by chromatography and obtained in 72% yield.

The structure of **125** was confirmed by ¹H NMR (Figure II.3), that shows the peaks of two vinylic protons as two doublets at 8.16 ppm and at 6.74 ppm with the same coupling constant of 15.3 Hz, which refers to the *trans* configuration of the double bond. In addition, the typical methine proton of the acetal group appears as a singlet at 5.75 ppm.

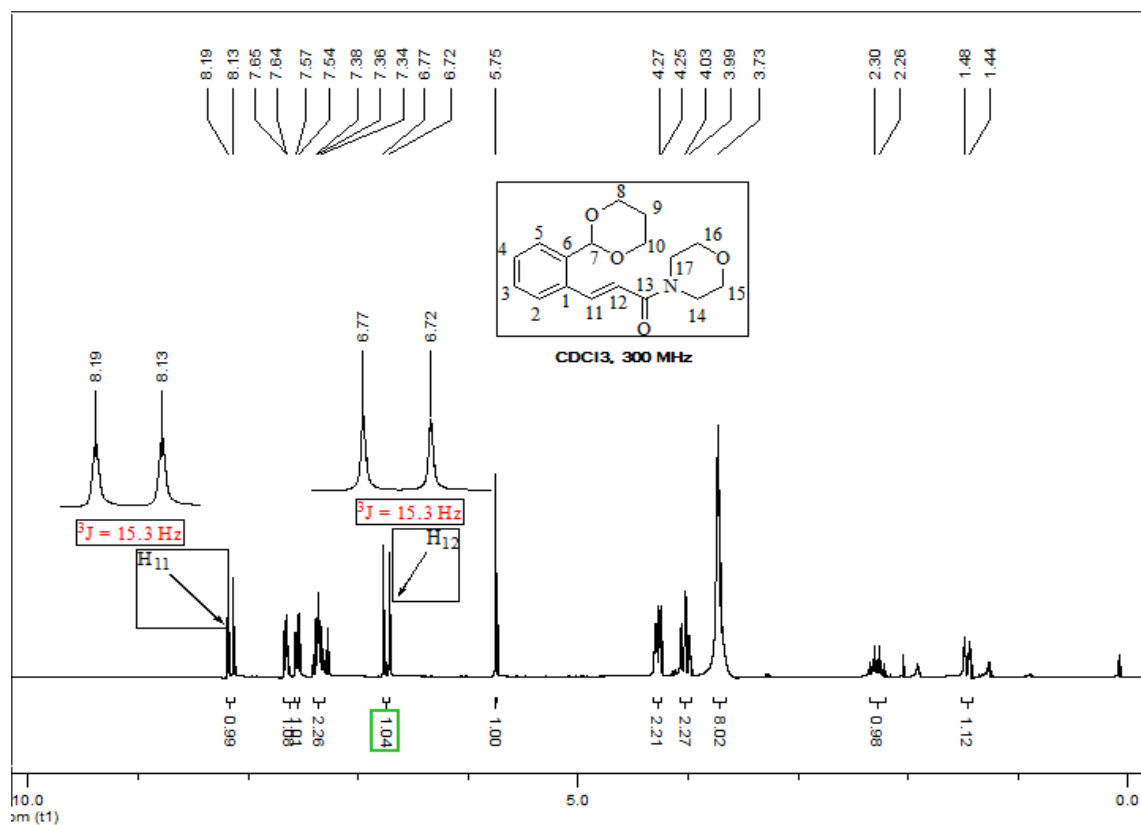


Fig. II. 3: ^1H NMR spectrum of α,β -unsaturated amide **125**

In the following step, hydrogenation of the double bond was required. Thus, compound **125** was treated with palladium on carbon under hydrogen atmosphere [89] affording the amide **126** in 68% yield. The ^1H NMR spectrum of **126** shows the disappearance of the two doublets at 8.16 ppm and at 6.74 ppm, and appearance of two triplets at 3.12 and 2.64 ppm each with coupling constants of 7.3 Hz (Figure II.4), which correspond to the newly formed two methylene groups.

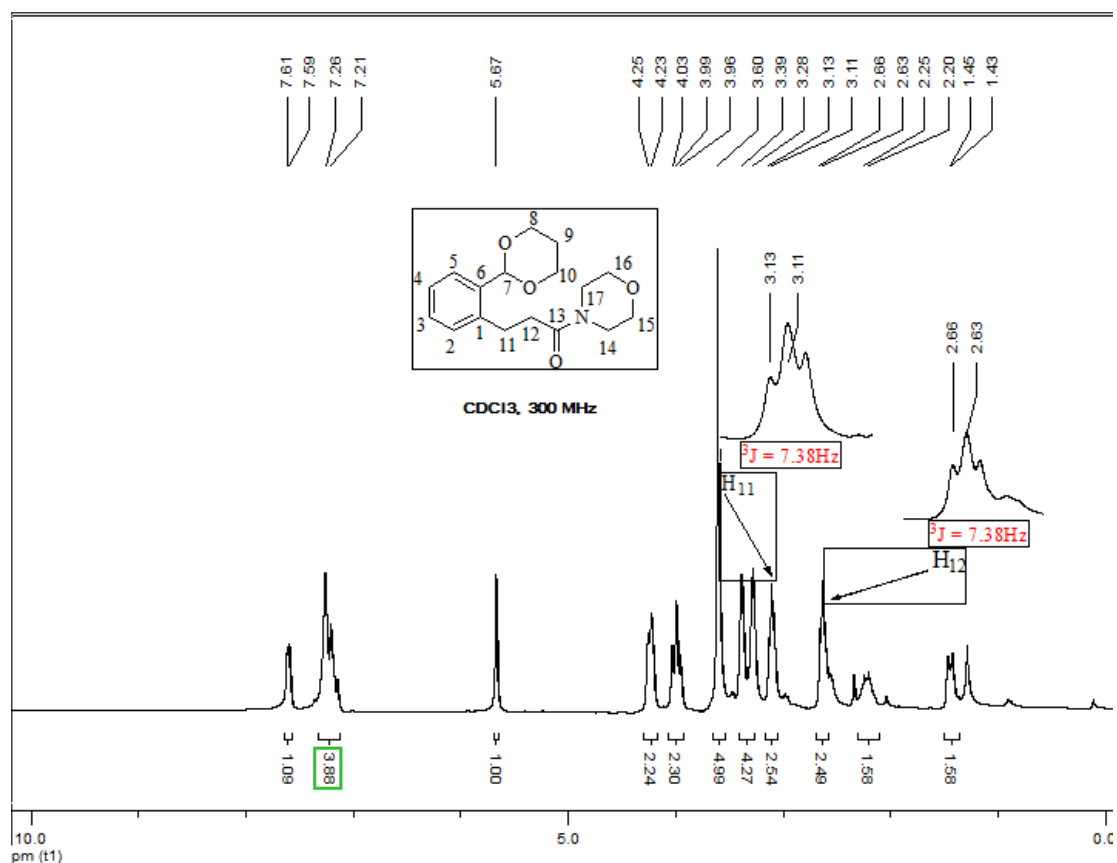


Fig. II. 4: ^1H NMR spectrum of saturated amide **126**

Having amide **126** in hands, we could now perform the addition reaction of the silyllithium derivative. Thus dimethylphenylsilyllithium, prepared from the commercially available chloro(dimethyl)phenylsilane, according to the literature procedure [90], was added slowly to **126** in THF at -78°C for 3-4h. Acylsilane **127** could be easily detected as a pink spot on the TLC plate, but different side products were also seen in the crude mixture and having very close R_f to the acylsilane **127**, which makes the separation difficult. Furthermore, this silyllithium addition was performed different times to optimize the yield from 12% to 44%.

The structure of acylsilane **127** was established by ^1H NMR (Figure II.5), where the two methyl groups attached to silicon atom appeared as two singlets at 0.48 and 0.41 ppm, and the four protons of the two methylene groups appeared as one multiplet at 2.90 ppm.

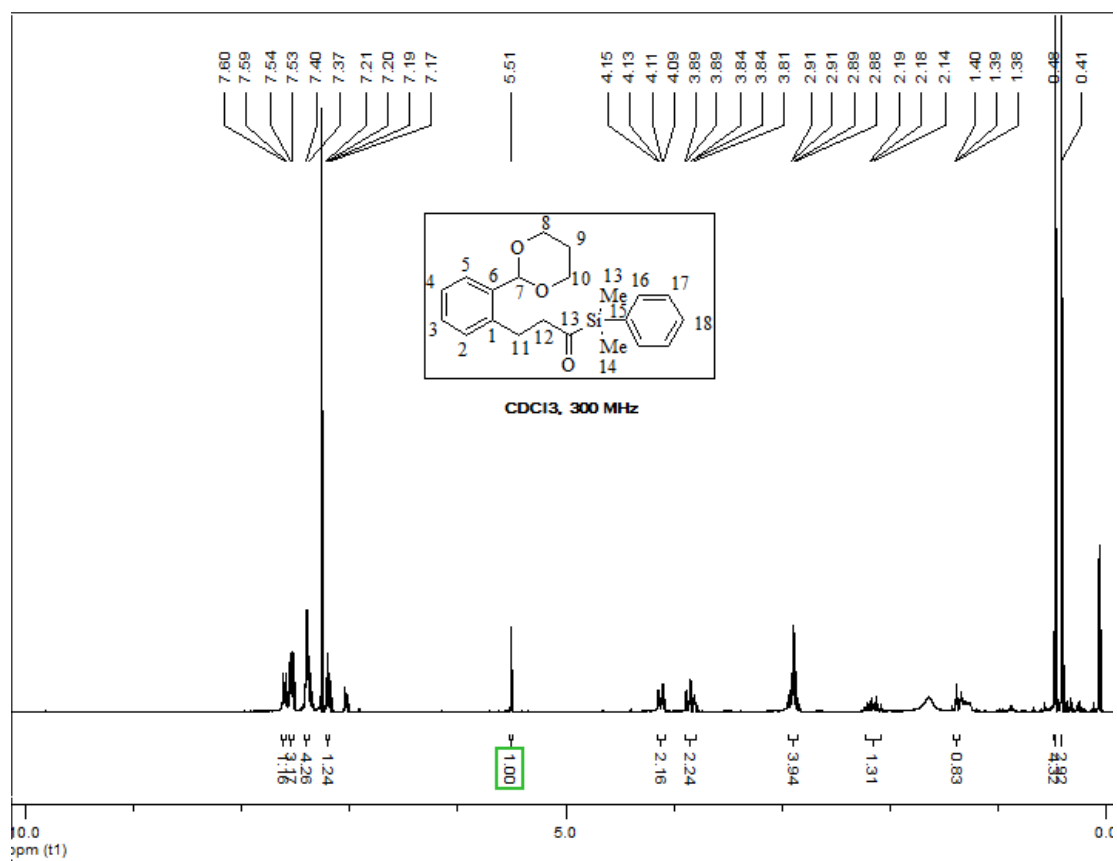


Fig. II. 5: ^1H NMR spectrum of acylsilane **127**

The last step to reach our desired acylsilane intermediate **128** was the hydrolysis of the acetal to unmask the aldehyde group. Therefore, acylsilane **127** was treated with a solution of hydrochloric acid (37%) in water and acetone to give the desired key intermediate **128** in 78% yield. The structure of **128** was confirmed by ^1H NMR (Figure II.6), which shows the presence of the aldehyde proton as a singlet at 10.12 ppm, and the disappearance of acetal protons signals, particularly the one that appears at 5.51 ppm.

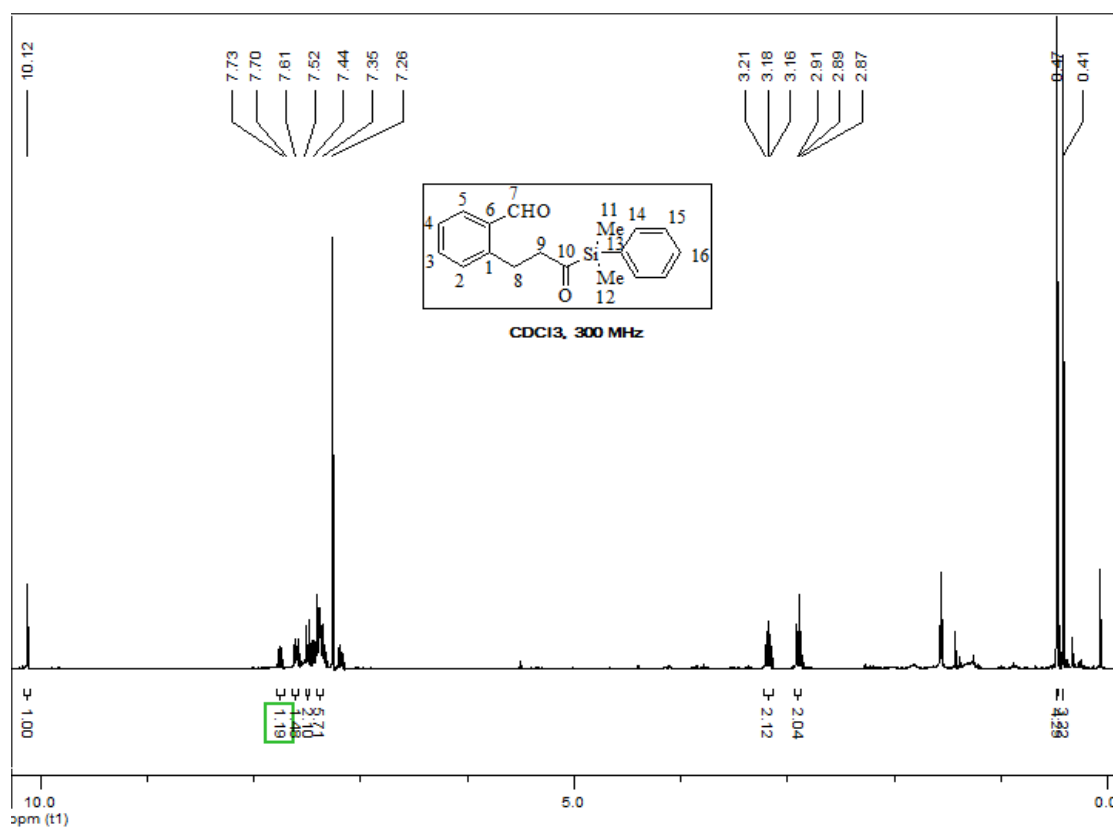
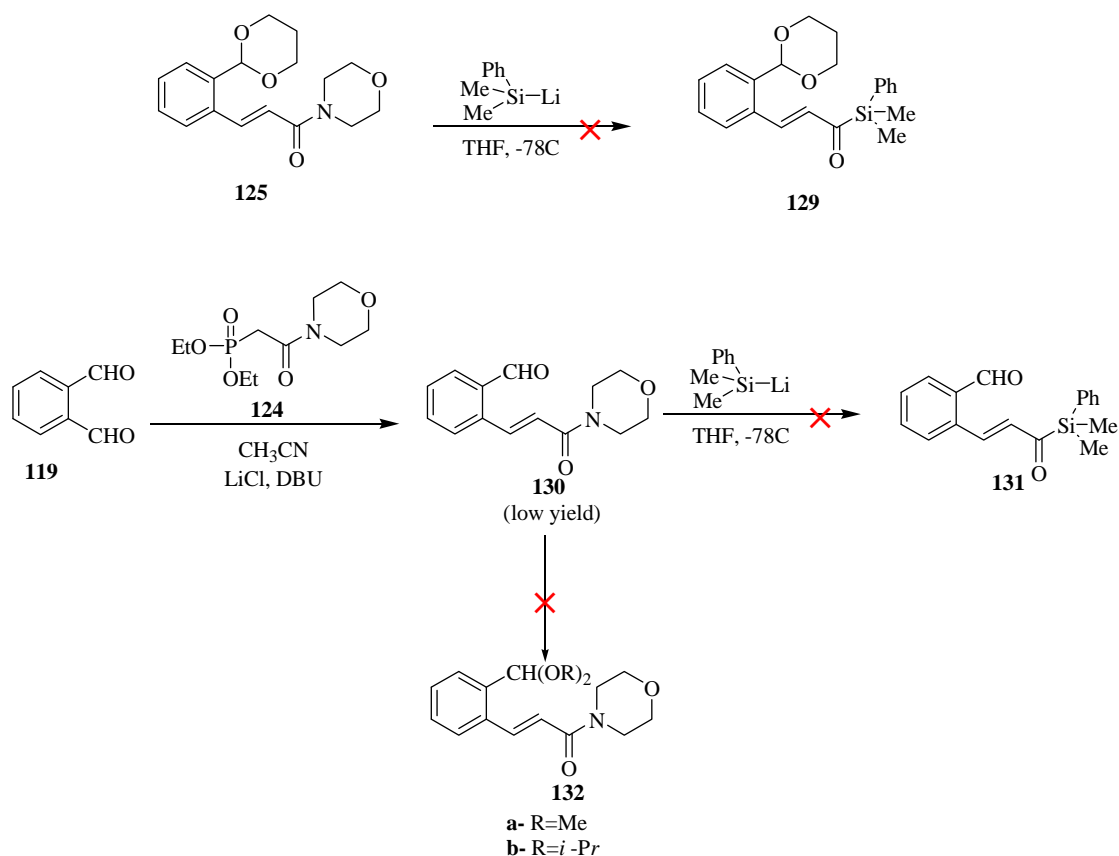


Fig. II. 6: ^1H NMR spectrum of the key intermediate **128**

It is important to note that, the addition of dimethylphenylsilyllithium was first performed on the conjugated amide **125**, before reducing the double bond (Scheme II.38), but unfortunately it was difficult to recover the conjugated system of acylsilane group, that's why we decided to hydrogenate the double bond first in order to get rid of the conjugated system that might affect the addition reaction of silyllithium.

On the other hand, and as a second attempt to obtain conjugated system of acylsilane, we tried to perform HWE reaction directly on the starting *o*-phthalaldehyde **119**, and we succeeded in obtaining the desired conjugated amide **130**, however in a very low yield (Scheme II.38).



Scheme II. 38: Direct addition of phosphonate **124** on the starting *o*-phthalaldehyde **119**

The recovered quantity of **130** was then treated with dimethylphenylsilyllithium in order to obtain the conjugated acylsilane derivative **131**, but the addition reaction didn't work in this case (Scheme II.38).

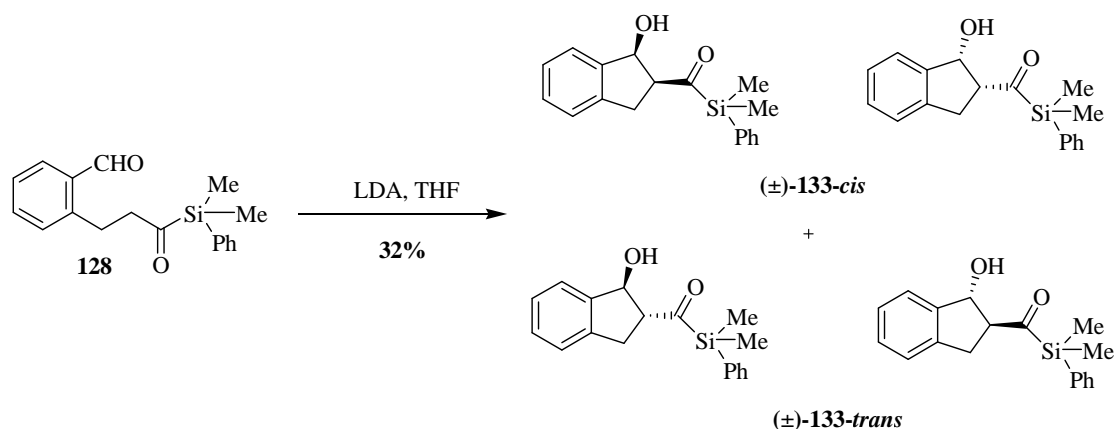
For this reason we tried to protect the aldehyde group that might affect or react with the added silyllithium, so aldehyde **130** was treated with methanol to get the acetal product **132a** (Scheme II.38), but the protection didn't work. Another attempt for such protection was performed using isopropanol to get acetal **132b**, but this didn't work too, and thus we could not get the desired acetal **132**.

Since we couldn't recover the conjugated system of silyllithium in this case, we focused our attention on the preparation of the non-conjugated acylsilane intermediate **128** as shown previously in scheme II.36.

2. Asymmetric intramolecular aldol reactions for model 1

Now, having acylsilane **128** in hand, we were ready to attempt the asymmetric intramolecular aldol reaction through different approaches, as described below.

The first point was to obtain authentic samples of the desired molecules in racemic form and this could be performed by using a simple aldol reaction, using LDA (1.2 equiv) as a base.



Scheme II. 39: Intramolecular aldolization reaction of **128** using LDA as a base

This reaction gave the desired indanols (±)-**133-cis** and (±)-**133-trans** but unfortunately these two diastereoisomers could not be separated by chromatography. The aldol reaction occurs with around 2:1 diastereoselectivity, but since these stereoisomers have not been separated and the NMR spectra of the mixture are complex, their *cis* or *trans* stereochemistry could not be established unambiguously.

Then, in an attempt to perform asymmetric intramolecular aldol reaction, the first trial was the use of mixed organocatalysts, a quinidine-derived molecule and proline (Figure II.7) both together, following literature procedures [91]. However, it is well known in the literature that asymmetric organocatalysis has two major pathways: the first, and the most commonly used one, is the enamine pathway by using proline-derived organocatalysts and other similar compounds, while the second, by H-bonding catalysis, where the thiourea-type catalysts are most representative examples.

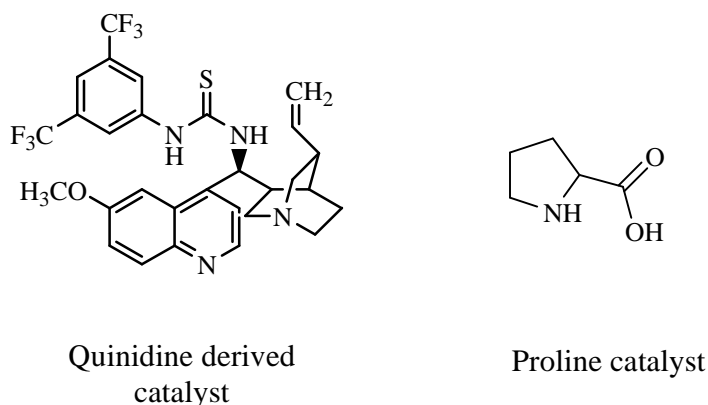
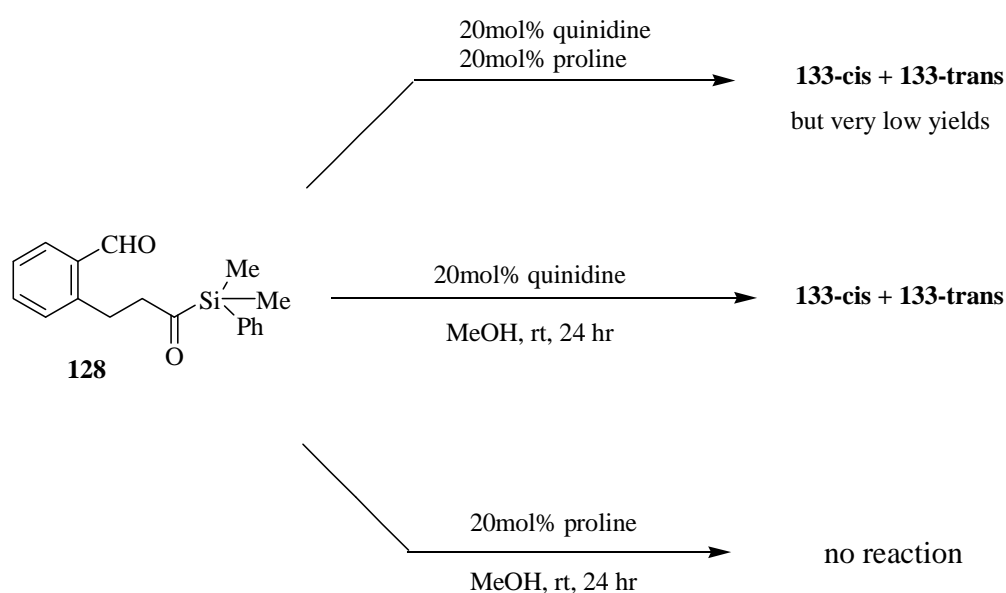


Fig. II. 7: Quinidine and proline catalysts

In some cases the two types of organocatalysts were combined and a very good example is the one reported by Zhao and coworkers [91], which was an important guideline for us at the beginning of our studies with acylsilanes.

Thus, our acylsilane key intermediate **128** was treated first with 20 mol% of quinidine/proline combined catalyts in methanol as shown in scheme II.40. But only a very slight formation of the desired product was detected by NMR.

On the other hand, the treatment of acylsilane intermediate **128** with the quinidine-derived catalyst alone was much more effective in the aldolization reaction, since we can easily detect by NMR of the crude reaction mixture the peaks of the two isomeric aldol product **133-cis** and **133-trans**. However, since they could not be separated easily, it has not been possible to establish the enantiomeric excess of this reaction.

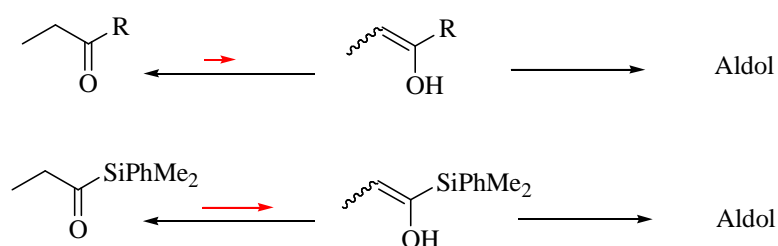


Scheme II. 40: Intramolecular aldolization using quinidine-derived catalyst

Finally, treatment of our key intermediate **128** with the proline catalyst alone didn't give any trace of the aldol products (Scheme II.40). Thus, the obvious conclusion of these interesting and useful preliminary experiments is that the acylsilane scaffold is not a suitable substrate for proline or amino acid-derived organocatalysis. Therefore, in our case, the best conditions for the intramolecular aldol reaction are the use of the quinidine-type catalyst alone.

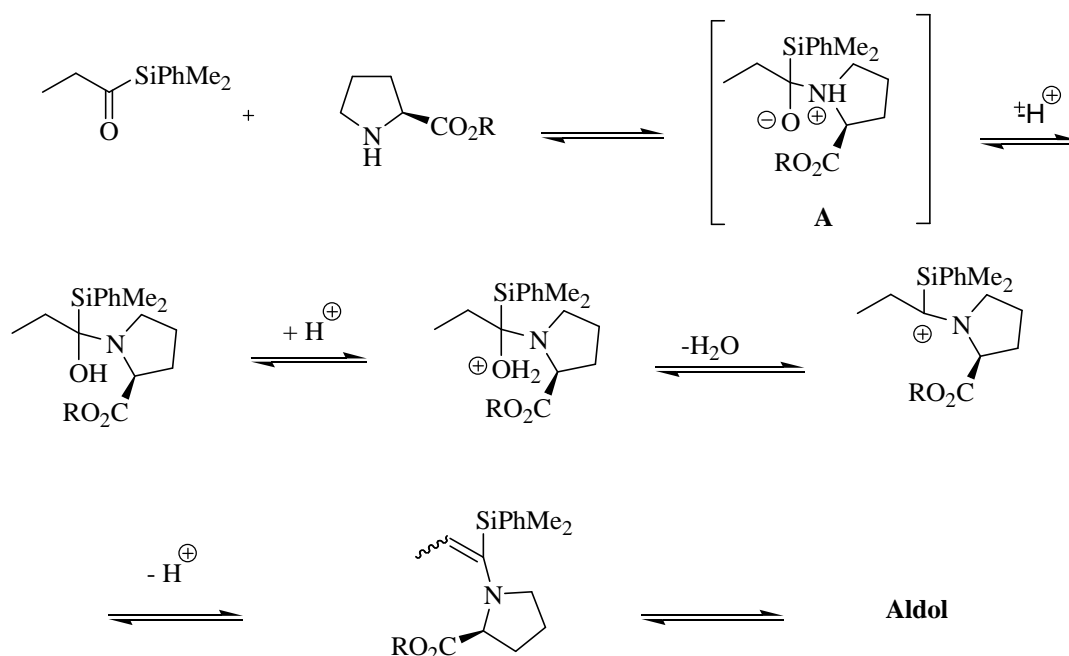
These results obtained with thiourea-derived catalyst were very exciting, since this type of catalyst (alone) has been used for several reactions like 1,4-addition reaction, but it has not been used for simple aldol reactions, possibly due to the other classical enamine pathway that was very successful.

Furthermore, the significance of thiourea-derived catalyst is that, it is working in the aldolization reaction of acylsilanes and not with a simple ketone. However, it is well known that the aldolization reaction of ketone could be generated either by enolate or enol nucleophilic species. Therefore an attractive possibility would be in the case of acylsilanes, to consider the enol contents. In that case, the keto-enol equilibrium could be somewhat more shifted to the right in the case of acylsilanes (Scheme II.41) [92], and since more enols are in the reaction mixture, ready for the next step (the aldol reaction), better yields and selectivities could be obtained.



Scheme II. 41: comparison of enol contents between ketone and acylsilane

At this stage, we do not have a clear explanation for the failure of asymmetric organocatalysis using proline derived catalyst, but if we follow the enamine pathway transposed to acylsilanes, as shown in the scheme below, some potential problems could explain this phenomenon.



Scheme II. 42: Mechanism for enamine formation

For instance, the nucleophilic addition of amino acid in the first step might be problematic in the case of acylsilanes, due to electronic effect of silicon (since it has lower electronegativity than carbon). On the other hand, at intermediate **A**, there is a possibility of competitive Brook rearrangement, which is often taking place in the case of acylsilanes. So, different factors could affect the aldolization reaction of acylsilane using proline catalyst.

The ¹H NMR spectrum of the *cis* and *trans* mixture of **133**-indanol (Figure II.8) shows in addition to the signals corresponding to the aromatic protons and the methyl groups, a signal at 5.24 ppm with a coupling constant of 7.2 Hz corresponding to the methine proton next to OH group.

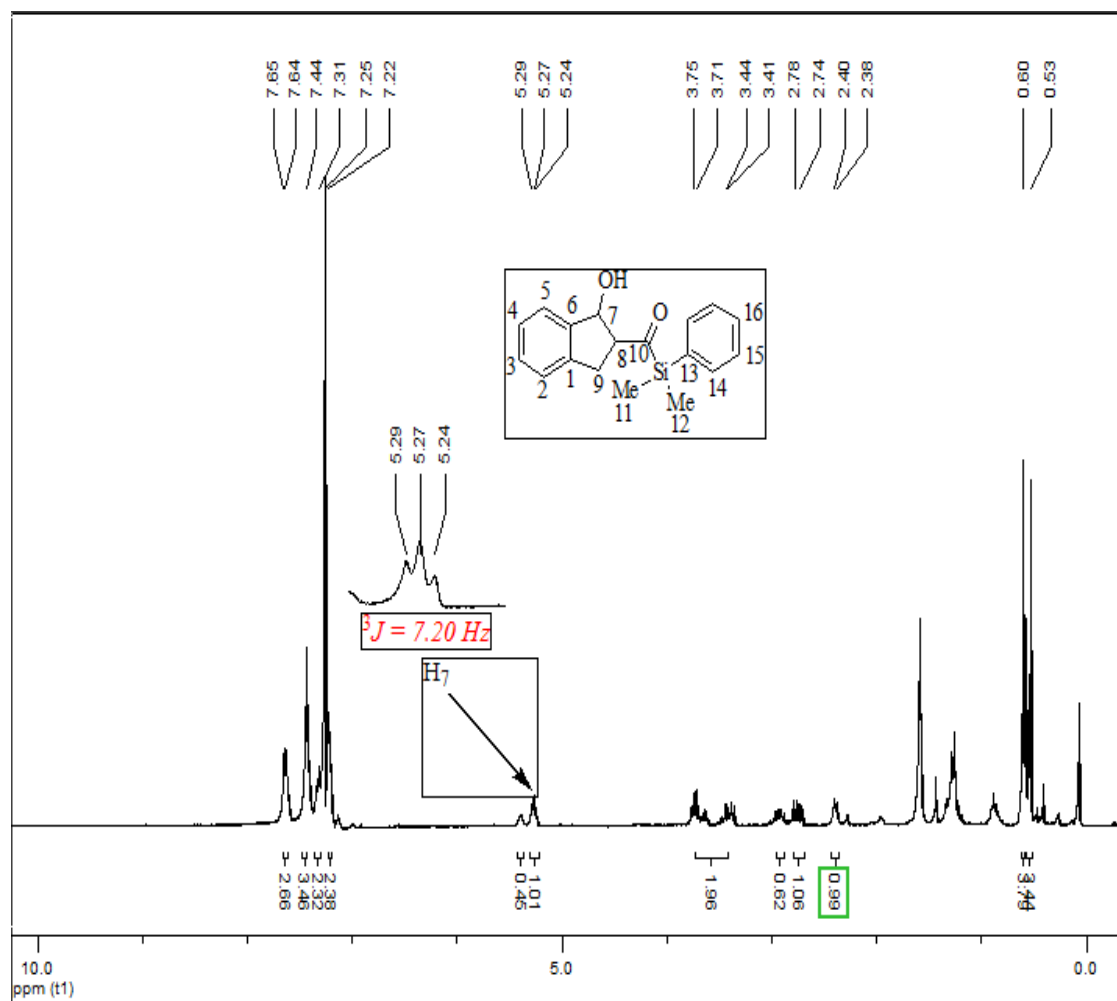
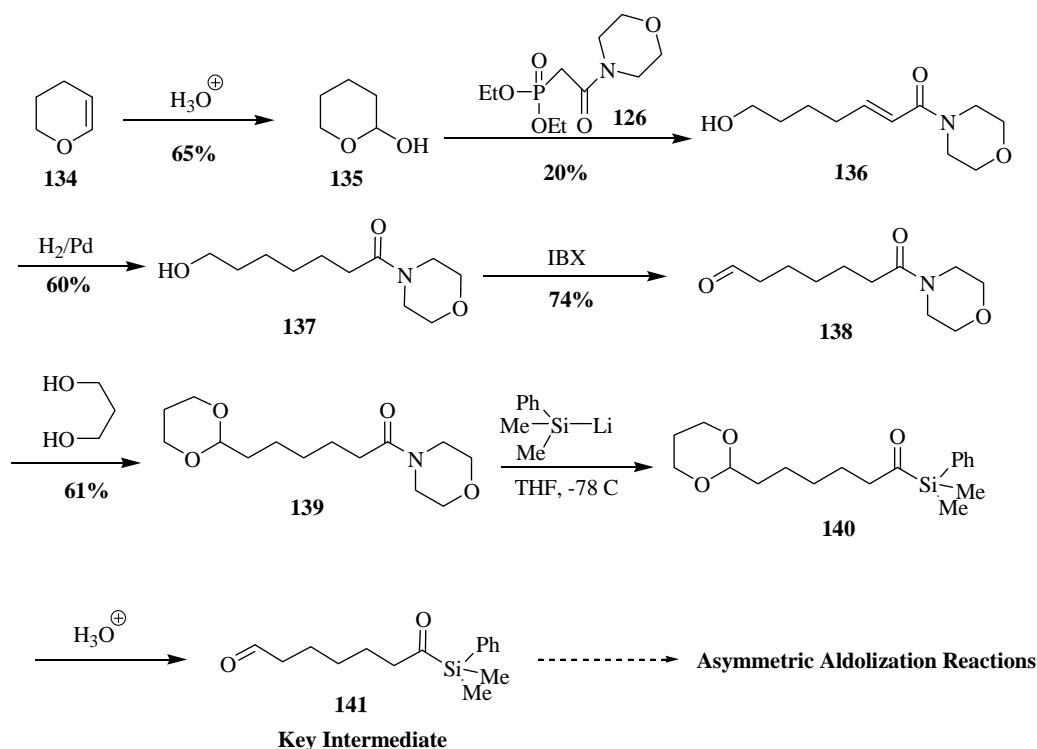


Fig. II. 8: ^1H NMR spectrum of the *cis* and *trans* mixture of **133**-indanole

The main problem that we faced later regarding the aromatic model was the addition reaction of silyllithium to amide **126** that gave many side products and makes the separation of the desired acylsilane product **127** very difficult and almost impossible! Many attempts were performed later to reproduce the results and try to get again better reaction mixture that give acylsilane **127** with less impurities, but unfortunately no more pure acylsilane **127** could be isolated after that, and this led us to stop our work at this stage, and use these results as a preliminary results for this study that might be developed later in our group.

2. Tentative synthesis of model 2 with aliphatic linker

On the other hand, and concerning the second model, 2,3-dihydropyran **134** was used as a starting material for an aliphatic linker, and the preparation of acylsilane intermediate **141** was performed with the same approach as for the first model, according to the sequence in scheme II.43.



Scheme II. 43: Preparation of acylsilane **141**

Hemiacetal **136** was obtained in 65% yield from the treatment of **134** in acidic medium, according to literature procedure [93], and the structure of **135** was established by comparison of its spectral data with the literature. This was followed by the HWE reaction of **135** [88] with the previously prepared phosphonate amide **124** (Scheme II.37), which gave the α,β -unsaturated amide **136** in a very low yield (20%). The structure of **136** was confirmed by 1H NMR data (Figure II.9) that shows the peaks of the vinylic protons as two doublets of triplets at 6.88 ppm (H_5 , $^3J_{trans}=15.1$ Hz, $^3J=6.9$ Hz) and at 6.22 ppm (H_6 , $^3J_{trans}=15.1$ Hz, $^4J=1.5$ Hz).

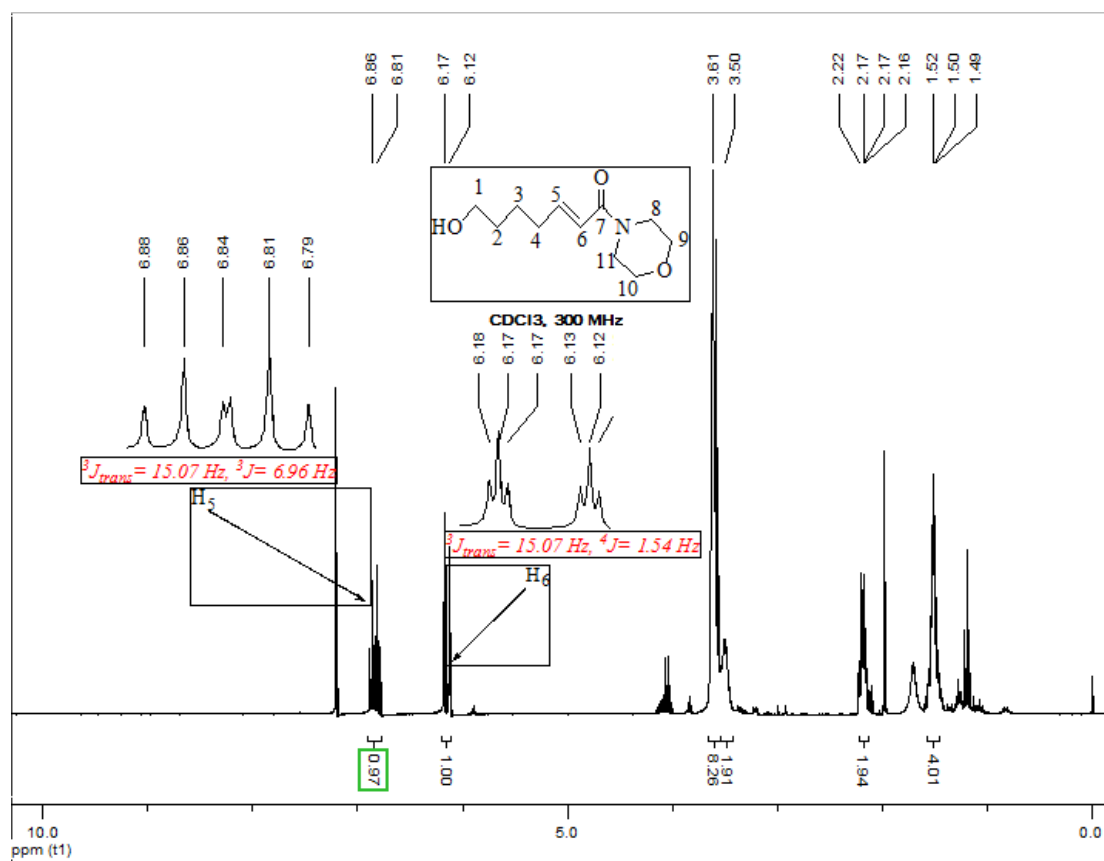


Fig. II. 9: ¹H NMR spectrum of amide **136**

Then, hydrogenation of the double bond in the following step, according to the literature procedure [89], gave the saturated amide **137** in 60% yield, where the ¹H NMR spectrum of **137** shows the disappearance of the two doublets of triplets at 6.88 ppm and at 6.22 ppm (Figure II.10).

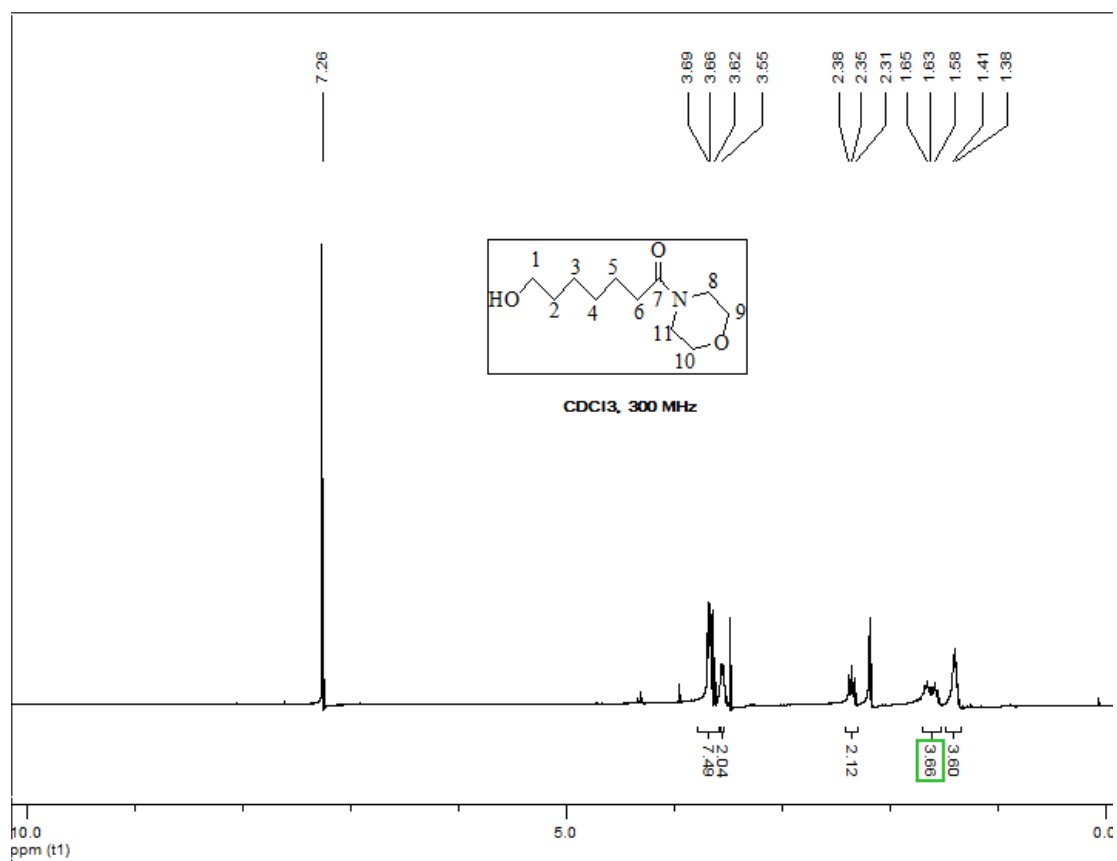


Fig. II. 10: ^1H NMR spectrum of amide **137**

The following step was the oxidation of alcohol **137** into aldehyde. Thus alcohol **137** was treated with IBX in DMSO and CH_2Cl_2 , and gave the desired aldehyde **138** in 74% yield. The structure of **138** was confirmed by ^1H NMR data that shows the appearance of the aldehyde proton at as a triplet at 9.66 ppm, with a coupling constant of 1.7 Hz (Figure II.11).

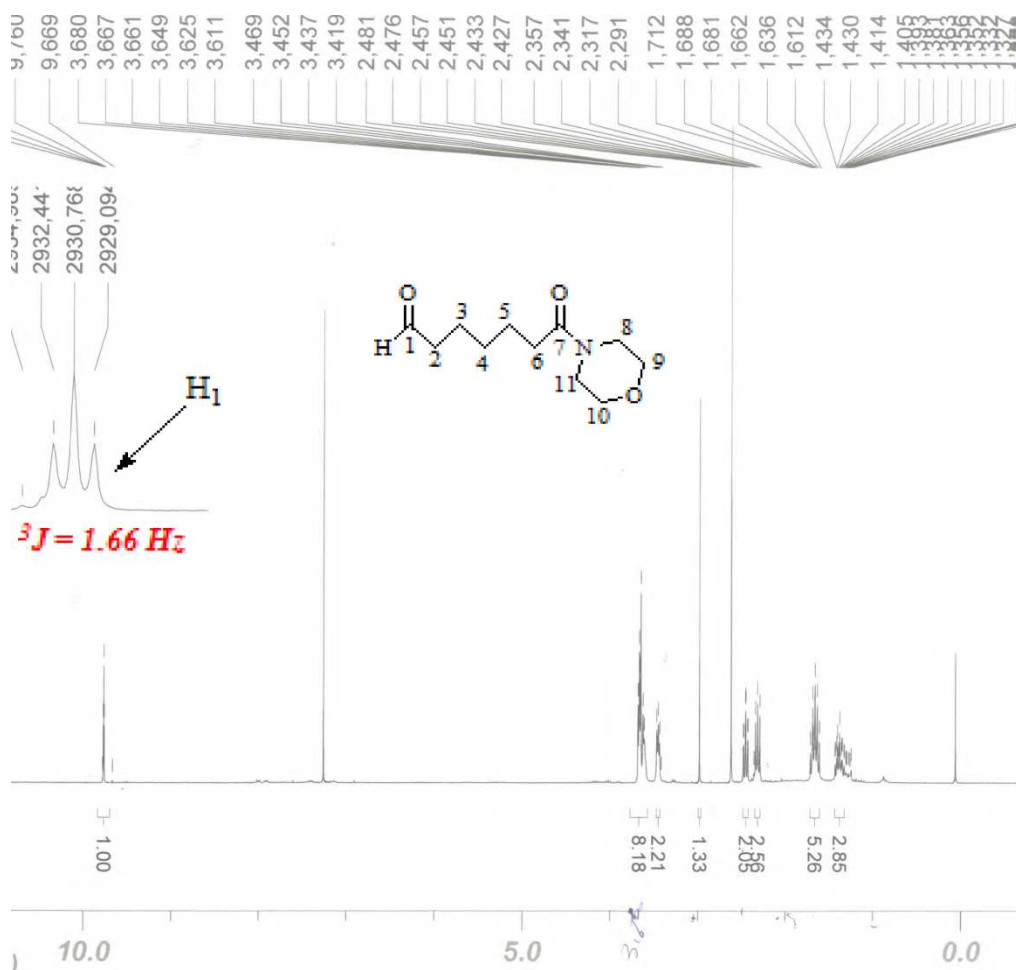


Fig.II. 11: ^1H NMR spectrum of aldehyde **138**

Protection of aldehyde **138** was then required in the following step. Thus aldehyde **138** was treated with propan-1, 3- diol and *p*-TsOH as catalyst giving acetal **139** in 61% yield. Structure of **139** was also confirmed by ^1H NMR data (Figure II.12) that shows the disappearance of the peak of aldehyde at 9.66 ppm, and the appearance of the signals corresponding to the acetal protons, especially the methine proton that appears as a triplet at 4.5 ppm with coupling constant of 5.1 Hz.

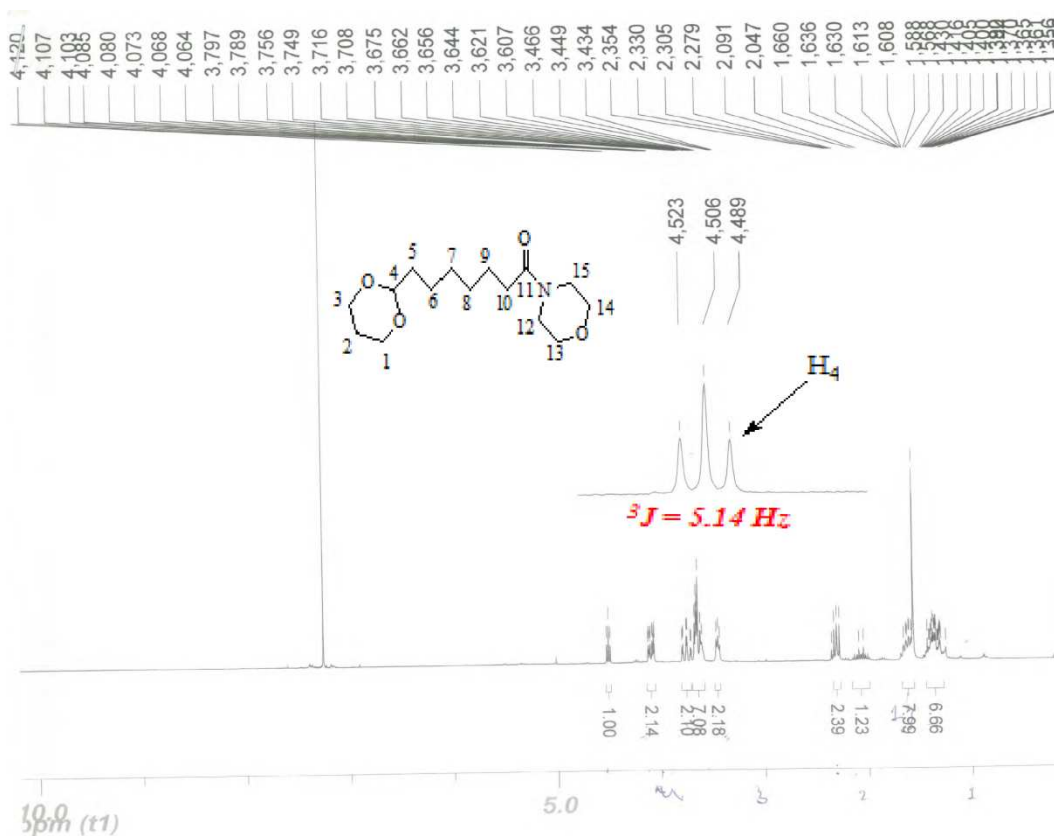


Fig.II. 12: ^1H NMR spectrum of acetal **139**

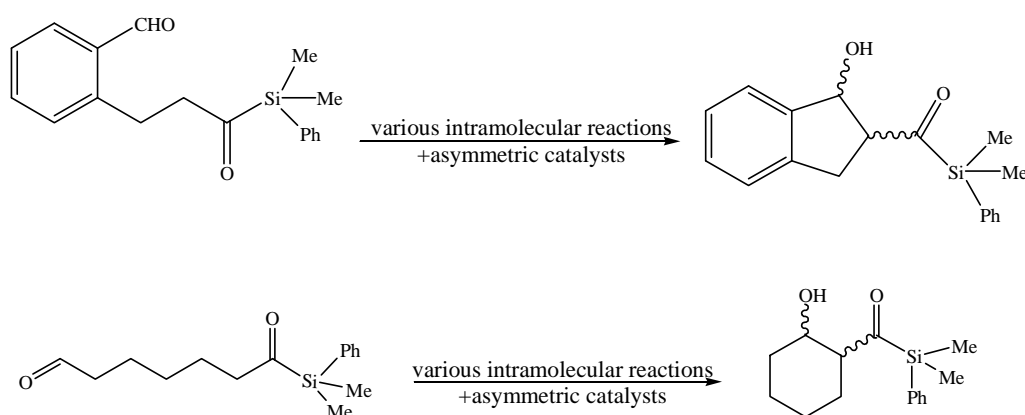
So, having intermediate **139** in hands, addition reaction of silyllithium was then performed. Thus, dimethylphenylsilyllithium was added slowly to a solution of **139** in THF at -78°C . Different side products were obtained during this reaction; however the peaks of the desired acylsilane product **140** were detected by ^1H NMR, but unfortunately purification of **140** was not possible, due to very small quantity of the crude mixture. Thus, deprotection of the acetal group was performed directly on the crude mixture, using hydrochloric acid (37%) in water and acetone, that gave the desired key intermediate **141**, where the proton of aldehyde group was detected at 9.69 ppm, but purification of this crude wasn't easy too.

It is important to note that, this sequence for the aliphatic linker was performed only once, due to the problem that we faced with the HWE reaction step, which was not sufficient with hemiacetal as aldehyde moiety, and thus very poor yield were always obtained by this step.

II.D. CONCLUSION

Conclusion:

As to conclude, synthesis of acylsilane intermediates could be achieved starting from morpholine amide as a precursor. Two models of acylsilane intermediates were chosen in our work (aliphatic and aromatic models) in order to perform intramolecular aldolization reaction (Scheme II.44).



Scheme II. 44: Two models of acylsilane intermediates

For the aromatic model, we could isolate a pure acylsilane intermediate, but in a very low yield, where the isolated quantity were used to perform asymmetric intramolecular aldolization reaction using chiral organocatalysts (quinidine and proline). Different attempts were performed, the use of quinidine derived catalyst alone showed to be the best choice for this asymmetric intramolecular aldolization, where the aldol products could be detected by NMR spectra. However, the use of proline catalyst alone or the mixture of quinidine/proline catalysts didn't give good results for the aldolization reaction.

On the other hand, and concerning the synthesis of the aliphatic model, very few milli-grams of acylsilane intermediate were obtained in the final step as a crude mixture, where their purification was difficult, and no attempts of aldolization reaction were performed at this stage.

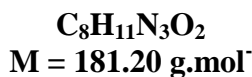
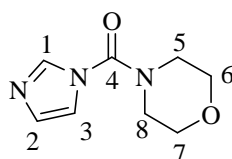
These preliminary results indicate that asymmetric organocatalysis should be possible starting from these new molecules, but more research is required in order to obtain the required precise data on the ee's of these reactions.

II.E. EXPERIMENTAL PART

Experimental Part

Preparation of imidazole-1-yl-morpholine-4-yl-methanone (**122**)

To a cooled (cold water bath) solution of CDI **121** (1 g, 6.16 mmol) in CH₂Cl₂ (5 ml), morpholine (0.48 g, 5.6 mmol) was added dropwise. After the solids dissolved, giving a slightly yellowish clear solution, the water bath was removed, and the mixture was stirred for a further 24h. After this time, the reaction was diluted with CH₂Cl₂ (3 ml), and quenched with water (7 ml), and the aqueous layer was extracted with CH₂Cl₂ (4×7 ml). The combined organic layer was dried over anhydrous MgSO₄, filtered and concentrated in vacuo. Carbamoylimidazole **122** was obtained as white solid 835 mg (82% yield).



White solid, mp = 92°C, **R_f** = 0.30 (pentane/ether 8/2);

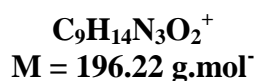
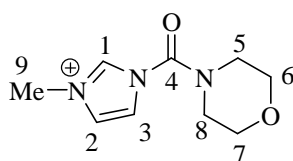
¹H NMR (CDCl₃, 300 MHz), δ ppm: 7.88 (s, 1H, H₁); 7.20 (d, 1H, H₂, ³J= 2.9 Hz); 7.11 (d, 1H, H₃, ³J= 2.9 Hz); 3.76 (m, 4H, H_{6,7}); 3.62 (m, 4H, H_{5,8}).

¹³C NMR (CDCl₃, 75 MHz), δ ppm: 150.72 (1C, C₄); 136.72 (1C, C₁); 129.69 (1C); 117.71 (1C); 66.33 (2C, C_{6,7}); 46.65 (2C, C_{5,8}).

HRMS (ESI) calculated for C₈H₁₁N₃O₂Na: [M +Na]⁺: m/z 204.0743 Found: m/z. 204.0743 (0ppm).

Preparation of 1-methyl-3-(morpholine-4-carbonyl)-3H-imidazole-1-ium (123)

To a solution of carbamoylimidazole **122** (0.835 g, 4.6 mmol) in acetonitrile (10 ml), methyl iodide was added (2.62 g, 18.4 mmol). The mixture was stirred at room temperature for 24h. The solvent was then removed under vacuo to yield the carbamoylimidazolium salt **123** as a white solid 780 mg (86% yield).



White solid, mp = 169°C, $R_f = 0.26$ (pentane/ether 7/3);

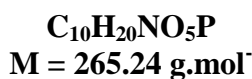
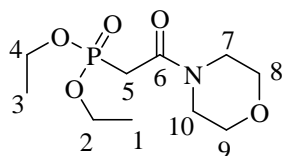
^1H NMR (CDCl_3 , 300 MHz), δ ppm: 9.58 (s, 1H, H_1); 8.02 (d, 1H, H_2 , $^3J = 3.7$ Hz); 7.86 (d, 1H, H_3 , $^3J = 3.7$ Hz); 3.92 (s, 3H, H_9); 3.68 (m, 4H, $\text{H}_{6,7}$); 3.54 (m, 4H, $\text{H}_{5,8}$).

^{13}C NMR (CDCl_3 , 75 MHz), δ ppm: 146.88 (1C, C_4); 137.42 (1C, C_1); 123.51 (1C); 120.83 (1C); 65.20 (2C, $\text{C}_{6,7}$); 46.13 (2C, $\text{C}_{5,8}$); 36.29 (1C, C_9).

HRMS (ESI) calculated for $\text{C}_9\text{H}_{14}\text{N}_3\text{O}_2\text{Na}$: $[\text{M} + \text{Na}]^+$: m/z 196.1080 Found: m/z 196.1081 (0 ppm).

Preparation of 2-(diethyl-phosphinoyl)-1-morpholine-4-yl-ethanone (124)

To a suspension of **123** (0.78 g, 5.1 mmol) in dry acetonitrile (30 ml) were added diethyl phosphonoacetic acid (1 g, 5.1 mmol) and triethylamine (0.7 ml, 5.1 mmol). The reaction mixture was refluxed for 24h. The solvent was removed in vacuo and the residue was dissolved in CH_2Cl_2 and washed with 0.2 N HCl. The aqueous layer was then extracted with CH_2Cl_2 (3 times), and the combined organic layers were washed with 0.2 N HCl, 0.5 M K_2CO_3 , and brine, then dried over anhydrous MgSO_4 and concentrated under vacuo. Phosphonate **124** was obtained without any further purification as yellow oil 820 mg (78% yield).



Yellow oil, $R_f = 0.31$ (pentane/ether 7/3);

¹H NMR (CDCl₃, 300 MHz), δ ppm: 3.88 (m, 4H, H_{2,4}); 3.36 (m, 8H); 2.78 (d, 2H, ²J_{H-P} = 22.0 Hz); 1.06 (t, 6H, H_{1,3}, ³J = 7.1 Hz).

¹³C NMR (CDCl₃, 75 MHz), δ ppm: 162.66 (d, 1C, C₆, ²J_{C-P} = 5.6 Hz); 66.00 (d, 2C, C_{2,4}, ²J_{C-P} = 6.8 Hz); 61.96 (1C, C₈); 61.90 (1C, C₉); 46.64 (1C, C₇); 41.68 (1C, C₁₀); 33.01 (1C, C₁); 31.96 (1C, C₃); 15.66 (d, 1C, C₅, ¹J_{C-P} = 6.1 Hz).

³¹P NMR (CDCl₃, 121 MHz), (ppm): 34.22.

HRMS (ESI) calculated for C₁₀H₂₀NO₅PNa: [M +Na]⁺: m/z 287.0501 Found: m/z. 287.0501 (0 ppm).

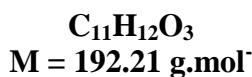
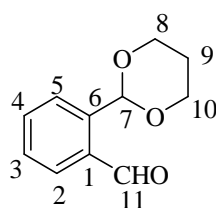
General procedure for the protection of aldehyde using 1,3-diol

A solution of the *o*-phthalaldehyde **119** (1 equiv), propan-1,3-diol (1 equiv) and *p*-toluenesulfonic acid (1% mol) in toluene was heated under reflux with a Dean-Stark apparatus for 6h. After this time, the reaction mixture was quenched with a saturated solution of sodium carbonate and water, decanted and the aqueous layer was extracted with ether (3 times). The combined organic phases were washed with brine, dried over MgSO₄ and concentrated.

Protection of *o*-phthalaldehyde

A solution of *o*-phthalaldehyde **119** (1 g, 7.46 mmol), propan-1,3-diol (0.55 ml, 7.46 mmol) and *p*-toluenesulfonic acid (14 mg, 0.25 mmol) in toluene (20 ml) was heated under reflux for 6h according to the procedure mentioned above. After purification by chromatography on silica gel, using pentane/ether 9/1 as an eluent, the protected aldehyde **120** was obtained as yellow oil 1.1 g (76% yield).

2-[1,3]Dioxan-2-yl-benzaldehyde (**120**)



Yellow oil, $R_f = 0.41$ (pentane/ether 9/1);

$^1\text{H NMR}$ (CDCl_3 , 300 MHz), δ ppm: 10.52 (s, 1H, H_{11}); 7.92 (dd, 1H, $^3J = 7.6$ Hz $^4J = 1.3$ Hz); 7.70 (dd, 1H, $^3J = 7.7$ Hz $^4J = 1.4$ Hz); 7.60 (td, 1H, $^3J = 7.4$ Hz, $^4J = 1.5$ Hz); 7.50 (td, 1H, $^3J = 7.1$ Hz, $^4J = 1.4$ Hz); 6.02 (s, 1H, H_7); 4.30 (m, 2H, H_8); 4.05 (m, 2H, H_{10}); 2.25 (m, 1H, H_9); 1.52 (m, 1H, H_9).

$^{13}\text{C NMR}$ (CDCl_3 , 75 MHz), δ ppm: 191.87 (1C, C_{11}); 139.47 (1C); 133.56 (1C); 133.14 (1C); 129.08 (1C); 128.85 (1C); 126.97 (1C); 99.86 (1C, C_7); 67.28 (2C, $\text{C}_{8,10}$); 25.33 (1C, C_9).

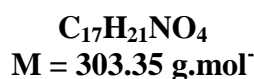
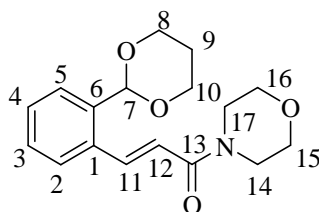
HRMS (ESI) calculated for $\text{C}_{11}\text{H}_{12}\text{O}_3\text{Na}$: $[\text{M} + \text{Na}]^+$: m/z 215.0678 Found: m/z . 215.0682 (2 ppm).

General procedure for the Horner-Wadworth-Emmons reaction of the aldehyde with phosphonate

To a suspension of LiCl (1.2 equiv) in acetonitrile, the phosphonate (1.2 equiv) was added, followed by the addition of DBU (1 equiv) and the aldehyde (1 equiv). The reaction mixture was stirred at room temperature for 16 h. After this time, the solvent was removed in vacuo and the crude product was dissolved in CH₂Cl₂ and washed with 0.1 N HCl, brine, dried over MgSO₄ and concentrated in vacuo.

Synthesis of 3-(2-[1,3]dioxane-2-yl-phenyl)-1-morpholin-4-yl-propenone (125)

To a suspension of LiCl (0.13 g, 3.1 mmol) in acetonitrile (30 ml), phosphonate **124** (0.82 g, 3.1 mmol) was added, followed by the addition of DBU (0.4 g, 2.57 mmol) and aldehyde **120** (0.5 g, 2.57 mmol), the reaction was stirred for 16 h according to the general procedure mentioned above. After purification by column chromatography on silica gel, using pentane/ether 8/2 as eluent, compound **125** was obtained as white solid 560 mg (72% yield).



White solid, mp = 139°C, R_f = 0.32 (pentane/ether 8/2);

¹H NMR (CDCl₃, 300 MHz), δ ppm: 8.16 (d, 1H, H₁₁, ³J_{trans} = 15.3 Hz); 7.65 (m, 1H); 7.58 (m, 1H); 7.36 (m, 2H); 6.74 (d, 1H, H₁₂, ³J_{trans} = 15.3 Hz); 5.75 (s, 1H, H₇); 4.25 (m, 2H, H₈); 4.00 (m, 2H, H₁₀); 3.73 (m, 8H); 2.30 (m, 1H, H₉); 1.48 (m, 1H, H₉).

¹³C NMR (CDCl₃, 75 MHz), δ ppm: 165.39 (1C, C₁₃); 140.47 (1C, C₁₁); 136.93 (1C); 133.55 (1C); 129.31 (1C); 128.88 (1C); 126.74 (1C); 126.40 (1C); 118.40 (1C,

C₁₂); 99.74 (1C, C₇); 67.43 (2C, C_{15,17}); 66.76 (2C, C_{8,10}); 45.76 (1C, C₁₄); 42.47 (1C, C₁₆); 25.63 (1C, C₉).

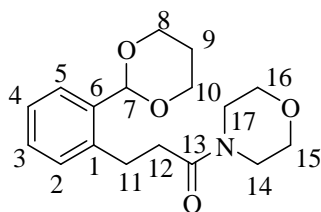
HRMS (ESI) calculated for C₁₇H₂₁NO₄Na: [M +Na]⁺: m/z 326.1362 Found: m/z. 326.1362 (0 ppm).

General procedure for the hydrogenation reaction of alkene

To a solution of alkene in methanol, 10% Pd/C (10% wt of alkene) was added and the mixture hydrogenated under hydrogen atmosphere at room temperature for 12 h. The reaction mixture was then filtered using celite, and the filtrate was concentrated under vacuo, and purified using column chromatography.

Synthesis of 3-(2-[1,3] dioxane-2-yl-phenyl)-1-morpholine-4-yl-propan-1-one (126)

To a solution of **125** (0.56 g, 1.85 mmol) in methanol (10 ml), Pd/C (56 mg, 10% mass) was added and the mixture hydrogenated under hydrogen atmosphere at room temperature for 12 h according to the general procedure mentioned above. After purification by chromatography on silica gel, using pentane/ether 7/3 as eluent, compound **126** was obtained as yellow oil 380 mg (68% yield).



C₁₇H₂₃NO₄
M = 305.36 g.mol⁻¹

Yellow oil, **R_f** = 0.32 (pentane/ether 7/3);

¹H NMR (CDCl₃, 300 MHz), δ ppm: 7.60 (d, 1H, ³J= 6.1 Hz); 7.24 (m, 3H); 5.67 (s, 1H, H₇); 4.25 (m, 2H, H₈); 4.00 (m, 2H, H₁₀); 3.60 (m, 4H, H_{15,16}); 3.32 (m, 4H,

H_{14,17}); 3.12 (t, 2H, H₁₁, ³J= 7.4 Hz); 2.64 (t, 2H, H₁₂, ³J= 7.4 Hz); 2.25 (m, 1H, H₉); 1.45 (m, 1H, H₉).

¹³C NMR (CDCl₃, 75 MHz), δ ppm: 170.77 (1C, C₁₃); 138.37 (1C); 136.08 (1C); 129.49 (1C); 128.50 (1C); 126.31 (1C); 126.06 (1C); 99.79 (1C, C₇); 67.02 (2C, C_{8,10}); 66.30 (1C, C₁₅); 65.99 (1C, C₁₆); 45.52 (1C, C₁₄); 41.51 (1C, C₁₇); 34.31 (1C, C₁₂); 27.98 (1C, C₉); 25.30 (1C, C₁₁).

HRMS (ESI) calculated for C₁₇H₂₃NO₄Na: [M +Na]⁺: m/z 328.1519 Found: m/z. 328.1521 (0 ppm).

Preparation of dimethylphenylsilyllithium from the commercially available chloro(dimethyl)phenylsilane

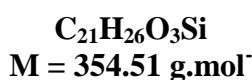
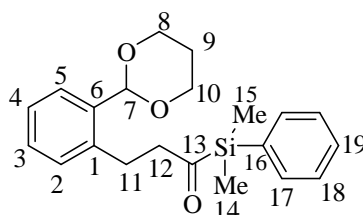
To a dry bi-necked flask was added THF under nitrogen atmosphere, followed by the addition of a well grinded lithium metal (1 g, 0.142 mol) (lithium was first rinsed with pentane, grinded, and then added slowly into the flask). The flask was then placed in an ice bath to reach 0°C, then chloro(dimethyl)phenylsilane (3.47 ml, 0.02 mol) was added dropwise to the solution. After few minutes (4-6 mins) the reaction mixture turned into blood red color. The reaction then kept on stirring at 0°C for additional 2h and then stored in the fridge.

General procedure for the addition reaction of dimethylphenylsilyllithium into morpholine amide

To a solution of morpholine amide (1 equiv) in THF, the prepared silyllithium (2 equiv) was added dropwise at -80°C. The mixture was stirred for 5h and quenched with a saturated solution of NH₄Cl (at -80°C), then kept to warm up till room temperature. The aqueous layer was extracted with ether (3 times), and the combined organic layers were dried over MgSO₄, filtered and concentrated under vacuo. The residue was purified by column chromatography.

Synthesis of 1-(dimethylphenyl-silanyl)-3-(2-[1,3] dioxane-2-yl-phenyl)-propan-1-one (127)

To a solution of morpholine amide **126** (0.38 g, 1.24 mmol) in THF, the prepared silyllithium (0.35 g, 2.48 mmol) was added dropwise at -80°C . The mixture was stirred for 5h according to the general procedure mentioned above. After purification by column chromatography on silica gel, using pentane/ether 9/1 as eluent, acylsilane **127** was obtained as yellow oil 194 mg (44% yield).

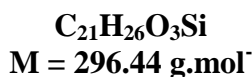
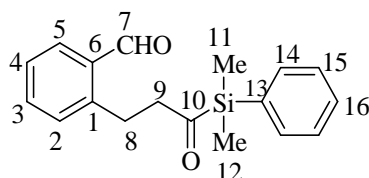


Yellow oil, $R_f = 0.48$ (pentane/ether 9/1);

$^1\text{H NMR}$ (CDCl_3 , 300 MHz), δ ppm: 7.60 (m, 1H); 7.54 (m, 3H); 7.40 (m, 4H); 7.20 (m, 1H); 5.51 (s, 1H, H_7); 4.12 (m, 2H, H_8); 3.84 (m, 2H, H_{10}); 2.90 (m, 4H, $\text{H}_{11,12}$); 2.18 (m, 1H, H_9); 1.40 (m, 1H, H_9), 0.48 (s, 3H, H_{14}); 0.41(s, 3H, H_{15}).

Preparation of 2-[3-(dimethylphenyl-silanyl)-3-oxo-propyl]-benzaldehyde (128)

To a solution of **127** (0.194 g, 0.55 mmol) in acetone (8 ml), 16 ml water was added followed by the addition of 5-6 drops of HCl. The reaction mixture was then stirred at room temperature for 2h. After this time, few drops of NaHCO_3 were added till pH reaches 7. The mixture was then extracted with ether (3 times) and the combined organic layer dried over MgSO_4 and concentrated under vacuo. After purification by chromatography on silica gel, using pentane/ether 8/2 as eluent, the key intermediate **128** was obtained as yellow oil 0.126 mg (78% yield).



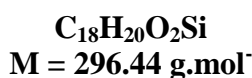
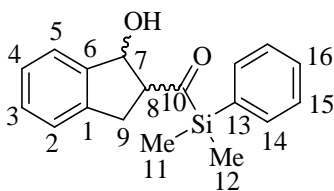
Yellow oil, **R_f** 0.56 (pentane/ether 8/2);

¹H NMR (CDCl₃, 300 MHz), δ ppm: 10.12 (s, 1H, H₇); 7.76 (m, 1H); 7.61 (m, 1H); 7.50 (m, 2H); 7.40 (m, 5H); 3.18 (t, 2H, H₈, ³J= 7.6 Hz); 2.88 (t, 2H, H₉, ³J= 7.2 Hz); 0.47 (s, 3H, H₁₁); 0.41(s, 3H, H₁₂).

Procedure for asymmetric intramolecular aldol reaction of acylsilane (130) using quinidine-derived catalyst

To a solution of **128** (0.126 g, 0.42 mmol) in methanol (5 ml), 20 mol % of quinidine thiourea (0.027 g, 0.084 mmol) was added. After few minutes, the reaction mixture turned into brown color. The reaction was kept on stirring for 24h at room temperature. After purification by chromatography on silica gel, using pentane/ether 9/1 as eluent, the mixture of aldol products **133** was obtained as a yellow oil 19 mg (15% yield).

(Dimethylphenyl-silanyl)-(1-hydroxy-indan-2-yl)-methanone (133)



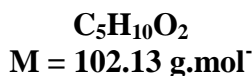
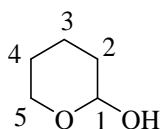
Yellow oil, **R_f** = 0.29 (pentane/ether 9/1);

¹H NMR (CDCl₃, 300 MHz), δ ppm: 7.65 (m, 2H); 7.44 (m, 3H); 7.25 (m, 2H); 7.22 (m, 2H); 5.24 (t, 1H, H₇, ³J= 7.2 Hz); 3.40 (m, 2H, H₉); 2.40 (m, 1H, H₈); 0.60 (s, 3H, H₁₁); 0.53 (s, 3H, H₁₂).

¹³C NMR (CDCl₃, 75 MHz), δ ppm: 247.96 (1C, C₁₀); 134.15 (1C); 133.02 (1C); 132.28 (1C); 130.04 (1C); 129.03 (1C); 128.88 (1C); 128.34 (1C); 128.30 (1C); 127.89 (1C); 127.10 (1C); 125.07 (1C); 124.14 (1C); 60.23 (1C, C₇); 35.54 (1C, C₈); 30.15 (1C, C₉); - 4.49 (1C, C₁₁); - 4.72 (1C, C₁₂).

Synthesis of tetrahydro-pyran-2-ol (135)

To a solution of 2, 3-dihydropyran **134** (2 g, 23.80 mmol) in water (8 ml), 1 ml of HCl (37%) was added slowly. The reaction mixture was stirred for 30 min at room temperature, and the solution was then neutralized using anhydrous sodium carbonate until pH reaches 7. Then 1.6g of NaCl was added upon stirring the mixture, and after the complete dissolution of NaCl, the aqueous layer was extracted twice with ether, and the combined organic layer was dried, and concentrated under vacuo. The crude product was then distilled at 60-62°C to get the desired product **135** as colorless oil 1.58 g (65% yield).



Colorless oil, **R_f** = 0.30 (pentane/ether 7/3);

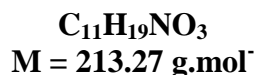
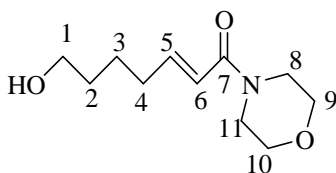
¹H NMR (CDCl₃, 300 MHz), δ ppm: 4.90 (m, 1H, H₁); 4.02 (m, 1H, H₅); 3.54 (m, 1H, H₅); 1.80 (m, 2H, H₂); 1.52 (m, 4H, H_{3,4}).

¹³C NMR (CDCl₃, 75 MHz), δ ppm: 98.32 (1C, C₁); 65.14 (1C, C₅); 37.42 (1C, C₂); 30.22 (1C, C₄); 20.26 (1C, C₃).

HRMS (ESI) calculated for C₅H₁₀O₂Na: [M +Na]⁺: m/z 125.0578 Found: m/z. 125.0578 (0 ppm).

Synthesis of 7-hydroxy-1-morpholin-4-yl-hept-2-en-1-one (136)

To a suspension of LiCl (0.20 g, 4.69 mmol) in acetonitrile (75 ml), phosphonate **124** (1.24 g, 4.69 mmol) was added, followed by the addition of DBU (0.60 g, 3.92 mmol) and hemiacetal **135** (0.4 g, 3.92 mmol). The reaction mixture was stirred for 16 h according to the general procedure mentioned above. After purification by column chromatography on silica gel, using pentane/ether 6/4 as eluent, alkene **136** was obtained as yellow oil 170 mg (20% yield).



Yellow oil, **R_f** = 0.33 (pentane/ether 6/4);

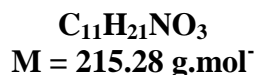
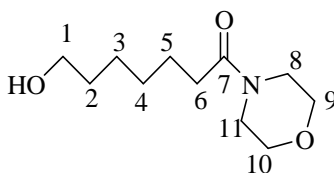
¹H NMR (CDCl₃, 300 MHz), δ ppm: 6.88 (dt, 1H, H₅, ³J_{trans} = 15.1 Hz, ³J = 6.9 Hz); 6.22 (dt, 1H, H₆, ³J_{trans} = 15.1 Hz, ⁴J = 1.5 Hz); 3.65 (m, 8H); 3.55 (m, 2H, H₁); 2.25 (m, 2H, H₂); 1.58 (m, 4H, H_{3,4}).

¹³C NMR (CDCl₃, 75 MHz), δ ppm: 162.18 (1C, C₇); 144.12 (1C, C₅); 120.96 (1C, C₆); 69.88 (2C, C_{9,10}); 62.16 (1C, C₁); 42.15 (2C, C_{8,11}); 31.20 (1C); 29.12 (1C); 24.36 (1C).

HRMS (ESI) calculated for C₁₁H₁₉NO₃Na: [M +Na]⁺: m/z 236.1263 Found: m/z. 236.1263 (0 ppm).

Synthesis of 7-hydroxy-1-morpholin-4-yl-heptan-1-one (137)

To a solution of **136** (0.12 g, 0.56 mmol) in methanol (15 ml), Pd/C (12 mg, 10% mass) was added and the reaction mixture was hydrogenated under hydrogen atmosphere at room temperature for 12 h according to the general procedure mentioned above. After purification by chromatography on silica gel, using pentane/ether 5/5 as eluent, compound **137** was obtained as yellow oil 70 mg (60% yield).



Yellow oil, **R_f** = 0.42 (pentane/ether 5/5);

¹H NMR (CDCl₃, 300 MHz), δ ppm: 3.66 (m, 8H); 3.55 (m, 2H, H₁); 2.35 (t, 2H, H₆, ³J = 7.3 Hz); 1.62 (m, 4H); 1.40 (m, 4H).

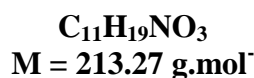
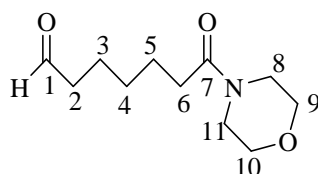
¹³C NMR (CDCl₃, 75 MHz), δ ppm: 168.13 (1C, C₇); 68.15 (2C, C_{9,10}); 61.28 (1C, C₁); 41.18 (2C, C_{8,11}); 32.19 (1C); 31.40 (1C); 27.11 (1C); 24.14 (1C); 21.26 (1C).

HRMS (ESI) calculated for C₁₁H₂₁NO₃Na: [M + Na]⁺: m/z 238.1419 Found: m/z. 238.1419 (0 ppm).

Oxidation of alcohol (137) using IBX

To a solution of IBX (0.136 g, 1.5 equiv) in DMSO (2 ml), a solution of alcohol **137** (0.07 g, 1 equiv) in CH₂Cl₂ (3 ml), was added slowly. The mixture was then heated at 60°C for 3h. After this time, the mixture was poured into cooled water and the precipitate was then filtrated. The filtrate was then extracted twice with diethyl ether, and the combined organic layer dried over MgSO₄, and concentrated under vacuo.

After purification by chromatography on silica gel, using pentane/ether 7/3 as eluent, aldehyde **138** was obtained as yellow oil 51.3 mg (74% yield).

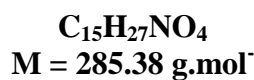
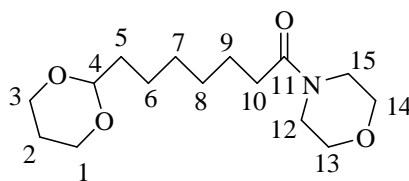


Yellow oil, **R_f** = 0.41 (pentane/ether 8/2);

¹H NMR (CDCl₃, 300 MHz), δ ppm: 9.66 (t, 1H, H₁, ³J = 1.7 Hz); 3.66 (m, 8H); 2.45 (m, 2H, H₂); 2.34 (m, 2H, H₆); 1.42 (m, 6H).

Preparation of 7-[1,3] dioxane-2-yl-1-morpholine-4-yl-heptan-1-one (**139**)

A solution of **138** (0.05 g, 0.24 mmol), propan-1,3-diol (18 μl, 0.24 mmol) and *p*-toluene sulfonic acid (0.45 mg, 0.0024 mmol) in toluene (1 ml) was heated under reflux for 6h according to the general procedure mentioned before. After purification by chromatography on silica gel, using pentane/ether 8/2 as an eluent, acetal **139** was obtained as yellow oil 41 mg (61% yield).



Yellow oil, **R_f** = 0.38 (pentane/ether 8/2);

¹H NMR (CDCl₃, 300 MHz), δ ppm: 4.50 (t, 1H, H₄, ³J = 5.1 Hz); 4.12 (m, 2H, H₁); 3.80 (m, 2H, H₃); 3.46 (m, 8H); 3.44 (m, 2H); 2.35 (m, 2H); 2.04 (m, 1H, H₂); 1.63 (m, 1H, H₂); 1.58 (m, 2H); 1.36 (m, 6H).

Synthesis of 1-(dimethylphenyl-silanyl)-3-(2-[1,3] dioxane-2-yl-phenyl)-propan-1-one (**140**)

To a solution of morpholine amide **139** (0.02 g, 0.07 mmol) in THF (2 ml), the prepared silyllithium (0.02 g, 0.14 mmol) was added dropwise at -78°C . The mixture was stirred for 5h according to the general procedure mentioned above. Many products were obtained by this reaction and the peaks of the desired acylsilane product **140** were detected by proton NMR. But due to very small quantity of the crude (since it was done only once), purification wasn't easy. However, the deprotection of the acetal group was performed directly on the crude reaction mixture and gave the desired key intermediate **141**, in which the proton of aldehyde group was detected at 9.69 ppm, but purification of this product from the crude reaction mixture was not successful.

II.F. REFERENCES

References:

1. Brook A. G., *J. Am. Chem. Soc.*, **1957**, 79, 4373.
2. Brook A. G., Mauris R. J., *J. Am. Chem. Soc.*, **1957**, 79, 971.
3. Kuwajima I., Matsumoto K., *Tetrahedron Lett.*, **1979**, 4095.
4. Ricci A., Deglinoenti A., *Synthesis*, **1989**, 647.
5. Page P. C., Klair S. S., Rosenthal S., *Chem. Soc. Rev.*, **1990**, 19, 147.
6. Cirillo P. F., Panek J. S., *Org. Prep. Proced. Int.*, **1992**, 24, 553.
7. Patrocinio A. F., Moran P. J., *J. Braz. Chem. Soc.*, **2001**, 12, 7.
8. Honda M., Segi M., *Synth. Org. Chem. Jpn.*, **2010**, 68, 601.
9. Miller J. A., Zweifel G., *J. Am. Chem. Soc.*, **1981**, 103, 6217.
10. Chung W. J., Omote., Welch J. T., *J. Org. Chem.*, **2005**, 70, 7784.
11. Wegert A., Behr J. B., Hoffmann N., Miethchen R., Portella C., Plantier-Royon R., *Synthesis*, **2006**, 2343.
12. Chu L. L., Zhang X. G., Qing F. L., *Org. Lett.*, **2009**, 11, 2197.
13. Mattson A. E., Bharadwaj A. R., Scheidt K. A., *J. Am. Chem. Soc.*, **2004**, 126, 2314.
14. Mattson A. E., Bharadwaj A. R., Zuhl A. M., Scheidt K. A., *J. Org. Chem.*, **2006**, 71, 5715.
15. Schmink J. R., Krska S. W., *J. Am. Chem. Soc.*, **2011**, 133, 19574.
16. Morihata K., Horiuchi Y., Taniguchi M., Oshima K., Utimoto K., *Tetrahedron Lett.*, **1995**, 36, 5555.
17. Boucley C., Cahiez G., Carini S., Cere V., Comes-Franchini M., Knochel P., Pollicino S., Ricci A., *J. Organomet. Chem.*, **2001**, 624, 223.
18. Cirillo P. F., Panek J. J., *Tetrahedron Lett.*, **1991**, 32, 457.
19. Scott E., M., *J. Org. Chem.*, **2007**, 72, 7050.
20. Yoshida J., Itoh M., Matsunaga S., Isoe S., *J. Org. Chem.*, **1992**, 57, 4877.
21. Denmark S. E., Xie M., *J. Org. Chem.*, **2007**, 72, 7050.
22. Patrocinio A. F., Moran P. J. S., *Synth. Commun.*, **2000**, 30, 1419.
23. Lettan R. B., Galliford C. V., Scheidt K. A., *J. Am. Chem. Soc.*, **2009**, 131, 8805.
24. Schinzer D., *Synthesis*, **1989**, 179.
25. Bouillon P., Portella C., *Eur. J. Org. Chem.*, **1999**, 1571.
26. Tamashima K., Iwasawa K., Kusama H., *J. Am. Chem. Soc.*, **2011**, 133, 3716.
27. Gao G., Bai X. F., Li F., Zheng L. S., Zheng Z. J., Lai G. Q., Jiang K. Z., Li F. W., Xu L. W., *Tetrahedron Lett.*, **2012**, 53, 2164.
28. Kresge A. J., Tobin J. B., *J. Org. Chem.*, **1993**, 58, 2652.

29. a) Ricci A., Degl'Innocenti A., *Synthesis* **1989**, 647; b) Page P. C. B., Klair S. S., Rosenthal S., *Chem. Soc. Rev.* **1990**, *19*, 147; c) Patrocínio A. F., Moran P. J. S., *J. Braz. Chem. Soc.* **2001**, *12*, 7; d) Page P. C. B., McKenzie M. J., *Product Subclass 25: Acylsilanes*, in: *Science of Synthesis*, **2001**, *4*, 513; e) Garrett M. N., Johnson J. S., *Product Subclass 4: Silicon Compounds*, in: *Science of Synthesis Knowledge Updates 2012/2*, **2012**, *4*, 1 ; f) Boyce G. R., Grezler S. N., Johnson J. S., Linghu X., Malinowski J. T., Nicewicz D. A., Satterfield A. D., Schmitt D. C., Steward K. M., *J. Org. Chem.* **2012**, *77*, 4503; g) Zhang H. J., Pribbeneau D. L., Bolm C., *Chem. Soc. Rev.* **2013**, *42*, 8540.
30. Brook A. G. "In Adv. Organomet. Chem., Stone, F. G. A., West, R. Eds", *Academic Press, N.Y.*, **1968**, *7*, 95.
31. Page P. C. B., Klair S. S., Rosenthal S. *Chem. Soc. Rev.* **1990**, *19*, 147.
32. Chieh P. C., Trotter J., *J. Chem. Soc.* **1969**, 1778.
33. (a) Brook A. G., Warner, C. M.; McGriskin, M. *J. Am. Chem. Soc.*, **1959**, *81*, 981. (b) Brook A. G. *Acc. Chem. Res.*, **1974**, *7*, 77. (c) Brook A. G., Bassindale A. R., "In: Rearrangements in Ground and Excited States"; *de Mayo P., Ed; Academic Press, New York*, **1980**.
34. (a) Mori A., Fujita A., Ikegashira K., Nishihara Y., Hiyama T. *Synlett*, **1997**, 693. (b) Wilson S. R., Hague M. S., Misra R. N., *J. Org. Chem.*, **1982**, *47*, 747. (c) Barrett A. G. M., Hill J. M., Wallace E. M., Flygare J. A., *Synlett*, **1991**, 764. (d) Hudrlik P. F., Abdallah Y. M., Kulkarni A. K. Hudrlik A. M., *J. Org. Chem.*, **1992**, *57*, 6552. (e) Hiyama T., Obayashi M., *J. Org. Chem.*, **1983**, *48*, 912.
35. (a) Linderman R. J., Ghannam A. *J. Am. Chem. Soc.*, **1990**, *112*, 2392. (b) Linderman R. J., Chen K., *Tetrahedron Lett.*, **1992**, *33*, 6767.
36. Danheiser R. L., Fink D. M., Okano K., Tsai Y. M., Szczepanski S. W., *J. Org. Chem.* **1985**, *50*, 5393.
37. Lipshutz B. H., Lindsley C., Susfalk R., Gross T. *Tetrahedron Lett.*, **1994**, *35*, 8999.
38. Brook A. G., Duff J. M., Jones P. F. Davis N. R. *J. Am. Chem. Soc.* **1967**, *89*, 431.
39. Corey E. J., Seebach D., Freedman R. *J. Am. Chem. Soc.* **1967**, *89*, 434.
40. Saleur D., Bouillon J. P., Portella C. *Tetrahedron Lett.*, **2000**, *41*, 321.
41. Suda K., Watanabe J., Takanami T., *Tetrahedron Lett.* **1992**, *33*, 1355.
42. Patrocínio A. F., Moran P. J. S., *J. Organomet. Chem.*, **2000**, *603*, 220.
43. Picard J. P., Calas R., Dunoguès J., Duffaut N., Gerval J., Lapouyade P. *J. Org. Chem.* **1979**, *44*, 420.
44. Fleming I., Roberts R. S., Smith S. C. *Tetrahedron Lett.*, **1996**, *37*, 9395.
45. Still W. C., *J. Org. Chem.*, **1976**, *41*, 3063.
46. Fleming I., Ghosh U., *J. Chem. Soc., Perkin Trans.*, **1994**, *1*, 257.

47. Kuwajima I., Abe T., Minami, N., *Chem. Lett.*, **1976**, 993.
48. Paredes M. D., Alonso R. *Tetrahedron Lett.*, **1999**, 40, 3973.
49. Christopher T. C., Benjamin C. M., Scheidt A., *Org. Lett.*, **2004**, 6, 3977.
50. Nakada M., Nakamura S., Kobayashi, S., Ohno, M. *Tetrahedron Lett.*, **1991**, 32, 4929.
51. Capperucci A., Degl'Innocenti A., Faggi C., Ricci A. *J. Org. Chem.* **1988**, 53, 3612.
52. (a) Fleming I., Marchi Jr. D. *Synthesis* 1981, 560. (b) Ager D., Fleming I., Patel S. K. *J. Chem. Soc., Perkin Trans.* **1981**, 1, 2521.
53. Bonini B. F., Franchini M. C., Mazzanti G., Passamonti U., Ricci A., Zani P. *Synthesis* **1995**, 92.
54. a) Bonini B. F., Franchini M. C., Fochi M., Mazzanti G., Ricci A. *Gazz. Chim. Ital.* **1997**, 127, 619; b) Bonini B. F., Franchini M. C., Fochi M., Mazzanti G., Ricci A. *J. Organomet. Chem.*, **1998**, 567, 181.
55. Yamamoto K., Suzuki S., Tsuji J. *Tetrahedron Lett.*, **1980**, 21, 1653.
56. Geng F., Maleczka Jr., R. E. *Tetrahedron Lett.*, **1999**, 40, 3113.
57. Fleming I., Barbero A., Walter D. *Chem. Rev.*, **1997**, 97, 2063.
58. Biernbaum M. S., Mosher H. S. *J. Org. Chem.* **1971**, 36, 3169.
59. Hudrlik P. F., Hudrlik A. M., Kulkarni A. K., *J. Am. Chem. Soc.* **1982**, 104, 6809.
60. Nakada M., Urano Y., Kobayashi S., Ohno M. *Tetrahedron Lett.* **1994**, 35, 741.
61. Chapeaurouge A., Bienz S. *Helv. Chim. Acta*, **1993**, 76, 1876.
62. Huber P., Bratovanov S., Bienz S., Syldatk C., Pietzsch M. *Tetrahedron: Asymmetry*, **1996**, 7, 69.
63. Bonini B. F., Masiero S., Mazzanti G., Zani P. *Tetrahedron Lett.*, **1991**, 32, 6801.
64. Takeda K., Nakatani J., Nakamura H., Sako K., Yoshii E., Yamaguchi K. *Synlett*, **1993**, 841.
65. Schinzer D. *Synthesis*, **1989**, 179.
66. (a) Tsai Y. M., Tang K. H., Jiaang W. T. *Tetrahedron Lett.*, **1993**, 34, 1303; (b) Chang S. Y., Jiaang W. T., Cherng C. D., Tang K. H., Huang C. H., Tsai Y. M. *J. Org. Chem.*, **1997**, 62, 9089; (c) Jiaang W. T., Lin H. C., Tang K. H., Chang L. B., Tsai Y. M. *J. Org. Chem.*, **1999**, 64, 618.
67. Siedem C. S., Molander G. A. *J. Org. Chem.*, **1996**, 61, 1140.
68. Saleur D., Bouillon J. P., Portella C. *Tetrahedron Lett.*, **1999**, 40, 1885.
69. Saleur D.; Bouillon J. P.; Portella C. *Tetrahedron Lett.* **2000**, 41, 321.
70. (a) Soderquist J. A., Anderson C. L., Miranda E. I., Rivera I., Kabalka G. W. *Tetrahedron Lett.*, **1990**, 31, 4677. (b) Buynak, J. D.; Geng, B.; Uang, S.; Strickland, J. B. *Tetrahedron Lett.*, **1994**, 35, 985.

71. Buynak J. D., Strickland J. B., Lamb G. W., Khasnis D., Modi S., Williams D., Zhang H. *J. Org. Chem.*, **1991**, *56*, 7076.
72. Takeda K., Ohnishi Y., Koizumi T. *Org. Lett.*, **1999**, *1*, 237.
73. Wang J., Li P., Choy P. Y., Chan A. S. C., Kwong F. Y. *Chem. Cat. Chem.*, **2012**, *4*, 917.
74. Howell G. P., *Org. Process Res. Dev.*, **2012**, *16*, 1258.
75. Chauhan P., Chimni S. S., *RSC Adv.*, **2012**, *2*, 6117.
76. Vicario J. L., Badia D., Carrillo L., *Synthesis*, **2007**, 2065.
77. Tsogoeva S. B., *Eur. J. Org. Chem.*, **2007**, 1701.
78. Leow D., Tan C. H., *Chem. Asian J.*, **2009**, *4*, 488.
79. Ishikawa T., *Chem. Pharm. Bull.*, **2010**, *58*, 1555.
80. Liu W. J., Li N., Gong L. Z., "In Asymmetric Catalysis from a Chinese Perspective, ed. S. M. Ma", *Springer-Verlag Berlin, Berlin*, **2011**, Vol. 36, 153.
81. Zhang Y., Kee C. W., Lee R., Fu X. A., Soh J. Y. T., Loh E. M. F., Huang K. W., Tan C. H., *Chem. Commun.* **2011**, *47*, 3897.
82. Qin B., Liu X., Shi J., Zheng K., Zhao H., Feng X., *J. Org. Chem.*, **2007**, *72*, 2374.
83. (a) Meijere A., Diederich F., "Metal-Catalyzed Cross-Coupling Reactions, 2nd ed.", *Wiley-VCH: Weinheim*, **2004**; (b) Negishi E., "Handbook of Organopalladium Chemistry for Organic Synthesis," *Wiley-Interscience: New York*, **2002**; (c) Tsuji J. "Palladium Reagents and Catalysts: New Perspectives for the 21st Century"; *Wiley-VCH: Weinheim*, **2004**. (d) Jana R., Pathak T. P., Sigman M. S. *Chem. Rev.* **2011**, *111*, 1417.
84. (a) Bumagin N. A., Korolev D. N., *Tetrahedron Lett.* **1999**, *40*, 3057. (b) Goossen L. J., Ghosh K. *Angew. Chem., Int. Ed.* **2001**, *40*, 3458. (c) Villalobos J. M., Srogl J., Liebeskind L. S. *J. Am. Chem. Soc.* **2007**, *129*, 15734. (d) Labadie J. W., Stille J. K. *J. Am. Chem. Soc.* **1983**, *105*, 6129. (e) Negishi, E.; Bagheri, V.; Chatterjee, S.; Luo F. T., Miller J. A., Stoll A. T. *Tetrahedron Lett.*, **1983**, *24*, 5181. (f) Fiandanese V., Marchese G., Martina V., Ronzini L. *Tetrahedron Lett.*, **1984**, *25*, 4805. (g) Barton D. H. R., Ozbalik N., Ramesh M. *Tetrahedron*, **1988**, *44*, 5661.
85. (a) Ishiyama T., Kizaki H., Hayashi T., Suzuki A., Miyaura N. *J. Org. Chem.* **1998**, *63*, 4726. (b) Jafarpour F., Rashidi-Ranjbar P., Kashani A. O. *Eur. J. Org. Chem.*, **2011**, 2128. (c) Hatanaka Y., Fukushima S., Hiyama T. *Tetrahedron*, **1992**, *48*, 2113. (d) Echavarren A. M., Stille J. K. *J. Am. Chem. Soc.*, **1988**, *110*, 1557.
86. Schmink J. R., Krska S. W., *J. Am. Chem. Soc.*, **2011**, *133*, 19574.
87. Petriguet J., Roisnel T., Gree R., *Chem. Eur. J.* **2007**, *1*, 7374.
88. Justyna A. Grzyb, Ming S., Chiaki Y., Chi W., Stanley B., Robert A., *Tetrahedron*, **2005**, *61*, 7153.

89. Vijaya L. K., Shiva S. K., Bhamidipati V. S. K., Rachapudi B. N., Bethala L.A., *Eur. J. Lipid Sci. Technol.*, **2013**, *115*, 921.
90. Woods G. F., *J. Org. Synthesis Coll.* **1965**, *3*, 470.
91. Sinha D., Mandal T., Gogoi S., Goldman G., Zhao J., *Chin. J. Chem.*, **2012**, *30*, 2624.
92. (a) Kresge A. K., Tobin J. B., *J. Org. Chem.* **1993**, *58*, 2652, (b) Apeloig Y., *J. Am. Chem. Soc.* **1990**, *112*, 9131.
93. Woods G. F., *J. Org. Synthesis Coll.* **1965**, *3*, 470.

II. THIRD CHAPTER

Medicinal Chemistry: Preparation of New Inhibitors of Anti-apoptotic MCL-1 Protein

III.A. INTRODUCTION

Introduction

Apoptosis

The elimination of normal or neoplastic cells via the induction of a cell death program has been recognized since the 1960s, with the term “apoptosis”[1]. Apoptosis has been described as a cell suicide mechanism by which multicellular organisms remove damaged or unwanted cells in order to maintain normal life development and homeostasis [2]. The failure of apoptosis system plays a causative role in carcinogenesis as well as the chemoresistance of tumor cells [3–5].

Apoptosis has been identified as a crucial process in physiological terms, for a number of reasons: for the maintenance of tissue homeostasis, for the safe removal of unwanted or damaged cells, for morphogenesis during embryonic development, and for the resolution of inflammation [6].

A number of ordered morphological changes had been identified in cells undergoing apoptosis, resulting in characteristic cellular changes, including chromatin condensation, nuclear fragmentation, breakdown of the cytoskeleton, and cell shrinkage. Most of the morphological changes associated with apoptosis are caused by a set of proteases that are specifically activated in apoptotic cells [7]. These homologous endopeptidases belong to the large family of proteins called caspases (c-asp-ases: cysteine dependent aspartate-specific protease). Caspases are among the most specific proteases, recognizing at least four contiguous amino acids.

Caspases involved in apoptosis are generally divided into two categories: the initiator caspases, which include caspase-2, caspase-8, caspase-9, and caspase-10, and the effector caspases, consisting of caspase-3, caspase-6, and caspase-7. An initiator caspase is characterized by an extended N-terminal prodomain of >90 amino acids, whereas an effector caspase contains only 20–30 residues in its prodomain [8]. In addition, only initiator caspases contain a caspase recruitment domain (CARD) or death effector domain (DED) preceding the catalytic domain. All caspases are

synthesized in cells as catalytically inactive zymogens. During apoptosis, they are usually converted to the active form by proteolytic processing. The activation of an effector caspase is performed by an initiator caspase through cleavage at specific internal Asp residues that separate the large and the small subunits of the effector caspases (Figure III.1). The initiator caspases, however, are autoactivated.

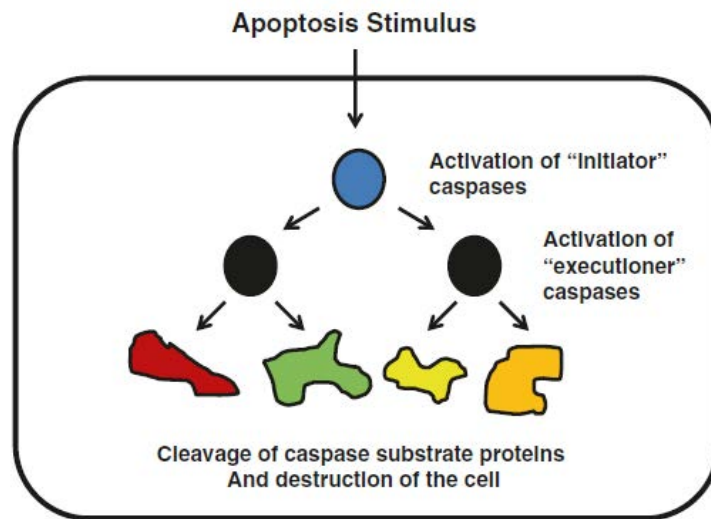


Fig.III. 1: Activation of the caspase protease cascade during apoptosis.

Thus, these caspases are responsible for the dismantling of the cell's components that are packaged into smaller apoptotic bodies. These apoptotic bodies were observed to be engulfed and degraded by macrophages or neighboring cells [1, 9, 10]. The early characterization of apoptotic cells also identified a few biochemical changes, including externalization of plasma membrane phospholipids, activation of cellular DNAses, and degradation of genomic DNA to oligonucleosomal- length fragments visualized as "apoptotic DNA ladders" on agarosegels [11].

In contrast, apoptosis plays a fundamental role in some physiological processes, especially in mammalian development and the immune system [12, 13]. Hence, the process of apoptosis is very important in both the development of immune cells and the execution of an immune response. T cells and B cells are lymphocytes, white blood cells that participate in the adaptive immune response. T cells mediate the cellular immune response (i.e., production of cytotoxic T cells, release of cytokines, antigen presentation, activation of macrophages and natural killer cells), and B cells mediate the humoral immune response (i.e., production of antibodies) [14].

Maturation process of T cell reveals the requirement for both apoptosis and survival mechanisms to modulate cell populations and fulfill their selection. In the early stages of thymocyte development (double negative stage, or CD4–CD8–), the presence of survival signals (e.g., the cytokine IL-7) is needed to prevent apoptosis. These signals control both the population of progenitors and T cell receptor (TCR) differentiation. In the following step, thymocytes start the first selection in the thymus cortex by binding their TCR to major histocompatibility complex (MHC) molecules of the surrounding epithelial cells. Cells which fail to interact will be eliminated since they didn't receive signals for their survival [15]. This process, termed positive selection, is necessary to ensure that T cells will be able to further participate in the immune response. In contrast, T cells bearing receptors that have too high affinity for MHC are dangerous for an organism as they have the potential to trigger the elimination of cells in healthy functional tissues. Consequently, these highly reactive cells are also eliminated by apoptosis. This constitutes the negative selection process. Similarly, B cell development and maturation involves positive and negative selection; and the early B cell populations are also dependent on survival cytokines such as IL-7 [16]. However, the development of B cells continues in the bone marrow and the selection signals are received through a different class of receptors, the B cell receptors (BCR) [17].

Apoptosis can be triggered either by activating receptors on the cell surface (the extrinsic pathway) or by the perturbation of mitochondria (the intrinsic pathway).

The extrinsic pathway:

In the death receptor pathway, caspase-8 is the key initiator caspase. Death receptors are members of the tumor necrosis factor (TNF) receptor super-family and comprise a subfamily that is characterized by the intracellular death domain (DD) [18]. The most

prominent death ligands are CD95-ligand/Fas ligand, TNF α , and TNF-related

apoptosis inducing ligand (TRAIL). Upon ligand binding, receptors oligomerize and

their death domains attract the intracellular adaptor protein FADD (Fas-associated death domain protein), which, in turn, recruits the inactive proform of caspase-8 or caspase-10 via their death-effector domain (DED). The formed multiprotein complex is called DISC (death-inducing signaling complex) [19]. Recruitment of procaspase-8 to the DISC results in a slight conformational change in the zymogen protein, resulting in modest activation of the enzyme activity and proximity-induced proteolytic processing of procaspase-8 proteins present in the DISC (Figure III.2) [20, 21, 22]. This process removes the inhibitory prodomain and produces large and small caspase-8 subunits.

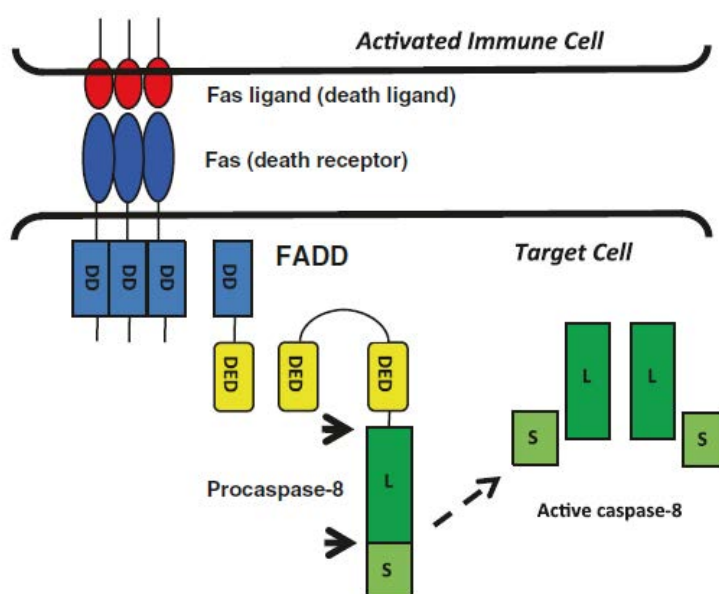


Fig.III. 2: DISC formation and caspase-8 activation in extrinsic pathway

Notably, the activation of caspase-8 is antagonized by FLICE-like inhibitory protein (FLIP), thus providing an additional level of regulation.

- The intrinsic pathway:

The intrinsic pathway (*via mitochondria*) plays a key role in regulating cell death in response to various stimuli. Apoptosis induced via mitochondria is highly regulated by finely balanced interactions between members of the BCL-2 family of proteins, which are divided into two main groups based on their structural and functional properties. The first group is termed as pro-survival proteins and includes BCL-2,

BCL-X_L, MCL-1 (myeloid cell leukemia-1), BCL-W, A1 etc... while the second group includes pro-apoptotic proteins and is divided into two further subclasses: the multi-domain BAK and BAX proteins, and the BH3-only proteins.

In response to apoptotic stimuli, BH3-only proteins activity can be up-regulated by increased expression, activation by proteolytic cleavage, or post translational modification. These BH3-only proteins then trigger apoptosis either by directly activating BAK/BAX [23, 24, 25, 26] (direct activators), or by disrupting complexes between pro-survival proteins and BAK/BAX proteins [27, 28] (sensitizer BH3-only). The activated or released BAK or BAX proteins then oligomerize on the outer mitochondrial membrane (OMM). This oligomeric assembly triggers mitochondrial outer membrane permeabilization (MOMP), allowing the release of cytochrome c and other apoptosis inducing factors (i.e. Smac/DIABLO, AIF etc...) from the mitochondrial inter-membrane space into the cytoplasm. Several cytochrome c molecules interact with several apoptotic protease-activating factor-1 (Apaf-1) molecules that themselves interact with caspases 9 molecules to form a structure known as apoptosome. Then apoptosome activates caspase-9 which in turn activates caspase-3 and thus initiating a caspases cascade that ultimately destroys the cell (Figure III.3) [29].

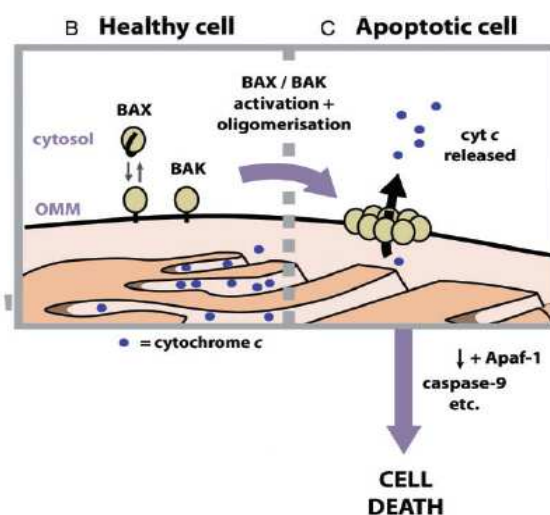


Fig.III. 3: Apoptosis via mitochondrial membrane

Apoptosome activity can be inhibited by various proteins belonging to the IAP family (Inhibitors of apoptosis) such as XIAP or survivin for instance. However, MOMP is

likely to constitute an irreversible step in the pathway as the amplification of the caspase activation cascade (upstream caspases activates downstream caspases) is difficult to interrupt. . The release of IAP inhibitors such as Smac/Diablo from mitochondria after MOMP can also contribute to the activation of caspases despite the presence of IAPs in cytosol.

Elevated level of one or more pro-survival proteins, as observed in many tumors, can inhibit MOMP and subsequent apoptosis. This blockade can occur through sequestration of activator BH3-only proteins, or capture and restrain of active forms of BAK/BAX, or both [30].

BCL-2 Family Proteins:

BCL-2 family proteins was identified in human B cell follicular lymphoma in which the chromosomal translocation $t(14;18)(q32;q21)$ induces BCL-2 gene overexpression [10].

Members of BCL-2 family are characterized by their domain of homology (BH1-BH4) and their functional activities. Based on these functional and structural homologies, the BCL-2 family was subdivided into two functional groups: the pro-survival proteins and the pro-apoptotic proteins [31]. The pro-survival group comprises BCL-2, BCL-X_L and BCL-W share up to four BH (BH1, BH2, BH3, and BH4) domains and a carboxyl terminal trans-membrane domain, where MCL-1 and A1 pro-survival members differ from the others in lacking a well-defined BH4 domain (Figure III.4). In general, pro-survival proteins are localized on the outer mitochondrial membrane (OMM). The second BCL-2 family group, pro-apoptotic proteins, is further subdivided in two classes based on their structures and associated functions. Members of the first class, the pro-apoptotic effector proteins, BAX and BAK are referred to as "*multi-domain proteins*" since they are composed of three BH (BH1, BH2, and BH3) domains, and oligomerize into proteolipid pores within the MOM. The formation of these pores and the subsequent release of proteins from the mitochondrial intermembrane space [32, 33] leads to mitochondrial outer membrane permeabilization (MOMP), which is considered to be the most significant

biochemical event in the initiation of the mitochondrial pathway of apoptosis. The second class of pro-apoptotic BCL-2 family members comprises proteins sharing only the BH3 domain and is referred to as the "*BH3-only proteins*" (such as Bad, Bim, Bid, Bik, Puma, and Noxa). BH3 only proteins are themselves divided into two groups: activators and sensitizers. The activators BH3-only (Bim, Puma and tBid) directly bind to Bak/Bax and lead to their oligomerization, leading to release of cytochrome c. The sensitizers BH3-only (such as Bad, Bim Bik, and Noxa) cannot directly activate Bax/Bak, but they inhibit pro-survival BCL-2 proteins and induce the release of activator proteins or Bax/Bak effectors from their anti-apoptotic partners [34].

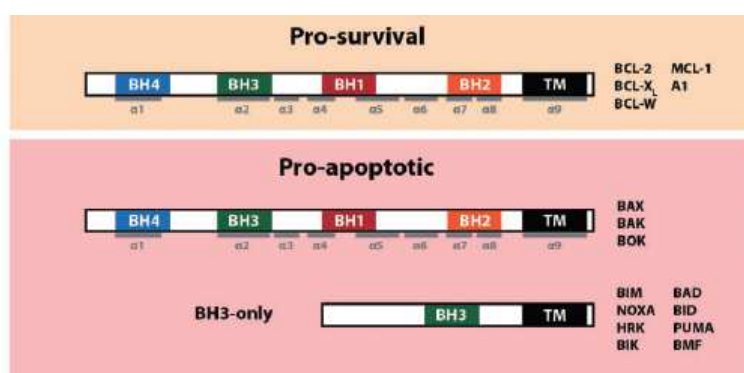


Fig.III. 4: Members of BCL-2 family proteins

Protein protein interactions (PPIs) play critical roles in numerous biological processes. Life and death decisions are, in particular, regulated by a network of PPIs among BCL-2 family members, with individual pro-survival BCL-2 homologues (such as BCL-2, BCL-X_L and BCL-W, MCL-1...) binding to, and inhibiting pro-apoptotic counterparts (the effector multi-domain proteins BAX/BAK, and their upstream regulators BH3 only proteins such as Bim, Bid, Puma, Noxa...) [35].

Structural studies revealed that BH1, BH2, and BH3 domains of the pro-survival BCL-2 family proteins form a hydrophobic groove on their surface. This structural property is important, since the hydrophobic groove of a pro-survival member can bind to α -helical BH3 domain of a pro-apoptotic protein and neutralize its pro-apoptotic function [36]. Furthermore, pro-survival BCL-2 family members prevent effector pro-apoptotic proteins Bax and Bak from being activated (previous studies show that all pro-survival members can bind to BAX, whereas only BCL-X_L and

MCL-1 can bind to BAK). When apoptotic signals are received, BH3-only proteins competitively bind to the hydrophobic groove of the pro-survival proteins which results in the release and conformational activation of BAX and BAK [37]. Bax and Bak can then oligomerize and induce MOMP.

Whereas Bim, Puma, and Bid can antagonize all pro-survival proteins, Bad inhibits BCL-2, BCL-X_L, and BCL-W and Noxa inhibits only MCL-1 and A1 (Figure III.5). Therefore, the specific interactions between the BCL-2 family proteins governs the balance between cell death and survival [38].

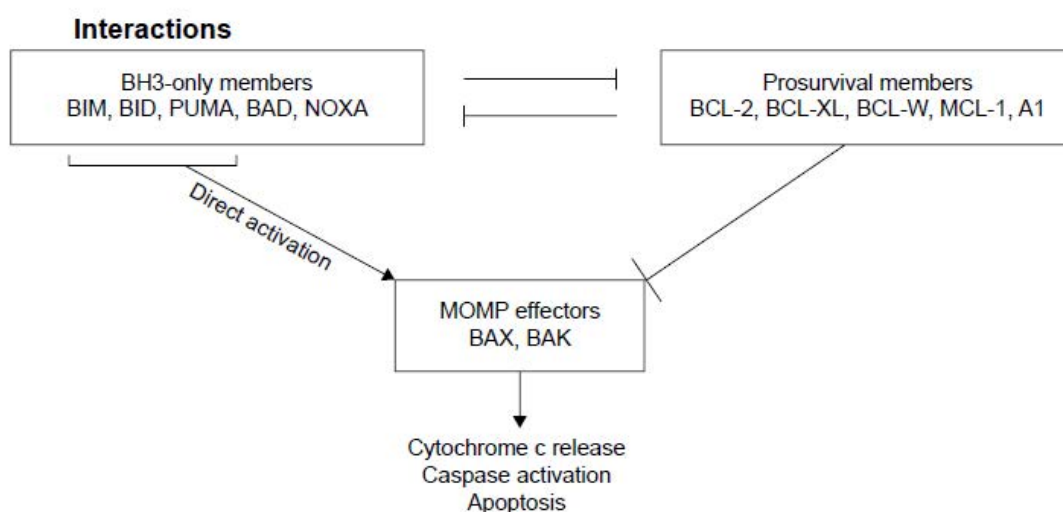


Fig.III. 5: Interaction between the three types of BCL-2 family proteins regulating MOMP and induce apoptosis.

Mcl-1 protein:

MCL-1 (myeloid cell leukemia 1) is a member of the BCL-2 family of proteins that prevents cells from undergoing programmed cell death, a hallmark of cancer [39]. By overexpression of the MCL-1 protein or amplification of the MCL-1 gene, a cancerous cell can avoid apoptosis, the normal fate for cells exhibiting abnormal and deregulated growth [28, 40]. Indeed, amplification of MCL-1 is one of the most common genetic aberrations observed in human cancers [41, 42], including lung, breast, prostate, pancreatic, ovarian, and cervical cancers, as well as melanoma and leukemia [43–50].

Like for the other anti-apoptotic BCL-2 proteins, there is a hydrophobic groove on the surface of MCL-1 that engages the BH3 “death” domains of BH3 only proteins (such as Bim, Bak and Bad). A number of residues in the binding groove differentiate MCL-1 from its homologues [51], in which its groove appears more electropositive than other pro-survival proteins (BCL-X_L groove for example is almost completely uncharged) [52]. As an alternative mechanism, activator BH3-only proteins (Bim, Puma, and tBid) bind and activate Bax and/or Bak directly if they are not bound and neutralized by BCL-2 like proteins including MCL-1 [37, 53, 54, 55]. However, Noxa can competitively bind to MCL-1 and prevent it from sequestering activator BH3-only proteins [55] (Figure III.6).

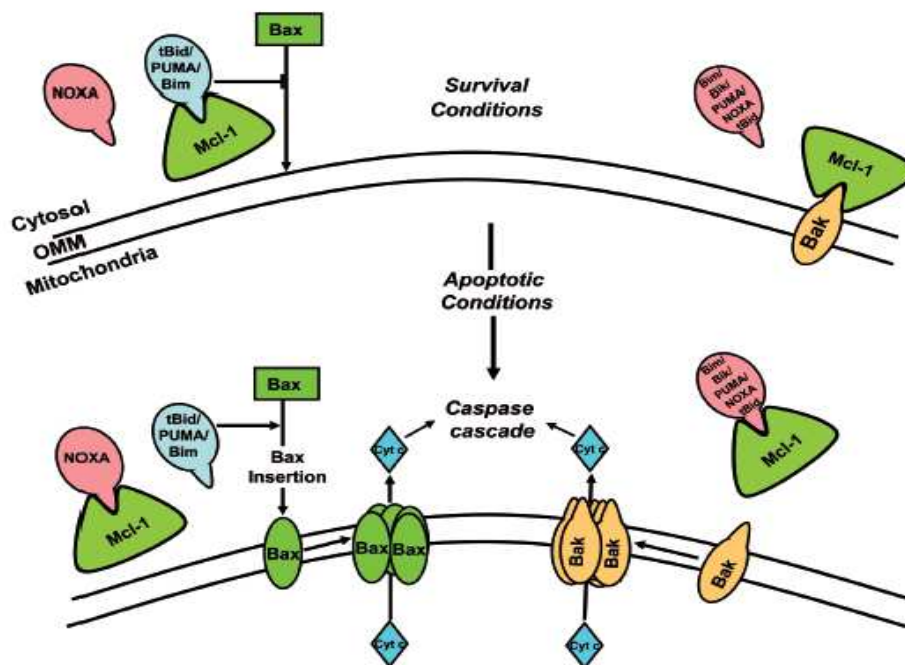


Fig.III. 6: Role of MCL-1 in survival and apoptotic conditions.

The BH3 domain is an amphipathic α -helix whose hydrophobic face recognizes four hydrophobic sub-pockets, p1, p2, p3 and p4, in the BH3-binding groove on MCL-1, while a critical Asp (Aspartic Acid) on the polar face of the BH3 helix binds Arg263 of MCL-1 [56, 57]. Through this protein–protein interaction (PPI), MCL-1 (and the other pro-survival BCL-2 proteins) “neutralizes” the cell-killing function of the pro-apoptotic BCL-2 proteins. In this way, overexpression of MCL-1 leads to the evasion of apoptosis and, hence, cancer.

Thus, MCL-1 is an important pro-survival oncogene that is overexpressed in the majority of cancers. In particular, multiple myeloma cells display high expression of MCL-1 and appear to be dependent on MCL-1 for survival [58]. Notably, gene alterations around the locus of MCL-1 on 1q21 have been identified as early as 1994, when it was discovered that 1q21 is duplicated or rearranged in many types of cancers [59], where MCL-1 has been identified as the most amplified gene in a screen of 3,000 individual cancers, highlighting its importance for cancer and suggesting a unique function of MCL-1 amongst the pro-survival BCL-2 proteins [60].

In contrast, MCL-1 shows to be required for the development and maintenance of B and T-lymphocytes [61], and for neural development [62], in addition to its critical role in the regulation of macrophage and neutrophil apoptosis [63, 64], and in the survival of haematopoietic stem cells [65].

BCL-2 Inhibitors:

Most cancer chemotherapeutic agents kill cancer cells by induction of apoptosis through perturbation of mitochondria and induction of the intrinsic pathway of apoptosis [66, 67]. Major efforts have been made over the last decade to develop small molecule inhibitors of the pro-survival members of the BCL-2 family of proteins, which are highly expressed in some cancers and are known to regulate mitochondrial membrane integrity. Although development of such inhibitors has proved particularly difficult due to the necessity to inhibit protein protein interactions, some success has been achieved. BH3 mimetics, for instance, proved to be highly potent inhibitors for different pro-survival members, and in many types of cancers.

These small molecules are capable of mimicking the BH3 domain of BH3-only proteins and bind to the pro-survival proteins with high affinity and inhibit their activity, leading to BAX/BAK activation and thus to caspase activation and apoptosis [38]. The BH3-mimetic concept has prompted the design of numerous small BH3 peptides or organic molecules [68, 69].

ABT-737 (Figure 7), for instance, is a highly potent inhibitor of BCL-2, BCL-X_L and BCL-W. It binds with very high affinity ($K_i < 1$ nM) to BCL-X_L, and binds also to BCL-2 and BCL-w (due to their similar structure as BCL-X_L). However, MCL-1 and

A1 that have less homologous structure are not inhibited by ABT-737. The potential of ABT-737 as an anticancer agent has further been demonstrated in a set of cancer cells including lung cancer cell lines. Different studies were performed and investigated the effect of ABT-737 in small cell line cancer (SCLC), and identified an essential role of MCL-1 in determining resistance to ABT-737 [70, 71, 72]. To this end, SCLC cell lines that have low expression of MCL-1 were more sensitive to ABT-737 than those with high expression of MCL-1. All of these pro-survival BCL-2 proteins inhibit apoptosis by sequestering pro-apoptotic BH3 containing BCL-2 proteins. In situations where the activity of BCL-2/ BCL-X_L /BCL-W is inhibited due to the binding of ABT-737 into their hydrophobic groove, this binding will compete with the binding of any pro-apoptotic BH3-containing proteins, for example, Bim or Bax and Bak. These pro-apoptotic proteins are subsequently amenable to induce release of cytochrome c. Unfortunately, high level of MCL-1 can compensate for the inhibition of BCL-2/ BCL-X_L /BCL-W and sequester the pro-apoptotic BCL-2 proteins previously displaced from BCL-2/ BCL-X_L /BCL-W.

The major limitation of ABT-737 as an anticancer drug is that it is not orally bio-available. For this reason, Abbott developed a related compound, ABT-263 (named Navitoclax) (Figure III.7), which is orally bio-available and also binds to BCL-2, BCL-X_L, and BCL-W but not to MCL-1 and A1 [73]. The biological activity of ABT-737 and ABT-263 appears to be comparable, although ABT-263 has been shown to be more readily sequestered by human serum albumin than ABT-737 [74].

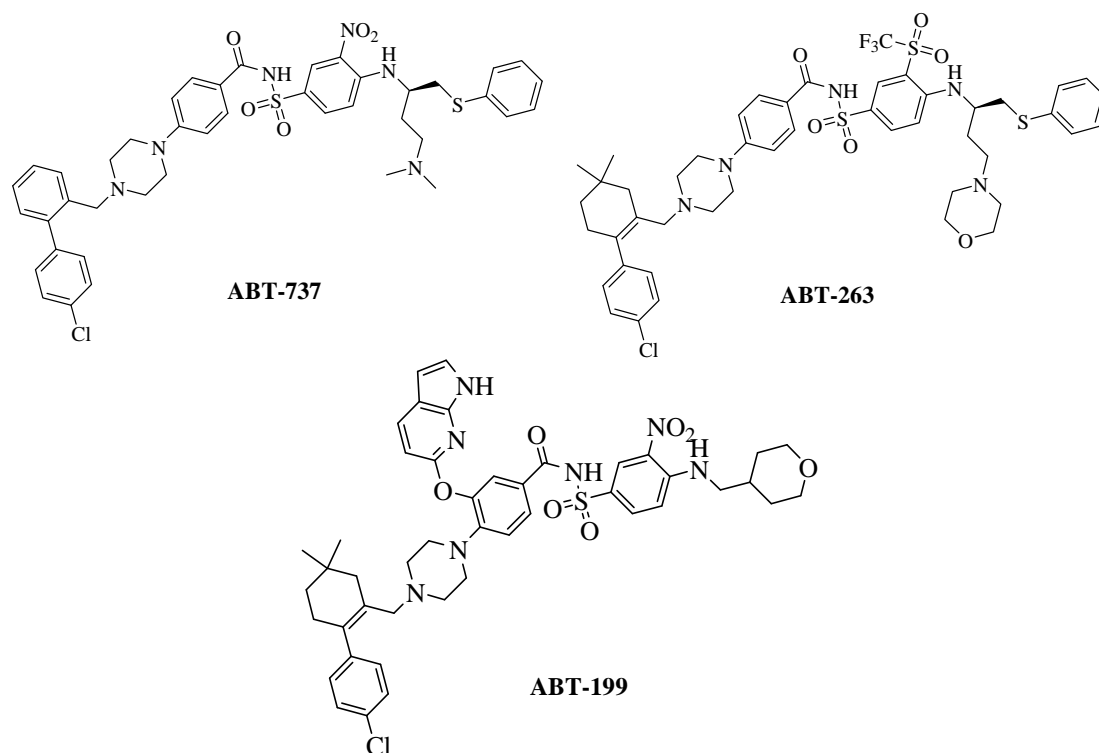


Fig.III. 7: Structures of ABT-737, ABT-263, and ABT-199 BCL-2 inhibitors

The major toxicity of ABT-263 was an on-target effect on BCL- X_L expressed in platelets [75, 76, 77]. The discovery that thrombocytopenia was a major mechanism based effect of ABT-263 led to studies that demonstrated the importance of BCL- X_L as a molecular clock in platelets [75]. To avoid this toxic side-effect, the ABT-199 derivative (Venetoclax) (Figure 7), which is specific for BCL-2 and does not bind to BCL- X_L , was then designed [79]. The first clinical trials with ABT-199 have yielded impressive results without thrombocytopenia [78, 79]

The effectiveness of these agents and others in several cancers is often limited by chemoresistance, which has most commonly been ascribed to high expression levels of other pro-survival BCL-2 family members, particularly MCL-1 [80-86]. Since, the survival of malignant cells depends at least partly on MCL-1 in many cancers, including chronic lymphocytic leukemia (CLL) (a disease characterizes by apoptosis deficiency), therefore, efforts focused on the identification of small molecules targeting selectively MCL-1.

MCL-1 inhibitors:

A variety of approaches for inhibiting MCL-1 have been described, including the use of BH3 peptides [87-90] and small molecules [92-95] that bind MCL-1 directly or inhibit its expression indirectly [95-97]. Indirect MCL-1 inhibitors include cyclin-dependent kinase (CDK) inhibitors such as roscovitine, flavopiridol, seliciclib, dinaciclib, and SNS-032, which inhibit the phosphorylation of the RNA polymerase 2 C-terminal domain and the elongation of transcripts, including MCL-1 [95-97]. Because of the short half-life time of MCL-1 protein (approximately 30 min), it is rapidly eliminated upon treatment with flavopiridol or dinaciclib [95]. Anthracyclines such as daunorubicin have also been shown to repress MCL-1 expression [42]. A potential liability of the indirect MCL-1 inhibitors is that they also reduce the expression of numerous other short-lived proteins, making them less selective and potentially more toxic. Therefore, direct MCL-1 inhibitors are more desirable and are often more potent. Here we introduce a series of direct and selective MCL-1 inhibitors that demonstrate clear on-target cellular activity, disrupting complexes of MCL-1 protein with the pro-apoptotic members and triggering apoptosis in cancer cell lines shown to rely on MCL-1 for survival.

IV.A.c.1.i. Indole-2-carboxylic acid derivatives:

A series of MCL-1 inhibitors derived from indole-2-carboxylic acid has been obtained by high-throughput screening and structure-guided design [98]. The compounds bind to MCL-1 with high affinity (0.45 nM) and selectivity over the other pro-survival BCL-2 family proteins. A mechanistic study has shown that the lead compound A-1210477 (Figure III.8), and its related analogs (A-1155905, A-1208746, and A-1248767), can disrupt the interactions of MCL-1 with BIM and Noxa. Further, it penetrates living cells, and acts via on-target mechanism [99]. These molecules induce the main hallmarks of the caspase-dependent mitochondrial apoptosis (including BAX/BAK activation) in multiple myeloma and non-small cell lung cancer cell lines that have been validated to be MCL-1 dependent. A-1210477 is a particularly strong binder of MCL-1 ($K_i = 0.45$ nM), representing an affinity improvement of at least two orders of magnitude over the other analogs, but it is a much weaker binder of BCL-2 ($K_i = 0.132$ μ M) and BCL-X_L ($K_i = 0.660$ μ M). These compounds are therefore the first BH3 mimetics targeting selectively MCL-1. Lastly, the fact that A-1210477

synergizes with navitoclax to trigger apoptosis is of interest given that MCL-1 is a key factor in the resistance of malignant cells to ABT-737 and navitoclax [80].

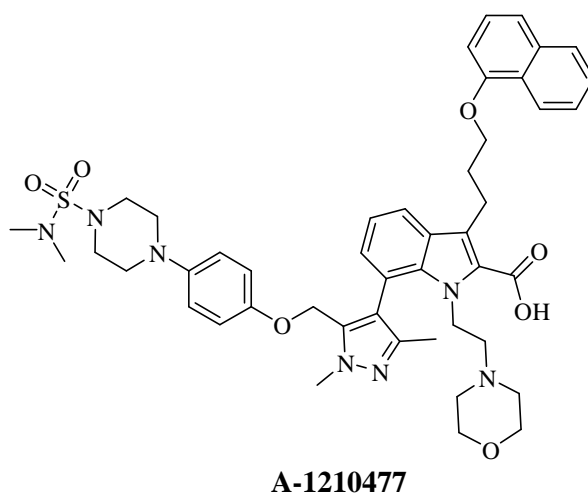


Fig.III. 8: Structures of Indole-2-carboxylic acid derivatives.

IV.A.c.1.ii. Merged Compounds: 2-Carboxylic Acid- Substituted Benzofurans, Benzothiophenes and Indoles:

Fesik and co-workers (at Vanderbilt University) used NMR-based screening of a large fragment library followed by structure-based design to generate potent MCL-1 inhibitors [57]. Two different classes of fragments were designed; Class I was mostly constituted of carboxylic acids attached to a 6,5-fused hetero cycle, for example **1** (Figure III.9), which binds to MCL-1 with a K_i of 131 μM , according to a fluorescence polarization competition assay (FPCA), whilst class II was populated by hydrophobic aromatics tethered to a polar functional group, most typically a carboxylic acid as in **2**, shown in Figure 9 ($K_i = 60 \mu\text{M}$). NOESY NMR-guided molecular modeling informed Fesik's group that the class I compounds were binding near Arg263, which was likely engaging in salt bridges with the carboxylic acids of the fragments. Also, it appeared that the class II compounds were binding deep into the hydrophobic p2 pocket and the carboxylic acid was located at the surface of this pocket near Arg263. The authors observed that the binding of class I and class II compounds to MCL-1 was mutually exclusive, suggesting that the carboxylic acid in each class was binding the same residue, possibly Arg263.

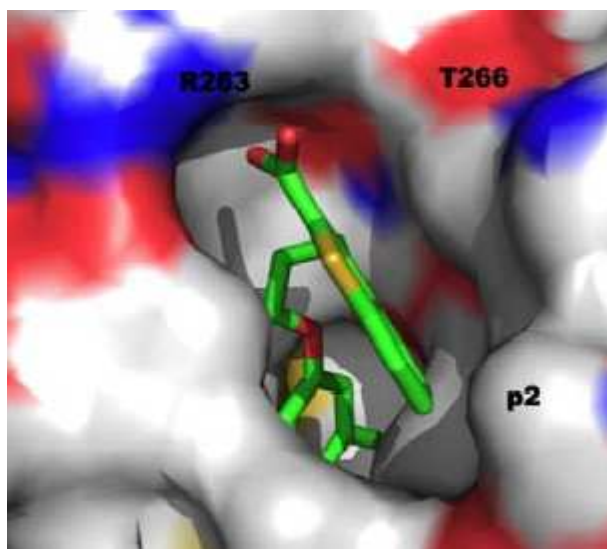
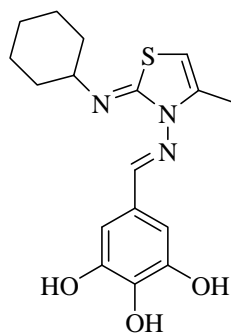


Fig.III. 10: Co-crystal structure of benzothiophene **3** with MCL-1

IV.A.c.1.iii. MIM1, A Substituted Pyrogallol:

Walensky and co-workers used a fluorescently-labeled, hydrocarbon-stapled MCL-1 BH3 helix as the probe to screen a large library of compounds, which led to the discovery of MIM1 (MCL-1 -1 Inhibitor Molecule 1, **6**) (Figure III.11) that binds in the BH3-binding groove on the surface of MCL-1 [91]. The screening process began with 71,296 small molecules, which were then decreased into 64 potent and selective MCL-1 inhibitors. The trihydroxy phenyl group (pyrogallol) in the structure of MIM1 showed to be required for the activity of such inhibitor against MCL-1. However, MIM1 is the first MCL-1 selective inhibitor that bears this motif: MIM1 disrupted the MCL-1/Bid BH3 peptide complex with an IC_{50} value of 4.8 μM , whilst MIM1 demonstrated no capacity to disrupt the BCL- X_L /Bid BH3 peptide complex ($IC_{50} > 50 \mu M$).



MIM1

Fig.III. 11: Structure of **6/MIM1**, a selective MCL-1 inhibitor.

NMR structural studies of MIM1 with ^{15}N - MCL-1 revealed that the small-molecule binds in the canonical BH3 binding groove. The cyclohexyl group was predicted to make hydrophobic contacts near the p3 pocket, while the thiazolyl core and its methyl substituent probe deeply into the p2 pocket (Figure III.12). In comparison with other MCL-1 selective inhibitors, this latter interaction may be a source of MIM1's selectivity. The pyrogallol motif forms hydrogen bonds with Asp256 and Arg263, which are residues that are engaged by the hydrophilic face of the amphipathic BH3 α -helices. Finally, MIM1 was shown to selectively inhibit MCL-1 based suppression of pro-apoptotic Bax activation through freeing up the BH3-only protein tBID, and selectively induced cell death in MCL-1 dependent leukemia cell line.

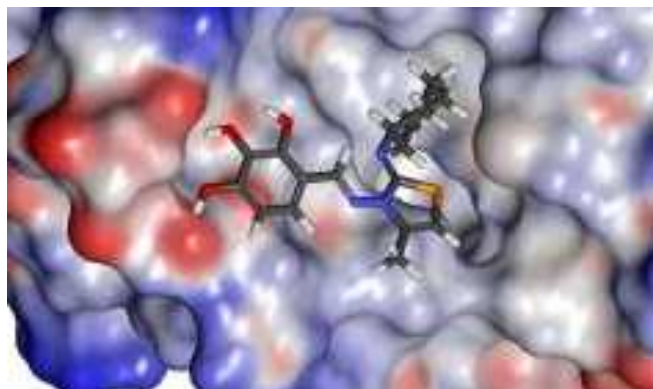


Fig.III. 12: Co-crystal structure of MIM-1 compound with MCL-1

IV.A.c.1.iv. 3-Substituted-N-(4-hydroxynaphthalen-1-yl) Aryl Sulfonamides:

Similarly to Walensky's approach, Nikolovska-Coleska's laboratory also applied a high throughput screening strategy to identify MCL-1 inhibitors [100]. After screening a small-molecule library of over 50,000 compounds, the authors discovered compound **7** (Figure III.13) that bound MCL-1 with a K_i of 1.55 μM , which is around the same affinity as MIM1.

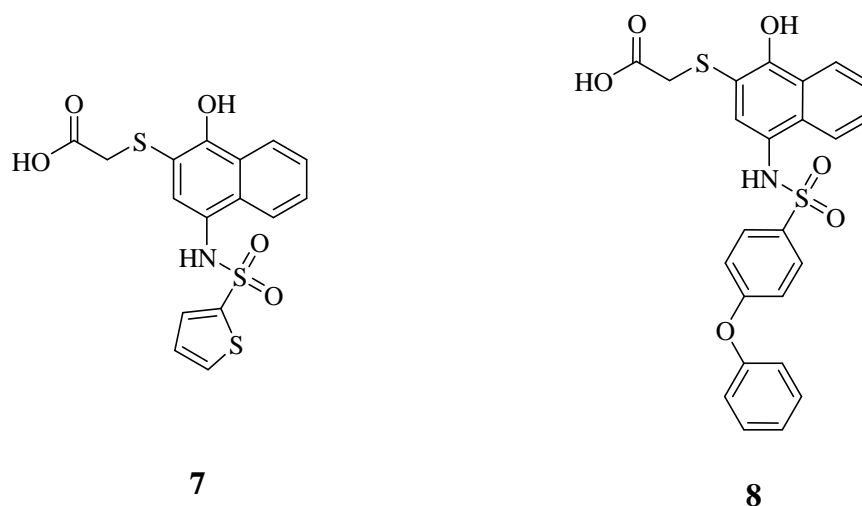


Fig.III. 13: MCL-1 inhibitors developed by Walensky.

Computational modeling predicted that the aromatic ether and naphthalene ring binds the hydrophobic pockets p2 and p3 in the MCL-1 protein (Figure III.14) [100]. The carboxylic acid forms a network of hydrogen bonds with Arg263 and Asn260, and the phenolic hydroxyl group binds His224. NMR structural studies confirmed that compound **7** was bound to the hydrophobic groove on the surface of MCL-1 and, therefore, was functioning as a BH3 mimetic. With this data in hand, Nikolovska-Coleska and co-workers focused on the structure-based design approach to optimize their target compound. A library of around 50 derivatives was prepared, of which the most potent member **8**, shown in Figure 13, bound MCL-1 with a K_i of 180 nM. Compound **8** was selective for Mcl-1 over the other anti-apoptotic BCL-2 proteins, most notably almost 60-fold selective over BCL- X_L .

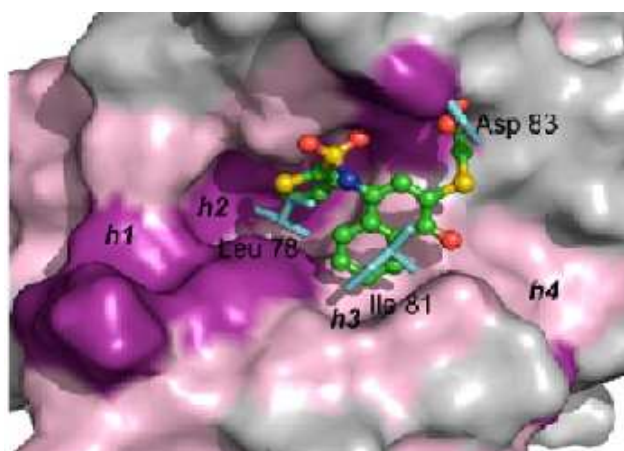


Fig.III. 14: Co-crystal structure of compound **8** with MCL-1

IV.A.c.1.v.8-Hydroxyquinolines:

In a collaborative effort between Eutropics Pharmaceuticals and researchers at The Scripps Research Institute, a high throughput screen of the NIH Molecular Libraries and Small Molecule Repository (MLSMR) led to the discovery of a selective MCL-1 inhibitor ($IC_{50} = 2.4 \mu M$) based on an 8-hydroxyquinoline-derivative scaffold **9** (Figure III.5) [101]. A subsequent round of SAR analysis revealed that the 8-hydroxyl group and the quinoline nitrogen were essential. Next, modification of the phenyl and amino-pyridine resulted in compound **10**, which exhibited improved affinity for MCL-1 ($IC_{50} = 0.31 \mu M$) and selectivity over BCL-X_L ($IC_{50} > 40 \mu M$).

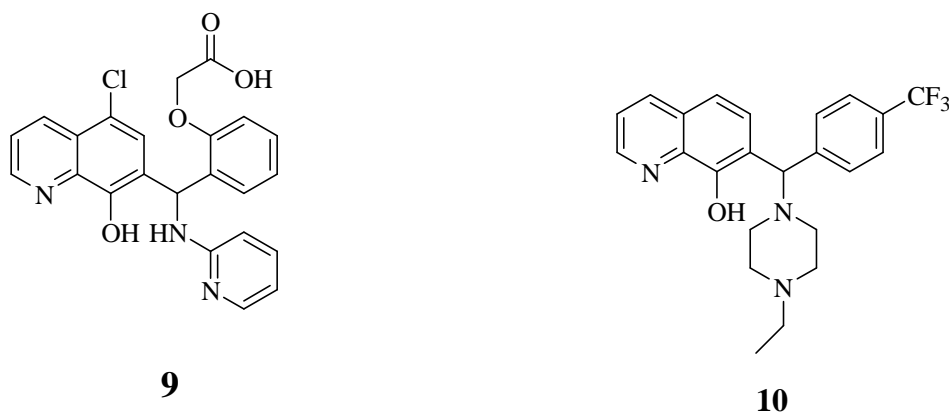


Fig.III. 15: Developed MCL-1 inhibitors.

Molecular modeling with the *R*-enantiomer of **10** suggested that the 8-hydroxyquinoline moiety engages in a hydrogen bond with Asn260, which orients the *N*-ethylpiperazine and *para*-CF₃-phenyl groups for delivery into the p2 and p4 pockets, respectively (Figure III.16).

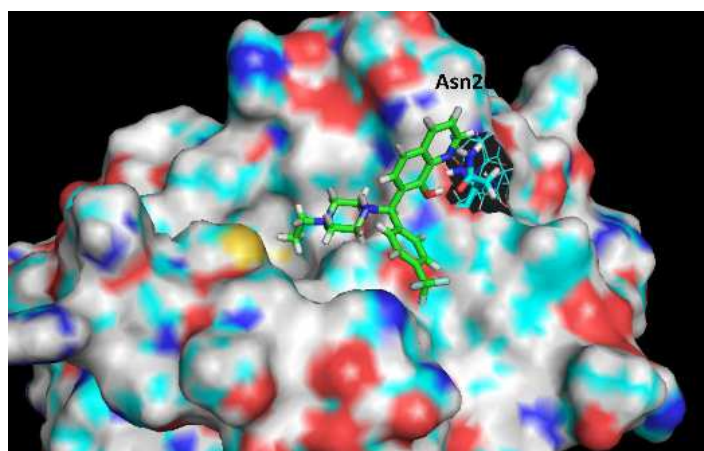


Fig.III. 16: Co-crystal structure of compound **8** with MCL-1

IV.A.c.1.vi. 2-(Arylsulfonamido) Benzoates and 2-Hydroxybenzoates (Salicylates):

Two novel series of MCL-1 inhibitors were developed by the researchers at AbbVie (a pharmaceutical company, formerly Abbott) using fragment-based methods. One based on 2-arylsulfonamido benzoate scaffold and the other on a salicylic acid motif [102]. NMR structural studies revealed that aryl sulfonamide salicylic acid derivatives exhibit important potency to MCL-1. According to NMR data obtained for aryl sulfonamide **11** (IC_{50} = 5 μ M; Figure III.17), it was suggested that the vinyl group oriented towards the p2 pocket normally occupied by Leu62 of the Bim-BH3 peptide. Replacement of the vinyl group with an aryl group afforded compound **12** (Figure III.17) which allows more than ten-fold improvement in MCL-1 inhibitory activity (IC_{50} of 0.4 μ M). Subsequent modification of the sulfonamide moiety resulted in compound **13** (IC_{50} = 30 nM, Figure III.17), a more potent inhibitors with the best of the series carrying a pyrazole moiety.

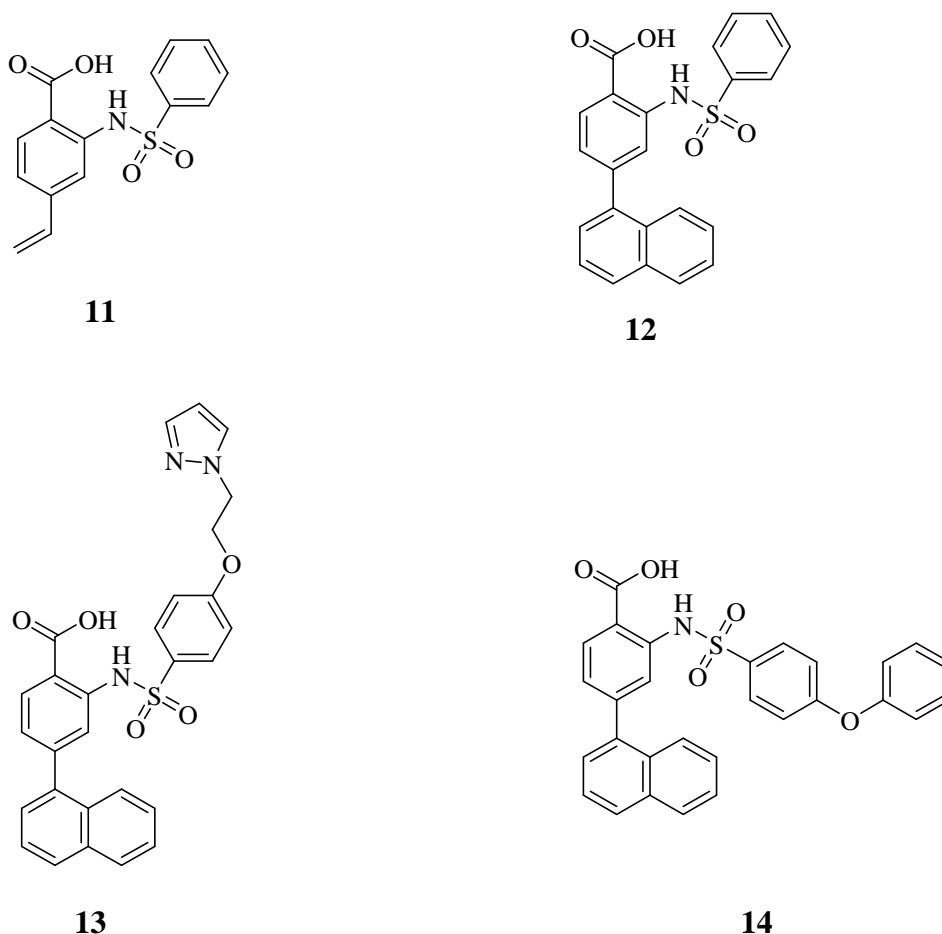


Fig.III. 17: AbbVie's aryl sulfonamide-based MCL-1 inhibitors

A co-crystal structure of **14** (IC_{50} = 0.5 μ M; Figure III.18; PDB ID: 4OQ5) revealed that the distal phenyl ring of the biphenyl ether moiety is projected into the p1 pocket, the naphthyl group into the p2 pocket and the carboxylic acid binds Arg263, close to Asp67 of the Bim-BH3 peptide [103]. It is particularly noteworthy that the p2 pocket opens up somewhat, allowing much deeper penetration of the naphthyl group than Leu62 of Bim-BH3. A similar finding was observed by Fesik and colleagues, and it has been proposed that this may be a source of MCL-1 selectivity by synthetic ligands.

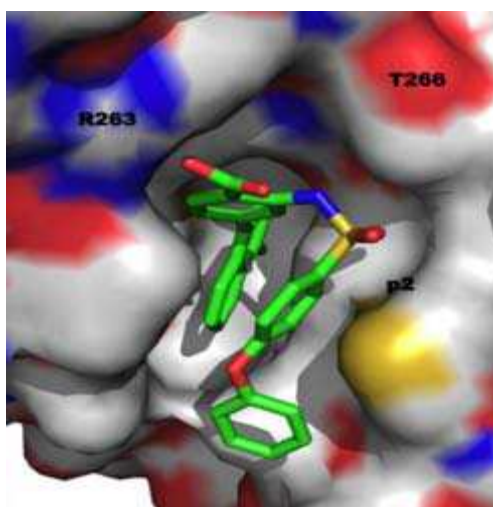


Fig.III. 18: Co-crystal structure of compound **14** with MCL-1

IV.A.c.1.vii. 8-Oxo-3-thiomorpholino-8H-acenaphtho [1, 2-b] pyrrole-9-carbonitrile and Fragments:

Zhang and colleagues used a fragment-based approach to convert their previously reported dual MCL-1/BCL-2 inhibitor 8-oxo- 3-thiomorpholino-8H-acenaphtho-[1, 2-*b*] pyrrole-9-carbonitrile (**15**: K_d = 58 nM (MCL-1), 310 nM (BCL-2), Figure III.19) into a more “drug-like” and MCL-1 selective inhibitor [104]. For this purpose, compound **15** was dissected into several fragments of which cyanoacetamide **16** exhibited good binding affinity to MCL-1 (K_d = 13.5 μ M). To gather information on the likely binding mode of **16**, the authors prepared an R263A mutant of MCL-1 since this arginine plays a significant role in the recognition of the Bim-BH3 helix. Fragment **16** demonstrated no appreciable affinity (K_d > 1000 μ M) to the mutant MCL-1 protein, indicating that it binds to R263, possibly through a hydrogen bond in

which the carbonyl of **16** serves as the hydrogen bond acceptor. Molecular modeling studies suggested that functionalization of the CH₂ and NH₂ groups of **16** might allow occupation of the p2 and p4 pockets, respectively. Accordingly, hydrophobic moieties were added to these functional groups.

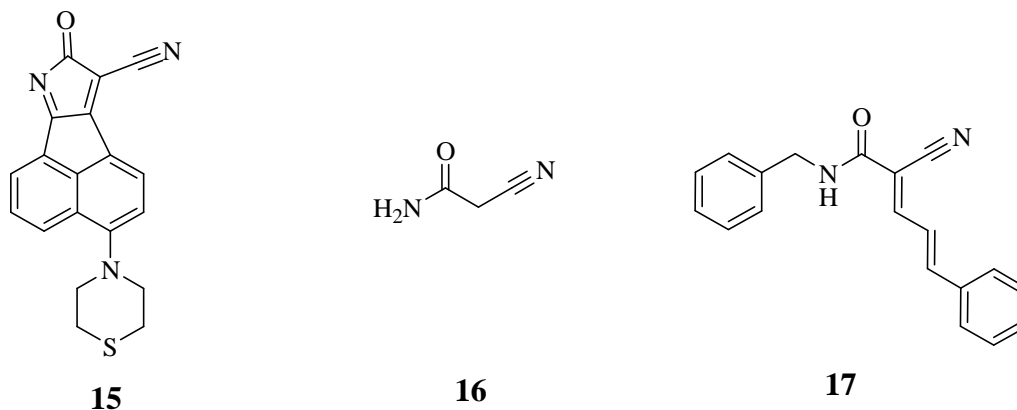


Fig.III. 19: Deconstruction of dual MCL-1/BCL-2 inhibitor **15** and rebuilding of MCL-1 selective inhibitor

This functionalization ends up with compound **17**, shown in Figure III.19, that exhibits an improved affinity towards MCL-1 ($K_d = 0.16 \mu\text{M}$) of almost two orders of magnitude over fragment **16**. In addition, FPCA indicated that **17** exhibited no affinity for BCL-2, and, therefore, that dual MCL-1/BCL-2 inhibitor **15** had been transformed into a selective MCL-1 inhibitor, since it selectively induced apoptosis in the MCL-1 dependent cell line NCI-H23 with an IC_{50} of $0.38 \mu\text{M}$ over cell lines that are dependent on BCL-2.

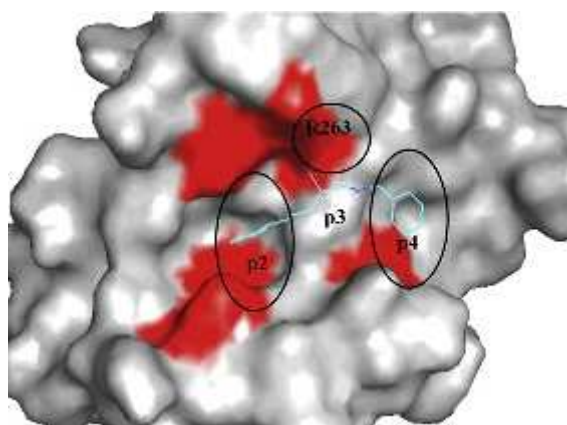
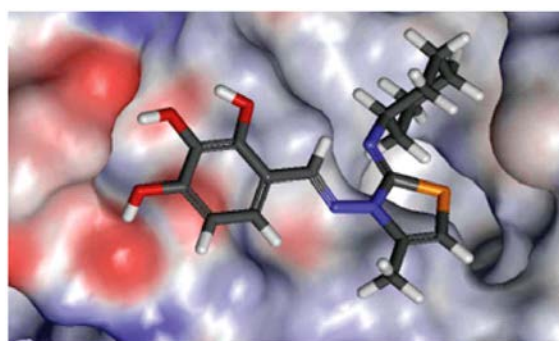


Fig.III. 20: Co-crystal structure of compound **17** with MCL-1

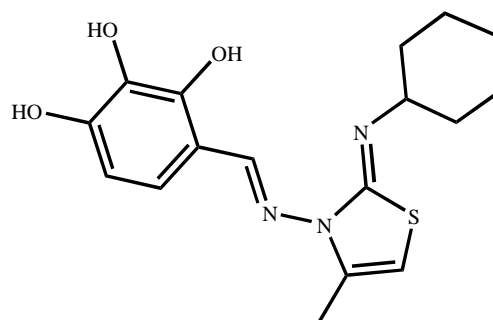
III.B. OBJECTIVE AND STRATEGY

Objective and Strategy

Very few MCL-1 inhibitors were reported in the literature at the beginning of the studies of our groups in this field and MIM-1 compound, which was discovered by Walenksy [91], showed an interesting interaction with the binding groove on the surface of MCL-1, as well as a promising bioactivity. Molecular modeling of MIM-1 shows both the hydrophobic interaction and hydrogen bonding interaction of MIM-1 substituents inside the pockets of MCL-1 protein (Figure III.21).



MIM-1 Docked in MCL-1 pocket



MIM-1 compound

Fig.III. 21: Molecular modeling of **MIM-1** in MCL-1 pocket

Thus, the synthesis of selected analogs of MIM-1, followed by in depth biological studies in order to obtain useful Structure-Activity Relationships, appeared to us as an attractive strategy to obtain more active and/or selective compounds in this area. Therefore on the basis of our own molecular modeling studies, in a first step, two different types of structures were selected and studied during the PhD thesis of Dr Assaad Nasr El Dine (Figure III.22). In a first series, he studied the role of the polyphenol moiety by replacing this part of the molecule with different aromatic groups. It was clearly demonstrated that, in agreement with molecular modeling studies, at least two phenols were required for bioactivity. In the second series he could establish that both the cyclohexyl and the methyl groups can be successfully replaced by aromatic, heteroaromatic and benzylic derivatives to afford new molecules with much higher bioactivity and selectivity than MIM-1 towards MCL-1. All the corresponding biological experiments were performed at the University of

Nantes (studies on breast cancer), the University of Caen (ovarian cancer) and University of Rennes (melanoma).

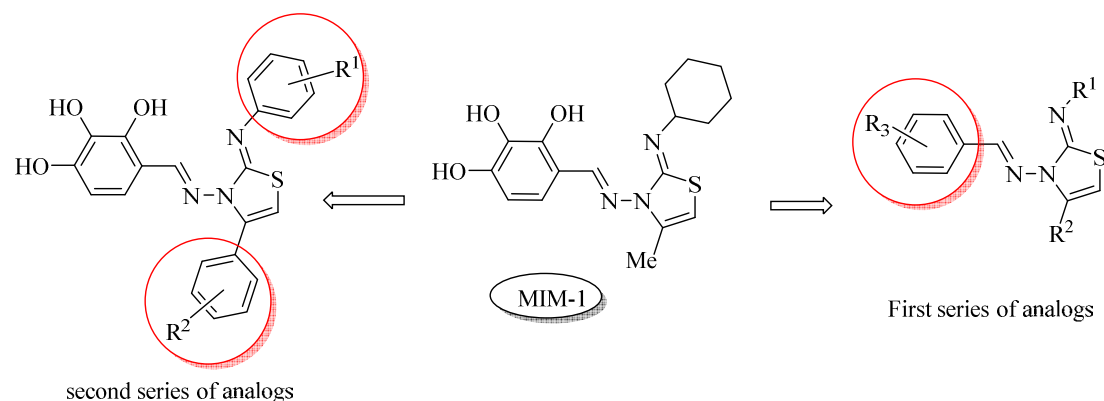


Fig.III. 22: First model prepared in our group

In a second step, which is part of my PhD work, our group wanted to explore the possibility of changing the heterocyclic core of MIM-1 with different five membered heterocycles as indicated in Figure III.23. This includes again the preparation of two different series. In the first series we keep anhydrazone type structure linked to a five membered heterocyclic core. In the second series we replace this hydrazone part by an alkene moiety, again linked to a five membered heterocycle.

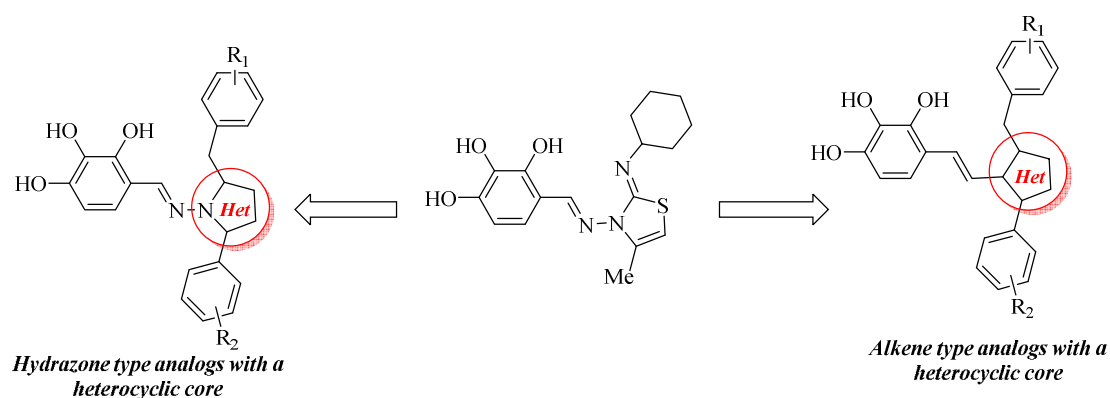


Fig.III. 23: Second model of synthesis

This design for these new molecules was supported by molecular docking studies performed by Dr Nicolas Levoin (Bioprojet-Biotech company, Rennes). Representative examples of such studies are given in Figures III.24 and III.25.

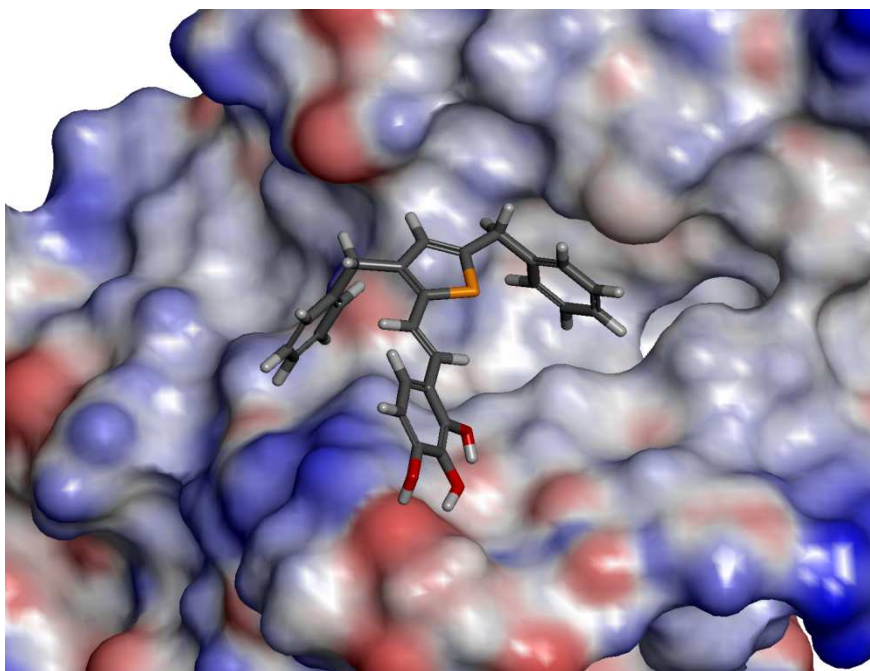


Fig. III.24: Thiophene docked in MCL-1 protein

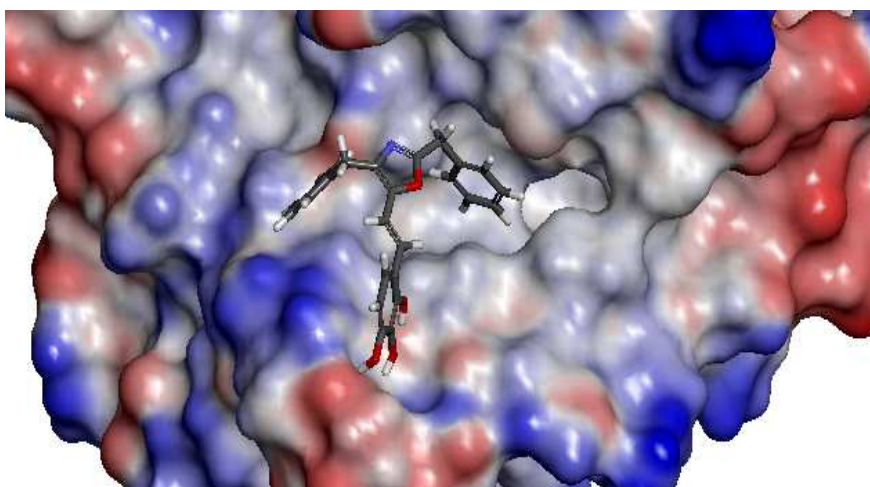


Fig. III.25: Oxazole docked in MCL-1 protein

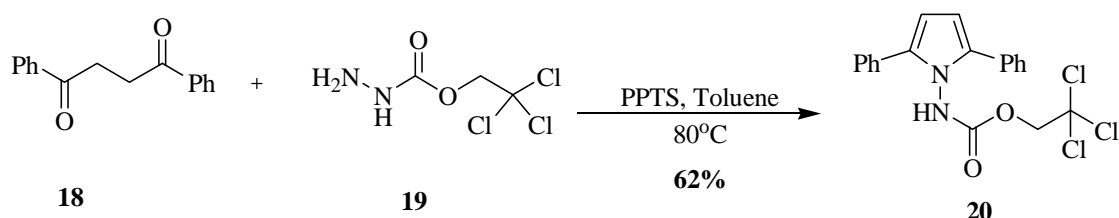
III.C. RESULTS AND DISCUSSION

Results and discussion

Hydrazone type analogs:

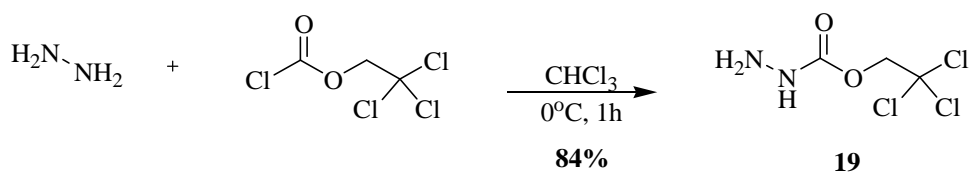
Pyrroles:

As to begin with the preparation of the first series compounds, pyrrole heterocycles were chosen as a core center for the hydrazone type analogs. Pyrrole **20** was obtained from the condensation reaction of commercially available 1, 4-Diphenylbutane-1,4-dione **18** and the protected hydrazine **19** according to the literature procedure [105] (Scheme III.1).



Scheme III. 1: Condensation of hydrazine **19** with diketone **18**

Hydrazine amide **19** itself was obtained from the protection of commercially available hydrazine with 2,2,2-dichloroethyl chloroformate according to the literature procedure [106] (Scheme III.2).



Scheme III. 2: Protection of hydrazine

Structure of pyrrole **20** was clearly established by NMR data (^1H , ^{13}C). ^1H NMR spectrum of **20** (Figure III.26) shows a singlet (two protons) at 6.37 ppm which could be assigned to the protons of the pyrrole ring **H₆** and **H₇**, in addition to another singlet at 4.69 ppm that refers to the methylene protons **H₁₄**.

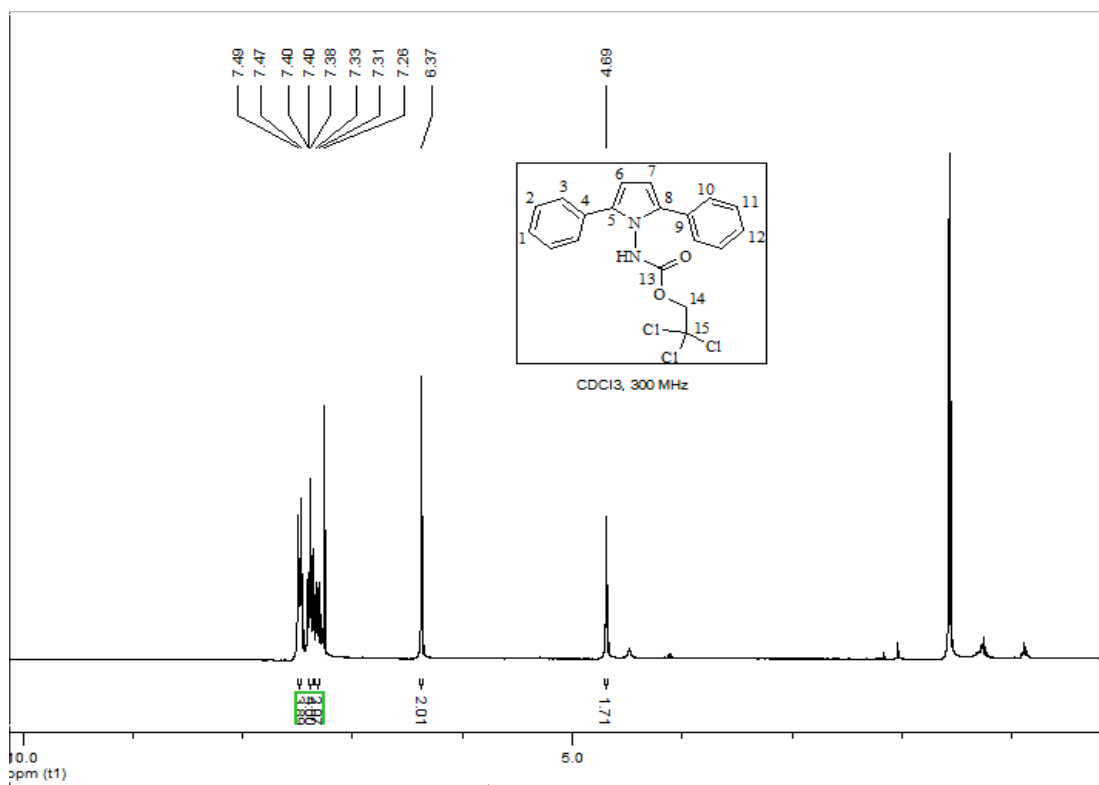


Fig.III. 26: ^1H NMR spectrum of **20**

^{13}C NMR spectrum of **20**, shown in Figure III.27, shows the peak of carbonyl amide at 153.72 ppm, in addition to the peak of methylene carbon C_{14} at 74.78 ppm and that of the methine carbon C_{15} at 94.70 ppm.

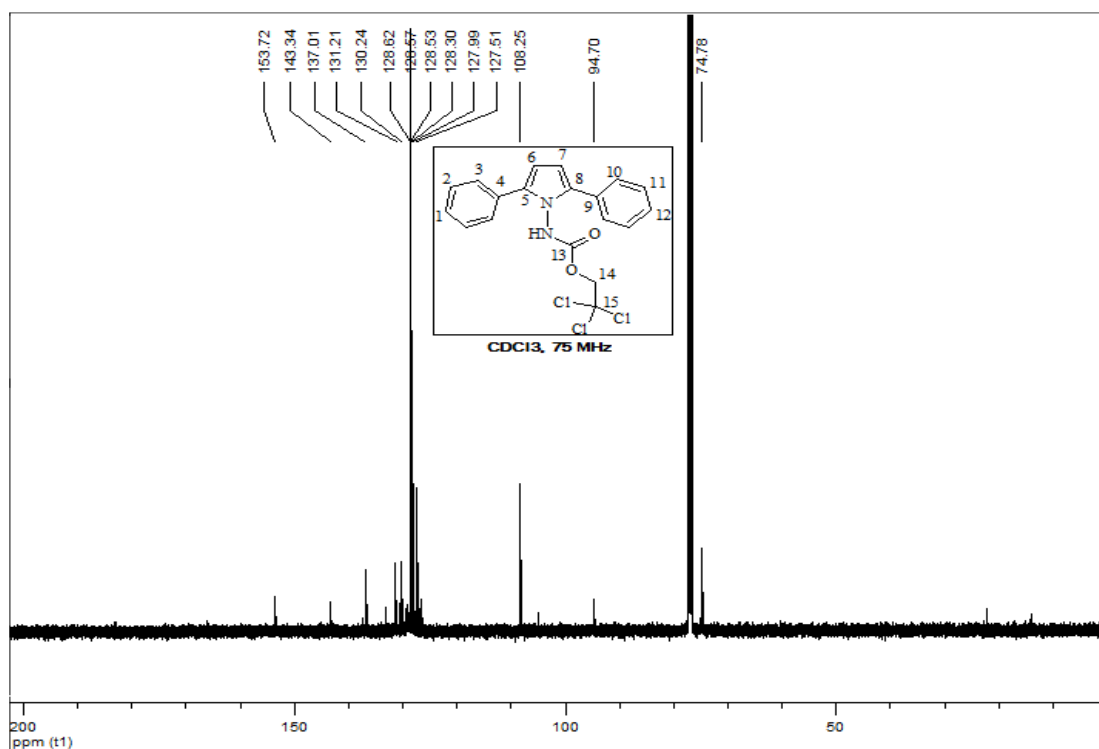
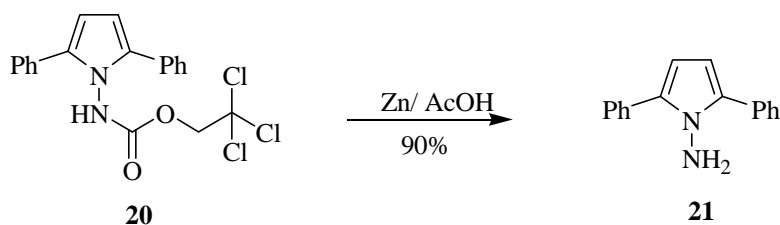


Fig.III. 27: ¹³C NMR spectrum of **20**

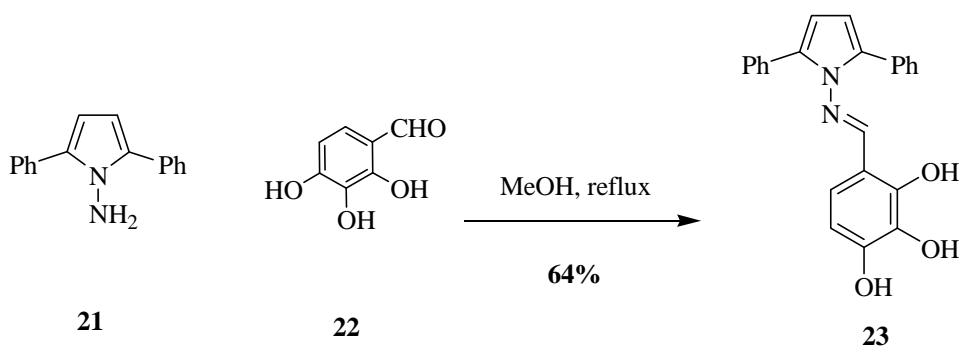
Pyrrole **20** was then deprotected in the following step according to the literature procedure [107], and yielded pyrrole **21** in 90% (Scheme III.3).



Scheme III. 3: Deprotection of pyrrole **20**

The structure of **21** was established by comparison of its spectral data with the literature [104].

In the last step, amine **21** was reacted with the commercially available trihydroxy benzaldehyde **22** in MeOH under reflux to afford the desired hydrazone **23** in 64% yield (Scheme III.4).



Scheme III. 4: Preparation of hydrazone **23**

Structure of **23** was clearly established by NMR data (^1H , ^{13}C). ^1H NMR spectrum of **23** shows the vinylic proton H_{13} as singlet at 8.20 ppm and the three hydroxyl protons as small broad peaks at 10.24, 9.88 and 8.60 ppm (Figure III.28). However, ^{13}C NMR spectrum of **23** shows the vinylic carbon C_{13} at 166.92 ppm (Figure III.29).

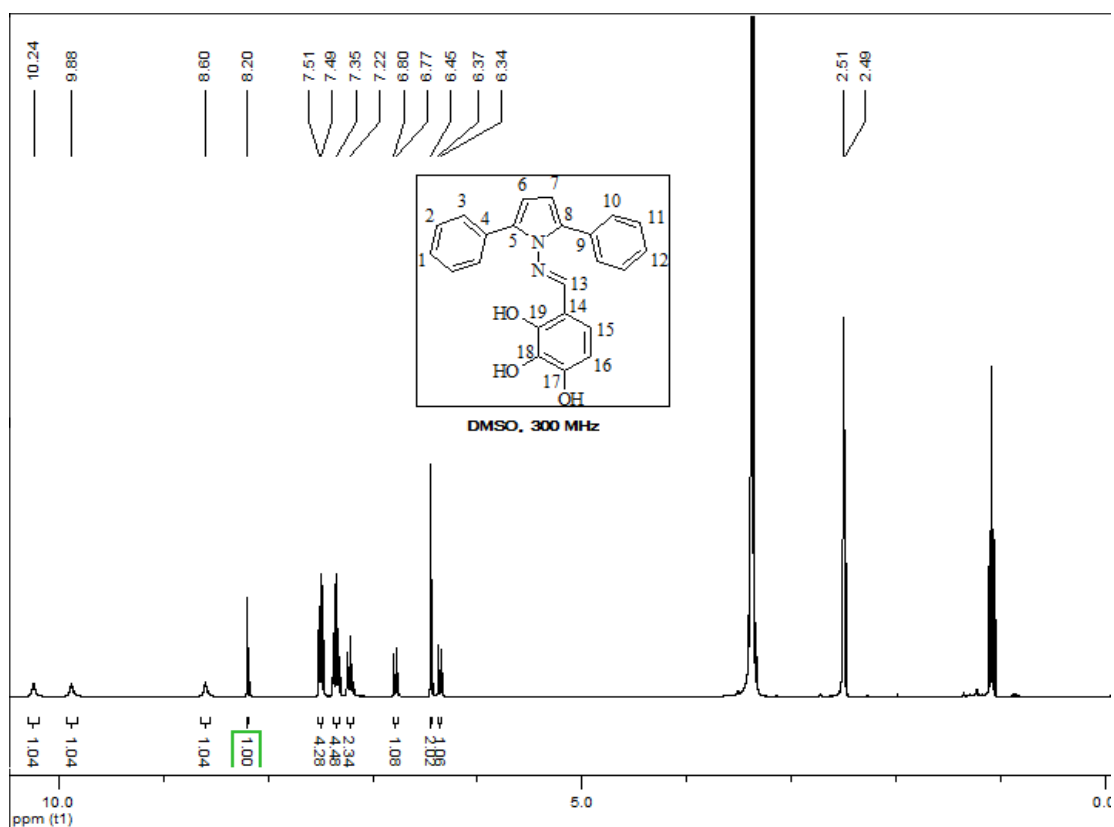


Fig.III. 28: ^1H NMR spectrum of **23**

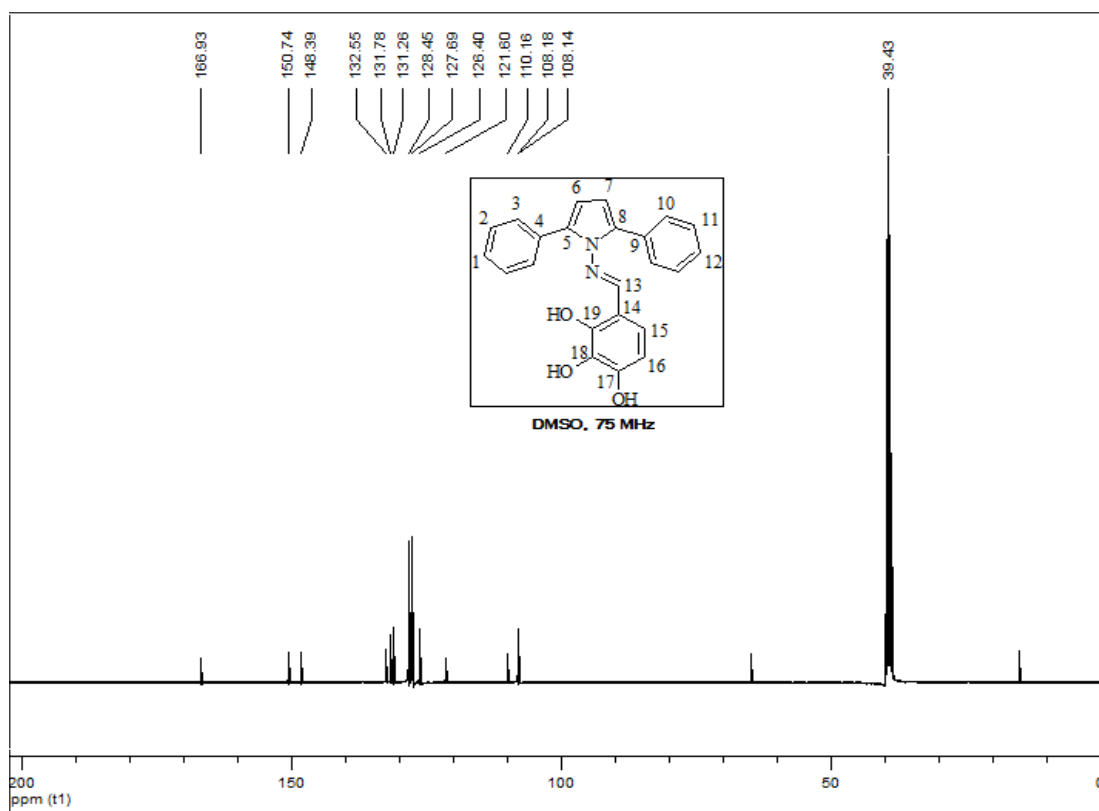
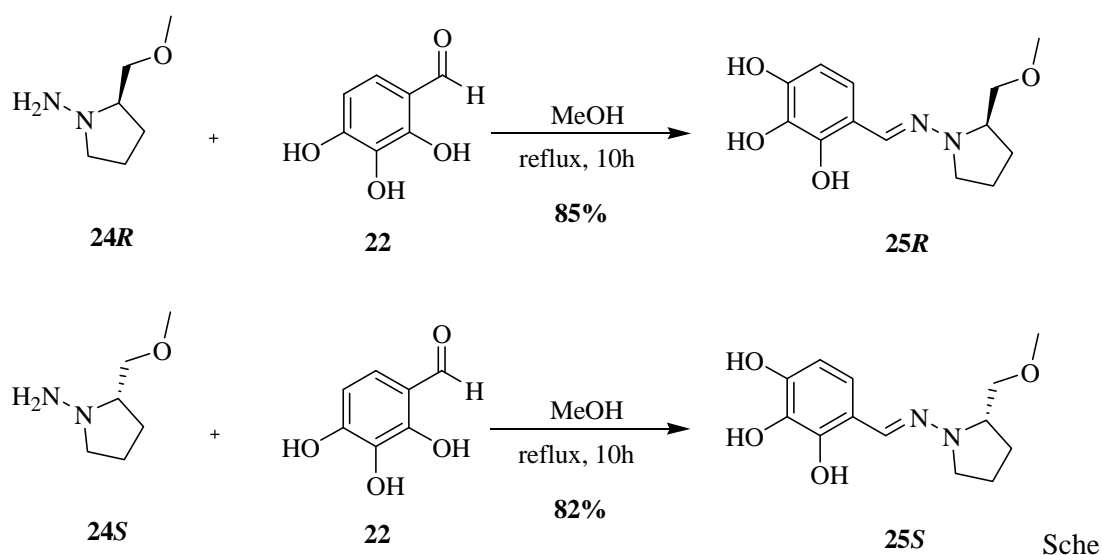


Fig.III. 29: ^{13}C NMR spectrum of **23**

Pyrrolidines:

On the other hand, in order to explore more simple models, the commercially available pyrrolidines **24R** and **24S** were condensed too with trihydroxybenzaldehyde **22** and afforded the desired hydrazones **25R** and **25S** in 85% and 82% respectively (Scheme III.5).



Scheme III. 5: Condensation reaction of pyrrolidines **24R** and **24S** with aldehyde **22**

Structures of hydrazones **25R** and **25S** were established clearly by NMR data (^1H , ^{13}C). ^1H NMR spectrum of **25R** (Figure III.30) shows the peak of the vinylic proton **H₇** as singlet at 7.45 ppm, in addition to the three hydroxyl groups that appear as small broad peaks at 11.41, 9.03 and 8.19 ppm. ^{13}C NMR spectrum of **25R** is shown in Figure III.31.

As expected, the NMR data of **25S** were found to be similar to those of **25R**.

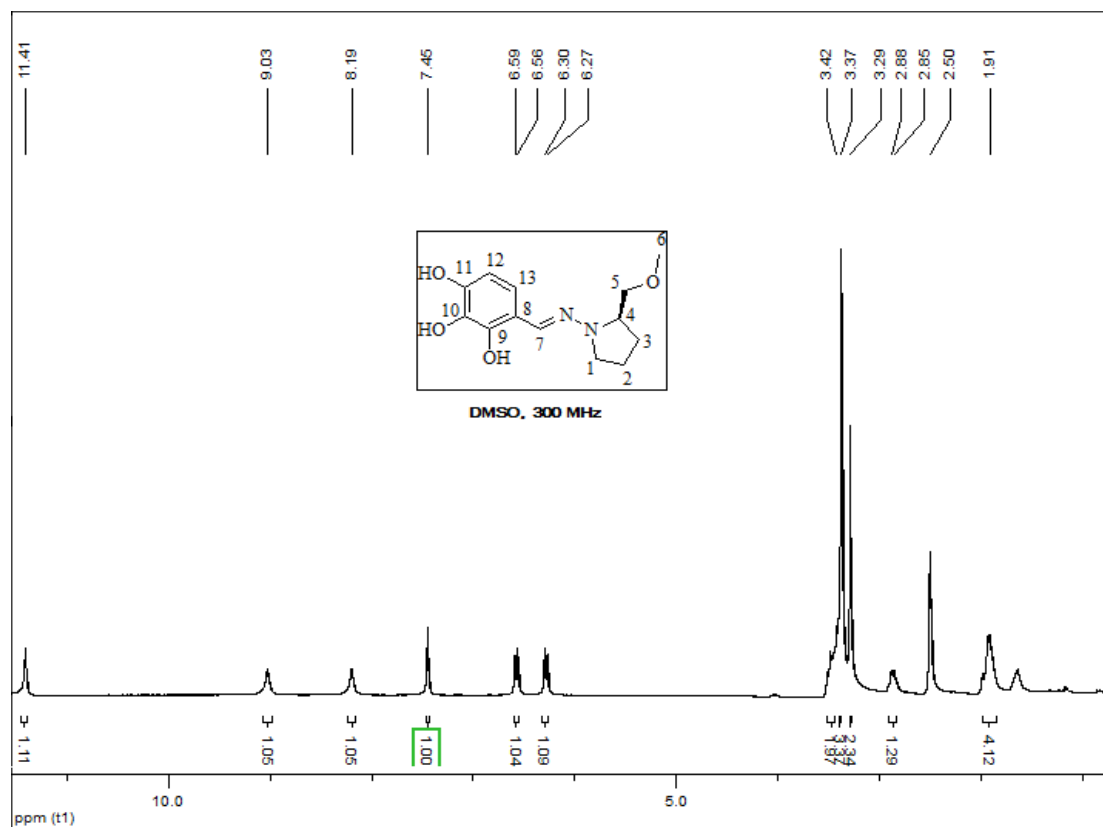


Fig.III. 30: ^1H NMR spectrum of **25R**

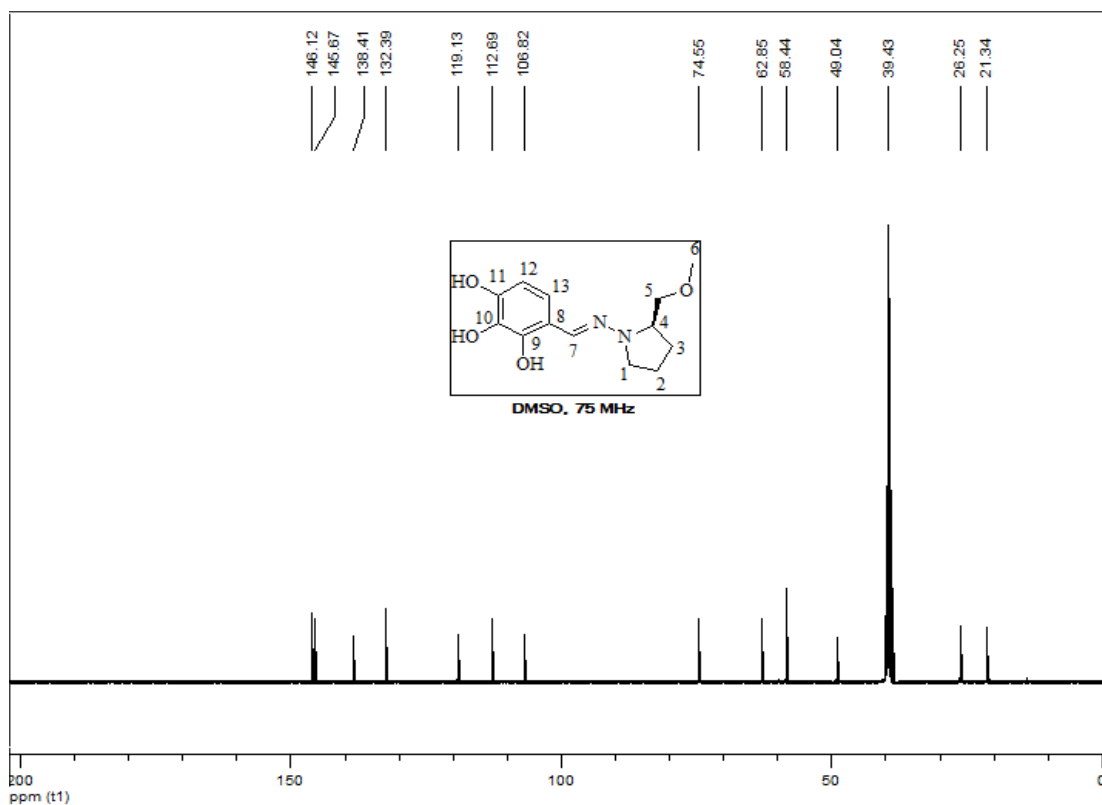
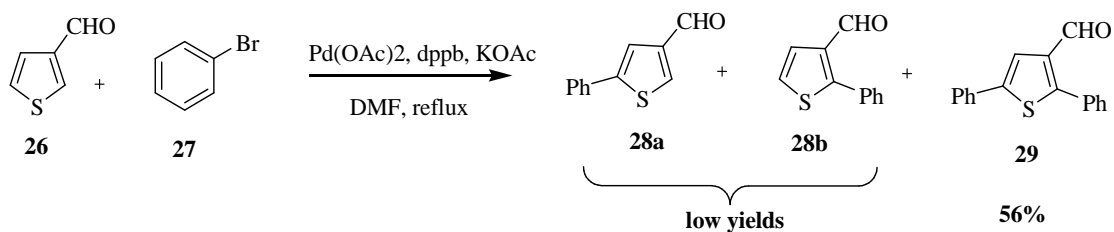


Fig.III. 31: ^{13}C NMR spectrum of **25R**

Alkene type analogs:

Thiophenes:

In the second series of molecules, thiophene heterocycles were chosen as a first heterocyclic core for alkene type analogs. Starting with the palladium catalyzed direct arylation of 3-formylthiophene **26** with bromobenzene **27** [108], a mixture of mono- and disubstituted phenyl thiophenes were obtained (Scheme III.6).



Scheme III. 6: Palladium catalyzed arylation of 3-formylthiophene **26** with bromobenzene **27**

Mono-substituted thiophenes **28a** and **28b** were isolated in a very low yield, and the recovered quantity of **28a** was treated again with the palladium acetate under the same reaction conditions which gave the desired disubstituted thiophene **29** in 56% yield.

Structure of **29** was clearly established by NMR data. The ^1H NMR spectrum of **29**, shown in Figure III.32, shows a small doublet at 9.88 ppm of coupling constant $^4J=0.2$ Hz which can be assigned to the aldehyde proton coupled weakly with H_6 .

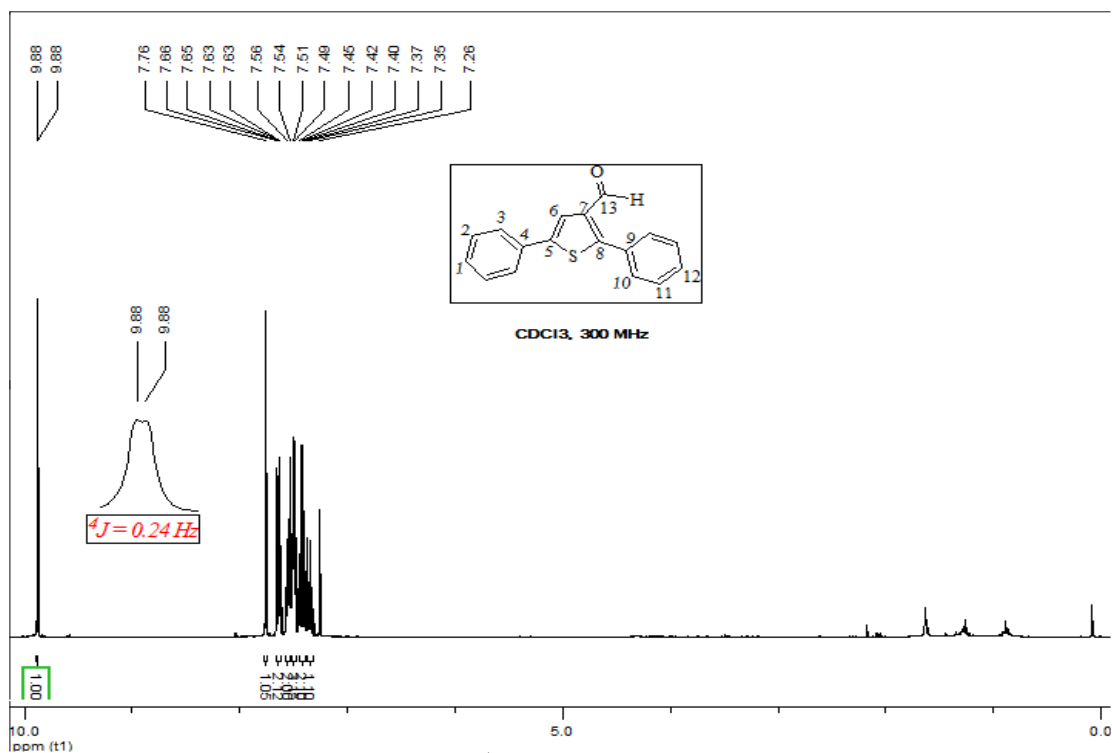


Fig.III. 32: ^1H NMR spectrum of **29**

^{13}C NMR spectrum of compound **29** (Figure III.33), shows the peak of the aldehyde carbon at 185.8 ppm.

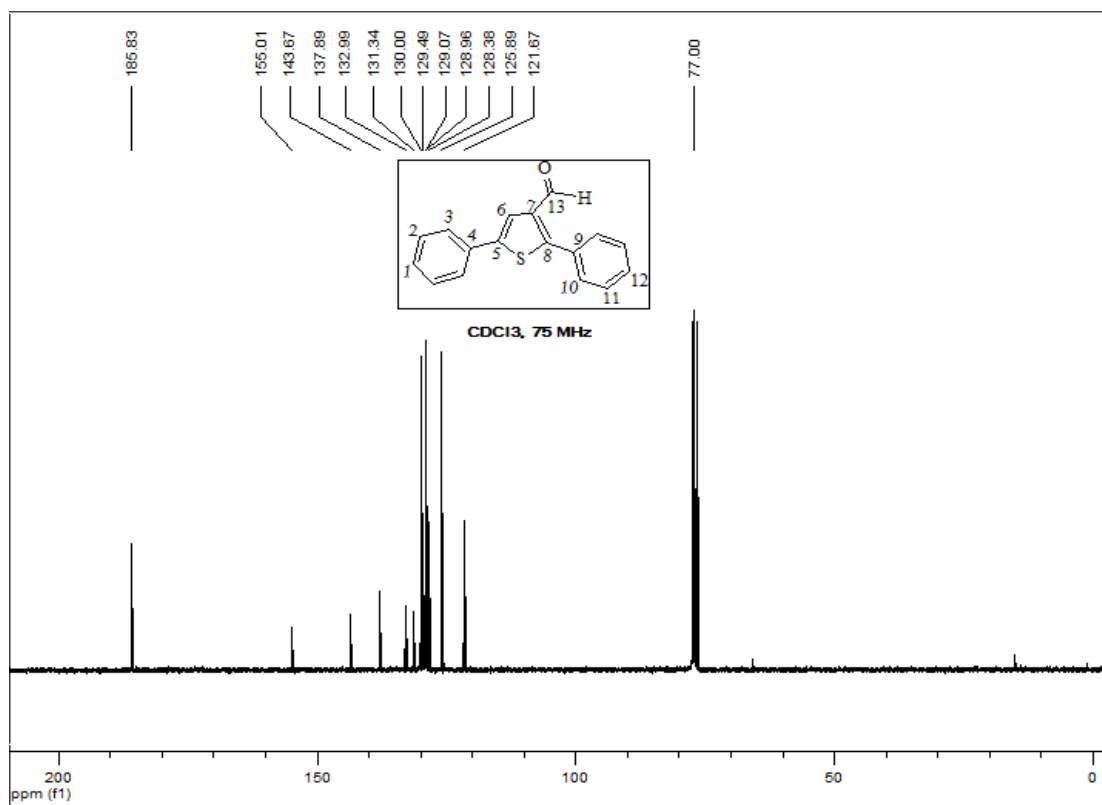


Fig.III. 33: ^{13}C NMR spectrum of **29**

Furthermore, ^1H - ^1H NOESY spectrum of **29** (Figure III.34) illustrates clearly the correlation between the aldehyde proton and **H₆**.

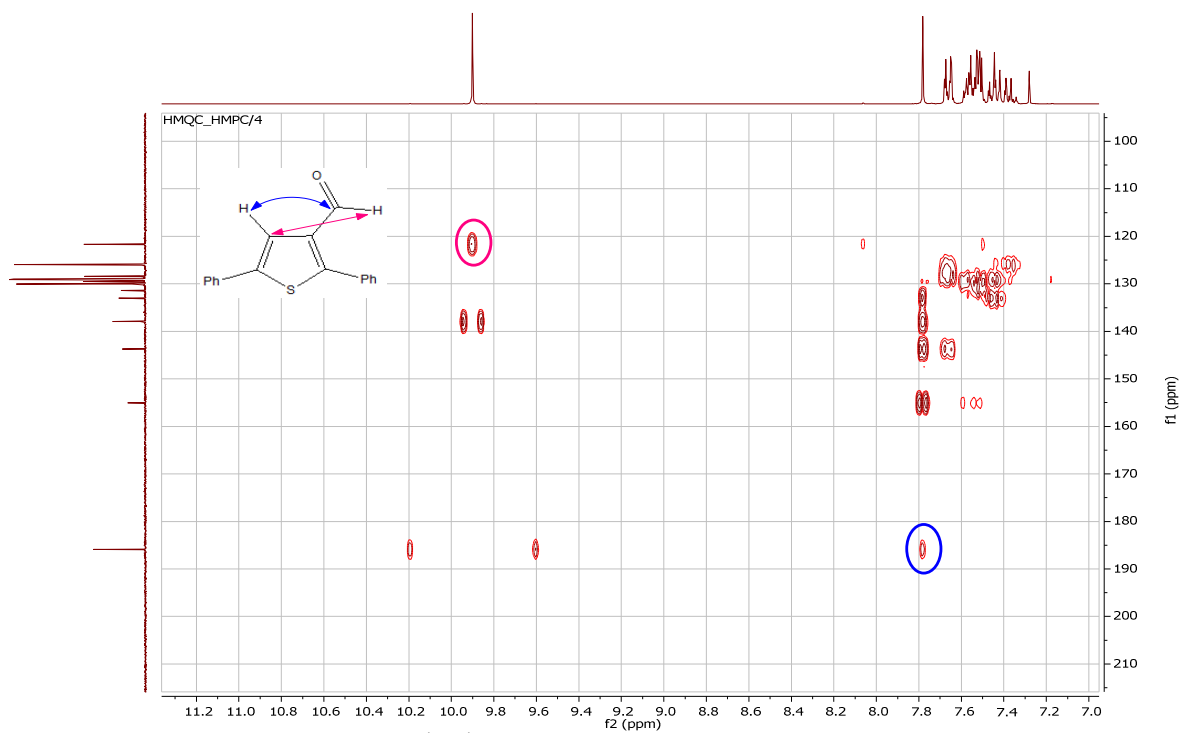


Fig.III. 34: ^1H - ^1H NOESY spectrum of **29**

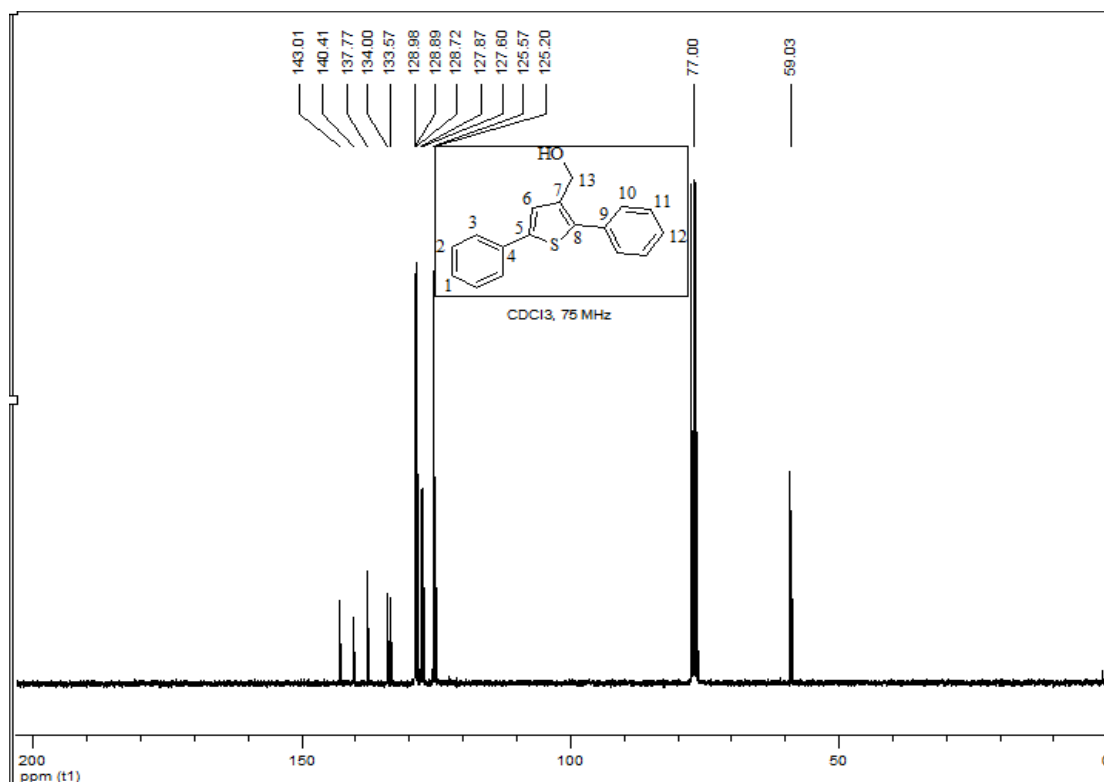
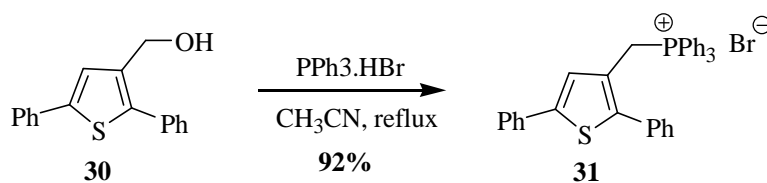


Fig.III. 36: ^{13}C NMR spectrum of **30**

Alcohol **30** was then transformed in the next step into phosphonium salt **31**, by treating it with triphenylphosphine hydrobromide (Scheme III.8), according to the literature procedure [109].



Scheme III. 8: Preparation of phosphonium salt **31**

Structure of **31** was illustrated by NMR data, where the ^1H NMR spectrum of **31** (Figure III.37) shows a doublet for two protons at 5.48 ppm with coupling constant of 13.7 Hz which could be assigned to the methylene protons coupled with the neighbour phosphorous.

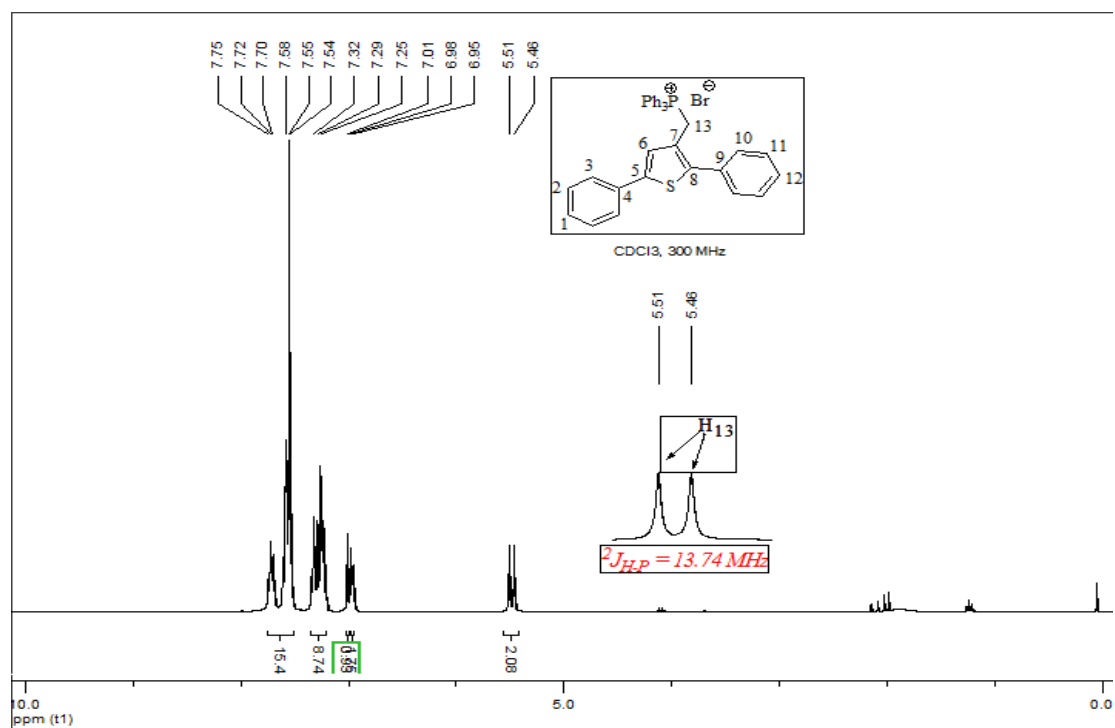


Fig.III. 37: ^1H NMR spectrum of **31**

^{13}C NMR spectrum of **31** (Figure III.38) shows also the appearance of a large doublet between 24.55 and 25.17 ppm of coupling constant 47.3 Hz, that could be assigned to C_{13} .

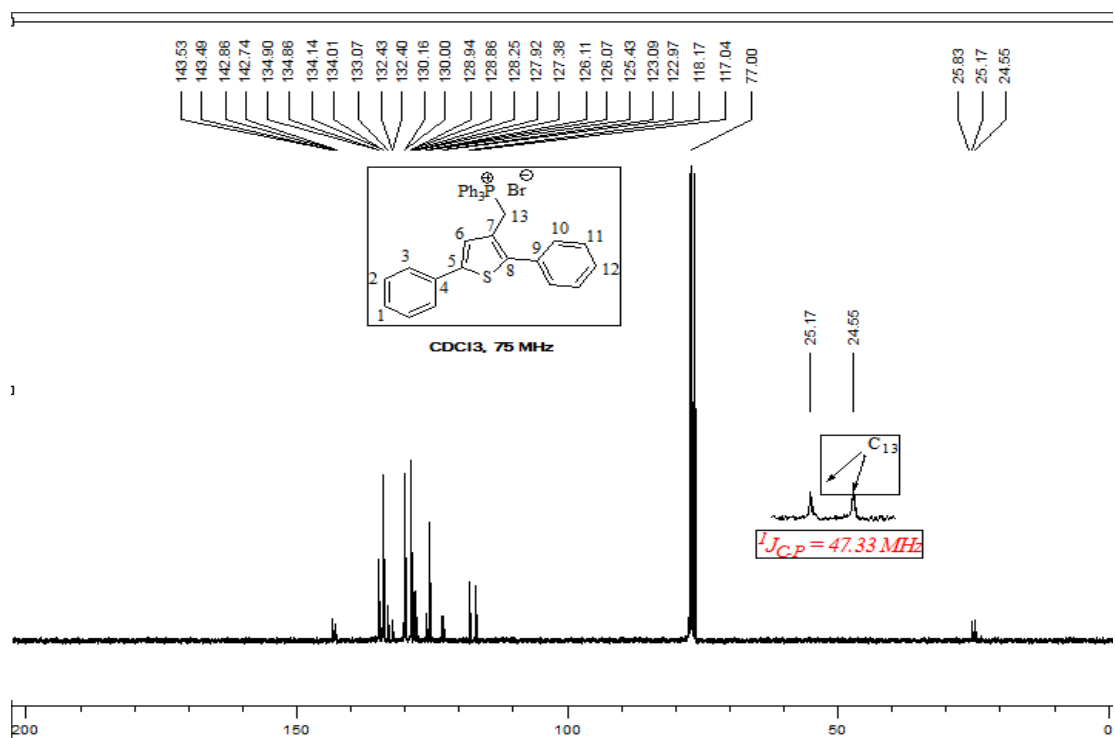


Fig.III. 38: ^{13}C NMR spectrum of **31**

protons with of the *cis* configuration. Figure III.42 shows also the ^{13}C NMR spectrum of **33Z**.

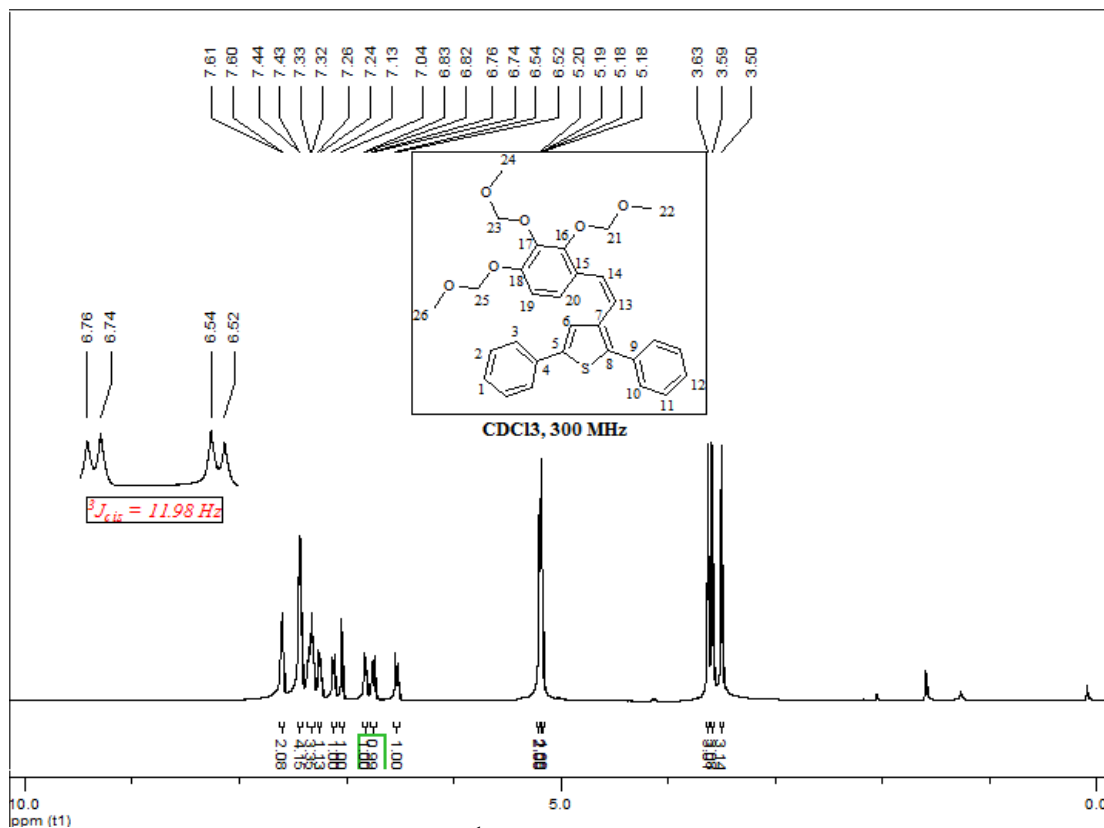


Fig.III. 41: ^1H NMR spectrum of **33Z**

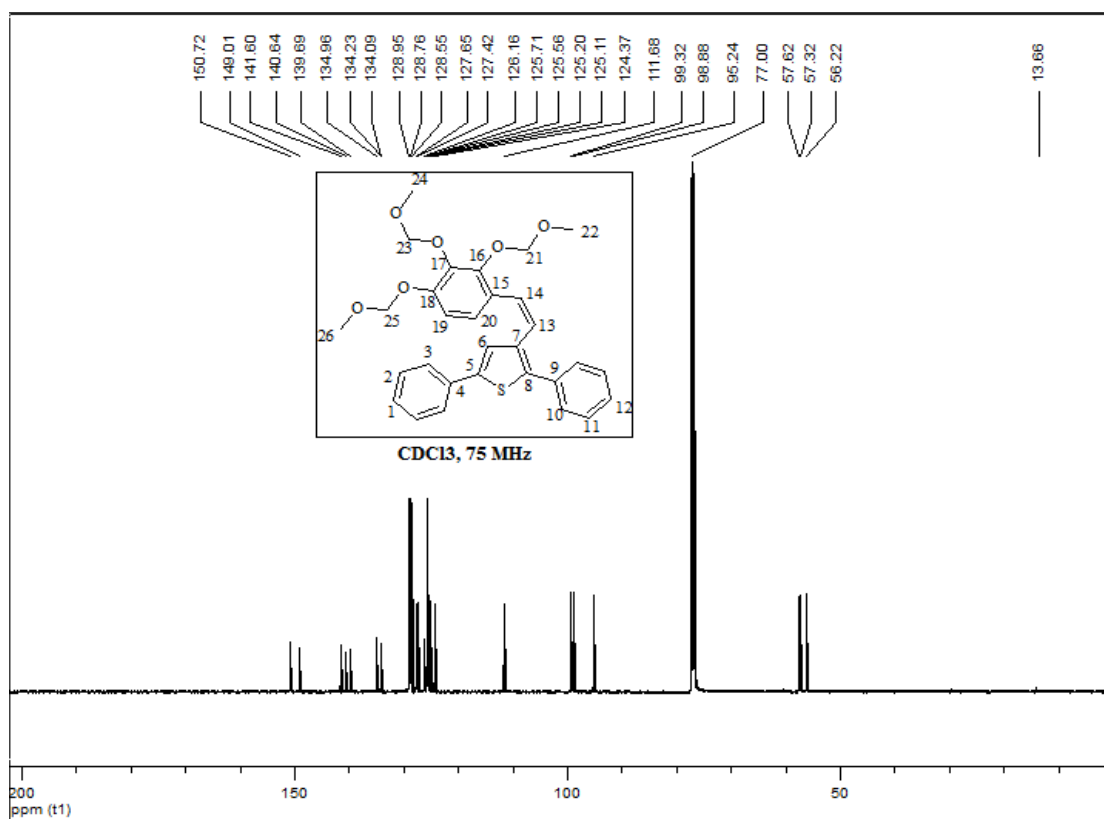
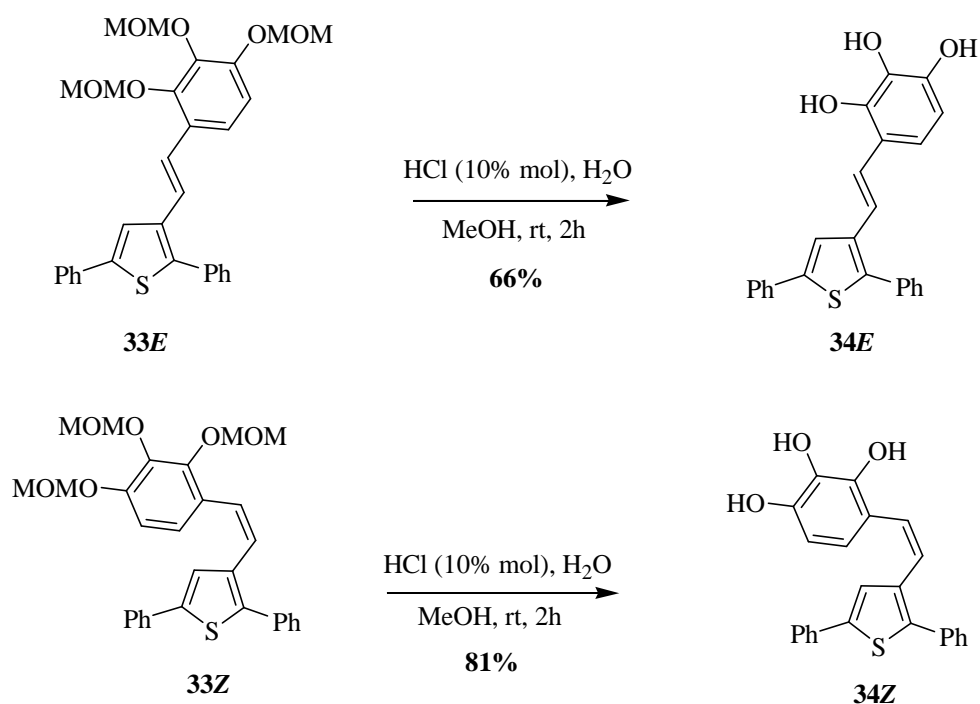


Fig.III. 42: ^{13}C NMR spectrum of **33Z**

In the last step, the deprotection of the MOM groups of **33E** and **33Z** yielded the desired target products **34E** and **34Z** in 81% yield for Z isomer and 66% for the E isomer (Scheme III.11).



Scheme III. 11: Deprotection of MOM groups

Structures of **34E** and **34Z** were established by NMR data. ^1H NMR spectrum of **34E** (Figure III.43) shows a doublet at 7.15 ppm with coupling constant of 16.4 Hz, which could be assigned to a vinylic proton, while the peak of the second vinylic proton is interfering with the aromatic peaks. In addition we observed also the disappearance of the methyl and methylene protons of the MOM group. Figure III.44 shows also ^{13}C NMR spectrum of **34E**.

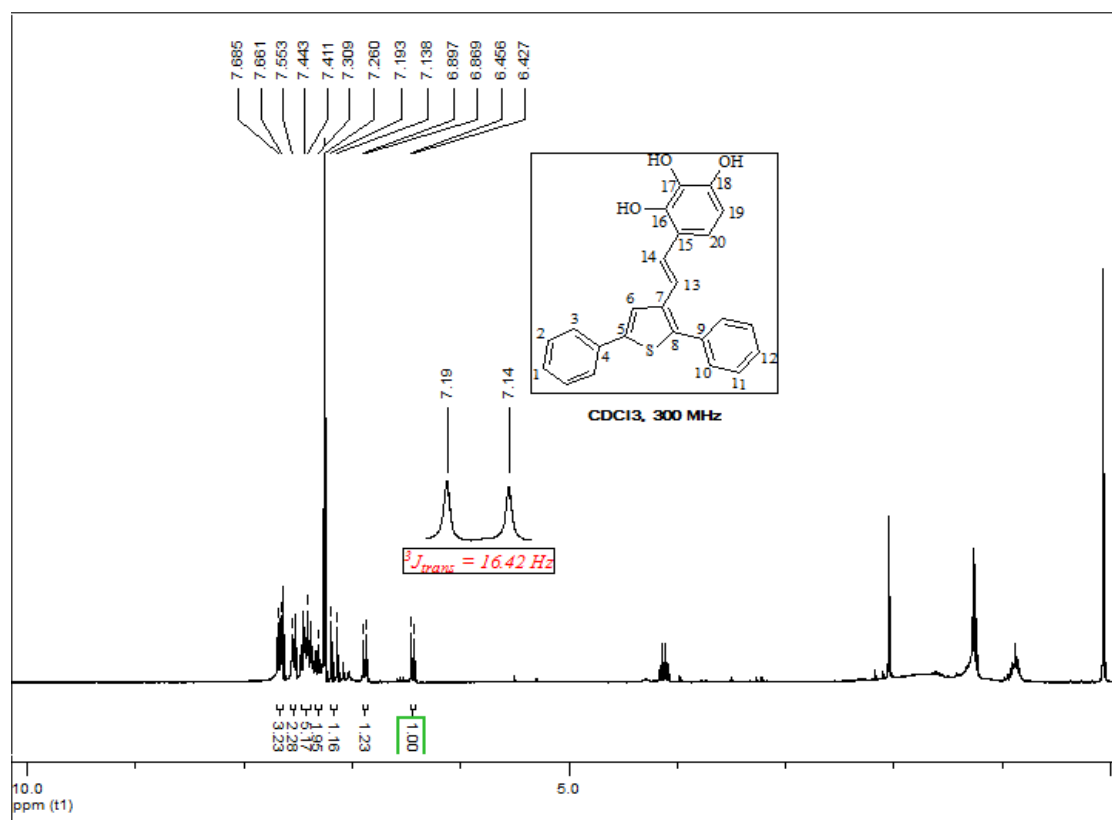


Fig.III. 43: ¹H NMR spectrum of **34E**

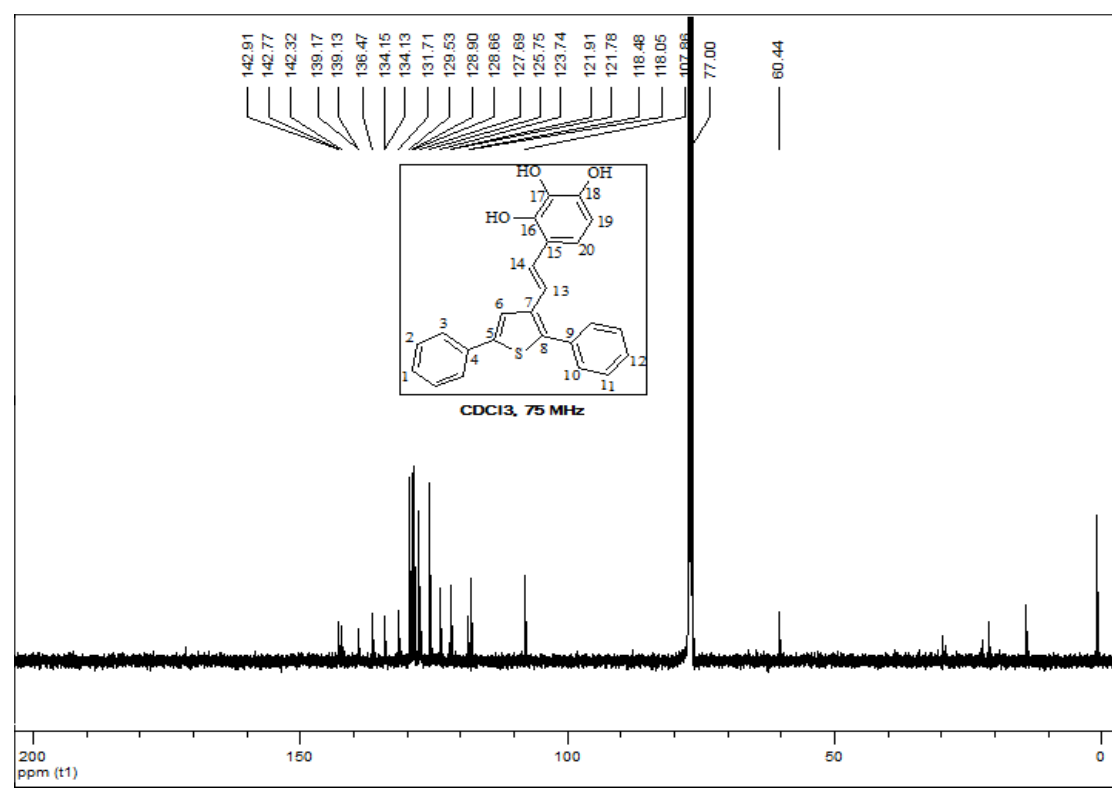


Fig.III. 44: ¹³C NMR spectrum of **34E**

On the other hand, ^1H NMR spectrum of **34Z** (Figure III.45) shows the appearance of the peaks of three hydroxyl protons (5.45-5.27 ppm) and the disappearance of the peaks of methyl and methylene protons. ^{13}C NMR spectrum of **34Z** is shown in Figure III.46.

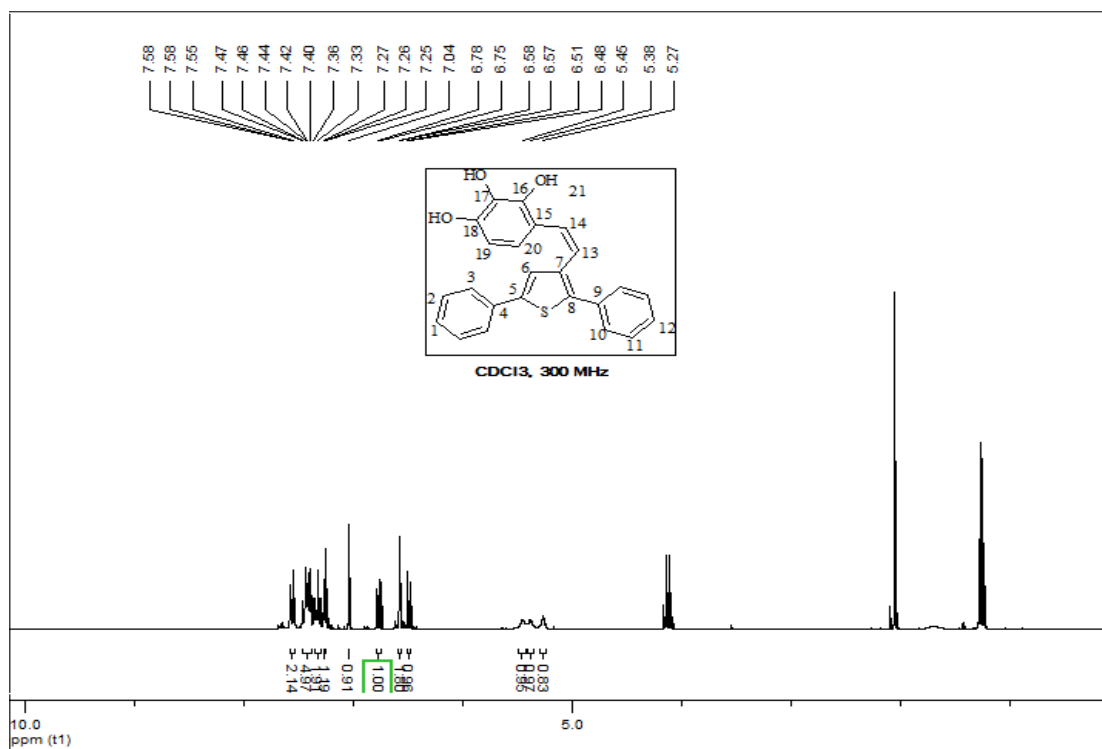


Fig.III. 45: ^1H NMR spectrum of **34Z**

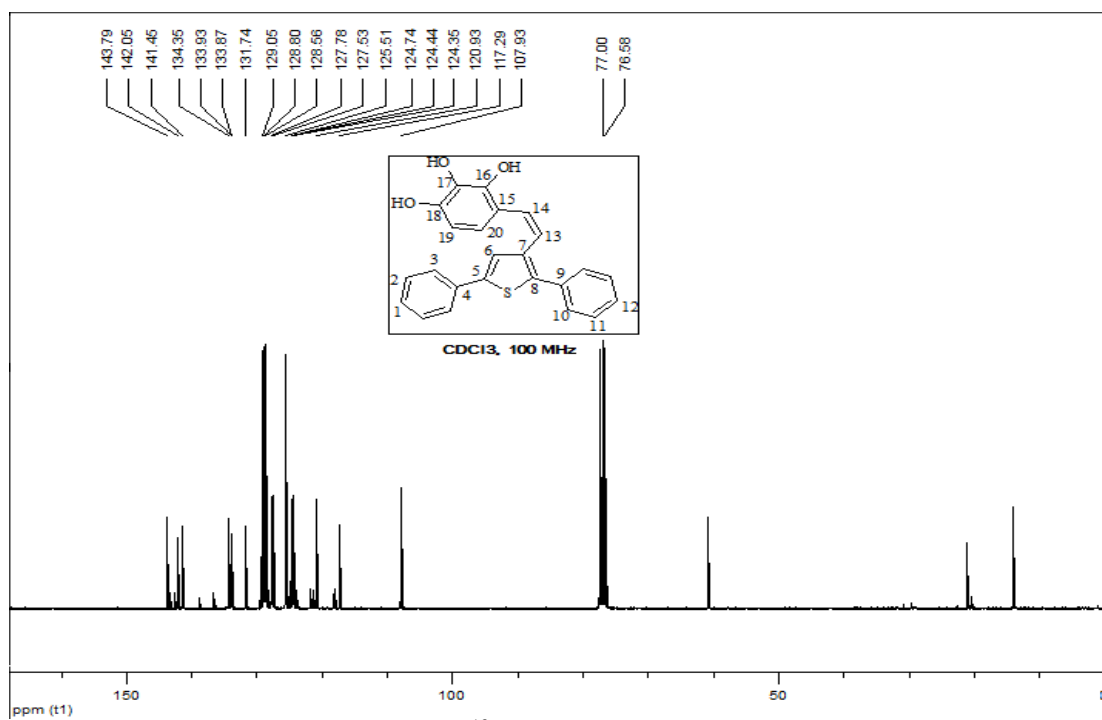
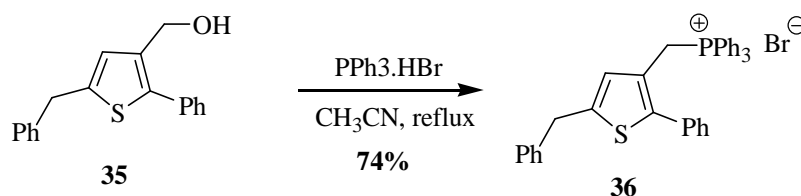


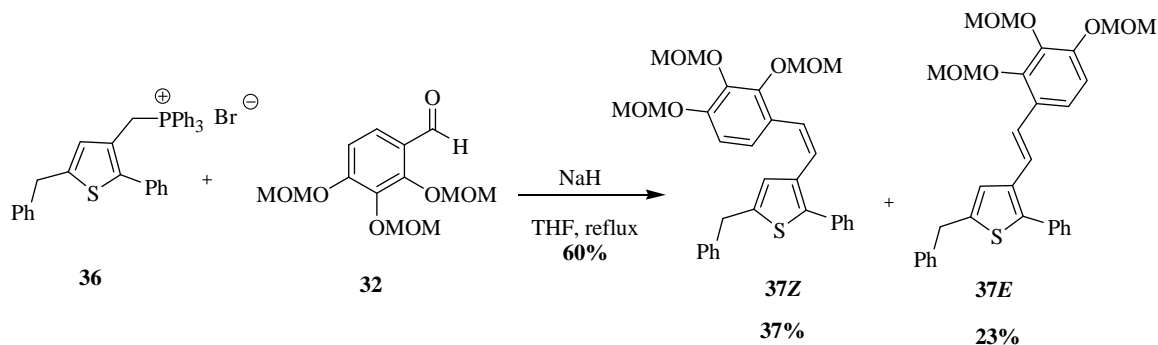
Fig.III. 46: ^{13}C NMR spectrum of **34Z**

Finally, another analog of thiophene with benzyl and phenyl substituents was also studied. It started from alcohol **35** which was already prepared during studies developed in the Indo-French Joint Laboratory between Rennes and Hyderabad [112]. Thus, this compound was treated with triphenylphosphine hydrobromide affording phosphonium salt **36** in 74% yield (Scheme III.12). Again, structure of **36** was also established by NMR data (^1H , ^{13}C), as for phosphonium salt **31**.



Scheme III. 12: Preparation of phosphonium salt **36**

Wittig reaction between **36** and the protected trihydroxybenzaldehyde **32** was then performed and afforded a mixture of **37E** and **37Z** in 60% overall yield, with 23% of *E* isomer and 37% of the *Z* isomer separated by silica gel chromatography (Scheme III.13).

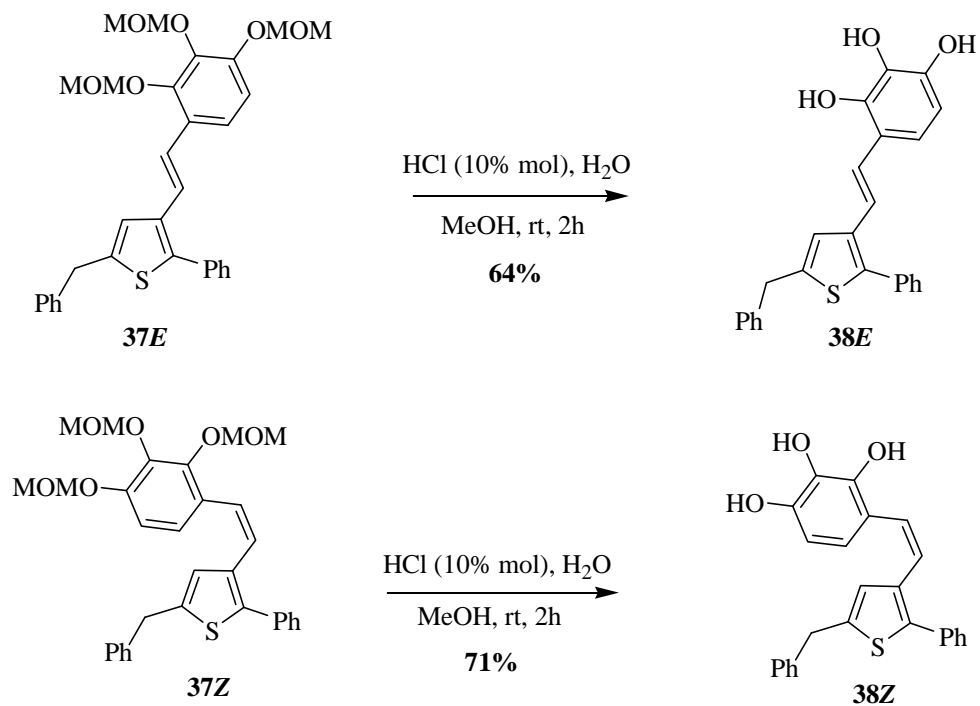


Scheme III. 13: Wittig reaction between phosphonium salt **36** and aldehyde **32**

Similarly, the structures of **37E** and **37Z** were clearly established by NMR data (^1H , ^{13}C) as for **33E** and **33Z**.

Then deprotection of the MOM groups of **37E** and **37Z** was performed and yielded the final desired products **38E** (in 64% yield) and **38Z** (71% yield) (Scheme III.14).

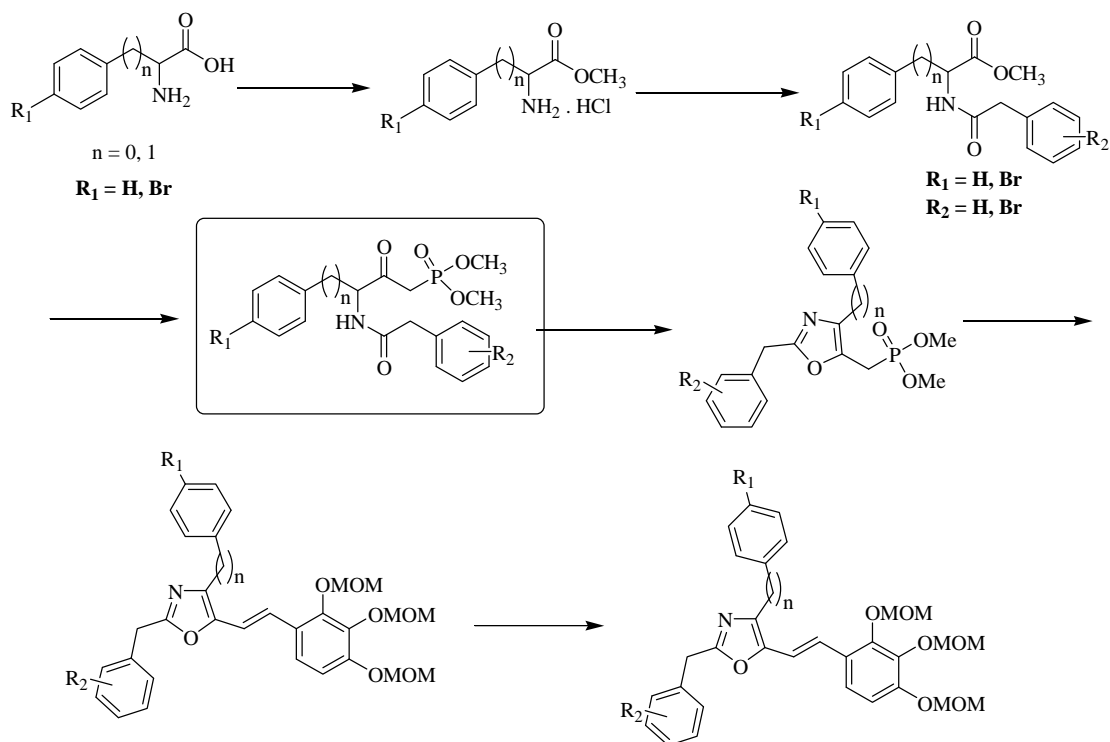
The structures of **38E** and **38Z** were clearly established by NMR data (^1H , ^{13}C) as for **34E** and **34Z**.



Scheme III. 14: Deprotection of MOM group of **37E** and **37Z**

Oxazoles:

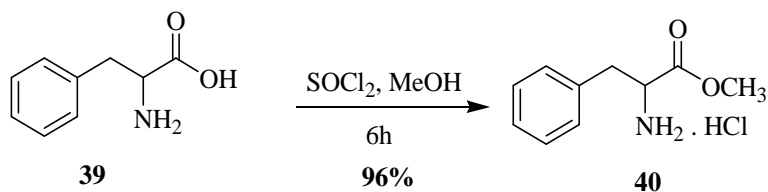
On the other hand, and as a second group in the alkenes type analog series, oxazole heterocycles were chosen as a new core center. The following scheme shows the general sequence designed for the preparation of such oxazole analogs.



Scheme III. 15: General sequence for the preparation of oxazoles

As shown in Scheme III.15, simple amino acids (Alanine or Glycine) were used as a starting material for the preparation of oxazoles.

Starting with the series of L-alanine amino acid, in the first step the carboxyl group was transformed into ester, according to the procedure mentioned in the literature [113], affording ester **40** as a white solid in 96% yield (Scheme III.16).



Scheme III. 16: Esterification reaction of carboxyl group

Structure of ester **40** was clearly established by NMR data (^1H , ^{13}C). ^1H NMR spectrum of **40** (Figure III.47) shows a singlet of two protons at 8.75 ppm that could be assigned to the amine protons, in addition to a triplet at 4.23 ppm with coupling constant of 6.8 Hz that refers to H_6 and a singlet of three protons at 3.65 ppm which refers to the methyl group H_8 .

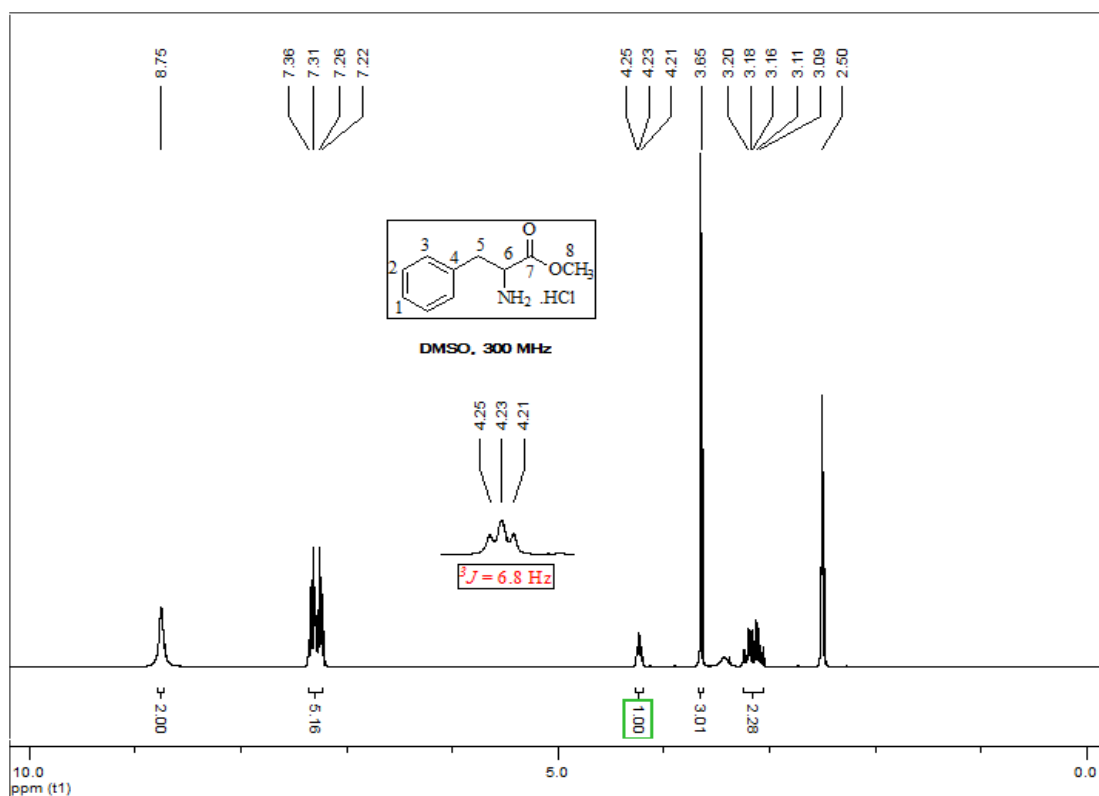


Fig.III. 47: ^1H NMR spectrum of **40**

Figure III.48 shows also the ^{13}C NMR spectrum of **40**, where the peak of the carbonyl carbon appears at 169.18 ppm.

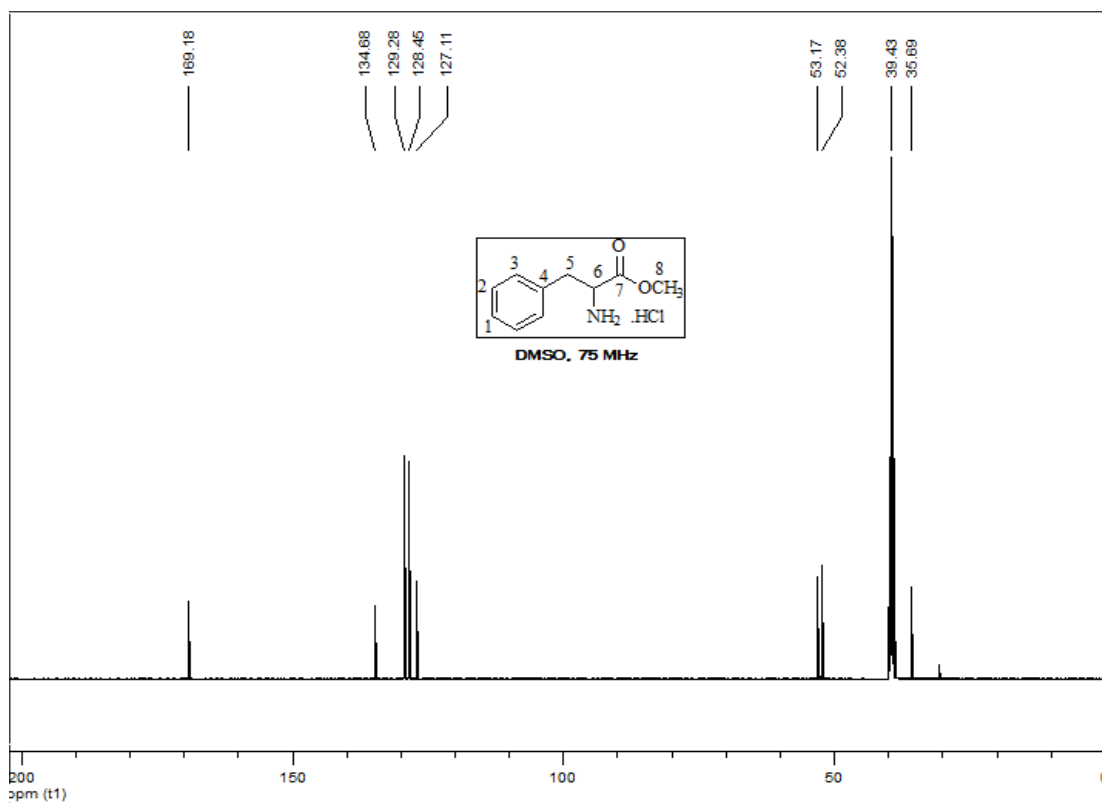
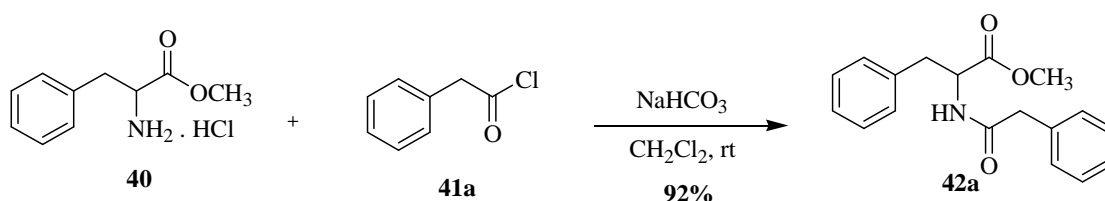


Fig.III. 48: ^{13}C NMR spectrum of **40**

The following step includes the formation of amide, where compound **40** was treated with phenyl acetyl chloride **41a** in CH_2Cl_2 using NaHCO_3 as a base (Scheme III.17), according to the literature procedure [113], affording the desired ester amide **42a** as a white solid in 92% yield.



Scheme III. 17: Preparation of amide **42a**

Structure of **42a** was clearly established by NMR data (^1H , ^{13}C), where the ^1H NMR spectrum of **42a** (Figure III.49) shows a doublet of one proton at 5.84 ppm which refers to the amine proton, and a doublets of triplets at 4.86 ppm which refers to the methine proton **H**₆, in addition to the methylene proton **H**₁₀ which appears as singlet at 3.55 ppm. Figure III.50 shows also the ^{13}C NMR spectrum of **42a**.

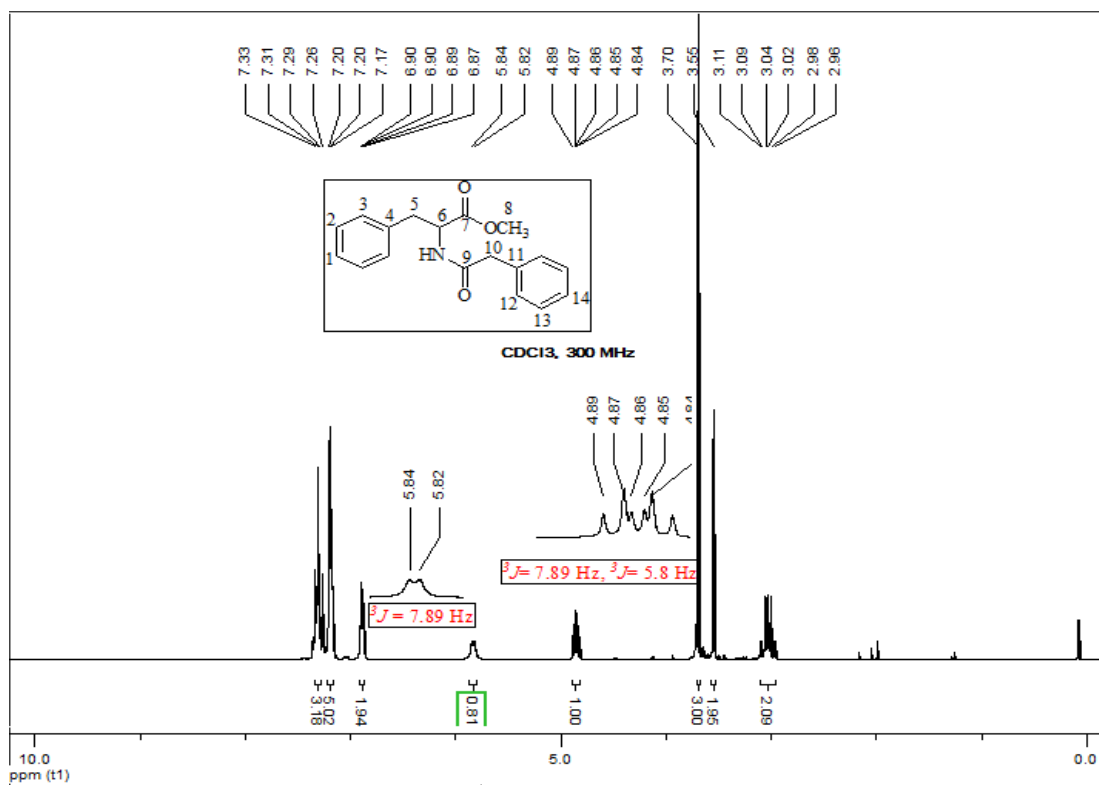


Fig.III. 49: ¹H NMR spectrum of **42a**

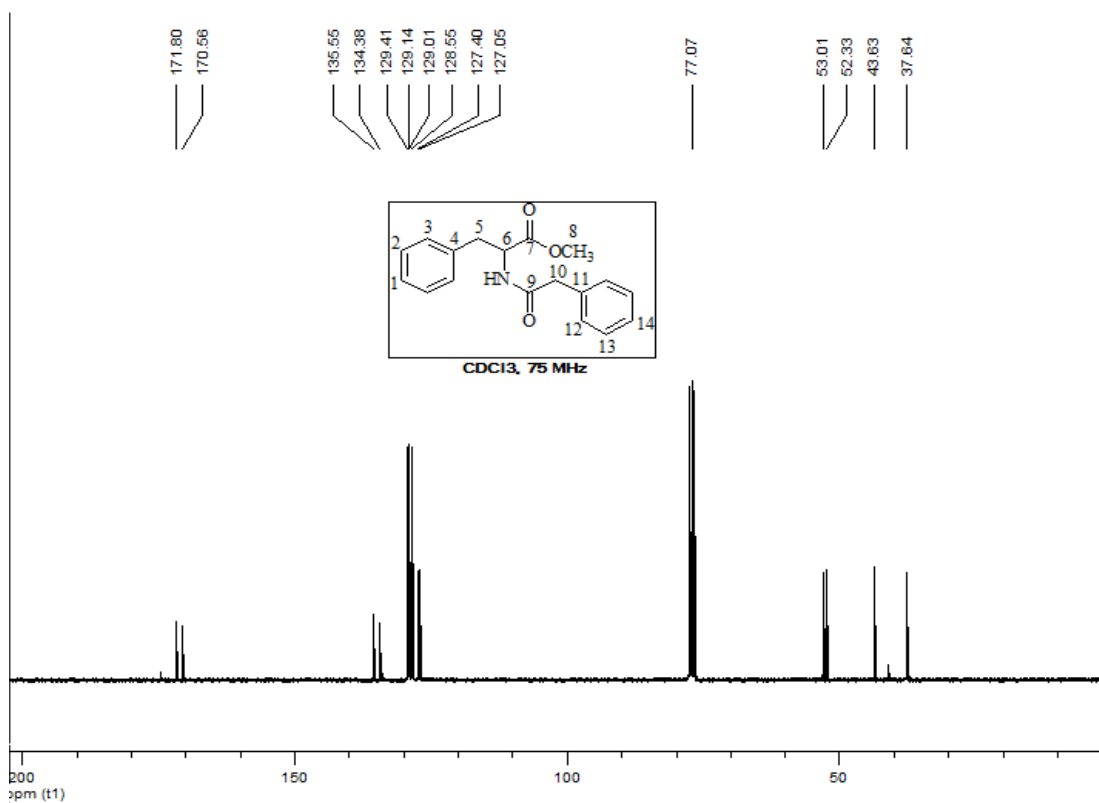
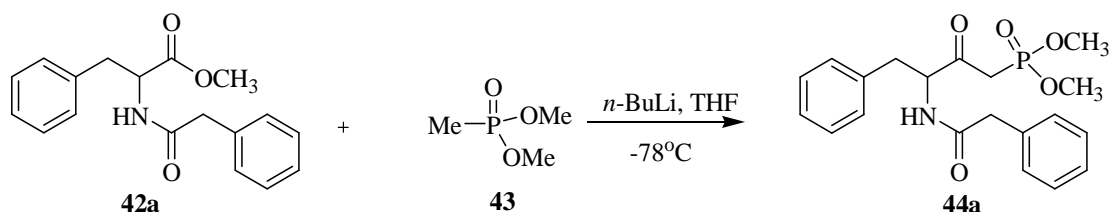


Fig.III. 50: ¹³C NMR spectrum of **42a**

As shown in the figure above, ¹³C NMR spectrum of **42a** shows the peak of the carbonyl carbon **C₉** of amide group at 170.56 ppm and that of the methylene carbon **C₁₀** at 43.63 ppm.

In the following step, formation of phosphonate group was required, thus the amide ester **42a** was treated with the commercially available dimethyl methyl phosphonate **43** in THF using *n*-BuLi as base affording the desired phosphonate **44a** as a white solid in 72% (Scheme III.18).



Scheme III. 18: Preparation of phosphonate **44a**

Structure of **44a** was clearly established by NMR data (^1H , ^{13}C , ^{121}P), where the ^1H NMR spectrum of **44a**(Figure III.51) shows two doublets at 3.72 and 3.68 ppm with the same coupling constant of 9.2 Hz, which could be assigned to the methoxy groups **H₉** and **H₁₀** attached to phosphorous atom.

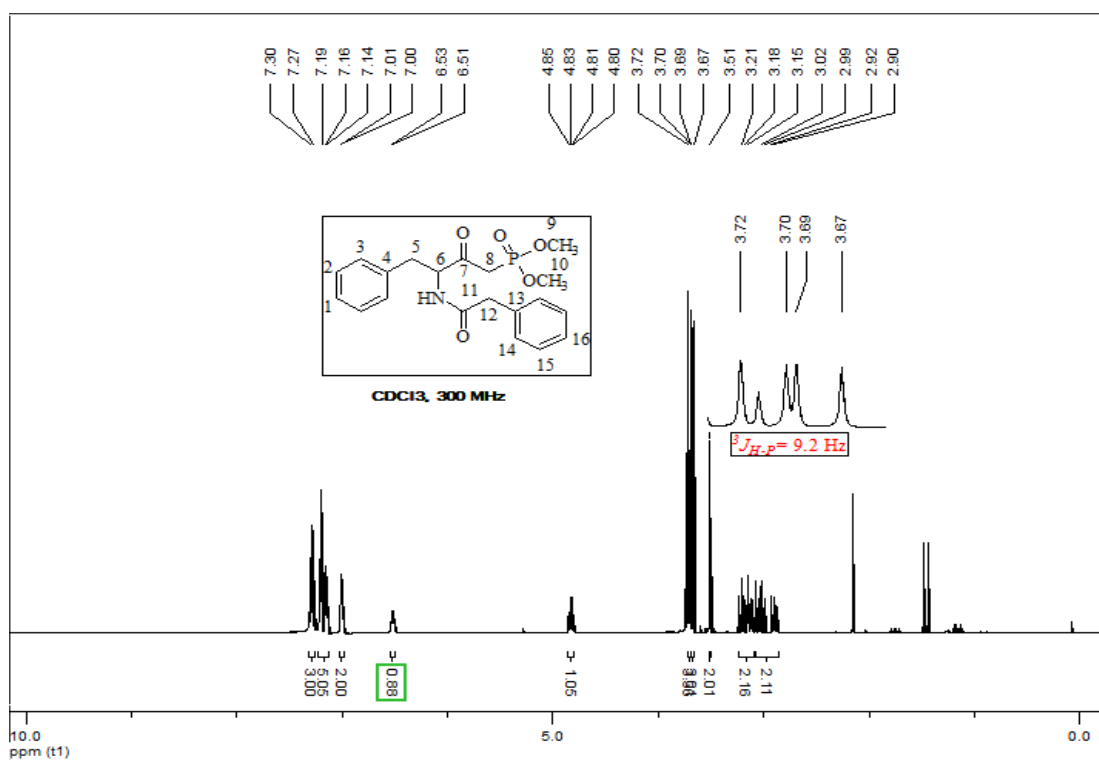


Fig.III. 51: ^1H NMR spectrum of **44a**

Furthermore, ^{13}C NMR spectrum of **44a** (Figure III.52) shows a doublet at 200.25 ppm with coupling constant of 6.5 Hz, which refers to the carbonyl carbon **C₇** of ketone group, in addition to another doublet at 38.48 ppm with coupling constant of 129.2 Hz that refers to **C₈** which is directly attached to phosphorus atom.

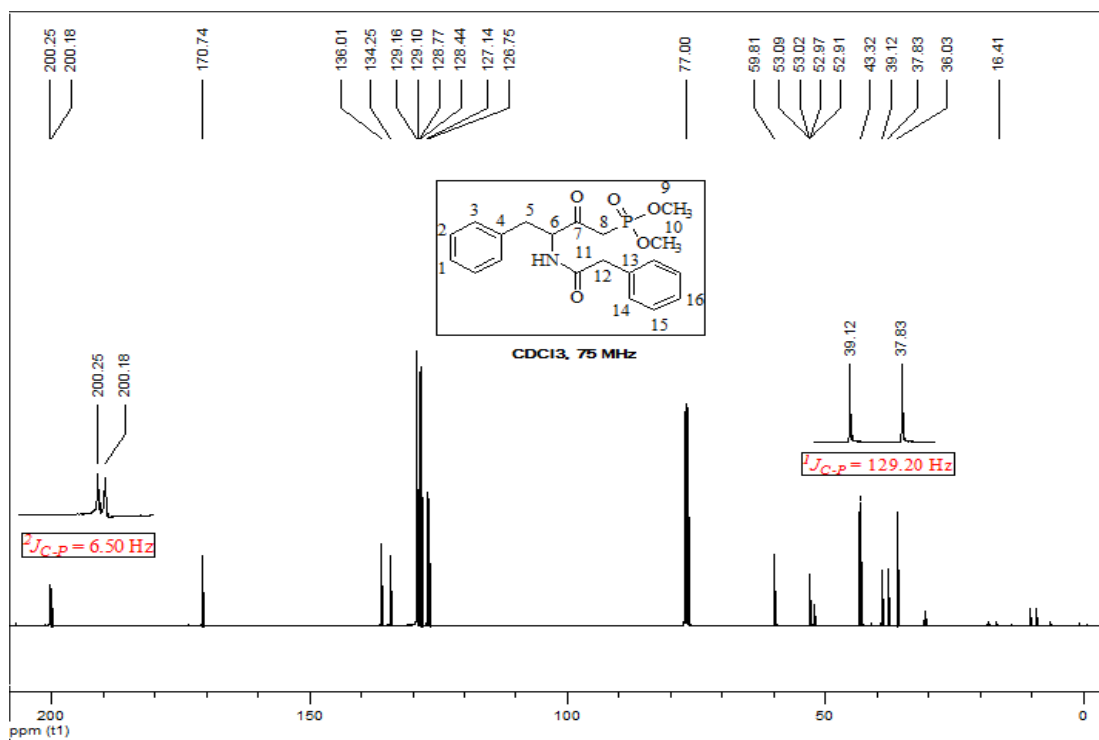


Fig.III. 52: ^{13}C NMR spectrum of **44a**

Finally, ^{31}P NMR spectrum of **44a**, shown in Figure III.53, shows the peak of the phosphorous atom at 22.08 ppm, where the peak at 33.16 ppm refers to the starting phosphonate.

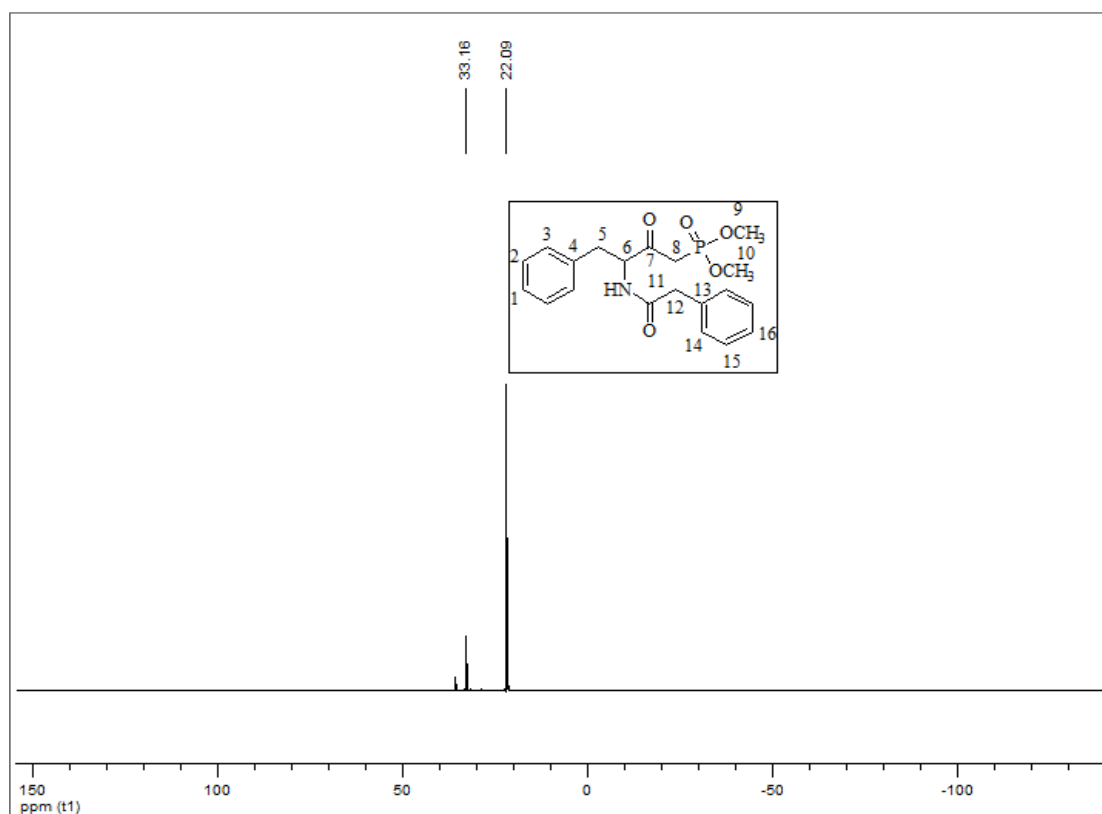


Fig.III. 53: ^{31}P NMR spectrum of **44a**

Using the same reaction conditions, different analogs of the phosphonates intermediate shown in Figure III.54 were also prepared starting from alanine amino acid.

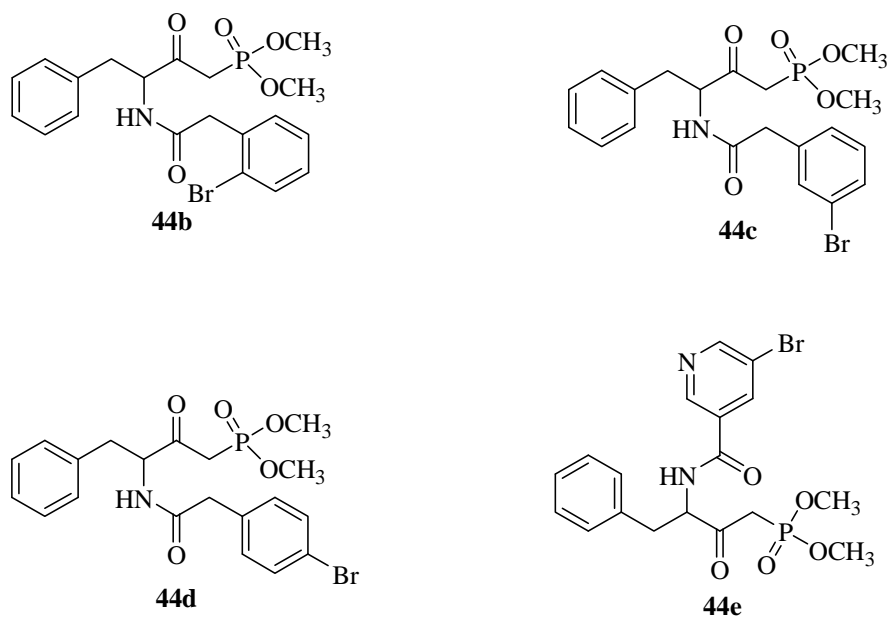
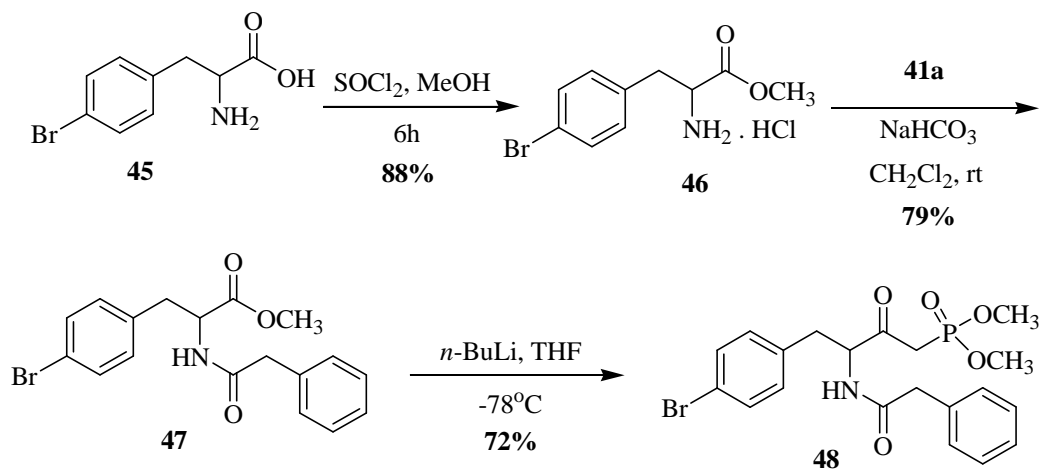


Fig.III. 54: Other analogs prepared starting from alanine amino acid

In addition to that, 4-bromo phenylalanine was also used as a starting amino acid which gave the desired phosphonate **48** as a white solid in 72% yield (Scheme III.19).



Scheme III. 19: Preparation of phosphonate **48**

Finally, glycine was used as another amino acid for the preparation of different phosphonate intermediates, using same reaction conditions as for phosphonate **44a** (Figure III.55).

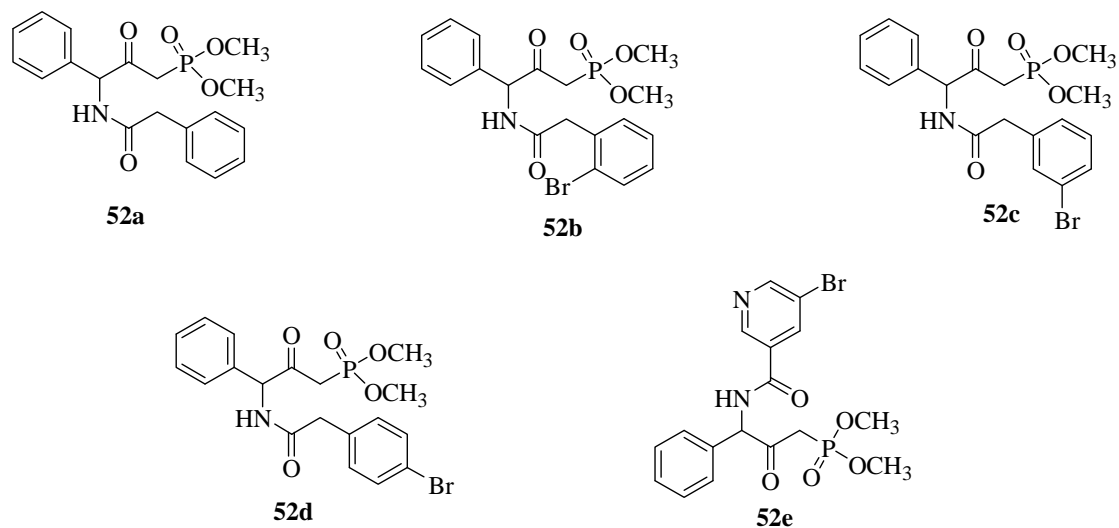
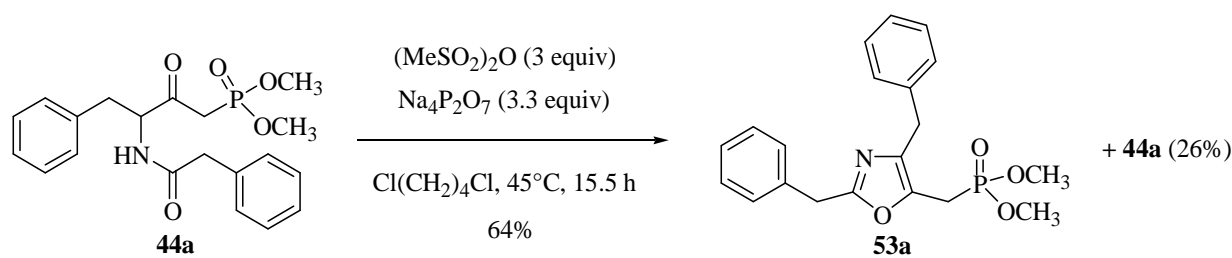


Fig.III. 55: Phosphonate intermediates prepared starting from glycine

The structure of all the amide ester and phosphonate intermediates were clearly established by NMR data (^1H , ^{13}C , ^{31}P) as for **42a** and **44a** respectively.

After extensive studies on model compound **53a**, the cyclization step was finally successfully performed by Dr P. Mosset to obtain the desired oxazole **53a** (Scheme III.20).



Scheme III. 20: Cyclization reaction of **44a** to obtain the oxazole product **53a**

Biological tests

Concerning the biological tests, hydrazone type analogs (Pyrrols and Pyrrolidines) and thiophene analogs were the only compounds subjected to biological tests at this stage. These molecules were tested with different lines of melanoma cancer cells, including HaCat cells and B16-F10 cells.

Results obtained by *Mrs F. Le Devehat* and *I. Rouaud* in the team of *Professor J. Boustie* (melanoma) in Rennes:

1. Principle of study:

1.1. HaCat cells:

HaCaT cells are derived from a non-cancerous line of human keratinocytes. This lineage approaches the composition of the human dermis. HaCaT cells are grown in of the RMPI 1640 medium supplemented with 5% fetal calf serum and antibiotic and under controlled atmosphere at 5% CO₂ and a temperature of 37 ° C.

1.2. The B16-F10 cells

B16-F10 cells are murine melanocytes (LGC, ATCC, CRL-6475-melanoma mouse). These cells are cultured in RMPI 1640 medium supplemented with 5% of calf serum fetal and antibiotic and under a controlled atmosphere at 5% CO₂ at a temperature of 37 ° C.

To perform 96-well plate seeding, the cells are reacted with the enzyme trypsin [or "trypsinized"]. The plates are then incubated in the oven for 24 hours to allow their adhesion to the support. After 24h of incubation, the cell viability is evaluated by the MTT test: this tetrazolium salt of yellow color is transformed by the mitochondrial dehydrogenases of viable cells into crystals of violet. This staining is proportional to the number of living cells and the reading is done with the Multi-scan FC spectrophotometer at 540 nm.

Two anti-cancer controls, doxorubicin and 5-fluorouracil were used.

2. Objective:

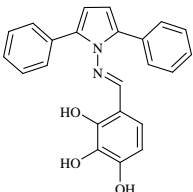
This study consisted of establishing the cellular toxicity of 8 products depending on their concentration. This will allow the determination of the IC₅₀ (concentration which results in 50% cell death).

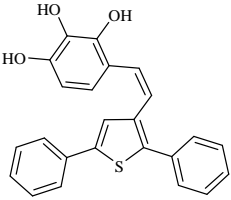
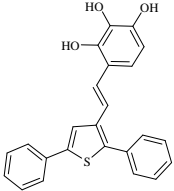
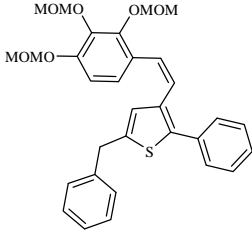
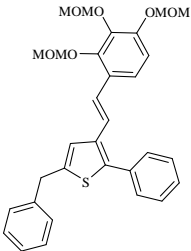
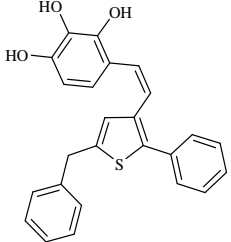
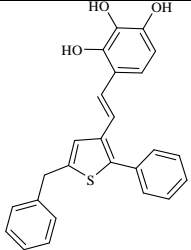
3. Preparation of the compounds:

Stock solutions of the compounds (Table 1) are prepared in DMSO at concentration of 100 mM or in a mixture of DMSO/ethanol (50/50) of 50 mM then placed in micro-tubes in fractions of 20 or 30 µl. These solutions are then frozen at -20 ° C.

A concentration range is established in the culture medium used: RPMI1640 supplemented with 5% calf serum. The final concentrations in the wells are 100 µM, 50 µM, 10 µM, 1 µM and 0.5 µM. Each concentration of each compound is tested in "Triplicate" (tests performed three times).

The results are given in Table III.1

Reference	Structure	IC ₅₀ in Mm			
		HaCat		B16	
		Average	Standard deviation	Average	Standard deviation
MH-92		29.00	9.00	10.00	4.00

MH102C		81.00	21.00	4.00	9.00
MH102T		> 100		> 100	
MH101C		> 100		> 100	
MH101T		> 100		> 100	
MH122		> 100		> 100	
MH125		> 100		60.00	13.00

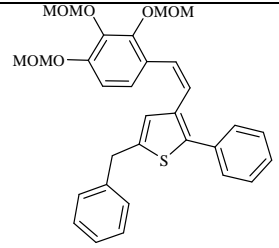
MH119		> 100		> 100	
5fluorouracile		> 100		43.00	6.00
doxorubicin		4.23	2.30	0.28	0.18

Table III. 1: Results of IC₅₀ (μM) of the compounds on HaCaT and B16 lines

From these results, the compounds can be divided into four categories:

For HaCaT:

- IC₅₀ >100μM: **MH-102T, MH-101C, MH-101T, MH-122T, MH-125C, MH-119C.**
- IC₅₀ >50μM et <100μM: **MH-102C.**
- IC₅₀ >10μM et <50μM: **MH-92.**
- IC₅₀ =10μM: **no compounds.**

For B16:

- IC₅₀ >100μM: **MH-102T, MH-101C, MH-101T, MH-122T, MH-119C.**
- IC₅₀ >50μM et <100μM : **MH-125C.**
- IC₅₀ >10μM et <50μM : **MH-102C.**
- IC₅₀ =10μM: **MH-92.**

As shown in the above results, the most active compound on both lines HaCat and B16 appeared to be MH-92 (HaCat: IC₅₀ = 29 ± 9 μM, B16: IC₅₀ = 10 ± 4 μM). In addition to MH-102C which appears greater activity on B16 (IC₅₀ = 34 ± 9 μM) than HaCat (: IC₅₀ = 81 ± 21 μM).

On the other hand, these eight products were also tested with other lines of cancer cells, including the ovarian cancer lineage (IGROV1-R10), which was performed by the team of *Pr. L. Poulain* at the university of *Caen*, and the breast cancer lineage, performed by the team of *Dr P. Juin* at the university of *Nantes*. But

unfortunately, none of the tested compounds showed a good selectivity towards MCL-1 protein.

III.D. CONCLUSION

Conclusion

In this study we investigated new inhibitors of the MCL-1 protein in order to restore apoptotic properties within cancer cells. We were able to design and synthesize several series of MIM-1 analogues depending on the molecular modeling carried out by Dr. N. Levoin, which helped us to rationalize the interaction of these compounds with the MCL-1 protein and to design new compounds.

Two different models were synthesized: the alkene type analogs and the hydrazone type analogs. Eight different compounds were prepared, by keeping the trihydroxyphenyl group (since it showed a key hydrophilic interaction with the MCL-1 pockets), while changing the core center and the other groups. Biological tests were performed on three different cancer cell lines at the universities of Rennes, Nantes and Caen. Results obtained showed a good activity only for the pyrrol compound (MH-92) that appeared to be a good inhibitor of both HaCat and B16 cells (melanoma); in addition to the other compound from the alkene type analog (MH-102C), that also showed a good activity on the B16 cells (melanoma).

More studies have to be performed in our groups in order to obtain the different molecules required for the biological studies, in particular the oxazole analogs which showed very promising docking properties.

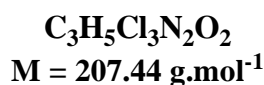
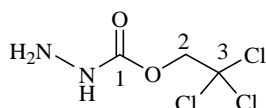
III.E. EXPERIMENTAL PART

Experimental Part

Part one: pyrrole derivatives

Synthesis of hydrazine carboxylic acid 2,2,2-trichloro-ethyl ester (**19**)

To a solution of commercially available hydrazine (11 ml, 0.35 mmol) in CHCl_3 (125 ml) at 0°C was added a solution of commercially available 2,2,2-trichloroethyl chloroformate (10.5 ml, 0.076 mmol) in CHCl_3 (25 ml). After a period of 1 hr at 0°C , the reaction mixture was partitioned between ethyl acetate and water. The organic phase was collected, dried over MgSO_4 and evaporated under reduced pressure. After purification on column chromatography, using 100% ethyl acetate, hydrazide **19** was obtained as a white solid in 92% yield.



White solid, mp= 42°C , $R_f = 0.34$ (EtOAc);

^1H NMR (CDCl_3 , 300 MHz), δ ppm: 6.06 (s, 1H, NH); 4.63 (s, 2H, H_2); 2.64 (s, 2H, NH_2).

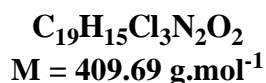
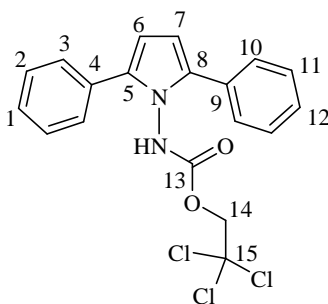
^{13}C NMR (CDCl_3 , 75 MHz), δ ppm: 154.78 (1C, C_1); 94.85 (1C, C_3); 74.34 (1C, C_2).

HRMS (ESI) calculated for $\text{C}_3\text{H}_5\text{N}_2\text{O}_2^{35}\text{Cl}_3\text{Na}$: $[\text{M} + \text{Na}]^+$: m/z 228.9314 Found: m/z. 228.9314 (0 ppm).

Condensation of 2,2,2-trichloroethyl hydrazide (19) with 1,4-diketone (18)

To a solution of hydrazide **19** (0.62 g, 3.51 mmol) in toluene (15 ml), were added the commercially available 1,2-dibenzoyl ethane **18** (0.7 g, 2.92 mmol) with a catalytic amount of pyridinium p-toluenesulfonate (PPTS) (0.035g, 0.15 mmol). The reaction mixture was stirred under nitrogen atmosphere at 80°C. After a period of 10 h, the solvent was removed under reduced pressure and the crude product was purified by column chromatography, using 7/3 of pentane/EtOAc mixture, compound **20** was obtained as white solid in 86 % yield.

(2,5-Diphenyl-pyrrol-1-yl)-carbamic acid-2,2,2-trichloro ethyl ester (20)



White solid, mp= 168°C, R_f = 0.38 (pentane/EtOAc 6/4);

$^1\text{H NMR}$ (CDCl_3 , 300 MHz), δ ppm: 7.48 (d, 4H, J = 6.9 Hz); 7.40 (tt, 4H, J = 6.9 Hz, J = 1.3 Hz); 7.32 (dt, 2H, J = 7.1 Hz, J = 1.2 Hz); 6.37 (s, 2H, $H_{6,7}$); 4.69 (s, 2H, H_{14}).

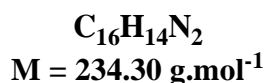
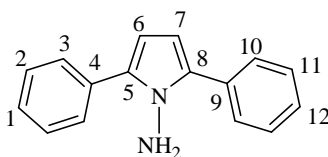
$^{13}\text{C NMR}$ (CDCl_3 , 75 MHz), δ ppm: 153.72 (1C, C_{13}); 143.34 (1C); 137.01 (1C); 131.21 (1C); 130.24 (1C); 128.62 (1C); 128.57 (1C); 128.53 (4C); 128.30 (2C); 127.99 (1C); 127.51 (1C); 108.25 (2C, $C_{6,7}$); 94.70 (1C, C_{15}); 74.78 (1C, C_{14}).

HRMS (ESI) calculated for $\text{C}_{19}\text{H}_{15}\text{N}_2\text{O}_2^{35}\text{Cl}_3\text{Na}$: $[\text{M} + \text{Na}]^+$: m/z 431.0091 Found: m/z . 431.0091 (0 ppm).

Deprotection of the primary amine in (20) using Zn/AcOH

To a solution of hydrazide **20** (0.5 g, 0.91 mmol) in glacial acetic acid (4.55 ml), under a nitrogen atmosphere, was added zinc dust (0.5 g) portion wise over 5 min. The reaction mixture was stirred at room temperature for 45 min. After this time, the reaction was quenched by adding water and sodium hydroxide (10 N) till PH 10 and extracted with ethyl acetate. The organic layer was dried over MgSO₄ and concentrated under vacuo. The crude mixture was then purified by column chromatography, using 100% EtOAc, and gave the desired amine **21** as a yellow solid in 88% yield.

2,5-Diphenyl-pyrrol-1-ylamine (21)



White solid, mp= 216°C, $R_f = 0.38$ (pentane/EtOAc 5/5);

¹H NMR (CDCl₃, 300 MHz), δ ppm: 7.71 (m, 4H); 7.40 (m, 6H); 6.23 (s, 2H, H_{6,7}); 5.70 (s, 2H, NH₂).

¹³C NMR (CDCl₃, 75 MHz), δ ppm: 134.92 (2C); 132.70 (2C); 128.06 (4C); 127.96 (4C); 126.10 (2C); 105.95 (2C, C_{6,7}).

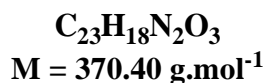
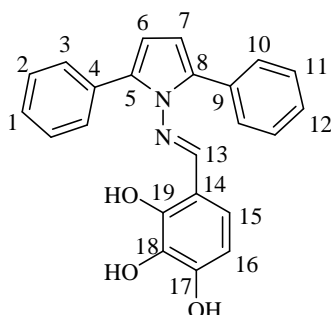
HRMS (ESI) calculated for C₁₆H₁₄N₂Na: [M +Na]⁺: m/z 257.1055 Found: m/z. 257.1055 (0 ppm).

General procedure for the condensation reaction of hydrazine with aldehyde

A methanolic (20 ml) solution of amine (1 mmol) was added to a solution of trihydroxybenzaldehyde (1 mmol) in methanol (15 ml), and the reaction mixture was refluxed for 6h. After this time, and after cooling of the reaction mixture, the solvent was removed under vacuo, and the residues were dissolved in ethyl acetate and purified by chromatography.

Synthesis of 4-[(2,5-diphenyl-pyrrol-1-ylimino)-methyl]-benzene-1,2,3-triol (**23**)

To a solution of amine **21** (0.4 g, 1.7 mmol) in methanol (34 ml), a solution of trihydroxybenzaldehyde **22** (0.26 g, 1.7 mmol) in methanol (22 ml) was added, and the reaction mixture was refluxed for 6h according to the general procedure. After purification by chromatography on silica gel, using pentane/ EtOAc 3/7 as eluent, hydrazone **23** was obtained as a yellow solid in 64% yield.



Yellow solid, mp= 88°C, R_f = 0.43 (pentane/EtOAc 7/3);

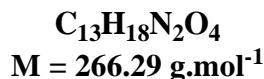
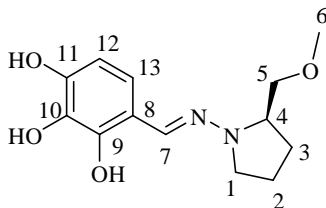
$^1\text{H NMR}$ (CDCl_3 , 300 MHz), δ ppm: 10.24 (s, 1H, OH); 9.88 (s, 1H, OH); 8.60 (s, 1H, OH); 8.20 (s, 1H, H₁₃); 7.50 (m, 4H); 7.35 (m, 4H); 7.22 (m, 2H); 6.78 (d, 1H, H₁₅, 3J = 8.6 Hz); 6.45 (s, 2H, H_{6,7}); 6.34 (d, 2H, H₁₆, 3J = 8.6 Hz).

$^{13}\text{C NMR}$ (DMSO, 75 MHz), δ ppm: 166.92 (1C, C₁₃); 150.74 (1C, C₁₇); 148.39 (1C, C₁₉); 132.55 (1C); 131.78 (2C); 131.26 (2C); 128.45 (4C); 127.68 (4C); 126.39 (2C); 121.59 (1C); 110.16 (1C); 108.17 (1C); 108.14 (2C, C_{6,7}).

HRMS (ESI) calculated for C₂₃H₁₈N₂O₃: [M +H]⁺: m/z 371.1390 Found: m/z. 371.1391 (0 ppm).

Synthesis of (R)-4-[(2-methoxymethyl-pyrrolidin-1-ylimino)-methyl]-benzene-1,2,3-triol (25R)

To a solution of commercially available 2,3,4-trihydroxybenzaldehyde **22** (0.5 g, 3.25 mmol) in MeOH (30 ml), a solution of commercially available (*R*)-1-amino-2-(methoxymethyl) pyrrolidine **24R** (0.42 g, 3.25 mmol) in MeOH (45 ml) was added according to the general procedure mentioned above. After purification by chromatography on silica gel, using pentane/EtOAc 8/2 as eluent, hydrazone **25R** was obtained as a white solid in 85% yield.



White solid, mp= 90°C, **R_f** = 0.32 (pentane/EtOAc 8/2);

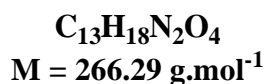
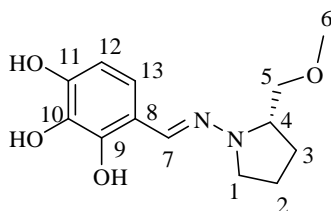
¹H NMR (DMSO, 300 MHz), δ ppm: 11.40 (s, 1H, OH); 9.03 (s, 1H, OH); 8.20 (s, 1H, H₇); 7.45 (s, 1H, OH); 6.56 (d, 1H, H₁₃, ³J= 8.3 Hz); 6.30 (d, 1H, H₁₂, ³J= 8.3 Hz); 3.42 (d, 2H, H₅, ³J= 7.5 Hz); 3.37 (s, 3H, H₆); 3.29 (s, 2H, H₁); 2.88 (m, 1H, H₄); 1.91 (m, 4H, H_{2,3}).

¹³C NMR (DMSO, 75 MHz), δ ppm: 146.12 (1C); 145.67 (1C); 138.41 (1C); 132.39 (1C); 119.13 (1C); 112.69 (1C); 106.82 (1C); 74.55 (1C, C₅); 62.85 (1C, C₄); 58.44 (1C, C₆); 49.04 (1C, C₁); 26.25 (1C, C₃); 21.34 (1C, C₂).

HRMS (ESI) calculated for C₁₃H₁₈N₂O₄: [M+H]⁺: m/z 289.1158 Found: m/z. 289.1161(1 ppm).

Synthesis of (S)-4-[(2-methoxymethyl-pyrrolidin-1-ylimino)-methyl]-benzene-1,2,3-triol (25S)

To a solution of commercially available 2,3,4-trihydroxybenzaldehyde **22** (0.5 g, 3.25 mmol) in MeOH (30 ml), a solution of commercially available (S)-1-amino-2-(methoxymethyl) pyrrolidine **24S** (0.42 g, 3.25 mmol) in MeOH (45 ml) was added according to the general procedure mentioned above. After purification by chromatography on silica gel, using pentane/EtOAc 8/2 as eluent, hydrazone **25S** was obtained as a white solid in 82% yield.



White solid, mp= 88°C, **R_f** = 0.30 (pentane/EtOAc 8/2);

¹H NMR (DMSO, 300 MHz), δ ppm: 11.43 (s, 1H, OH); 9.12 (s, 1H, OH); 8.21 (s, 1H, H₇); 7.43 (s, 1H, OH); 6.55 (d, 1H, H₁₃, ³J= 8.4 Hz); 6.30 (d, 1H, H₁₂, ³J= 8.4 Hz); 3.41 (m, 4H, H_{1,5}); 3.27 (s, 3H, H₆); 2.86 (dd, 1H, H₄, ³J= 8.9 Hz, ³J= 8.0 Hz); 1.91 (m, 4H, H_{2,3}).

¹³C NMR (DMSO, 75 MHz), δ ppm: 146.26 (1C); 145.86 (1C); 138.64 (1C); 132.58 (1C); 119.43 (1C); 112.94 (1C); 107.03 (1C); 74.75 (1C, C₅); 63.09 (1C, C₄); 58.85 (1C, C₆); 49.25 (1C, C₁); 26.43 (1C, C₃); 21.55 (1C, C₂).

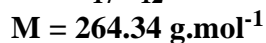
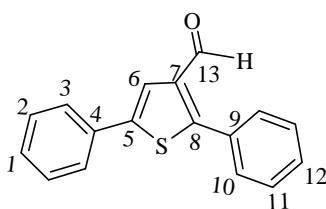
HRMS (ESI) calculated for C₁₃H₁₈N₂O₄: [M +H]⁺: m/z 289.1158 Found: m/z. 289.1156 (1 ppm).

Part two: Thiophene derivatives

Procedure for palladium catalyzed C₂ and C₅ direct arylation of 3-formylthiophene

In a typical experiment, the aryl bromide **27** (0.314 g, 2 mmol), the commercially available 3-formylthiophene **26** (0.336g, 3 mmol), and potassium acetate (0.392 g, 4 mmol) were introduced in an oven dried Schlenk tube, equipped with a magnetic stirring bar. Then palladium acetate (0.44 mg, 0.002 mmol), dppb ligand (0.84 mg, 0.002 mmol) and DMF (6 ml) were added, and the Schlenk tube was purged several times with nitrogen. The Schlenk tube was placed in a preheated oil bath at 150°C, and the reactants were allowed to stir for 16 h. After this time, the solvent was removed under vacuo, and the residues were dissolved and extracted with ether (3 times), and the organic phase was then dried over MgSO₄, and then concentrated under vacuo. After purification on column chromatography, using 98/2 of pentane/ether mixture, 2,5-diphenyl-thiophene-3-carbaldehyde **29** was obtained as a white solid in 52 % yield.

2, 5-Diphenyl thiophene-3-carbaldehyde (29)



White solid, mp= 71°C, R_f = 0.34 (pentane/ether 9/1);

¹H NMR (CDCl₃, 300 MHz), δ ppm: 9.88 (d, 1H, H₁₃, ⁴J= 0.2 Hz); 7.76 (d, 1H, H₆, ⁴J= 0.2 Hz); 7.65 (m, 2H); 7.56 (m, 2H); 7.50 (m, 3H); 7.49 (m, 2H); 7.34 (m, 1H).

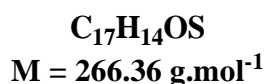
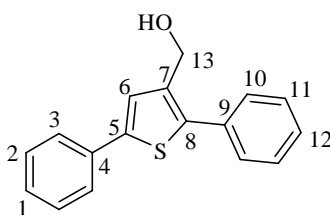
¹³C NMR (CDCl₃, 75 MHz), δ ppm: 185.83 (1C, C₁₃); 155.00 (1C, C₈); 143.67(1C, C₅); 137.88(1C, C₇); 132.99 (1C); 131.34 (1C); 130.00 (2C); 129.49 (1C); 129.07 (2C); 128.96 (2C); 128.38 (1C); 125.89 (2C); 121.66 (1C, C₆).

HRMS (ESI) calculated for $C_{17}H_{12}ONaS$: $[M + Na]^+$: m/z 287.0501 Found: m/z . 287.0501 (1 ppm).

Reduction of 2,5-diphenyl-thiophene-3-carbaldehyde (29)

To a solution of **29** (0.264 g, 1 mmol) in MeOH (5ml), $NaBH_4$ (0.038 g, 1 mmol) was added portionwise and the reaction was stirred for 10 min. The reaction was then quenched with saturated ammonium chloride solution, and extracted with CH_2Cl_2 (3 times). The combined organic phase was washed with brine, dried over $MgSO_4$, and concentrated under vacuo. A white solid of alcohol **30** was obtained without purification in 94% yield.

(2, 5-Diphenyl-thiophen-3-yl)-methanol (30)



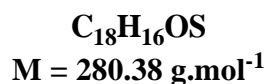
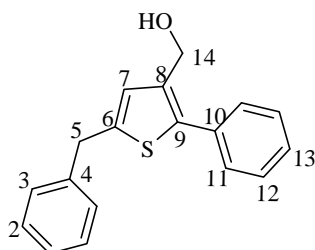
White solid, $mp = 108^\circ C$, $R_f = 0.30$ (pentane/ether 7/3);

1H NMR ($CDCl_3$, 300 MHz), δ ppm: 7.64 (m, 2H); 7.55 (m, 2H); 7.42 (m, 6H); 7.30 (m, 1H, H_6); 4.69 (s, 2H, H_{13}).

^{13}C NMR ($CDCl_3$, 75 MHz), δ ppm: 143.01 (1C, C_5); 140.40 (1C, C_7); 137.77 (1C, C_8); 134.00 (1C); 133.57 (1C); 128.98 (2C); 128.89 (2C); 128.71 (2C); 127.87 (1C); 127.59 (1C); 125.56 (2C); 125.20 (1C); 59.03 (1C, C_{13}).

HRMS (ESI) calculated for $C_{17}H_{14}ONaS$: $[M + Na]^+$: m/z 289.0657 Found: m/z . 289.0656 (1 ppm).

(5-Benzyl-2-phenyl-thiophen-3-yl)-methanol (35)



Yellow solid, mp= 53°C, **R_f** = 0.30 (pentane/ether 7/3);

¹H NMR (CDCl₃, 300 MHz), δ ppm: 7.46 (m, 2H); 7.44 (m, 2H); 7.32 (m, 6H); 6.88 (s, 1H, H₇); 4.60 (s, 2H, H₁₄); 4.14 (s, 2H, H₅).

¹³C NMR (CDCl₃, 75 MHz), δ ppm: 143.01 (1C, C₅); 140.40 (1C, C₇); 137.77 (1C, C₈); 134.00 (1C); 133.57 (1C); 128.98 (2C); 128.89 (2C); 128.71 (2C); 127.87 (1C); 127.59(1C); 125.56 (2C); 125.20 (1C); 59.03 (1C, C₁₃).

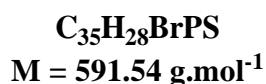
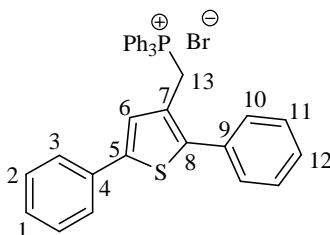
HRMS (ESI) calculated for C₁₈H₁₆ONaS: [M +Na]⁺: m/z 303.0814 Found: m/z. 303.0812 (1 ppm).

General procedure for the conversion of alcohol into phosphonium salt

Triphenylphosphine hydrobromide (1 equiv) was added to a solution of alcohol (1 equiv) in acetonitrile, and the reaction mixture was refluxed for 3h. After cooling to room temperature, the solvent was removed in vacuo and the residue was crystallized from EtOH/AcOEt.

Synthesis of (2,5-diphenyl-thiophen-3-ylmethyl)-triphenyl-phosphonium bromide (31)

The reaction was performed between alcohol **30** (0.266 g, 1 mmol) and triphenylphosphine hydrobromide (0.343 g, 1 mmol) according to the general procedure mentioned above, and yielded the desired phosphonium salt **31** as a white solid in 84 % yield.



White solid, mp > 266°C, **R_f** = 0.38 (pentane/ether 9/1);

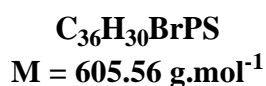
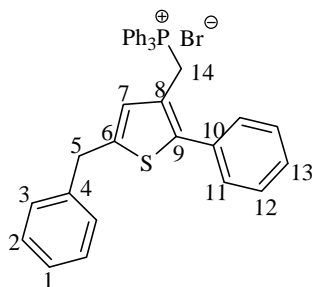
¹H NMR (CDCl₃, 300 MHz), δ ppm: 7.75-7.54 (m, 15H, PPh₃); 7.32-7.25 (m, 8H); 7.01 (d, 1H, H₆, ⁴J = 1.3 Hz); 6.96 (m, 2H); 5.48 (d, 2H, H₁₃, ²J_{H-P} = 13.7 Hz).

¹³C NMR (CDCl₃, 75 MHz), δ ppm: 143.50 (d, 1C, J_{C-P} = 2.3 Hz); 142.88 (d, 1C, J_{C-P} = 9.1 Hz); 134.88 (d, 2C, J_{C-P} = 2.9 Hz); 134.14 (s, 4C); 134.00 (s, 4C); 133.07 (s, 1C); 132.42 (d, 1C, J_{C-P} = 2.4 Hz); 130.16 (s, 2C); 129.99 (s, 4C); 128.94 (s, 4C); 128.86 (s, 2C); 128.25 (s, 1C); 127.92 (s, 1C); 126.08 (d, 1C, J_{C-P} = 2.8 Hz); 125.42 (s, 2C); 122.97 (d, 1C, J_{C-P} = 8.9 Hz); 118.17 (s, 1C); 117.04 (s, 1C); 25.18 (d, 1C, C₁₃, ¹J_{C-P} = 47.3 Hz).

HRMS (ESI) calculated for C₃₅H₂₈PS: C⁺: m/z 511.1643 Found: m/z. 511.1641 (1 ppm).

Synthesis of (5-Benzyl-2-phenyl-thiophen-3-ylmethyl)-triphenyl-phosphonium bromide (36)

The reaction was performed between alcohol **35** (0.280 g, 1 mmol) and triphenylphosphine hydrobromide (0.343 g, 1 mmol) according to the general procedure mentioned above, and yielded the desired phosphonium salt **36** as a yellow solid in 80 % yield.



Yellow solid, mp = 209°C, **R_f** = 0.41 (pentane/ether 9/1);

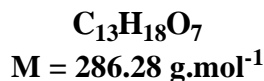
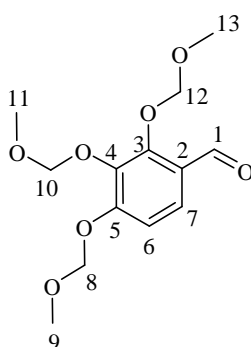
¹H NMR (CDCl₃, 300 MHz), δ ppm: 7.70 (m, 3H); 7.50 (m, 10H); 7.28 (m, 6H); 7.22 (m, 2H) 7.10 (dd, 2H, J= 7.6 Hz, J= 1.6 Hz); 6.90 (dd, 2H, J= 7.6 Hz, J= 1.6 Hz); 6.49 (s, 1H, H₇); 5.45 (d, 2H, H₁₄, ²J_{H-P}= 13.7 Hz); 3.93 (s, 2H, H₅).

¹³C NMR (CDCl₃, 75 MHz), δ ppm: 144.24 (d, 1C, J_{C-P}= 2.4 Hz); 139.85 (s, 1C); 134.75 (d, 2C, J_{C-P}= 1.1 Hz); 134.15 (s, 4C); 134.07 (s, 4C); 130.07 (s, 4C); 129.97 (s, 4C); 129.12 (d, 2C, J_{C-P}= 1.1 Hz); 128.82 (s, 2C); 128.60 (s, 2C); 128.48 (s, 2C); 128.22 (d, 1C, J_{C-P}= 2.7 Hz); 128.01 (s, 1C); 126.57 (s, 1C) 118.19 (s, 1C); 117.51 (s, 1C); 36.04 (s, 1C, C₅); 24.95 (d, 1C, C₁₄, ¹J_{C-P}= 46.7 Hz).

HRMS (ESI) calculated for C₃₆H₃₀PS: C⁺: m/z 525.1800 Found: m/z. 525.1797 (1 ppm).

Synthesis of 2,3,4-Tris-methoxymethoxy-benzaldehyde (**32**)

To a solution of 2,3,4-trihydroxybenzaldehyde **22** (0.77 g, 5 mmol), in CH₂Cl₂ (20 ml) was added N,N-diisopropylethylamine (3.48 ml, 20 mmol) followed by chloromethyl methyl ether (0.58 ml, 7.33 mmol). The reaction was stirred at room temperature for 18 h then quenched with saturated sodium bicarbonate solution (14 ml). The aqueous layer was extracted with CH₂Cl₂ (3× 20 ml). The combined organic layer was then washed with saturated sodium chloride (26 ml), dried over MgSO₄, and concentrated under vacuo. After purification on column chromatography, using 8/2 of pentane/EtOAc, aldehyde **32** was obtained as yellow oil in 95 % yield.



Yellow oil, **R_f** = 0.52 (pentane/ EtOAc 8/2);

¹H NMR (CDCl₃, 300 MHz), δ ppm: 10.26 (s, 1H, H₁); 7.56 (d, 1H, H₇, ³J= 8.8 Hz); 7.00 (d, 1H, H₆, ³J= 8.8 Hz); 5.24 (s, 2H); 5.23 (s, 2H); 5.12 (s, 2H); 3.58 (s, 3H); 3.53 (s, 3H); 3.47 (s, 3H).

¹³C NMR (CDCl₃, 75 MHz), δ ppm: 188.84 (1C, C₁); 156.55 (1C, C₅); 154.14 (1C, C₃); 138.81 (1C, C₄); 124.82 (1C); 124.42 (1C); 111.29 (1C); 100.20 (1C); 98.70 (1C); 94.70 (1C); 57.89 (1C); 57.35 (1C); 56.43 (1C).

HRMS (ESI) calculated for C₁₃H₁₈O₇Na: [M +Na]⁺: m/z 309.0944 Found: m/z. 309.0945 (0 ppm).

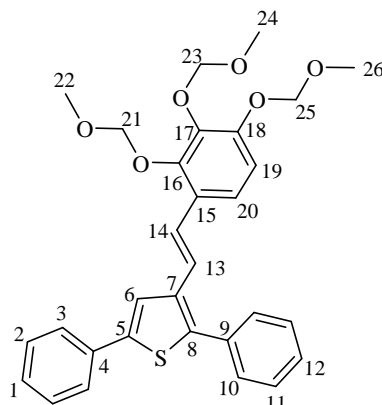
General procedure for the Wittig reaction between phosphonium salt and aldehyde

Sodium hydride (1 mmol) was added to a suspension of the appropriate phosphonium halide (1 mmol) in dry THF under nitrogen atmosphere, and the reaction mixture was refluxed with stirring for 5-15 min till the appearance of orange color; that indicates the formation of ylide. Then appropriate aldehyde (1 mmol) was added and the reaction mixture refluxed for 16 hr. After this time, and after cooling of the reaction mixture, the solvent was removed under vacuo, and the residues were dissolved in ethyl acetate and purified by chromatography.

Wittig reaction between phosphonium **31** and aldehyde **32**

To a solution of phosphonium salt **31** (1 g, 1.68 mmol) in THF (45 ml), sodium hydride (0.04 g, 1.68 mmol), and aldehyde **32** (0.48 g, 1.68 mmol) was added according to the general procedure mentioned above. After purification by chromatography on silica gel, using pentane/EtOAc as eluent (80/20), two isomers of the desired alkene products **33E** and **33Z** were purely isolated; where *E* isomer obtained in 25% and *Z* isomer obtained in 39%. The combined yield of the reaction is 64%.

**(E)-2, 5-Diphenyl-3-[2-(2,3,4-tris-methoxymethoxy-phenyl)-vinyl]-thiophene
(33E)**



C₃₀H₃₀O₆S
M = 518.62 g.mol⁻¹

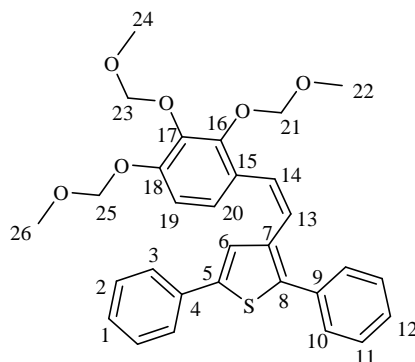
White solid, mp= 84°C, **R_f** = 0.37 (pentane/ EtOAc 8/2);

¹H NMR (CDCl₃, 300 MHz), δ ppm: 7.68 (d, 1H, J= 1.4 Hz); 7.64 (m, 2H); 7.54 (m, 2H); 7.46 (m, 3H); 7.38 (m, 4H); 7.22 (d, 1H, H₂₀, ³J= 8.8 Hz); 7.08 (d, 1H, ³J_{trans} = 16.4 Hz); 6.92 (d, 1H, H₁₉, ³J= 8.8 Hz); 5.20 (s, 4H); 5.17 (s, 2H); 3.64 (s, 3H); 3.62 (s, 3H); 3.51 (s, 3H).

¹³C NMR (CDCl₃, 75 MHz), δ ppm: 150.60 (1C, C₁₈); 148.64 (1C, C₁₆); 142.81 (1C); 139.66 (1C); 139.48 (1C); 136.38 (1C); 134.05 (1C); 134.02 (1C); 129.51 (2C); 128.91 (2C); 128.67 (2C); 127.75 (1C); 127.71 (1C); 126.48 (1C); 125.70 (2C); 124.01 (1C); 122.05 (1C); 121.66 (1C); 121.04 (1C); 112.20 (1C); 99.72 (1C); 98.82 (1C); 95.18 (1C); 57.90 (1C); 57.35 (1C); 56.22 (1C).

HRMS (ESI) calculated for C₃₀H₃₀O₆NaS: [M +Na]⁺: m/z 541.1655 Found: m/z. 541.1655 (0 ppm).

**(Z)-2, 5-Diphenyl-3-[2-(2,3,4-tris-methoxymethoxy-phenyl)-vinyl]-thiophene
(33Z)**



C₃₀H₃₀O₆S
M = 518.62 g.mol⁻¹

White solid, mp= 96°C, **R_f** = 0.64 (pentane/EtOAc 8/2);

¹H NMR (CDCl₃, 300 MHz), δ ppm: 7.60 (d, 2H, J= 7.1 Hz); 7.44 (m, 4H); 7.32 (m, 3H); 7.24 (m, 1H); 7.13 (d, 1H, H₂₀, ³J= 8.6 Hz); 7.04 (s, 1H, H₆); 6.82 (d, 1H, H₁₉, ³J= 8.6 Hz); 6.76 (d, 1H, H₁₄, ³J_{cis}= 11.9 Hz); 6.54 (d, 1H, H₁₃, ³J_{cis}= 11.9 Hz); 5.20 (s, 2H); 5.19 (s, 2H); 5.18 (s, 2H); 3.63 (s, 3H); 3.59 (s, 3H); 3.50 (s, 3H).

¹³C NMR (CDCl₃, 75 MHz), δ ppm: 150.72 (1C, C₁₈); 149.01 (1C, C₁₆); 141.60 (1C); 140.64 (1C); 139.69 (1C); 134.96 (1C); 134.23 (1C); 134.09 (1C); 128.95 (2C); 128.76 (2C); 128.55 (2C); 127.65 (1C); 127.42 (1C); 126.16 (1C); 125.71 (1C); 125.58 (2C); 125.20 (1C); 125.11 (1C); 124.37 (1C); 111.68 (1C); 99.32 (1C); 98.88 (1C); 95.24 (1C); 57.62 (1C); 57.32 (1C); 56.22 (1C).

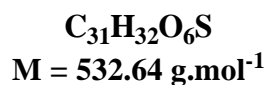
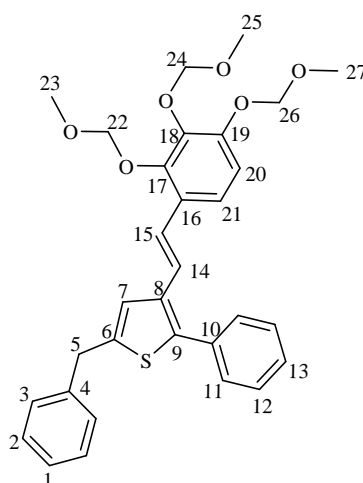
HRMS (ESI) calculated for C₃₀H₃₀O₆NaS: [M +Na]⁺: m/z 541.1655 Found: m/z. 541.1657 (0 ppm).

Wittig reaction between phosphonium 36 and aldehyde 32

To a solution of phosphonium salt **36** (0.5 g, 0.82 mmol) in THF (25 ml), sodium hydride (0.02 g, 0.82 mmol), and aldehyde **32** (0.24 g, 0.82 mmol) was added according to the general procedure mentioned above. After purification by chromatography on silica gel, using pentane/EtOAc as eluent (80/20), two isomers of the desired alkene products **37E** and **37Z** were purely isolated; where **E** isomer

obtained in 28% and **Z** isomer obtained in 32%. The combined yield of the reaction is 60%.

(E)-5-Benzyl-2-phenyl-3-[2-(2,3,4-tris-methoxymethoxy-phenyl)-vinyl]-thiophene
(37E)



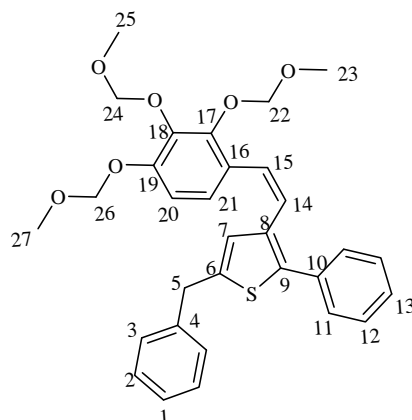
Yellow oil, **R_f** = 0.36 (pentane/EtOAc 8/2);

¹H NMR (CDCl₃, 300 MHz), δ ppm: 7.44 (m, 2H); 7.41 (m, 2H); 7.34 (m, 4H); 7.28 (m, 2H); 7.24 (d, 1H, H₁₅, ³J_{trans} = 16.5 Hz); 7.18 (d, 1H, H₂₁, ³J = 8.8); 7.09 (s, 1H, H₇); 7.02 (d, 1H, H₁₄, ³J_{trans} = 16.5 Hz); 6.90 (d, 1H, H₂₀, ³J = 8.8 Hz); 5.20 (s, 2H); 5.16 (s, 2H); 5.15 (s, 2H), 4.16 (s, 2H, H₅); 3.63 (s, 3H); 3.55 (s, 3H); 3.51 (s, 3H).

¹³C NMR (CDCl₃, 75 MHz), δ ppm: 150.49 (1C, C₁₉); 148.59 (1C, C₁₇); 143.21 (1C); 139.76 (1C); 139.69 (1C); 138.78 (1C); 135.23 (1C); 134.29 (1C); 129.53 (2C); 128.75 (2C); 128.61 (1C); 128.55 (2C); 127.46 (1C); 126.64 (1C); 126.63 (1C); 123.84 (2C); 123.56 (1C); 122.17 (1C); 120.90 (1C); 112.25 (1C); 99.70 (1C); 98.83 (1C); 95.24 (1C); 57.83 (1C); 57.36 (1C); 56.24 (1C); 36.39 (1C, C₅).

HRMS (ESI) calculated for C₃₁H₃₂O₆NaS: [M +Na]⁺: m/z 555.1811 Found: m/z. 555.1811 (0 ppm).

**(Z)-5-Benzyl-2-phenyl-3-[2-(2,3,4-tris-methoxymethoxy-phenyl)-vinyl]-thiophene
(37Z)**



C₃₁H₃₂O₆S
M = 532.64 g.mol⁻¹

Yellow oil, **R_f** = 0.62 (pentane/EtOAc 8/2);

¹H NMR (CDCl₃, 300 MHz), δ ppm: 7.55 (m, 2H); 7.40 (m, 2H); 7.32 (m, 4H); 7.22 (m, 2H); 7.10 (d, 1H, H₂₁, ³J = 8.7 Hz); 6.84 (d, 1H, H₂₀, ³J = 8.7 Hz); 6.68 (d, 1H, H₁₅, ³J_{cis} = 12.0 Hz); 6.60 (s, 1H, H₇); 6.50 (d, 1H, H₁₄, ³J_{cis} = 12.0 Hz); 5.24 (s, 2H); 5.19 (s, 2H); 5.17 (s, 2H); 4.02 (s, 2H, H₅); 3.66 (s, 3H) 3.59 (s, 3H); 3.58 (s, 3H).

¹³C NMR (CDCl₃, 75 MHz), δ ppm: 150.68 (1C, C₁₉); 148.99 (1C, C₁₇); 141.77 (1C); 140.09 (1C); 139.95 (1C); 139.55 (1C); 134.47 (1C); 133.77 (1C); 128.88 (2C); 128.48 (2C); 128.41 (2C); 127.38 (1C); 127.31 (1C); 126.39 (2C); 126.15 (2C); 125.30 (1C); 125.15 (1C); 124.47 (1C); 111.38 (1C); 99.30 (1C); 99.85 (1C); 95.27 (1C); 57.61 (1C); 57.31 (1C); 58.28 (1C); 36.14 (1C, C₅).

HRMS (ESI) calculated for C₃₁H₃₂O₆NaS: [M +Na]⁺: m/z 555.1811 Found: m/z. 555.1809 (0 ppm).

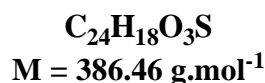
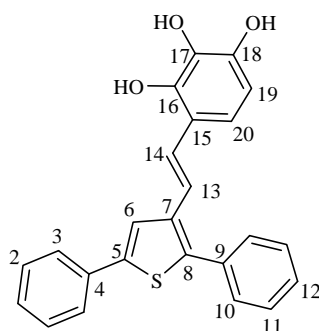
General procedure for the deprotection of MOM group

To a stirred solution of the protected alcohol (0.5 mmol) in methanol (15 ml), 6M HCl (15 ml) was added dropwise. The mixture was stirred for 1h, then diluted with water and extracted with ethyl acetate (3 times). The organic layer was then washed with water, dried over anhydrous MgSO₄, and concentrated under vacuo.

Deprotection of (*E*)-2, 5-Diphenyl-3-[2-(2,3,4-tris-methoxymethoxy-phenyl) vinyl]-thiophene (**33E**)

To a stirred solution of **33E** (0.1 g, 0.2mmol) in methanol (6 ml), 6M HCl (6 ml) was added dropwise. The mixture was stirred for 1h according to general procedure mentioned before. After purification by chromatography on silica gel, using pentane/EtOAc as eluent (60/40), **34E** was obtained as yellow solid in 76% yield.

(*E*)-4-[2-(2, 5-diphenyl-thiophen-3-yl)-vinyl]-benzene-1,2,3-triol (**34E**)



Yellow solid, mp= 192°C, $R_f = 0.30$ (pentane/EtOAc 5/5);

¹H NMR (CDCl₃, 300 MHz), δ ppm: 7.68 (m, 3H); 7.55 (m, 2H); 7.42 (m, 5H); 7.30 (m, 2H); 7.16 (d, 1H, ³J_{trans} = 16.4 Hz); 6.86 (d, 1H, H₂₀, ³J = 8.6 Hz); 6.42 (d, 1H, H₁₉, ³J = 8.6 Hz).

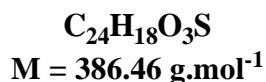
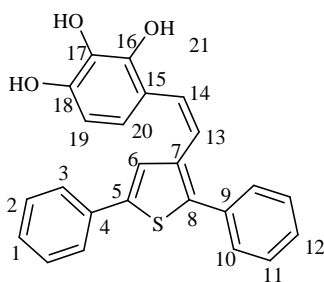
^{13}C NMR (CDCl_3 , 75 MHz), δ ppm: 142.91 (1C); 142.32 (1C); 139.17(1C); 136.47 (1C); 134.15 (1C); 131.71 (1C); 129.53 (2C); 128.90 (2C); 128.66 (2C); 127.69 (2C); 125.75 (2C); 123.74 (2C); 121.91 (1C); 121.78 (2C); 118.48 (1C); 118.05 (2C).

HRMS (ESI) calculated for $\text{C}_{24}\text{H}_{18}\text{O}_3\text{NaS}$: $[\text{M} + \text{Na}]^+$: m/z 409.0868 Found: m/z. 409.0867 (0 ppm).

Deprotection of (Z)-2, 5-Diphenyl-3-[2-(2,3,4-tris-methoxymethoxy-phenyl)-vinyl]-thiophene (33Z)

To a stirred solution of **33Z** (0.2 g, 0.4mmol) in methanol (12 ml), 6M HCl (12 ml) was added dropwise. The mixture was stirred for 1h according to general procedure mentioned before. After purification by chromatography on silica gel, using pentane/EtOAc as eluent (60/40), **34Z** was obtained as yellow solid in 70% yield.

(Z)-4-[2-(2, 5-Diphenyl-thiophen-3-yl)-vinyl]-benzene-1,2,3-triol (34Z)



Yellow solid, mp= 198°C, $R_f = 0.54$ (pentane/EtOAc 5/5);

^1H NMR (CDCl_3 , 300 MHz), δ ppm: 7.58 (m, 2H); 7.44 (m, 5H); 7.32 (m, 2H); 7.28 (m, 1H); 7.04 (s, 1H, H_6); 6.78 (d, 1H, H_{20} , $^3J = 8.5$ Hz); 6.58 (d, 2H, $J = 2.1$ Hz); 6.50 (d, 1H, H_{19} , $^3J = 8.5$ Hz); 5.45 (s, 1H, OH); 5.38 (s, 1H, OH); 5.26 (s, 1H, OH).

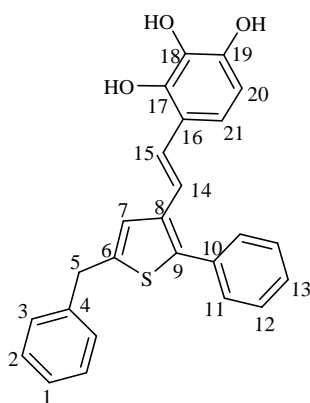
^{13}C NMR (CDCl_3 , 75 MHz), δ ppm: 143.79 (1C, C_{18}); 142.05 (1C, C_{16}); 141.05 (1C); 134.35 (1C); 133.87 (1C); 131.74 (1C); 129.05 (2C); 128.80 (2C); 128.58 (2C); 127.78 (2C); 127.53 (2C); 125.51 (2C); 124.74 (2C); 124.44 (1C); 124.36 (1C); 120.93 (1C); 117.29 (1C).

HRMS (ESI) calculated for $\text{C}_{24}\text{H}_{18}\text{O}_3\text{NaS}$: $[\text{M} + \text{Na}]^+$: m/z 409.0868 Found: m/z . 409.0869 (0 ppm).

Deprotection of (*E*)-5-Benzyl-2-phenyl-3-[2-(2,3,4-tris-methoxymethoxy-phenyl)-vinyl]-thiophene (**37E**)

To a stirred solution of **37E** (0.2 g, 0.37 mmol) in methanol (12 ml), 6M HCl (12 ml) was added dropwise. The mixture was stirred for 1h according to general procedure mentioned before. After purification by chromatography on silica gel, using pentane/EtOAc as eluent (60/40), **38E** was obtained as yellow oil in 66% yield.

(*E*) 4-[2-(5-Benzyl-2-phenyl-thiophen-3-yl)-vinyl]-benzene-1,2,3-triol (**38E**)



$\text{C}_{25}\text{H}_{20}\text{O}_3\text{S}$
 $M = 400.48 \text{ g}\cdot\text{mol}^{-1}$

Yellow oil, $R_f = 0.31$ (pentane/EtOAc 5/5);

^1H NMR (CDCl₃, 300 MHz), δ ppm: 7.48 (m, 2H); 7.38 (m, 2H); 7.32 (m, 4H); 7.22 (m, 1H); 7.14 (m, 2H); 6.68 (d, 1H, H₂₁, $^3J = 8.5$ Hz); 6.56 (d, 1H, $^3J_{\text{cis}} = 11.8$ Hz); 6.50 (s, 1H, H₇); 6.48 (d, 1H, H₂₀, $^3J = 8.5$ Hz); 5.45 (s, 1H, OH); 5.35 (s, 1H, OH); 5.17 (s, 1H, OH); 3.97 (s, 2H, H₅).

^{13}C NMR (CDCl₃, 75 MHz), δ ppm: 143.90 (1C, C₁₉); 142.50 (1C, C₁₇); 141.00 (1C); 139.74 (1C); 134.13 (1C); 132.93 (1C); 131.79 (1C); 129.07 (2C); 128.49 (2C); 128.45 (2C); 127.56 (1C); 126.52 (2C); 126.49 (2C); 125.06 (2C); 124.50 (2C); 120.85 (1C); 117.19 (1C); 36.11 (1C, C₅).

HRMS (ESI) calculated for C₂₅H₂₀O₃NaS: [M +Na]⁺: m/z 423.1025 Found: m/z. 423.1027 (0 ppm).

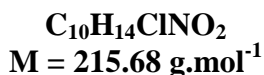
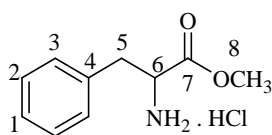
Part three: Oxazole derivatives

General procedure of esterification reaction using SOCl₂

To a solution of the amino acid (1 equiv) in methanol, a solution of thionyl chloride (1.5 equiv) in anhydrous dichloromethane was added dropwise under nitrogen atmosphere at room temperature. The reaction mixture was then stirred at 40°C for 16 h. After this time, the mixture was cooled to room temperature and the solvent was removed under vacuo.

Synthesis of 2-amino-3-phenyl propionic acid methyl ester hydrochloride (**40**)

To a solution of L-phenylalanine **39** (1.5 g, 1 equiv) in MeOH (40 ml), a solution of thionyl chloride (1 ml, 1.5 equiv) in anhydrous CH₂Cl₂ (3 ml) was added drop wise according to the general procedure mentioned above. The product **40** was obtained as a white solid without any purification in 92% yield.



White solid, mp = 164°C, R_f = 0.28 (CH₂Cl₂/ 4% MeOH).

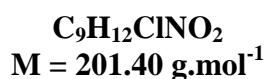
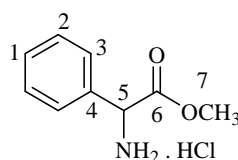
¹H NMR (DMSO, 300 MHz), δ ppm: 8.75 (s, 2H, NH₂); 7.30 (m, 5H); 4.23 (t, 1H, H₆, ³J = 6.8 Hz); 3.65 (s, 3H, H₈); 3.16 (m, 2H, H₅).

¹³C NMR (DMSO, 75 MHz), δ ppm: 169.18 (1C, C₇); 134.68 (1C, C₄); 129.28 (2C); 128.45 (2C); 127.11 (1C, C₁); 53.17 (1C, C₆); 52.38 (1C, C₈); 35.69 (1C, C₅).

HRMS (ESI) calculated for C₁₀H₁₄NO₂Na: [M +Na]⁺ : m/z 202.0838, Found: m/z. 202.0824 (7 ppm).

Synthesis of 1-amino-2-phenyl acetic acid methyl ester hydrochloride (50)

To a solution of phenyl glycine **49** (1g, 1 equiv) in MeOH (30 ml), a solution of thionyl chloride (0.72 ml, 1.5 equiv) in anhydrous CH₂Cl₂ (2.6 ml) was added drop wise according to the general procedure mentioned above. The product **50** was obtained as a white solid without any purification in 90% yield.



White solid, mp = 245°C, R_f = 0.31 (CH₂Cl₂/ 4% MeOH).

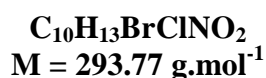
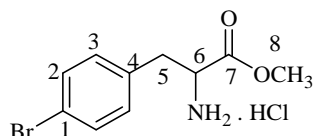
¹H NMR (DMSO, 300 MHz), δ ppm: 9.27 (s, 2H, NH₂); 7.45 (m, 5H); 5.23 (s, 1H, H₅); 3.69 (s, 3H, H₇).

¹³C NMR (DMSO, 75 MHz), δ ppm: 168.87 (1C, C₆); 132.50 (1C); 129.37 (1C); 128.85 (2C); 128.21 (2C); 55.22 (1C, C₅); 53.01 (1C, C₇).

HRMS (ESI) calculated for C₉H₁₁NO₂Na: [M +Na]⁺ : m/z 188.0682, Found: m/z. 188.0684 (1 ppm).

Synthesis of 2-amino-3-(4-bromo phenyl)-propionic acid methyl ester hydrochloride (**46**)

To a solution of 4-bromo phenylalanine **45** (1 g, 1 equiv) in MeOH (32 ml), a solution of thionyl chloride (0.45 ml, 1.5 equiv) in anhydrous CH₂Cl₂ (2.2 ml) was added drop wise according to the general procedure mentioned above. The product **46** was obtained as a white solid without any purification in 88% yield.



White solid, mp = 200°C, R_f = 0.30 (CH₂Cl₂/ 4% MeOH).

¹H NMR (DMSO, 300 MHz), δ ppm: 8.78 (s, 2H, NH₂); 7.52 (d, 2H, ³J = 8.1 Hz); 7.22 (d, 2H, ³J = 8.1 Hz); 4.25 (s, 1H, H₆); 3.67 (s, 3H, H₈); 3.16 (m, 2H, H₅).

¹³C NMR (DMSO, 75 MHz), δ ppm: 169.65 (1C, C₇); 134.69 (1C, C₄); 132.23 (2C); 131.93 (2C); 121.06 (1C, C₁); 53.44 (1C, C₆); 53.14 (1C, C₈); 35.50 (1C, C₅).

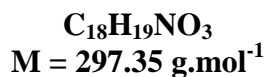
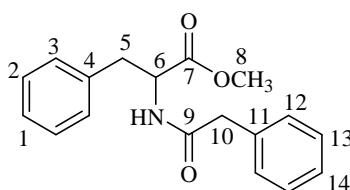
HRMS (ESI) calculated for C₁₀H₁₂NO₂⁷⁹BrNa: [M +Na]⁺ : m/z 279.9943, Found: m/z. 279.9939 (2 ppm).

General procedure for the preparation of amide from primary amine and phenyl acetyl chloride

To a solution of amine (1 equiv) and sodium bicarbonate (5 equiv) in acetonitrile, a solution of phenyl acetyl chloride (1.26 equiv) in acetonitrile was added drop wise. The reaction mixture was kept on stirring over night at room temperature. After that, the reaction mixture was quenched with water and extracted directly. The organic layer was washed with brine, and the combined aqueous phase was extracted twice with ethyl acetate, then the combined organic phase was dried over magnesium sulfate and concentrated under vacuo.

Synthesis of 3-phenyl-2-phenylacetyl-amino-propionic acid methyl ester (**42a**)

To a solution of amine ester **40** (1.2 g, 1 equiv) and sodium bicarbonate (2.34 g, 5 equiv) in acetonitrile (16 ml), a solution of phenyl acetyl chloride **41a** (1.1 g, 1.26 equiv) in acetonitrile (4 ml) was added drop wise, according to the general procedure. After evaporation of the solvent, the amide ester **42a** was obtained without any purification as a white solid in 90% yield.



White solid, mp = 89°C, R_f = 0.62 (CH₂Cl₂/ 4% MeOH).

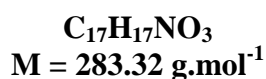
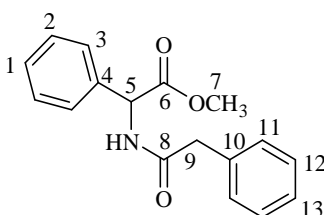
¹H NMR (CDCl₃, 300 MHz), δ ppm: 7.30 (m, 3H); 7.20 (m, 5H); 6.90 (m, 2H); 5.84 (d, 1H, NH, ³J = 7.9 Hz); 4.86 (dt, 1H, H₆, ³J = 7.9 Hz, ³J = 5.8 Hz); 3.70 (s, 3H, H₈); 3.55 (s, 2H, H₁₀); 3.04 (m, 2H, H₅).

¹³C NMR (CDCl₃, 75 MHz), δ ppm: 170.80 (1C, C₇); 170.56 (1C, C₉); 136.55 (1C, C₁₁); 134.38 (1C, C₄); 129.41 (2C); 129.14 (2C); 129.01 (2C); 128.55 (2C); 127.40 (1C, C₁₄); 127.05 (1C, C₁); 53.01 (1C, C₆); 52.33 (1C, C₈); 43.63 (1C, C₁₀); 37.64 (1C, C₅).

HRMS (ESI) calculated for C₁₈H₁₉NO₃Na: [M + Na]⁺ : m/z 320.1257, Found: m/z. 320.1257 (0 ppm).

Synthesis of phenyl-phenylacetyl-amino-propionic acid methyl ester (**51a**)

To a solution of amine ester **50** (0.9 g, 1 equiv) and sodium bicarbonate (1.88 g, 5 equiv) in acetonitrile (10 ml), a solution of phenyl acetyl chloride **41a** (0.86 g, 1.26 equiv) in acetonitrile (2 ml) was added drop wise, according to the general procedure. After evaporation of the solvent, the amide ester **51a** was obtained without any purification as a white solid in 93% yield.



White solid, mp = 111°C, $R_f = 0.59$ (CH_2Cl_2 / 4% MeOH).

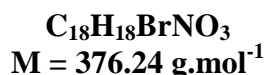
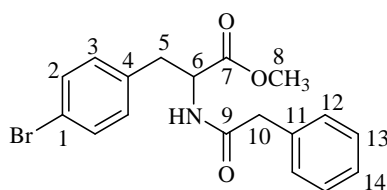
$^1\text{H NMR}$ (CDCl_3 , 300 MHz), δ ppm: 7.30 (m, 10H); 6.48 (d, 1H, NH, $^3J = 6.4$ Hz); 5.55 (d, 1H, H_5 , $^3J = 6.4$ Hz); 3.69 (s, 3H, H_7); 3.61 (s, 2H, H_9).

$^{13}\text{C NMR}$ (CDCl_3 , 75 MHz), δ ppm: 171.20 (1C, C_6); 170.26 (1C, C_8); 136.30 (1C, C_{10}); 134.36 (1C, C_4); 129.34 (2C); 128.96 (2C); 128.90 (2C); 128.48 (1C); 127.40 (1C); 127.08 (2C); 56.40 (1C, C_5); 52.76 (1C, C_7); 43.42 (1C, C_9).

HRMS (ESI) calculated for $\text{C}_{17}\text{H}_{17}\text{NO}_3\text{Na}$: $[\text{M} + \text{Na}]^+$: m/z 306.1100, Found: m/z. 306.1102 (0 ppm).

Synthesis of 3-(4-bromo-phenyl)-2-phenylacetyl-amino-propionic acid methyl ester (**47**)

To a solution of amine ester **46** (0.8 g, 1 equiv) and sodium bicarbonate (1.14 g, 5 equiv) in acetonitrile (10 ml), a solution of phenyl acetyl chloride **41a** (0.52 g, 1.26 equiv) in acetonitrile (1.6 ml) was added drop wise, according to the general procedure. After purification by chromatography on silica gel, using CH_2Cl_2 as the only eluent, the amide ester **47** was obtained as a white solid in 79% yield.



White solid, mp = 140°C, R_f = 0.58 (CH₂Cl₂/ 4% MeOH).

¹H NMR (CDCl₃, 300 MHz), δ ppm: 7.32 (m, 5H); 7.22 (m, 2H); 6.75 (dt, 2H, ³J= 8.3 Hz, ⁴J= 2.3 Hz); 5.85 (d, 1H, NH, ³J= 7.5 Hz); 4.86 (dt, 1H, H₆, ³J_{NH-H}= 7.5 Hz, ³J_{H-H}= 5.7 Hz); 3.72 (s, 3H, H₈); 3.56 (s, 2H, H₁₀); 3.03 (m, 2H, H₅).

¹³C NMR (CDCl₃, 75 MHz), δ ppm: 171.52 (1C, C₇); 170.39 (1C, C₉); 134.54 (1C, C₁₁); 134.33 (1C, C₄); 131.57 (2C); 130.79 (2C); 129.28 (2C); 129.02 (2C); 127.44 (1C); 121.03 (1C, C₁); 52.68 (1C, C₆); 52.40 (1C, C₈); 43.66 (1C, C₁₀); 36.99 (1C, C₅).

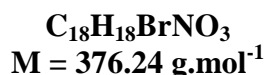
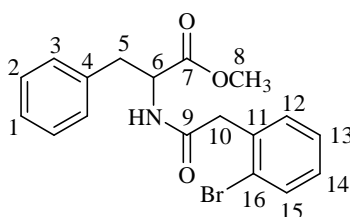
HRMS (ESI) calculated for C₁₈H₁₈NO₃⁷⁹BrNa: [M +Na]⁺ : m/z 398.0362, Found: m/z. 398.0363 (0 ppm).

General procedure for the preparation of amide from primary amine and bromo-phenyl acetic acid

To a solution of amine (1 equiv) and sodium bicarbonate (5 equiv) in acetonitrile, a solution of bromo-phenyl acetic acid (1.26 equiv) in acetonitrile was added, followed by addition of DCC. The reaction mixture was kept on stirring over night at room temperature. After that, the reaction mixture was quenched with water and extracted directly. The organic layer was washed with brine, and the combined aqueous phase was extracted twice with ethyl acetate, then the combined organic phase was dried over MgSO₄ and concentrated under vacuo.

Synthesis of 2-[2-(2-bromo-phenyl)-acetylamino]-3-phenyl-propionic acid methyl ester (42b)

To a solution of amine ester **40** (1.2 g, 1 equiv) and sodium bicarbonate (2.34 g, 5 equiv) in acetonitrile (16 ml), a solution of 2-bromo-phenyl acetic acid **41b** (1.51 g, 1.26 equiv) in acetonitrile (6 ml) was added, followed by addition of DCC (1.45g, 1.26 equiv) according to the general procedure. After purification by chromatography on silica gel, using CH₂Cl₂ as the only eluent, the amide ester **42b** was obtained as a white solid in 82% yield.



White solid, mp = 123°C, R_f = 0.63 (CH₂Cl₂/ 4% MeOH).

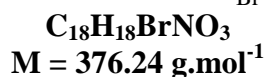
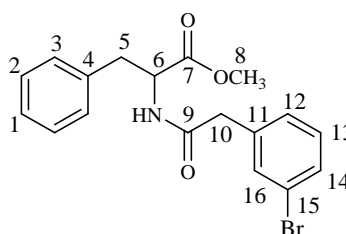
¹H NMR (CDCl₃, 300 MHz), δ ppm: 7.58 (d, 1H, H₁₅, ³J = 7.9 Hz); 7.28 (m, 2H); 7.20 (m, 4H); 6.97 (m, 2H); 5.92 (d, 1H, NH, ³J = 7.8 Hz); 4.88 (dt, 1H, H₆, ³J_{NH-H} = 7.8 Hz, ³J_{H-H} = 5.8 Hz); 3.73 (s, 2H, H₁₀); 3.71 (s, 3H, H₈); 3.08 (m, 2H, H₅).

¹³C NMR (CDCl₃, 75 MHz), δ ppm: 171.68 (1C, C₇); 168.99 (1C, C₉); 135.53 (1C, C₁₁); 134.42 (1C, C₄); 133.07 (1C); 131.59 (1C); 129.12 (3C); 128.51 (2C); 127.93 (1C); 127.01 (1C); 124.93 (1C, C₁₆); 53.05 (1C, C₆); 52.25 (1C, C₈); 43.75 (1C, C₁₀); 37.69 (1C, C₅).

HRMS (ESI) calculated for C₁₈H₁₈NO₃⁷⁹BrNa: [M +Na]⁺ : m/z 398.0362, Found: m/z. 398.0360 (1ppm).

Synthesis of 2-[2-(3-bromo phenyl)-acetylamino]-3-phenyl-propionic acid methyl ester (42c)

To a solution of amine ester **40** (1.3 g, 1 equiv) and sodium bicarbonate (2.54 g, 5 equiv) in acetonitrile (20 ml), a solution of 3-bromo-phenyl acetic acid **41c** (1.63 g, 1.26 equiv) in acetonitrile (8 ml) was added, followed by addition of DCC (1.57 g, 1.26 equiv) according to the general procedure. After purification by chromatography on silica gel, using CH₂Cl₂ as the only eluent, the amide ester **42c** was obtained as a white solid in 78% yield.



White solid, mp = 105°C, R_f = 0.62 (CH₂Cl₂/ 4% MeOH).

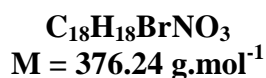
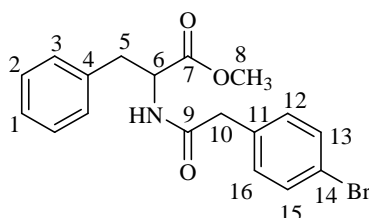
¹H NMR (CDCl₃, 300 MHz), δ ppm: 7.45 (m, 2H); 7.20 (m, 5H); 6.96 (m, 2H); 5.95 (d, 1H, NH, ³J = 7.5 Hz); 4.88 (dt, 1H, H₆, ³J_{NH-H} = 7.5 Hz, ³J_{H-H} = 5.8 Hz); 3.76 (s, 3H, H₈); 3.52 (s, 2H, H₁₀); 3.10 (m, 2H, H₅).

¹³C NMR (CDCl₃, 75 MHz), δ ppm: 171.70 (1C, C₇); 169.49 (1C, C₉); 136.62 (1C, C₁₁); 135.40 (1C, C₄); 132.29 (1C); 130.43 (1C); 130.34 (1C); 129.06 (2C); 128.54 (2C); 127.92 (1C); 127.12 (1C); 122.80 (1C, C₁₅); 52.99 (1C, C₆); 52.34 (1C, C₈); 42.99 (1C, C₁₀); 37.52 (1C, C₅).

HRMS (ESI) calculated for C₁₈H₁₈NO₃⁷⁹BrNa: [M +Na]⁺ : m/z 398.0362, Found: m/z. 398.0363 (0 ppm).

Synthesis of 2-[2-(4-bromo-phenyl)-acetylamino]-3-phenyl propionic acid methyl ester (42d)

To a solution of amine ester **40** (1 g, 1 equiv) and sodium bicarbonate (1.95 g, 5 equiv) in acetonitrile (12 ml), a solution of 4-bromo-phenyl-acetic acid **41d** (1.26 g, 1.26 equiv) in acetonitrile (5 ml) was added, followed by addition of DCC (1.57 g, 1.26 equiv) according to the general procedure. After purification by chromatography on silica gel, using CH_2Cl_2 as the only eluent, the amide ester **42d** was obtained as a white solid in 80% yield.



White solid, mp = 90°C, $R_f = 0.62$ (CH_2Cl_2 / 4% MeOH).

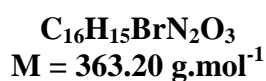
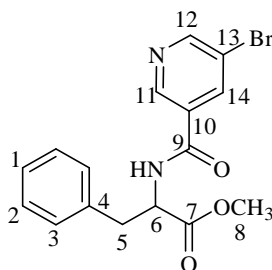
^1H NMR (CDCl_3 , 300 MHz), δ ppm: 7.44 (m, 2H); 7.22 (m, 3H); 7.06 (m, 2H); 6.89 (m, 2H); 5.78 (d, 1H, NH, $^3J = 7.2$ Hz); 4.83 (dt, 1H, H_6 , $^3J_{\text{NH-H}} = 7.2$ Hz, $^3J_{\text{H-H}} = 5.8$ Hz); 3.72 (s, 3H, H_8); 3.48 (s, 2H, H_{10}); 3.04 (m, 2H, H_5).

^{13}C NMR (CDCl_3 , 75 MHz), δ ppm: 171.75 (1C, C_7); 169.69 (1C, C_9); 135.38 (1C, C_{11}); 133.37 (1C, C_4); 131.98 (2C); 130.98 (2C); 129.04 (2C); 128.56 (2C); 127.11 (1C); 121.36 (1C, C_{14}); 52.89 (1C, C_6); 52.35 (1C, C_8); 42.88 (1C, C_{10}); 37.52 (1C, C_5).

HRMS (ESI) calculated for $\text{C}_{18}\text{H}_{18}\text{NO}_3^{79}\text{BrNa}$: $[\text{M} + \text{Na}]^+$: m/z 398.0362, Found: m/z. 398.0362 (0 ppm).

Synthesis of 2-[5-bromo pyridine-3-carbonyl]-amino]-3-phenyl propionic acid methyl ester (42e)

To a solution of amine ester **40** (0.5 g, 1 equiv) and sodium bicarbonate (0.98 g, 5 equiv) in acetonitrile (7 ml), a solution of 5-bromopyridine-3-carboxylic acid **41e** (0.6 g, 1.26 equiv) in acetonitrile (2.5 ml) was added, followed by addition of DCC (0.6 g, 1.26 equiv) according to the general procedure. After purification by chromatography on silica gel, using CH₂Cl₂ as the only eluent, the amide ester **42e** was obtained as a white solid in 71% yield.



White solid, mp = 100°C, R_f = 0.58 (CH₂Cl₂/ 4% MeOH).

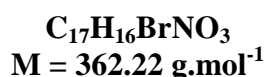
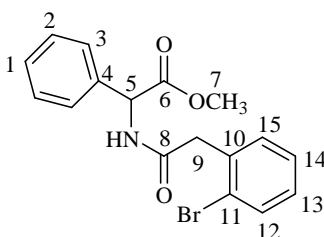
¹H NMR (CDCl₃, 300 MHz), δ ppm: 8.76 (m, 2H); 8.18 (m, 1H); 7.28 (m, 3H); 7.12 (m, 2H); 6.72 (d, 1H, NH, ³J = 7.6 Hz); 5.05 (dt, 1H, H₆, ³J_{NH-H} = 7.6 Hz, ³J_{H-H} = 5.8 Hz); 3.78 (s, 3H, H₈); 3.25 (m, 2H, H₅).

¹³C NMR (CDCl₃, 75 MHz), δ ppm: 171.66 (1C, C₇); 163.64 (1C, C₉); 153.54 (1C, C₁₁); 145.85 (1C, C₁₂); 137.76 (1C); 135.41 (1C); 130.94 (1C); 129.17 (2C); 128.73 (2C); 127.39 (1C); 120.91 (1C, C₁₃); 53.63 (1C, C₆); 52.61 (1C, C₈); 37.70 (1C, C₅).

HRMS (ESI) calculated for C₁₆H₁₇N₂O₃⁷⁹BrNa: [M +Na]⁺ : m/z 385.0158. Found: m/z. 385.0159 (0 ppm).

Synthesis of [2-(2-bromo phenyl)-acetylamino]-phenyl acetic acid methyl ester (51b)

To a solution of amine ester **50** (1g, 1 equiv) and sodium bicarbonate (2.1 g, 5 equiv) in acetonitrile (12 ml), a solution of 2-bromo-phenyl-acetic acid **41b** (1.35 g, 1.26 equiv) in acetonitrile (5 ml) was added, followed by addition of DCC (1.21 g, 1.26 equiv) according to the general procedure. After purification by chromatography on silica gel, using CH₂Cl₂ as the only eluent, the amide ester **51b** was obtained as a white solid in 75% yield.



White solid, mp = 152°C, R_f = 0.60 (CH₂Cl₂/ 4% MeOH).

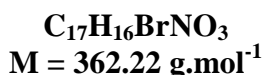
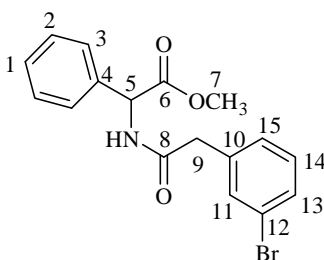
¹H NMR (CDCl₃, 300 MHz), δ ppm: 7.60 (d, 1H, H₁₂, ³J= 7.9 Hz); 7.32 (m, 7H); 7.18 (td, 1H, ³J= 7.8 Hz, ⁴J= 2.0 Hz); 6.56 (d, 1H, NH, ³J= 6.3 Hz); 5.58 (d, 1H, H₅, ³J_{NH-H}= 6.3 Hz); 3.78 (s, 2H, H₉); 3.78 (s, 3H, H₇).

¹³C NMR (CDCl₃, 75 MHz), δ ppm: 171.11 (1C, C₆); 168.83 (1C, C₈); 136.30 (1C, C₁₀); 134.44 (1C, C₄); 133.06 (1C); 131.63 (2C); 129.15 (1C); 128.87 (2C); 128.46 (1C); 127.95 (1C); 127.14 (1C); 124.88 (1C, C₁₁); 56.50 (1C, C₅); 52.76 (1C, C₇); 43.66 (1C, C₉).

HRMS (ESI) calculated for C₁₇H₁₆NO₃⁷⁹BrNa: [M +Na]⁺ : m/z 384.0205, Found: m/z. 384.0208 (1 ppm).

Synthesis of [2-(3-bromo-phenyl)-acetylamino]-phenyl acetic acid methyl ester (51c)

To a solution of amine ester **50** (1g, 1 equiv) and sodium bicarbonate (2.1 g, 5 equiv) in acetonitrile (12 ml), a solution of 3-bromo phenyl acetic acid **41c** (1.35 g, 1.26 equiv) in acetonitrile (5 ml) was added, followed by addition of DCC (1.21 g, 1.26 equiv) according to the general procedure. After purification by chromatography on silica gel, using CH₂Cl₂ as the only eluent, the amide ester **51c** was obtained as a white solid in 76% yield.



White solid, mp = 128°C, R_f = 0.61(CH₂Cl₂/ 4% MeOH).

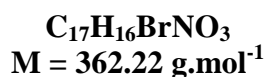
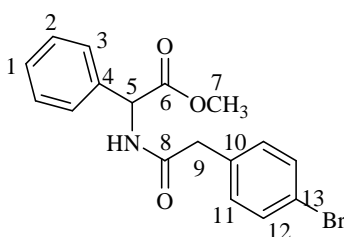
¹H NMR (CDCl₃, 300 MHz), δ ppm: 7.42 (m, 2H); 7.32 (m, 5H); 7.22 (m, 2H); 6.56 (d, 1H, NH, ³J = 6.6 Hz); 5.56 (d, 1H, H₅, ³J_{NH-H} = 6.6 Hz); 3.70 (s, 3H, H₇); 3.55 (s, 2H, H₉).

¹³C NMR (CDCl₃, 75 MHz), δ ppm: 171.13 (1C, C₆); 169.35 (1C, C₈); 136.62 (1C, C₁₀); 136.18 (1C, C₄); 132.28 (1C); 130.41 (1C); 130.29 (1C); 128.95 (2C); 128.56 (1C); 127.88 (1C); 127.13 (2C); 122.76 (1C, C₁₂); 56.52 (1C, C₅); 52.79 (1C, C₇); 42.68 (1C, C₉).

HRMS (ESI) calculated for C₁₇H₁₆NO₃⁷⁹BrNa: [M +Na]⁺ : m/z 384.0205, Found: m/z. 384.0206 (0 ppm).

Synthesis of [2-(4-bromo-phenyl)-acetylamino]-phenyl acetic acid methyl ester (51d)

To a solution of amine ester **50** (1.1 g, 1 equiv) and sodium bicarbonate (2.3 g, 5 equiv) in acetonitrile (14 ml), a solution of 4-bromo phenyl acetic acid **41d** (1.48 g, 1.26 equiv) in acetonitrile (6 ml) was added, followed by addition of DCC (1.42 g, 1.26 equiv) according to the general procedure. After purification by chromatography on silica gel, using CH₂Cl₂ as the only eluent, the amide ester **51d** was obtained as a white solid in 79% yield.



White solid, mp = 150°C, R_f = 0.61 (CH₂Cl₂/ 4% MeOH).

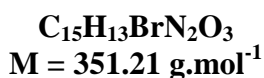
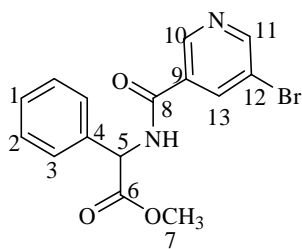
¹H NMR (CDCl₃, 300 MHz), δ ppm: 7.45 (m, 2H); 7.30 (m, 5H); 7.14 (m, 2H); 6.50 (d, 1H, NH, ³J = 6.6 Hz); 5.55 (d, 1H, H₅, ³J_{NH-H} = 6.6 Hz); 3.70 (s, 3H, H₇); 3.54 (s, 2H, H₉).

¹³C NMR (CDCl₃, 75 MHz), δ ppm: 171.19 (1C, C₆); 169.51 (1C, C₈); 136.20 (1C, C₁₀); 133.36 (1C, C₄); 131.96 (2C); 130.98 (2C); 128.96 (2C); 128.58 (1C); 127.13 (2C); 121.37 (1C, C₁₃); 56.48 (1C, C₅); 52.80 (1C, C₇); 42.63 (1C, C₉).

HRMS (ESI) calculated for C₁₇H₁₆NO₃⁷⁹BrNa: [M +Na]⁺ : m/z 384.0205, Found: m/z. 384.0207 (0 ppm).

Synthesis of [(5-bromo pyridine-3-carbonyl)-amino]-phenyl acetic acid methyl ester (51e)

To a solution of amine ester **50** (0.5 g, 1 equiv) and sodium bicarbonate (1 g, 5 equiv) in acetonitrile (7 ml), a solution of 5-bromopyridine-3- carboxylic acid **41e** (0.63 g, 1.26 equiv) in acetonitrile (3 ml) was added, followed by addition of DCC (0.64 g, 1.26 equiv) according to the general procedure. After purification by chromatography on silica gel, using CH₂Cl₂ as the only eluent, the amide ester **51e** was obtained as a white solid in 70% yield.



White solid, mp = 153°C, R_f = 0.57 (CH₂Cl₂/ 4% MeOH).

¹H NMR (CDCl₃, 300 MHz), δ ppm: 8.88 (d, 1H, ⁴J = 2.0 Hz); 8.70 (d, 1H, ⁴J = 2.2 Hz); 8.24 (d, 1H, ⁴J = 2.0 Hz); 7.56 (d, 1H, NH, ³J = 6.8 Hz); 7.35 (m, 5H); 5.74 (d, 1H, H₅, ³J = 6.8 Hz); 3.74 (s, 3H, H₇).

¹³C NMR (CDCl₃, 75 MHz), δ ppm: 171.04 (1C, C₆); 163.48 (1C, C₈); 153.41 (1C, C₁₀); 146.14 (1C, C₁₁); 137.81 (1C); 135.70 (1C); 130.62 (1C); 129.00 (2C); 128.75 (1C); 127.32 (2C); 120.74 (1C, C₁₂); 56.90 (1C, C₅); 52.93 (1C, C₇).

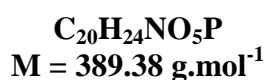
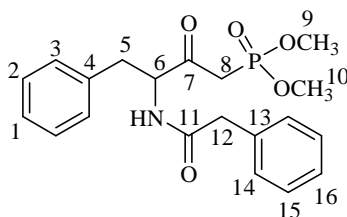
HRMS (ESI) calculated for C₁₆H₁₇N₂O₃⁷⁹BrNa: [M +Na]⁺: m/z 371.0001, Found: m/z. 371.0003 (0 ppm).

General procedure for the preparation of phosphonates

In a dry tri-necked flask, dimethyl methyl phosphonate (3.6 equiv) was weighted; the flask was then placed under nitrogen, followed by the addition of THF. After that, the flask was cooled till -65°C , and n-BuLi (3.6 equiv) was added drop wise, then the reaction mixture was stirred for 30 min at -65°C to -60°C . After this time, the flask cooled down to -75°C , and the solution of amide ester (1 equiv) in THF was added drop wise. The reaction mixture was then kept on stirring till the temperature increased to -10°C , where the reaction was controlled by TLC at this temperature, after completion of the reaction, the reaction mixture was quenched with citric acid (2 equiv) in water, extracted twice with CH_2Cl_2 , and the combined organic layer dried over MgSO_4 , and concentrated under vacuo.

Synthesis of (2-oxo-4-phenyl-3-phenylacetyl-amino-butyl)-phosphonic acid dimethyl ester (**44a**)

To a solution of dimethyl methyl phosphonate **43** (3 g, 3.6 equiv) and n-BuLi (15.15 ml, 3.6 equiv) in THF (110 ml), a solution of amide ester **42a** (2 g, 1 equiv) in THF (25 ml) was added dropwise according to the general procedure mentioned above. The color starts to appear as pink and turned directly into deep orange during the addition of amide ester **42a**, then it turned into bright yellow when the temperature reaches around -55°C . After purification by chromatography on silica gel, using CH_2Cl_2 as the only eluent, the desired phosphonate **44a** was obtained as a yellow solid in 72% yield.



Yellow solid, mp = < 52°C, R_f = 0.33 (CH₂Cl₂/ 4% MeOH)

¹H NMR (CDCl₃, 300 MHz), δ ppm: 7.28 (m, 3H); 7.16 (m, 5H); 7.00 (m, 2H); 6.52 (d, 1H, NH, ³J = 7.9 Hz); 4.82 (dt, 1H, H₆, ³J_{NH-H} = 7.9 Hz, ³J_{H-H} = 5.6 Hz); 3.72 (d, 3H, H₉, ³J_{H-P} = 9.2 Hz); 3.68 (d, 3H, H₁₀, ³J_{H-P} = 9.2 Hz); 3.50 (s, 2H, H₁₂); 3.18 (m, 2H, H₈); 2.96 (m, 2H, H₅).

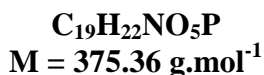
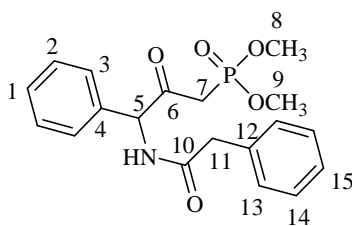
¹³C NMR (CDCl₃, 75 MHz), δ ppm: 200.25 (d, 1C, C₇, ²J_{C-P} = 6.5 Hz); 170.74 (1C, C₁₁); 136.01 (1C, C₁₃); 134.25 (1C, C₄); 129.16 (2C); 129.10 (2C); 128.77 (2C); 128.44 (2C); 127.14 (1C), 126.75 (1C); 59.01 (d, 1C, C₆, ³J_{C-P} = 2.1 Hz); 53.09 (d, 1C, C₉, ²J_{C-P} = 6.5 Hz); 52.97 (d, 1C, C₁₀, ²J_{C-P} = 6.5 Hz); 43.32 (1C, C₁₂); 38.48 (d, 1C, C₈, ¹J_{C-P} = 129.2 Hz); 36.03 (1C, C₅).

³¹P NMR (CDCl₃, 121 MHz), (ppm): 22.09

HRMS (ESI) calculated for C₂₀H₂₄NO₅NaP: [M +Na]⁺ : m/z 412.1284, Found: m/z. 412.1286 (0 ppm).

Synthesis of (2-oxo-3-phenyl-3-phenylacetyl-amino-butyl)-phosphonic acid dimethyl ester (**52a**)

To a solution of dimethyl methyl phosphonate **43** (3.8 g, 3.6 equiv) and n-BuLi (19 ml, 3.6 equiv) in THF (120 ml), a solution of amide ester **51a** (2.4 g, 1 equiv) in THF (30 ml) was added dropwise according to the general procedure mentioned above. The color turned rapidly into light lemon yellow during the addition of the amide ester **51a**, and remains the same till the end of the reaction. The crude was then dissolved in cyclohexane and heated at 75°C; after a period of 20 to 30 mins and when a white solid starts to precipitate, the flask was placed aside to cool, then decanted to obtain the desired phosphonate **52a** in 85% yield.



White solid, mp = 84°C, R_f = 0.30 (CH₂Cl₂/ 4% MeOH).

¹H NMR (CDCl₃, 300 MHz), δ ppm: 7.32 (m, 6H); 7.22 (m, 4H); 6.82 (d, 1H, NH, ³J = 6.6 Hz); 5.66 (d, 1H, H₅, ³J_{NH-H} = 6.6 Hz); 3.73 (d, 3H, H₈, ³J_{H-P} = 11.3 Hz); 3.66 (d, 3H, H₉, ³J_{H-P} = 11.3 Hz); 3.56 (s, 2H, H₁₁); 3.10 (AB_{sys}, 1H, H₇, J = 14.5 Hz); 3.02 (AB_{sys}, 1H, H₇, J = 14.5 Hz)

¹³C NMR (CDCl₃, 75 MHz), δ ppm: 197.16 (d, 1C, C₆, ²J_{C-P} = 6.4 Hz); 170.13 (1C, C₁₀); 135.28 (1C, C₁₂); 134.39 (1C, C₄); 129.27 (2C); 129.20 (2C); 128.83 (1C); 128.79 (2C); 128.13 (2C), 127.24 (1C); 63.60 (d, 1C, C₅, ³J_{C-P} = 3.3 Hz); 53.26 (d, 1C, C₈, ²J_{C-P} = 6.3 Hz); 52.96 (d, 1C, C₉, ²J_{C-P} = 6.4 Hz); 43.28 (1C, C₁₁); 38.76-37.01 (d, 1C, C₇, ¹J_{C-P} = 132.1 Hz).

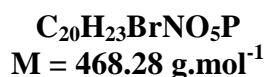
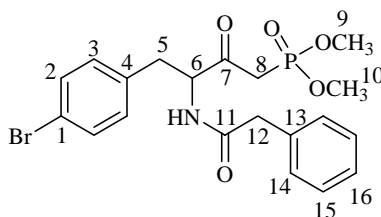
³¹P NMR (CDCl₃, 121 MHz), (ppm): 21.21

HRMS (ESI) calculated for C₁₉H₂₂NO₅NaP: [M +Na]⁺ : m/z 398.1127, Found: m/z. 398.1128 (0 ppm).

Synthesis of [4-(4-bromo-phenyl)-2-oxo-3-phenylacetyl-amino-butyl]-phosphonic acid dimethyl ester (48)

To a solution of dimethyl methyl phosphonate **43** (3.56 g, 3.6 equiv) and n-BuLi (18 ml, 3.6 equiv) in THF (140 ml), a solution of amide ester **47** (3 g, 1 equiv) in THF (16 ml) was added dropwise according to the general procedure. The color turned directly into deep yellow during the addition of amide ester **47**, and remains the same till the end of the reaction. After purification by chromatography on silica gel, using

CH₂Cl₂ as the only eluent, the desired phosphonate **48** was obtained as a white solid in 72% yield.



Yellow solid, mp = 92°C, R_f = 0.32 (CH₂Cl₂/ 4% MeOH).

¹H NMR (CDCl₃, 300 MHz), δ ppm: 7.26 (m, 5H); 7.12 (m, 2H); 6.86 (d, 2H, ³J= 8.3 Hz); 6.52 (d, 1H, NH, ³J= 8.1 Hz); 4.80 (dt, 1H, H₆, ³J_{NH-H}= 8.1 Hz, ³J_{H-H}= 5.5 Hz); 3.73 (d, 3H, H₉, ³J_{H-P}= 9.9 Hz); 3.69 (d, 3H, H₁₀, ³J_{H-P}= 10.1 Hz); 3.51 (s, 2H, H₁₂); 3.16 (m, 2H, H₈); 2.96 (m, 2H, H₅).

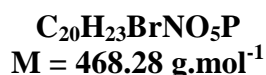
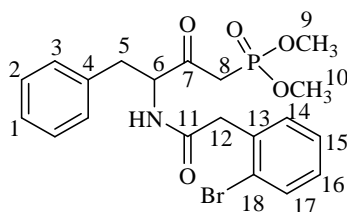
¹³C NMR (CDCl₃, 75 MHz), δ ppm: 200.12 (d, 1C, C₇, ²J_{C-P}= 6.4 Hz); 170.89 (1C, C₁₁); 135.13 (1C, C₁₃); 134.26 (1C, C₄); 131.54 (2C); 130.93 (2C); 129.16 (2C); 128.92 (2C); 127.32 (1C), 120.77 (1C, C₁); 59.56 (d, 1C, C₆, ³J_{C-P}= 1.6 Hz); 53.20 (d, 1C, C₉, ²J_{C-P}= 6.6 Hz); 53.12 (d, 1C, C₁₀, ²J_{C-P}= 6.8 Hz); 43.53 (1C, C₁₂); 39.43-37.73 (d, 1C, C₈, ¹J_{C-P}= 128.5 Hz); 35.43 (1C, C₅).

³¹P NMR (CDCl₃, 121 MHz), (ppm): 21.94

HRMS (ESI) calculated for C₂₀H₂₃NO₅⁷⁹BrNaP: [M +Na]⁺ : m/z 490.0389, Found: m/z. 490.0387 (0 ppm).

**Synthesis of {3-[2-(2-bromo-phenyl)-acetyl-amino]-2-oxo-4-phenyl-butyl}-
phosphonic acid dimethyl ester (44b)}**

To a solution of dimethyl methyl phosphonate **43** (2.96 g, 3.6 equiv) and n-BuLi (15 ml, 3.6 equiv) in THF (114 ml), a solution of amide ester **42b** (2.5 g, 1 equiv) in THF (15 ml) was added dropwise according to the general procedure. The color turned directly into deep yellow during the addition of amide ester **42b**, and remains the same till the end of the reaction. After purification by chromatography on silica gel, using CH₂Cl₂ as the only eluent, the desired phosphonate **44b** was obtained as a white solid in 70% yield.



Yellow solid, mp = < 54°C, R_f = 0.33 (CH₂Cl₂/ 4% MeOH).

¹H NMR (CDCl₃, 300 MHz), δ ppm: 7.54 (dd, 1H, H₁₇, ³J = 7.9 Hz, ⁴J = 1.1 Hz); 7.18 (m, 6H); 7.04 (m, 2H); 6.40 (d, 1H, NH, ³J = 7.6 Hz); 4.82 (dt, 1H, H₆, ³J_{NH-H} = 7.6 Hz, ³J_{H-H} = 5.7 Hz); 3.73 (d, 3H, H₉, ³J_{H-P} = 10.5 Hz); 3.66 (d, 3H, H₁₀, ³J_{H-P} = 10.5 Hz); 3.65 (s, 2H, H₁₂); 3.22 (m, 2H, H₈); 2.98 (m, 2H, H₅).

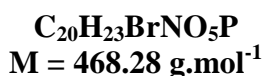
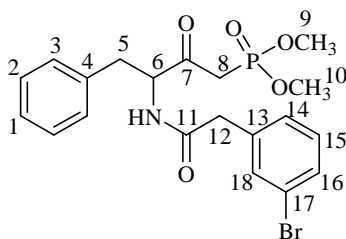
¹³C NMR (CDCl₃, 75 MHz), δ ppm: 200.34 (d, 1C, C₇, ²J_{C-P} = 6.4 Hz); 169.43 (1C, C₁₁); 136.05 (1C, C₁₃); 134.20 (1C, C₄); 132.97 (1C); 131.59 (1C); 129.19 (2C); 129.06 (1C); 128.54 (2C), 127.87 (1C); 126.86 (1C); 124.88 (1C, C₁₈); 59.94 (d, 1C, C₆, ³J_{C-P} = 1.8 Hz); 53.09 (d, 1C, C₉, ²J_{C-P} = 6.6 Hz); 52.96 (d, 1C, C₁₀, ²J_{C-P} = 6.6 Hz); 43.54 (1C, C₁₂); 39.52-37.81 (d, 1C, C₈, ¹J_{C-P} = 129.0 Hz); 36.31 (1C, C₅).

³¹P NMR (CDCl₃, 121 MHz), (ppm): 22.06

HRMS (ESI) calculated for C₂₀H₂₃NO₅⁷⁹BrNaP: [M +Na]⁺ : m/z 490.0389, Found: m/z. 490.0389 (0 ppm).

**Synthesis of {3-[2-(3-bromo-phenyl)-acetylamino]-2-oxo-4-phenyl-butyl}
phosphonic acid dimethyl ester (44c)**

To a solution of dimethyl methyl phosphonate **43** (1.5 g, 3.6 equiv) and n-BuLi (7.6 ml, 3.6 equiv) in THF (58 ml), a solution of amide ester **42c** (1.26 g, 1 equiv) in THF (8 ml) was added drop wise according to the general procedure. The color turned directly into deep yellow during the addition of amide ester **42c**, and remains the same till the end of the reaction. After purification by chromatography on silica gel, using CH₂Cl₂ as the only eluent, the desired phosphonate **44c** was obtained as a white solid in 65% yield.



Yellow solid, mp = < 48°C, R_f = 0.34 (CH₂Cl₂/ 4% MeOH).

¹H NMR (CDCl₃, 300 MHz), δ ppm: 7.34 (m, 2H); 7.18 (m, 3H); 7.08 (m, 2H); 7.00 (m, 2H); 6.80 (d, 1H, NH, ³J = 7.6 Hz); 4.79 (dt, 1H, H₆, ³J_{NH-H} = 7.6 Hz, ³J_{H-H} = 5.6 Hz); 3.71 (d, 3H, H₉, ³J_{H-P} = 10.8 Hz); 3.67 (d, 3H, H₁₀, ³J_{H-P} = 10.8 Hz); 3.43 (s, 2H, H₁₂); 3.20 (m, 2H, H₈); 2.92 (m, 2H, H₅).

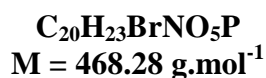
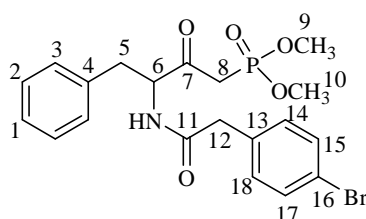
¹³C NMR (CDCl₃, 75 MHz), δ ppm: 200.24 (d, 1C, C₇, ²J_{C-P} = 6.4 Hz); 169.93 (1C, C₁₁); 136.55 (1C, C₁₃); 135.91 (1C, C₄); 132.24 (1C); 130.43 (1C); 130.35 (1C); 129.20 (2C); 128.60 (2C), 127.93 (1C); 127.02 (1C); 122.80 (1C, C₁₇); 59.94 (d, 1C, C₆, ³J_{C-P} = 1.5 Hz); 53.32 (d, 1C, C₉, ²J_{C-P} = 6.5 Hz); 53.15 (d, 1C, C₁₀, ²J_{C-P} = 6.5 Hz); 42.96 (1C, C₁₂); 37.34 (d, 1C, C₈, ¹J_{C-P} = 128.4 Hz); 36.27 (1C, C₅).

³¹P NMR (CDCl₃, 121 MHz), (ppm): 21.86

HRMS (ESI) calculated for C₂₀H₂₃NO₅⁷⁹BrNaP: [M +Na]⁺ : m/z 490.0389, Found: m/z. 490.0383 (1 ppm).

**Synthesis of {3-[2-(4-bromo-phenyl)-acetyl-amino]-2-oxo-4-phenyl-butyl}
phosphonic acid dimethyl ester (44d)**

To a solution of dimethyl methyl phosphonate **43** (2.11 g, 3.6 equiv) and n-BuLi (10.6 ml, 3.6 equiv) in THF (82 ml), a solution of amide ester **42d** (1.78 g, 1 equiv) in THF (10 ml) was added dropwise according to the general procedure. The color turned directly into deep yellow during the addition of amide ester **42d**, and remains the same till the end of the reaction. After purification by chromatography on silica gel, using CH₂Cl₂ as the only eluent, the desired phosphonate **44d** was obtained as a white solid in 68% yield.



Yellow solid, mp = 108°C, R_f = 0.33 (CH₂Cl₂/ 4% MeOH).

¹H NMR (CDCl₃, 300 MHz), δ ppm: 7.40 (m, 2H); 7.22 (m, 3H); 7.02 (m, 4H); 6.46 (d, 1H, NH, ³J = 7.8 Hz); 4.84 (dt, 1H, H₆, ³J_{NH-H} = 7.8 Hz, ³J_{H-H} = 5.7 Hz); 3.72 (d, 3H, H₉, ³J_{H-P} = 10.9 Hz); 3.68 (d, 3H, H₁₀, ³J_{H-P} = 10.9 Hz); 3.44 (s, 2H, H₁₂); 3.22 (m, 2H, H₈); 2.94 (m, 2H, H₅).

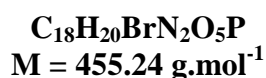
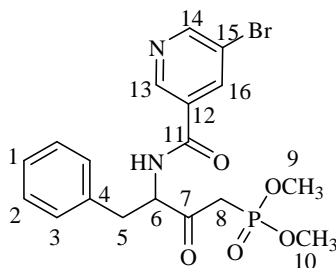
¹³C NMR (CDCl₃, 75 MHz), δ ppm: 200.28 (d, 1C, C₇, ²J_{C-P} = 6.4 Hz); 170.13 (1C, C₁₁); 135.91 (1C, C₁₃); 133.33 (1C, C₄); 131.92 (2C); 130.90 (2C); 129.17 (2C); 128.57 (2C); 126.95 (1C), 121.27 (1C, C₁₆); 59.86 (d, 1C, C₆, ³J_{C-P} = 1.8 Hz); 53.26 (d, 1C, C₉, ²J_{C-P} = 6.6 Hz); 53.03 (d, 1C, C₁₀, ²J_{C-P} = 6.6 Hz); 42.79 (1C, C₁₂); 38.82 (d, 1C, C₈, ¹J_{C-P} = 128.6 Hz); 36.21 (1C, C₅).

³¹P NMR (CDCl₃, 121 MHz), (ppm): 21.94

HRMS (ESI) calculated for C₂₀H₂₃NO₅⁷⁹BrNaP: [M +Na]⁺ : m/z 490.0389, Found: m/z. 490.0387 (0 ppm).

Synthesis of {3-[(5-bromo-pyridine-3-carbonyl)-amino]-2-oxo-4-phenyl-butyl} phosphonic acid dimethyl ester (44e)

To a solution of dimethyl methyl phosphonate **43** (1.08 g, 3.6 equiv) and n-BuLi (5.5 ml, 3.6 equiv) in THF (40 ml), a solution of amide ester **42e** (0.88 g, 1 equiv) in THF (5 ml) was added dropwise according to the general procedure. The color turned directly into deep red during the addition of the amide ester **42e**, and then turned into deep yellow when the temperature reaches -30°C. After purification by chromatography on silica gel, using CH₂Cl₂ as the only eluent, the desired phosphonate **44e** was obtained as a white solid in 60% yield.



Yellow oil, R_f = 0.35 (CH₂Cl₂/ 4% MeOH).

¹H NMR (CDCl₃, 300 MHz), δ ppm: 8.90 (s, 1H); 8.74 (s, 1H); 8.26 (s, 1H); 8.00 (d, 1H, NH, ³J = 8.1 Hz); 7.22 (m, 5H); 5.08 (dt, 1H, H₆, ³J_{NH-H} = 8.1 Hz, ³J_{H-H} = 6.0 Hz); 3.73 (d, 3H, H₉, ³J_{H-P} = 11.3 Hz); 3.70 (d, 3H, H₁₀, ³J_{H-P} = 11.3 Hz); 3.34 (m, 2H, H₈); 3.12 (m, 2H, H₅).

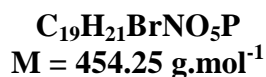
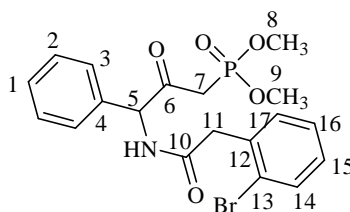
¹³C NMR (CDCl₃, 75 MHz), δ ppm: 198.94 (d, 1C, C₇, ²J_{C-P} = 6.2 Hz); 163.86 (1C, C₁₁); 153.44 (1C, C₁₃); 146.43 (1C, C₁₄); 137.84 (1C); 136.18 (1C); 130.57 (1C); 129.28 (2C); 128.61 (2C), 127.06 (1C); 120.79 (1C, C₁₅); 60.60 (d, 1C, C₆, ³J_{C-P} = 1.8 Hz); 53.48 (d, 1C, C₉, ²J_{C-P} = 6.6 Hz); 53.12 (d, 1C, C₁₀, ²J_{C-P} = 6.6 Hz); 38.88 (d, 1C, C₈, ¹J_{C-P} = 128.8 Hz); 36.29 (1C, C₅).

³¹P NMR (CDCl₃, 121 MHz), (ppm): 22.12

HRMS (ESI) calculated for $C_{18}H_{20}N_2O_5^{79}Br NaP$: $[M + Na]^+$: m/z 477.01854, Found: m/z . 477.0182 (1 ppm).

Synthesis of {3-[2-(2-bromo-phenyl)-acetyl-amino]-2-oxo-3-phenyl-propyl}-phosphonic acid dimethyl ester (52b**)**

To a solution of dimethyl methyl phosphonate **43** (2.4 g, 3.6 equiv) and n-BuLi (12.10 ml, 3.6 equiv) in THF (90 ml), a solution of amide ester **51b** (1.95 g, 1 equiv) in THF (10 ml) was added dropwise according to the general procedure. The color turned directly into deep yellow during the addition of amide ester **51b**, and remains the same till the end of the reaction. After purification by chromatography on silica gel, using CH_2Cl_2 as the only eluent, the desired phosphonate **52b** was obtained as a white solid in 71% yield.



Yellow solid, mp = 107°C, $R_f = 0.31$ (CH_2Cl_2 / 4% MeOH).

1H NMR ($CDCl_3$, 300 MHz), δ ppm: 7.52 (d, 1H, H_{14} , $^3J = 7.6$ Hz); 7.30 (m, 7H); 7.12 (m, 1H); 7.06 (d, 1H, NH, $^3J = 6.5$ Hz); 5.68 (d, 1H, H_5 , $^3J_{NH-H} = 6.5$ Hz); 3.72 (d, 3H, H_8 , $^3J_{H-P} = 10.7$ Hz); 3.66 (d, 3H, H_9 , $^3J_{H-P} = 10.7$ Hz); 3.60 (s, 2H, H_{11}); 3.12 (AB_{sys} , 1H, H_7 , $J = 14.5$ Hz); 3.01 (AB_{sys} , 1H, H_7 , $J = 14.5$ Hz).

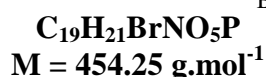
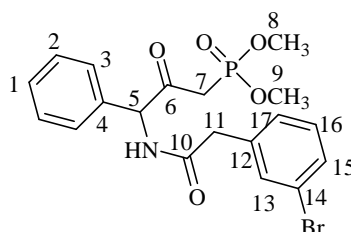
^{13}C NMR ($CDCl_3$, 75 MHz), δ ppm: 197.12 (d, 1C, C_6 , $^2J_{C-P} = 6.4$ Hz); 168.67 (1C, C_{10}); 135.21 (1C, C_{12}); 134.38 (1C, C_4); 132.86 (1C); 131.53 (1C); 129.12 (2C); 128.96 (1C); 128.70 (1C), 128.09 (2C); 127.77 (1C); 124.76 (1C, C_{13}); 63.64 (d, 1C, C_5 , $^3J_{C-P} = 3.3$ Hz); 53.10 (d, 1C, C_8 , $^2J_{C-P} = 6.5$ Hz); 52.98 (d, 1C, C_9 , $^2J_{C-P} = 6.4$ Hz); 43.47 (1C, C_{11}); 37.82 (d, 1C, C_7 , $^1J_{C-P} = 131.8$ Hz).

^{31}P NMR ($CDCl_3$, 121 MHz), (ppm): 21.28

HRMS (ESI) calculated for $C_{19}H_{21}NO_5^{79}BrNaP$: $[M + Na]^+$: m/z 476.0232, Found: m/z . 476.0230 (0 ppm).

Synthesis of {3-[2-(3-bromo-phenyl)-acetylamino]-2-oxo-3-phenyl-propyl}-phosphonic acid dimethyl ester(52c)

To a solution of dimethyl methyl phosphonate **43** (2.34 g, 3.6 equiv) and n-BuLi (11.8 ml, 3.6 equiv) in THF (190 ml), a solution of amide ester **51c** (1.9 g, 1 equiv) in THF (10 ml) was added dropwise according to the general procedure. The color turned directly into deep yellow during the addition of amide ester **51c**, and remains the same till the end of the reaction. After purification by chromatography on silica gel, using CH_2Cl_2 as the only eluent, the desired phosphonate **52c** was obtained as a white solid in 73% yield.



Yellow solid, mp = 99°C, $R_f = 0.30$ (CH_2Cl_2 / 4% MeOH).

1H NMR ($CDCl_3$, 300 MHz), δ ppm: 7.38 (m, 5H); 7.18 (m, 2H); 7.16 (m, 2H); 7.02 (d, 1H, NH, $^3J = 6.4$ Hz); 5.68 (d, 1H, H₅, $^3J_{NH-H} = 6.4$ Hz); 3.73 (d, 3H, H₈, $^3J_{H-P} = 9.2$ Hz); 3.68 (d, 3H, H₉, $^3J_{H-P} = 9.2$ Hz); 3.57 (s, 2H, H₁₁); 3.11 (AB_{sys}, 1H, H₇, J= 14.5 Hz); 3.03 (AB_{sys}, 1H, H₇, J= 14.5 Hz).

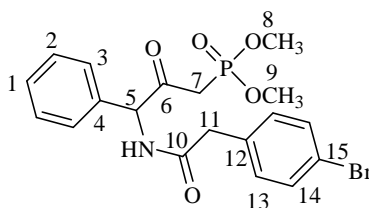
^{13}C NMR ($CDCl_3$, 75 MHz), δ ppm: 197.26 (d, 1C, C₆, $^2J_{C-P} = 6.3$ Hz); 169.22 (1C, C₁₀); 136.70 (1C, C₁₂); 135.23 (1C, C₄); 132.21 (1C); 130.30 (1C); 130.22 (1C); 129.31 (2C); 128.88 (1C), 128.12 (2C); 127.86 (1C); 122.66 (1C, C₁₄); 63.70 (d, 1C, C₅, $^3J_{C-P} = 3.2$ Hz); 53.14 (d, 1C, C₈, $^2J_{C-P} = 6.2$ Hz); 52.15 (d, 1C, C₉, $^2J_{C-P} = 6.6$ Hz); 42.64 (1C, C₁₁); 38.90-37.15 (d, 1C, C₇, $^1J_{C-P} = 131.6$ Hz).

³¹P NMR (CDCl₃, 121 MHz), (ppm): 21.22

HRMS (ESI) calculated for C₁₉H₂₁NO₅⁷⁹BrNaP: [M +Na]⁺ : m/z 476.0232, Found: m/z. 476.0233 (0 ppm).

Synthesis of {3-[2-(4-bromo-phenyl)-acetyl-amino]-2-oxo-3-phenyl-propyl} phosphonic acid dimethyl ester (52d)

To a solution of dimethyl methyl phosphonate **43** (2.19 g, 3.6 equiv) and n-BuLi (11 ml, 3.6 equiv) in THF (84 ml), a solution of amide ester **51d** (1.78 g, 1 equiv) in THF (10 ml) was added dropwise according to the general procedure. The color turned directly into deep yellow during the addition of amide ester **51d**, and remains the same till the end of the reaction. After purification by chromatography on silica gel, using CH₂Cl₂ as the only eluent, the desired phosphonate **52d** was obtained as a white solid in 76% yield.



C₁₉H₂₁BrNO₅P
M = 454.25 g.mol⁻¹

Yellow solid, mp = 127°C, R_f = 0.31 (CH₂Cl₂/ 4% MeOH).

¹H NMR (CDCl₃, 300 MHz), δ ppm: 7.44 (m, 2H); 7.34 (m, 3H); 7.24 (m, 2H); 7.14 (m, 2H); 6.96 (d, 1H, NH, ³J = 6.4 Hz); 5.72 (d, 1H, H₅, ³J_{NH-H} = 6.4 Hz); 3.74 (d, 3H, H₈, ³J_{H-P} = 11.2 Hz); 3.70 (d, 3H, H₉, ³J_{H-P} = 11.2 Hz); 3.62 (s, 2H, H₁₁); 3.12 (AB_{sys}, 1H, H₇, J = 14.5 Hz); 3.04 (AB_{sys}, 1H, H₇, J = 14.5 Hz).

¹³C NMR (CDCl₃, 75 MHz), δ ppm: 197.28 (d, 1C, C₆, ²J_{C-P} = 6.3 Hz); 169.34 (1C, C₁₀); 135.24 (1C, C₁₂); 133.39 (1C, C₄); 131.85 (2C); 130.95 (2C); 129.31 (2C); 128.89 (1C); 128.10 (2C), 121.24 (1C, C₁₅); 63.66 (d, 1C, C₅, ³J_{C-P} = 3.2 Hz); 53.23

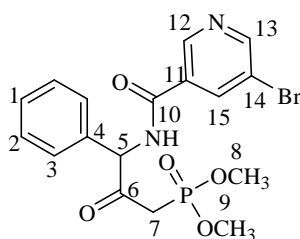
(d,1C, C₈, ²J_{C-P}= 6.8 Hz); 53.04 (d,1C, C₉, ²J_{C-P}= 6.8 Hz); 42.55 (1C, C₁₁); 38.86-37.12 (d,1C, C₇, ¹J_{C-P}= 131.6 Hz).

³¹P NMR (CDCl₃, 121 MHz), (ppm): 21.21

HRMS (ESI) calculated for C₁₉H₂₁NO₅⁷⁹BrNaP: [M +Na]⁺ : m/z 476.0232, Found: m/z. 476.0232 (0 ppm).

Synthesis of {3-[(5-bromo-pyridine-3-carbonyl)-amino]-2-oxo-3-phenyl-propyl}-phosphonic acid dimethyl ester (52e)

To a solution of dimethyl methyl phosphonate **43** (1.2 g, 3.6 equiv) and n-BuLi (6.1 ml, 3.6 equiv) in THF (42 ml), a solution of amide ester **51e** (0.94 g, 1 equiv) in THF (5 ml) was added dropwise according to the general procedure. The color turned directly into deep red during the addition of the amide ester **51e**, and then turned into deep yellow when the temperature reaches -30°C. After purification by chromatography on silica gel, using CH₂Cl₂ as the only eluent, the desired phosphonate **52e** was obtained as yellow oil in 63% yield.



C₁₇H₁₈BrN₂O₅P
M = 441.21 g.mol⁻¹

Yellow oil, R_f = 0.37 (CH₂Cl₂/ 4% MeOH).

¹H NMR (CDCl₃, 300 MHz), δ ppm: 8.95 (d, 1H, ⁴J = 1.6 Hz); 8.76 (d, 1H, ⁴J = 2.0 Hz); 8.28 (d, 1H, ⁴J = 2.0 Hz); 7.92 (d, 1H, NH, ³J = 6.3 Hz); 7.38 (m, 5H); 5.92 (d, 1H, H₅, ³J_{NH-H} = 6.3 Hz); 3.76 (d, 3H, H₈, ³J_{H-P} = 11.2 Hz); 3.69 (d, 3H, H₉, ³J_{H-P} = 11.0 Hz); 3.14 (AB_{sys}, 1H, H₇, J = 14.2 Hz); 3.08 (AB_{sys}, 1H, H₇, J = 14.2 Hz).

¹³C NMR (CDCl₃, 75 MHz), δ ppm: 197.22 (d, 1C, C₆, ²J_{C-P} = 6.1 Hz); 163.12 (1C, C₁₀); 153.50 (1C, C₁₂); 146.30 (1C, C₁₃); 137.78 (1C); 135.01 (1C); 130.62 (1C);

129.44 (2C); 129.12 (1C), 128.27 (2C); 120.79 (1C, C₁₄); 64.00 (d,1C, C₅, ³J_{C-P}= 2.7 Hz); 53.35 (d,1C, C₈, ²J_{C-P}= 6.6 Hz); 53.20 (d,1C, C₉, ²J_{C-P}= 6.5 Hz); 38.22 (d,1C, C₇, ¹J_{C-P}= 130.6 Hz).

³¹P NMR (CDCl₃, 121 MHz), (ppm): 21.11

HRMS (ESI) calculated for C₁₇H₁₈N₂O₅⁷⁹Br NaP: [M +Na]⁺: m/z 463.00289 Found: m/z. 463.0034 (1 ppm).

III.F. REFERENCES

References:

1. Kerr J. F., Wyllie A. H., Currie A. R., *Br. J. Cancer*, **1972**, 26(4), 239.
2. Fuchs Y., Steller, H. *Cell*, **2011**, 147, 742.
3. Hanahan D., Weinberg R. A. *Cell*, **2011**, 144, 646.
4. Ziegler D. S., Kung A. L. *Curr. Opin. Oncol.* **2008**, 20, 97.
5. Reed J. C., *Nature Rev. Drug Discovery*, **2002**, 1, 111.
6. Luke W. T., Connie L., Steven W. E., *FEBS Letters*, **2010**, 584, 2981.
7. McIlwain D. R., Berger T., Mak T. W., *Cold Spring Harbor Perspectives in Biology*, **2013**, 5, a008656.
8. Drag M. and Salvesen G. S., *Nature Rev. Drug Discovery*, **2010**, 9, 690.
9. Cleary M. L, Sklar J., *Proc. Natl. Acad. Sci. USA* **1985**, 21, 7439.
10. Tsujimoto Y., Cossman J., Jaffe E., Croce C. M., *Science*, **1985**, 228, 1440.
11. Wyllie A. H., Morris R. G., Smith A. L., Dunlop D., *J. Pathol.* **1984**, 1, 67.
12. Vaux D. L., *Cell Death & Differentiation*, **1999**, 6, 493.
13. Krammer P. H., *Nature*, **2000**, 407, 789.
14. Murphy K., *8th ed. New York: Garland Science*, **2011**.
15. Hernandez J. B., Newton R. H., Walsh C. M. *Curr. Opin. Cell. Biol.*, **2010**, 22, 865.
16. Corfe S. A., Paige C. J. *Semin. Immunol.* **2012**, 24,198.
17. Hardy R. R., Hayakawa K., *Annu. Rev. Immunol.* **2001**, 19, 595.
18. Peter M. E., Krammer P. H., *Current Opinion in Immunology*, **1998**, 10, 545.
19. Dickens L. S., Powley I. R., Hughes M. A., MacFarlane M., *Experimental Cell Research*, **2012**, 318, 1269.
20. Muzio M., Stockwell B. R., Stennicke H. R., Salvesen G. S., Dixit V. M. *J. Biol. Chem.* **1998**, 5, 2926.
21. Martin D. A, Siegel R. M, Zheng L, Lenardo M. J. *J. Biol. Chem.* **1998**, 8, 4345.
22. Yang X., Chang H. Y., Baltimore D. *Mol. Cell*, **1998**, 1, 319.
23. Cartron P. F., Gallenne T., Bougras G., Gautier F., Manero F., Vusio P. *Mol. Cell*, **2004**, 16, 807.
24. Certo M., Del Gaizo M. V., Nishino M., Wei G., Korsmeyer S., Armstrong S. A. *Cancer Cell*, **2006**, 9, 351.
25. Deng J., Carlson N., Takeyama K., Dal C. P., Shipp M., Letai A., *Cancer Cell*, **2007**, 12, 171.
26. Gavathiotis E., Suzuki M., Davis M. L., Pitter K., Bird G. H, Katz S.G., *Nature*, **2008**, 455, 1076.

27. Oltvai Z. N., Milliman C. L., Korsmeyer S. J., *Cell*, **1993**, 74, 609.
28. Willis S. N., Fletcher J. I., Kaufmann T., van Delft M. F., Chen L., Czabotar P. E., *Science*, **2007**, 315, 856.
29. Bratton S. B., Salvesen G. S., *J. Cell Sc.*, **2010**, 123, 3209.
30. Llambi F., Moldoveanu T., Tait S. W., Bouchier-Hayes L., Temirov J., McCormick L.L., *Mol. Cell*, **2011**, 44, 517.
31. Thibaud T. R., Jerry E. Chipuk; *Ann. N.Y. Acad. Sci.*, **2013**, 1285, 59.
32. Liu X., Kim C. N., Yang J., *Cell*, **1996**, 86, 147.
33. Kluck R. M., Bossy-Wetzl E., Green D. R., Newmeyer D. D., *Science*, **1997**, 275, 1132.
34. Letai A., Bassik M. C., Walensky L. D., Sorcinelli M. D., Weiler S., Korsmeyer S. J. *Cancer Cell*, **2002**, 2, 183.
35. Vo D. D., Gautier F., Barillé-Nion S., Juin P., Levion N., Grée R., *Bioorg. Med. Chem. Lett.*, **2014**, 24, 1758.
36. Petros A. M., Olejniczak E. T. and Fesik S. W., *Biochim. Biophys. Acta*, **2004**, 1644, 83.
37. Adams J. M. and Cory S., *Curr. Opin. Immunol.*, **2007**, 19, 488.
38. Czabotar P. E., Lessene G., Strasser A., Adam J. M., *Nat. Rev. Mol. Cell Biol.*, **2014**, 15, 49.
39. Danial N. N., Korsmeyer S. J. *Cell*, **2004**, 116, 205.
40. Adams J. M., Cory S., *Oncogene*, **2007**, 26, 1324.
41. Beroukhi R., Mermel C. H., Porter D., Wei G., Raychaudhuri S., Donovan J., Barretina J., Boehm J. S., Dobson J., Urashima M., Mc Henry K. T., Pinchback R. M., Ligon A. H., Cho Y.-J., Haery L., Greulich H., Reich M., Winckler W., Lawrence M. S., Weir B. A., Tanaka K. E., Chiang D. Y., Bass A. J., Loo A., Hoffman C., Prensner J., Liefeld T., Gao Q., Yecies D., Signoretti S., Maher E., Kaye F. J., Sasaki H., Tepper J. E., Fletcher J. A., Taberero J., Baselga J., Tsao M.-S., Demichelis F., Rubin M. A., Janne P. A., Daly M. J., Nucera C., Levine R. L., Ebert B. L., Gabriel S., Rustgi A. K., Antonescu C. R., Ladanyi M., Letai A., Garraway L. A., Loda M., Beer D. G., True L. D., Okamoto A., Pomeroy S. L., Singer S., Golub T. R., Lander E. S., Getz G., Sellers W. R., Meyerson M., *Nature*, **2010**, 463, 899.
42. Wei G., Margolin A. A., Haery L., Brown E., Cucolo L., Julian B., Shehata S., Kung A. L., Beroukhi R., Golub T. R., *Cancer Cell*, **2012**, 21, 547.
43. Song L., Coppola D., Livingston S., Cress D., Haura E. B. *Cancer Biol. Ther.*, **2005**, 4, 267.
44. Ding Q., He X., Xia W., Hsu, J.-M., Chen C.-T., Li L.-Y., Lee D.- F., Yang J.-Y., Xie X., Liu J.-C., Hung M. C., *Cancer Res.*, **2007**, 67, 4564.

45. Krajewska M., Krajewski S., Epstein J. I., Shabaik A., Sauvageot J., Song K., Kitada S., Reed J. C. *Am. J. Pathol.*, **1996**, *148*, 1567.
46. Miyamoto Y., Hosotani R., Wada M., Lee J. U., Koshiba T., Fujimoto K., Tsuji S., Nakajima, S., Doi R., Kato M., Shimada Y., Imamura M. *Oncology*,**1999**, *56*, 73.
47. Brotin E., Meryet-Figuière M., Simonin K., Duval R. E., Villedieu M., Leroy-Dudal J., Saison-Behmoaras E., Gauduchon P., Denoyelle C., Poulain L., *Int. J. Cancer*, **2010**, *126*, 885.
48. Derenne S., Monia B., Dean N. M., Taylor J. K., Rapp M. J., Harousseau, J. L., Bataille R., Amiot M., *Blood*, **2002**, *100*, 194.
49. Andersen M. H., Becker J. C., Thor Straten P., *Leukemia*,**2005**, *19*, 484.
50. Kang M. H., Wan Z., Kang Y. H., Sposto R., Reynolds C. P., *J. Natl. Cancer Inst.*, **2008**, *100*, 580.
51. Han, J., Goldstein, L. A., Hou, W., Rabinowich, H., *J. Biol. Chem.*, **2007**, *282*, 16223.
52. Day, C. L., Chen, L., Richardson, S. J., Harrison, P. J., Huang, D.C., Hinds, M. G., *J. Biol. Chem.*, **2005**, *280*, 4738.
53. Quinn B. A., Dash R., Azab B., Sarkar S., Das S. K., Kumar S., Oyesanya R. A., Dasgupta S., Dent P., Grant S., Rahmani M., Curiel D. T., Dmitriev I. Hedvat M., Wei J.; Wu, B.; Stebbins J. L.; Reed J. C., Pellicchia M., Sarkar D., Fisher P. B., *Expert Opin. Invest. Drugs*, **2011**, *20*, 1397.
54. Clohessy J. G., Zhuang J., Boer J., Gil-Gmez, G., Brady H. J., *J. Biol. Chem.*, **2006**, *281*, 5750.
55. Kim H., Rafiuddin-Shah M., Tu, H. C., Jeffers J. R., Zambetti G. P., Hsieh, J. J., Cheng, E. H. *Nat. Cell Biol.*, **2006**, *8*, 1348.
56. Youle R.J., Strasser A., *Nat. Rev. Mol. Cell Biol.*, 2008, *9*, 47.
57. Friberg A., Vigil D., Zhao B., Daniels R.N., Burke J.P., Garcia-Barrantes P.M., *J. Med. Chem.*, 2013, *56*, 15.
58. Zhang B., Gojo I., Fenton R. G., *Blood*, *99*,**2002**, 1885.
59. Craig R.W., Jabs E.W., Zhou P. et al., *Genomics*, **1994**, *23*, 457.
60. Beroukhim R., Merml C. H., Porter D, *Nature*, **2010**, *463*, 899.
61. Opferman J.T. et al., *Nature*, **2003**, *426*, 671.
62. Arbour N. et al., *J. Neurosci*, *28*, **2008**, *24*, 6068.
63. Steimer D. A. et al., *Blood*, **2009**, *12*, 2805.
64. Edwards S.W. et al. *Biochem. Soc. Trans.*, **2004**, *32*, 489.
65. Opferman J. T. et al., *Science*, **2005**, *5712*, 1101.
66. Decaudin D., Marzo I., Brenner C., Kroemer G. *Int. J. Oncol.*, **1998**, *12*,141.
67. Green D. R., Kroemer G., *Science*, **2004**, *305*, 626.
68. Billard C. *Mol. Cancer Ther.* **2013**, *12*, 1691.

69. Roy M. J., Vom A., Czabotar P. E., Lessene G. *Br. J. Pharmacol.* **2014**, *171*, 1973.
70. Tahir S. K., Yang X., Anderson M. G., *Cancer Res.*, **2007**, *67*, 1176.
71. Lin X., Morgan-Lappe S., Huang X., *Oncogene*, **2007**, *26*, 3972.
72. Hann C. L., Daniel V. C., Sugar E. A., *Cancer Res.*, **2008**, *68*, 2321.
73. Tse C., Shoemaker A. R., Adickes J., *Cancer Res.*, **2008**, *68*, 3421.
74. Vogler M., Furdas S. D., Jung M., Kuwana T., Dyer M. J. S., Cohen G. M., *Clinical Cancer Research*, **2010**, *16*, 4217.
75. Mason K. D., Carpinelli M. R., Fletcher J. I., *Cell*, **2007**, *128*, 1173.
76. Vogler. M., Hamali H. A., Sun X., *Blood*, **2011**, *117*, 7145.
77. Schoenwaelder S. M. Yuan Y., Josefsson E. C., *Blood*, **2009**, *114*, 663.
78. Souers A. J., Levenson J. D., Boghaert E. R., *Nat. Med.*, **2013**, *19*, 202.
79. Seymour J. F., Davids M. S., Pagel J. M., *Blood*. **2013**, *122*, 293.
80. Van Delft M. F., Wei A. H., Mason K. D., Vandenberg C. J., Chen L., Czabotar P. E., Willis S.N., Scott C. L., Day C. L., Cory S, Adams J.M., Roberts A.W., Huang D.C., *Cancer Cell*, **2006**, *10*, 389.
81. Vogler M., Dinsdale D., Dyer M. J. S, Cohen GM., *Cell Death Differ.*, **2009**, *16*, 360.
82. Souers A. J., Levenson J. D., Boghaert E. R., Ackler S. L., Catron N. D., Chen J, Dayton B. D., Ding H., Enschede S.H., Fairbrother W. J., Huang D. C. S, Hymowitz S. G, Jin S, Khaw S. L., *Nat Med*, **2013**, *19*, 202.
83. Vogler M., Dinsdale D., Dyer M.J. S, Cohen G. M., *Br. J. Haematol*, **2013**, *163*, 139.
84. Dai Y, Grant S., *Cancer Res.* **2007**, *67*, 2908.
85. Gores G. J, Kaufmann S. H., *Genes Dev.*, **2012**, *26*, 305.
86. Zhang H, Guttikonda S, Roberts L, Uziel T, Semizarov D, Elmore S. W, Levenson J. D, Lam L. T. *Oncogene*, **2010**, *1*.
87. Stewart M. L, Fire E, Keating A. E, Walensky L. D., *Nat. Chem. Biol.*, **2010**, *6*, 595.
88. Placzek W. J, Sturlese M, Wu B, Cellitti J. F, Wei J, Pellecchia M., *J Biol. Chem.*, **2011**, *286*, 39829.
89. Muppidi A., Doi K, Edwardraja S., Drake E. J., Gulick A. M., Wang H. G., *J. Am. Chem. Soc.*, **2012**, *134*, 14734.
90. Smith B. J., Lee E. F., Checco J. W., Evangelista M., Gellman S. H., Fairlie W. D. *Biochem*, **2013**, *14*, 1564.
91. Cohen N. A., Stewart M. L., Gavathiotis E., Tepper J. L., Bruekner S. R., Koss B., *Chem. Biol*, **2012**, *19*, 1175.
92. Doi K., Li R., Sung S. S., Wu H., Liu Y., Manieri W., *J. Biol. Chem.*, **2012**, *287*, 10224.
93. Abulwerdi F., Liao C., Liu M., Azmi A. S., Aboukameel A., Mady A. S., *Mol. Cancer Ther.*, **2014**, *13*, 565.

94. Richard D. J, Lena R., Bannister T., Blake N., Pierceall W. E., Carlson N. E., *Bioorg. Med. Chem.*, **2013**, *21*, 6642.
95. Gojo I., Zhang B., Fenton R. G. *Clin. Cancer Res.*, **2002**, *8*, 3527.
96. MacCallum D. E., Melville J., Frame S., Watt K., Anderson S., Gianella-Borradori A., *Cancer Res.*, **2005**, *65*, 5399.
97. Xie G., Tang H., Wu S., Chen J., Liu J., Liao C. *Int. J. Oncol.*, **2014**, *45*, 804.
98. Bruncko M., Wang L., Sheppard G. S., *J. Med. Chem.*, **2015**, *58*, 2180.
99. Levenson J. D., Zhang H., Chen J., *Cell Death Dis.*, **2015**, *6*, 1590.
100. Abulwerdi F. A., Liao C, Mady A. S., Gavin J., Shen C., Cierpicki T., *J Med. Chem.*, **2014**, *57*, 4111.
101. Richard D. J, Lena R, Bannister T, Blake N, Pierceall W.E, Carlson N. E, *Bioorg Med Chem.*, 2013, *21*, 6642.
102. Petros A. M, Swann S. L, Song D., Swinger K., Park C., Zhang H., *Bioorg Med. Chem. Lett.*, 2014, *24*, 1484.
103. Jeremy L., Chen Y. L., Lanning M., E, Fletcher S., *J. Med. Chem*, **2016**, 5b01888.
104. Zhang Z, Song T, Li X, Wu Z, Feng Y, Xie F., *Eur. J. Med. Chem.*, 2013, *59*, 141.
105. McLeod M., Boudreault N., Leblanc Y., *J. Org. Chem.* **1996**, *61*, 1180.
106. Boudreault N., Ball R. G., Bayly C., Micheal A., Leblanc Y., *Tetrahedron*, **1994**, *Vol. 50*, 7947.
107. Mitchell H., Leblanc Y., *J. Org. Chem.* **1994**, *59*, 682.
108. Jia J. D., Henri D., *Eur. J. Org. Chem.* **2010**, 611.
109. Desideri N., *Lett. Org. Chem.*, **2006**, *3*, 546.
110. Sandulache A., Artor M. S., Diana C. G., Lucia M. P., Jose A. S., *New J. Chem.*, **2003**, *27*, 1592.
111. Peter G.M., Theodora W., *Greene's Protective group in organic synthesis*, **2007**.
112. Raji R., Rani V., Damoder R., *J. Org. Chem.* **2013**, *78*, 6495.
113. Bera S., Panda G., *Org. Biomol. Chem.*, **2014**, *12*, 3976.

General Conclusion

This thesis is divided into three independent chapters:

- β -lactams chemistry: a new and direct synthesis of α -methylene and α -alkylidene- β -lactams using the Kinugasa reaction.
- Acylsilane chemistry: synthesis of new acylsilane derivatives bearing an aldehyde group in a remote position of the same molecule to perform asymmetric intramolecular aldol reaction.
- Medicinal chemistry: synthesis of new molecules of MIM-1 analog that induce apoptosis of cancer cells.

In the first chapter, Kinugasa reaction was applied to alkynes bearing a nucleofuge in propargylic position that allowed us to discover a direct entry to new α -methylene and α -alkylidene β -lactams.

In the second chapter, Two models of acylsilane derivatives that bear an aldehyde group in a remote position of the same molecule were synthesized starting from morpholine amide as a precursor, and asymmetric intramolecular aldol reaction was then performed.

In the last chapter, our goal was to reinduce the pro-apoptotic properties in cancer cells in order to obtain new antitumor compounds. Depending on the molecular modeling carried out by Dr. N. Levoïn, two different models of MIM-1 analog (inhibitor of anti-apoptotic protein MCL-1) were synthesized and tested on three types of cancer cells (breast, ovarian and melanoma).

Thus this work shows good results for medicinal chemistry, since the new entry that we discovered toward α -methylene and α -alkylidene- β -lactams may open a gate for the synthesis of β -Lactamase inhibitors. In addition to the synthesis of new interesting bioactive molecules that exhibit anti-apoptotic properties. Furthermore, asymmetric synthesis of acylsilanes compound could be developed towards new bioactive molecules.

Résumé

La thèse est divisée en trois chapitres indépendants. - Chimie des β -lactames: Synthèse d' α -méthylène et d' α -alkylidène- β -lactames en utilisant la réaction de Kinugasa. - Chimie des acylsilanes: essai d'application d'une réaction aldol intramoléculaire asymétrique sur un dérivé d'acylsilane nouvellement synthétisé. - Chimie médicinale: synthèse de nouvelles molécules à visée anticancéreuse. Dans le premier chapitre la réaction de Kinugasa a été appliquée pour la première fois à des alcynes vrais, portant en position propargylique un groupe partant ce qui permet d'accéder directement et en une étape aux méthylène- et alkylidène β -lactames recherchés. Dans le second chapitre la synthèse de molécules originales possédant à la fois une fonction acylsilane et un aldéhyde en position éloignée, puis l'aldolisation intramoléculaire asymétrique ont été explorées. Dans le dernier chapitre, notre objectif était de restaurer les propriétés apoptotiques au sein des cellules cancéreuses afin d'obtenir de nouveaux composés à activité antitumorale. A partir de données obtenues par modélisation moléculaire, nous avons fait le design de plusieurs séries d'analogues d'un inhibiteur connu (MIM-1) de la protéine anti-apoptotique Mcl-1. Huit composés ont été synthétisés et testés pour trois types de cellules cancéreuses (sein, ovaire et le mélanome).

Abstract

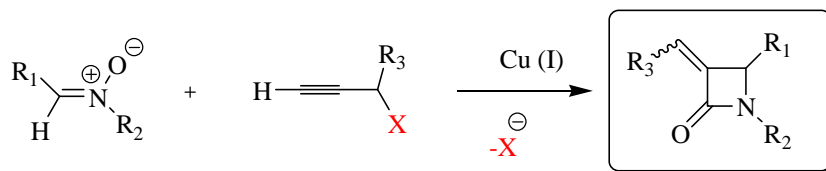
The thesis is divided into three chapters: - β -lactams chemistry: synthesis of α -methylene and α -alkylidene- β -lactams using the Kinugasa reaction. - Acylsilane chemistry: applying asymmetric intramolecular aldol reaction on newly synthesized acylsilane derivatives. - Medicinal chemistry: synthesis of new molecules with anticancer aims. In the first chapter, Kinugasa reaction was applied for the first time with an alkyne bearing a nucleofuge in propargylic position that allowed us to discover a new pathway for the synthesis of exoalkylidene β -lactams. In the second chapter, new acylsilane derivatives bearing an aldehyde functional group in a remote position of the molecule were prepared, and asymmetric intramolecular aldolization reaction was performed. In the last chapter, our goal was to reinduce the pro-apoptotic properties in cancer cells in order to obtain new antitumor compounds. Starting from data obtained through molecular modeling studies, we designed and prepared several series of analogs for a known inhibitor (MIM-1) of the anti-apoptotic protein Mcl-1. Eight compounds have been synthesized and screened towards three types of cancer cells (breast, ovarian and melanoma).

Key words: nucleofuge, propargylic derivatives, Kinugasa reaction, α -methylene and α -alkylidene- β -lactams, acylsilane derivatives, asymmetric intramolecular aldolization reaction, anti-tumor, MIM-1, MCL-1, apoptosis, cancer.

Abstract-Résumé

Cette thèse, réalisée en cotutelle entre l'Université Libanaise à Beyrouth (Laboratoire de Chimie Médicinale et des Produits Naturels, Pr Ali Hachem) et l'Université de Rennes 1 (Institut des Sciences Chimiques de Rennes, CNRS UMR 6226, Equipe Dr R. Grée), s'intègre dans la grande thématique du développement de nouvelles méthodologies en synthèse organique et leur application à la préparation de composés bioactifs. Elle est organisée en trois chapitres indépendants.

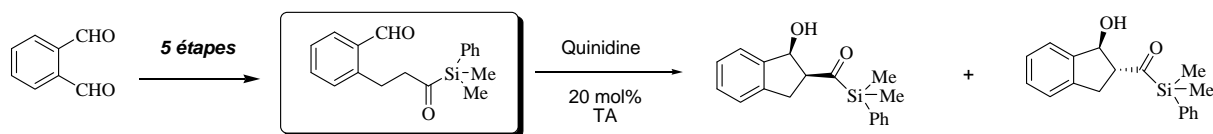
Dans le premier chapitre on décrit une méthodologie très originale d'accès à des méthylène- et alkylidène- β -lactames. Il s'agit d'une famille de composés importante sur le plan biologique, notamment dans le domaine des antibiotiques : un certain nombre de composés de cette famille ont déjà montré des propriétés d'inhibition des β -lactamases, enzymes impliquées dans les phénomènes de résistance aux antibiotiques. Dans le cadre de ce travail il a été montré, pour la première fois, que l'application de la réaction de Kinugasa à des alcynes vrais, portant en position propargylique un groupe partant (halogène, tosylate, mesylate, carbonate...) permettait d'accéder directement et en une étape aux méthylène- et alkylidène- β -lactames recherchés. Une étude détaillée a permis d'optimiser les conditions de réaction et de montrer que le groupe partant carbonate était le plus approprié pour cette réaction. Ensuite a été réalisée une étude visant à cerner les possibilités et limites d'utilisation de cette voie de synthèse : cette réaction tolère des groupes R3 variés en donnant des rendements satisfaisants à bons à partir de nitrones linéaires mais ne marche pas avec des nitrones cycliques.



Au bilan, cette nouvelle approche permet d'accéder rapidement (1 étape à partir de produits commerciaux ou faciles à préparer) et avec des rendements corrects, à de nouveaux méthylène- et alkylidène- β -lactames. Ceci permettra donc d'explorer plus en détail les propriétés biologiques de cette famille de composés importants. Ce travail a fait l'objet d'une publication à *Tetrahedron Letters* en 2016.

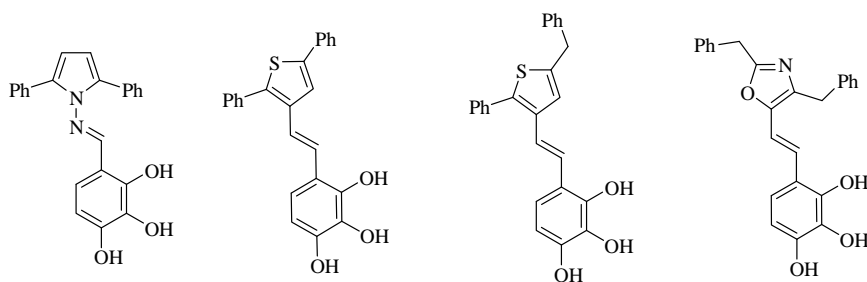
Dans le second chapitre on s'intéresse à la chimie des acylsilanes, composés qui ont été nettement moins étudiés dans la littérature que d'autres groupements fonctionnels mais qui possèdent des potentialités synthétiques très intéressantes. Le premier objectif dans ce cas concernait la synthèse de molécules originales possédant à la fois une fonction acylsilane et un aldéhyde en position éloignée et ceci avec deux espaceurs différents. A partir de ces molécules le second problème était d'explorer les possibilités d'aldolisation intramoléculaire asymétrique. Après un travail de synthèse intense, il a été possible de préparer un premier composé modèle possédant un groupe aromatique comme espaceur. L'aldolisation intramoléculaire asymétrique a été explorée, montrant que les meilleures conditions impliquaient l'utilisation de la quinidine seule comme catalyseur. L'emploi de la proline seule, ou de la

combinaison proline+quinidine donnait de moins bons rendements en produits d'aldolisation. Malheureusement, cette réaction a donné un mélange de deux diastéréoisomères inséparables par les techniques classiques de chromatographie et il n'a pas été possible de déterminer les excès énantiomériques potentiels.



La synthèse d'une seconde molécule cible, possédant cette fois un espaceur linéaire avec cinq atomes de carbone, a été explorée malheureusement sans succès. Ceci est lié à la difficulté de réaliser des réactions compatibles avec deux groupes fonctionnels sensibles comme les aldéhydes et les acylsilanes. Ce chapitre a donc montré qu'il était possible de réaliser la réaction d'aldolisation intramoléculaire souhaitée mais des travaux complémentaires seront nécessaires pour une analyse complète de sa stéréo/énantiosélectivité.

Dans la troisième et dernière partie de la thèse les recherches concernent la découverte de nouveaux composés à activité anticancéreuse. L'idée directrice consiste à rechercher des molécules susceptibles de lever les freins à l'apoptose très couramment observés avec les cellules tumorales : en échappant à l'apoptose (mort cellulaire programmée) les cellules cancéreuses vont survivre très longtemps, ce qui à l'évidence va augmenter leur dangérosité. Une grande partie des phénomènes biologiques liés à l'apoptose est sous le contrôle de l'interaction de protéines pro- et anti-apoptotiques. Les protéines antiapoptotiques sont très souvent surexprimées ans les cellules tumorales et, en se liant très fortement aux protéines proapoptotiques, empêchent ces dernières d'agir et de déclencher la mort des cellules cancéreuses. Il s'agit donc de trouver des composés qui libèrent les protéines proapoptotiques de leurs partenaires antiapoptotiques, notamment Bcl-xL ou Mcl-1. Suite aux recherches antérieures des deux équipes, et après des études de modélisation moléculaire et docking dans Mcl-1, plusieurs familles de molécules cibles ont été définies. Ce sont des composés possédant des coeurs hétérocycliques liés à un motif polyphénolique et à des branches aromatiques ou benzyliques.



Structures des molécules cibles

Des composés à squelette thiophénique et pyrrolique ont été préparés et testés biologiquement. Ils se sont malheureusement révélés inactifs dans les tests anticancéreux réalisés. Une étude préliminaire a été réalisée également pour dégager une voie d'accès originale vers des molécules à cœur oxazole. Ces travaux seront poursuivis pour préparer et tester les produits cibles correspondants.